THE BIOCHEMISTRY OF HYPOXIA. DRUG METABOLISM, TYROSINE DEGRADATION AND MITOCHONDRIAL RESPIRATION BY ISOLATED HEPATOCYTES AT LOW $P(O_2)$

by

Dean P. Jones

A THESIS

Presented to the Department of Biochemistry
and the Graduate Division of the University of Oregon
Health Sciences Center
in partial fulfillment of
the requirements for the degree of

Doctor of Philosophy
June 1976

APPROVED:

[redacted]

(Professor in Charge of Thesis)

[redacted]

(Chairman, Graduate Council)

ACKNOWLEDGEMENTS

Financial support through a National Institutes of Health pre-doctoral traineeship and through grants from the United States Public Health Service is gratefully acknowledged.

I am indebted to Professor H.S. Mason for academic stimulation and critique and for continued support during my graduate studies. I also thank Dr. J.H. Fellman, Dr. D. Kabat and Dr. N. Gerber for helpful discussions and comments, and Mr. R. Jones for assistance with electron microscopy.

I want to express special appreciation to my wife, Diane, who spent many hours typing drafts of the manuscript and, more importantly, provided emotional support during this period.

TABLE OF CONTENTS

LIST OF TABLES

LIST OF FIGURES

LIST OF APPENDIX FIGURES

LIST OF ABBREVIATIONS

ADP	Adenosine diphosphate
AMP	Adenosine monophosphate
ASC	Ascorbate
ATP	Adenosine triphosphate
BSA	bis-(Trimethylsilyl)acetamide
BSTFA	bis-(Trimethylsilyl)trifluoroacetamide
E.C.	Adenylate energy charge
EPR	Electron paramagnetic resonance
GDH	Glutamic dehydrogenase
GLU	Glutamic acid
HEX	hexobarbital
HG	Homogentisic acid
HGO	Homogentisate oxidase
pHPP	p-Hydroxyphenylpyruvic acid
pHPPO	p-Hydroxyphenylpyruvic acid oxidase
Km	Michaelis constant
LAC	Lactic acid
LDH	Lactic dehydrogenase
3-MC	3-Methylcholanthrene
Mk	Myokinase
NAD^+	Nicotinamide adenine dinucleotide, oxidized form
NADH	Nicotinamide adenine dinucleotide, reduced form
$NADP^+$	Nicotinamide adenine dinucleotide phosphate, oxidized form
NADPH	Nicotinamide adenine dinucleotide phosphate, reduced form
2-OG	2-Oxoglutarate
PEP	Phosphoenol pyruvate
Pk	Pyruvate kinase
$P(O_2)$	Oxygen partial pressure

POPOP	p-bis-[2-(5-Phenyloxazolyl)]-benzene
PPO	2,5-Diphenyloxazole
PYR	Pyruvic acid
$Q(O_2)$	Respiratory rate
TAT	Tyrosine aminotransferase
TMPD	N, N, N', N', -tetramethyl-P-phenylenediamine
TYR	Tyrosine
Vmax	Maximum velocity at infinite substrate concentration

I. INTRODUCTION

"Hypoxia" is a general term for decreased oxygen availability to cells. The decrease may be small or great (anoxia=without oxygen), and the resulting physiological variations from normal may be acute or chronic, reversible or irreversible, innocuous or deadly. Usually hypoxia is a consequence of or concomitant with other medical problems. When cells are deprived of oxygen, however, the severity and duration of deprivation is important in determining the capability of recovery of normal cellular function. Unraveling mechanisms of cell injury at the biomolecular level is indeed complex. It requires a thorough knowledge of oxygen utilizing enzymes and their dependence upon oxygen. The purpose of this dissertation is to develop a model for the study of the biochemistry of hypoxia on a cellular level.

Part I.A of this introduction deals with the history of the biochemistry of hypoxia and contains a brief summary of some major developments of oxygen metabolism and cellular responses to hypoxia. Part I.B reviews the current knowledge of the biochemistry of hypoxia and includes theories on the mechanism of hypoxic lesions at the biomolecular level. Part I.C presents a statement of the problem of this dissertation.

I.A. History

A comprehensive history of hypoxia is not available. The understanding of physiological responses to hypoxia was closely tied to the development of the general field of respiratory physiology (Haldane and Priestley, 1935; Perkins, 1964; van Liere and Stickney, 1963). The development of the biochemistry of hypoxia was greatly dependent upon understanding of cellular respiration. The treatment here is a brief overview of major concepts of hypoxia. Additional information may be obtained from an excellent book by Keilin (1966), "The History of Cell Respiration and Cytochrome," and a series of scientific papers and essays collected by Kalckar (1969), "Biological Phosphorylations: Development of Concepts." A chronology of discoveries in the broad context of hypoxia is given in Appendix I.

A fundamental step in the history of hypoxia was development of the concept that oxygen is essential for normal function of the body. Robert Boyle (1670) published a series of experiments using an air pump to evacuate a vessel containing small animals. He concluded that an unknown part of air is necessary for life. Robert Hooke corroborated this conclusion (1667). He carved away the ribcage of a dog and pricked tiny holes in the lungs to allow escape of air. Using a pair of bellows to maintain the lung constantly inflated, he showed that the dog survived perfectly well so long as there was a

continual supply of fresh air. As soon as the supply stopped, the animal went into convulsive fits. John Mayow (Medico-Physical Works, 1674) discussed a "nitro-aereal" spirit found in the air which is consumed during animal respiration and during combustion. Although oxygen itself had not been discovered at this time, two of its important properties were known, namely, that it is present in air and that it is required during respiration and combustion.

The preparation of pure oxygen marked a new age of science; Priestley and Scheele prepared and characterized oxygen independently (1771-1774). Lavoisier (1789) utilized this discovery along with his own quantitative experiments to establish a firm basis for the development of modern chemistry and extended the observations of Priestley that oxygen is the component of air essential for life.

Lavoisier made other important contributions to understanding respiration, notably the use of calorimetry to show that the same amount of heat is produced during respiration and combustion. He showed that the quantity of oxygen consumed by an animal is not affected by concentration changes, but that the quantity consumed is greatly influenced by exercise, digestion and external temperature (Keilin, 1966). Thus, he established that oxygen utilization by the body is determined by the needs of the body and was not merely by oxygen concentration.

Oxygen consumption was demonstrated to occur in tissues by Spallanzani (1791), but this work was not published for several years (Keilin, 1966). Its acceptance was further delayed because it challenged the accepted view of a central life force. The shift of scientific thinking followed additional studies by Liebig (1850). Measurement of oxygen consumption by various tissues was accomplished during the period 1910-1930 by improved methods of manometry introduced by Barcroft and Haldane and used widely by Warburg (Dickens and Simers, 1930; Dixon, 1934; see Section I. B.).

The concept that oxygen consumption occurs primarily in the tissues produced the question of how cells in a tissue are supplied with oxygen. The Kroghs (1919) applied Fick's diffusion theory to oxygen diffusion through tissue. They measured this diffusion and studied capillary patterns to provide a description of oxygen supply to cells in terms of capillaries supplying surrounding tissue cylinders with oxygen by radial diffusion (Krogh, 1922).

The development of polarographic electrodes which can be used for measurement of oxygen tension within living tissues has recently allowed the commencement of a systematic analysis of tissue oxygen supply. Salomon discovered that oxygen reduction affected the current of a platinum wire (1897). Its use for oxygen determination became possible after the development of the polarographic electrode system (Heyrovsky, 1925). The first accurate tissue oxygen

measurements were made by Davies and Brink (1942) using a recessed platinum electrode with a collodion film to cover the platinum. Clark (1956) introduced a further modification, a membrane-coated platinum electrode containing a silver-silver chloride reference electrode. This electrode is valuable for blood and solution oxygen measurements, but because of its size, is of limited value for tissue work. A platinum micro-electrode consisting of a 100 μm platinum core) coated with glass and with an exposed 10 μm platinum tip which is suitable for tissue oxygen measurements was described by Cater and Silver (1961).

Introduction of hot air balloons by the Montgolfier brothers (1783) had a great impact on the study of hypoxia since it produced a method for rapid induction of altitude sickness without complicating affects of exercise and dietary changes. Paul Bert (1878) showed that oxygen deprivation alone was sufficient to cause all manifestations of altitude sickness. Thus, the study of altitude sickness and mountain sickness became the study of oxygen deprivation. During the subsequent half century the physiology of oxygen deprivation was intensely investigated, resulting in a classification of anoxemias by Barcroft (1920; see Table I-A), and a general understanding of the physiological responses to hypoxia (see Haldane and Priestley, 1935).

An understanding of the relationship of cellular energetics to biological oxidations was essential for a biochemical interpretation of

hypoxia. Liebig (1824) showed that carbohydrates, fats and protein are burned by the body. The discovery of catalysis by Vogel in 1812 and independently by Davy in 1820, formulated into a theory of catalysis by Berzelius in 1837, led to the view that cells contain a chemical catalyst responsible for the oxidation of foodstuffs (Keilin, 1966). Arthur Harden observed that addition of boiled yeast extract to a yeast extract incubation with glucose greatly stimulated alcoholic fermentation. Subsequent research (Harden and Young, 1906) established that the specific effect was due to inorganic phosphate and cozymase (NAD^+). This investigation led to the study of the affect of these substances on muscle metabolism (Dickens, 1951) and ultimately to an understanding of glycolysis, the tricarboxylic acid cycle, and oxidative phosphorylation.

The presence of lactic acid in tissues was known at the time Lavosier established the foundations of modern chemistry, but its role in metabolism was not understood. Araki (1890) noted that large quantities of lactate were produced in the body at high altitudes. Fletcher and Hopkins (1907) found that electrical stimulation of muscle contraction resulted in an accumulation of lactate. Embden and coworkers studied the precursors of lactate; they reasoned from the work of Harden and Young that sugar phosphates in the presence of muscle extract should yield lactic acid and inorganic phosphate. Their results showed this correlation (Kalckar, 1969). Warburg

(1923) concluded that glycolysis supplied energy requirements for mammalian cells in the same manner that carbohydrates are used by bacteria. Further, the inhibitory effect of oxygen upon fermentation (glycolysis), originally discovered by Pasteur, was recognized (Warburg, 1926) as a link between respiration and glycolysis. Hill and coworkers (1924) and Bang (1935) showed that lactate accumulation during exercise is related to oxygen debt. Lipmann (1941) explained this phenomenon in terms of a switch between a more efficient aerobic energy yielding system, respiration, and the less efficient system, glycolysis.

During the years 1912-1922, Wieland and coworkers actively studied the class of oxido-reductases known as dehydrogenases and advanced the theory that the oxidative processes in cells are due to the enzymatic activation of hydrogen and subsequent reaction with a suitable electron acceptor such as molecular oxygen (Keilin, 1966). Concomitantly, Warburg searched for a respiratory enzyme containing iron which could react with oxygen to increase the valence state of the iron. The iron could then react with organic substances and revert back to its bivalent state, thus catalyzing respiration. The conflict between these theories was resolved by Keilin (1929) only six years after his rediscovery of cytochromes. He showed that these pigments could undergo oxidation and reduction and proposed that they act as a link between dehydrogenases and oxygen.

The final segment between pyruvate and the dehydrogenases was provided by Krebs (1937). He observed the biochemical synthesis of citric acid from a mixture of oxaloacetic acid and pyruvic acid, and proposed a cycle commencing with this condensation and leading to oxaloacetate (Section I. B. 4.).

Adenosine triphosphate and phosphocreatine were isolated from muscle by Fiske and Subbarow (1927, 1929). Respiratory dependent phosphorylation by lysed erythrocytes was demonstrated by Englehardt (1930, 1932) and in iodoacetate poisoned muscle by Lundsgaard (1930). Kalckar (1937) showed that phosphorylation in renal cortex is proportional to oxygen consumption. Belister and Tsybokova (1939) and Ochoa (1940) determined ratios of phosphorylation relative to oxygen consumption of 2 to 3, which suggested that transfer of reducing equivalents between carriers could be harnessed for phosphorylation (Kalckar, 1969). The localization of these reactions in mitochondria was demonstrated by Kennedy and Lehninger (1948).

The central role of ATP in the transfer of energy from oxidative metabolism to support cellular functions was proposed by Lipmann (1941). Eggleton and Eggleton (1927) had previously observed that an acid labile phosphoric ester is rapidly decreased in muscle during fatigue. Stone, Marshall and Nims (1941) showed that phosphocreatine decreases in the brain during short periods of anoxia, and

Gurdjian, Webster and Stone (1949) showed that under severe hypoxia decomposition of adenosine triphosphate occurs.

The cellular oxygen requirement was accounted for in terms of oxidative phosphorylation by Chance (1957). However, other oxygen utilizing enzymes have been known since Bertrand (1894) described laccase. Mason, Folkes and Peterson (1955) and Hayaishi, Katagiri and Rothberg (1955) independently used $^{18}O_2$ to show that molecular oxygen is directly incorporated into enzymatic products. Subsequently, numerous oxygen-dependent enzymes have been discovered and their oxygen dependence studied (Section I. B.).

I. B. The Biochemistry of Hypoxia

This section contains discussions of 1) the definition and classification of hypoxias, 2) systemic affects of hypoxia, 3) the cellular oxygen supply, 4) cellular metabolism of oxygen, 5) biochemical studies of hypoxia, and 6) theories of hypoxic pathophysiology.

I. B. 1. Definition and Classification of Hypoxias

Hypoxia is a condition of oxygen insufficiency in whole animals or isolated tissues (Bendixen and Laver, 1964; Van Liere and Stickney, 1963). This definition implies that oxygen tension, decreased from normal, causes a functional change. A schematic diagram showing the causal relationship of oxygen deprivation to

functional changes is presented in Figure I-1. The primary hypoxic events are probably enzymatic oxygen deficiencies. If oxygen deficiency affects cytochrome oxidase, it alters the available energy supply or redox state of the cell and is consequently a bioenergetic hypoxia. If it affects the metabolic incorporation of molecular oxygen by an oxidase, it is a metabolic hypoxia. Biochemical changes which occur as a consequence of the primary hypoxia are secondary hypoxic events. Bioenergetic hypoxia results in decreased ATP, phosphoryl potential, adenylate energy charge, and a more negative redox potential. Consequently, effects of these changes upon cell functions such as protein synthesis, active transport, enzyme reactions, cellular pH, or muscle contraction, are secondary events characteristic of bioenergetic hypoxia. Metabolic hypoxia results in decreased rate of substrate oxygenation and product formation, and may also affect the redox state of the cell. Secondary consequences may occur by diversion of substrates into alternate pathways, lack of a reaction product which is needed for another function, or prolonged biological activity of a hormone or drug due to incapacity for removal.

On a physiological basis, hypoxia is defined operationally with respect to oxygen tensions found in normal healthy individuals at sea level. The following may be used as criteria for hypoxia: 1) the $P(O_2)$ of inspired air is below 154 torr ; 2) the arterial $P(O_2)$ is below 95 torr ; 3) the median or average $P(O_2)$ for a specific tissue

Figure I-1. Schematic representation of the pedigree of causes during hypoxia. This scheme relates the hypothetical sequence of events during hypoxia as described by the current theory. The simplifying assumption that the initiating physiological event is an uncomplicated cellular hypoxia was used. The primary biochemical events are enzymatic oxygen deficiencies and all other biochemical and physiological changes occur as a consequence of these primary hypoxic events.

Figure I-1

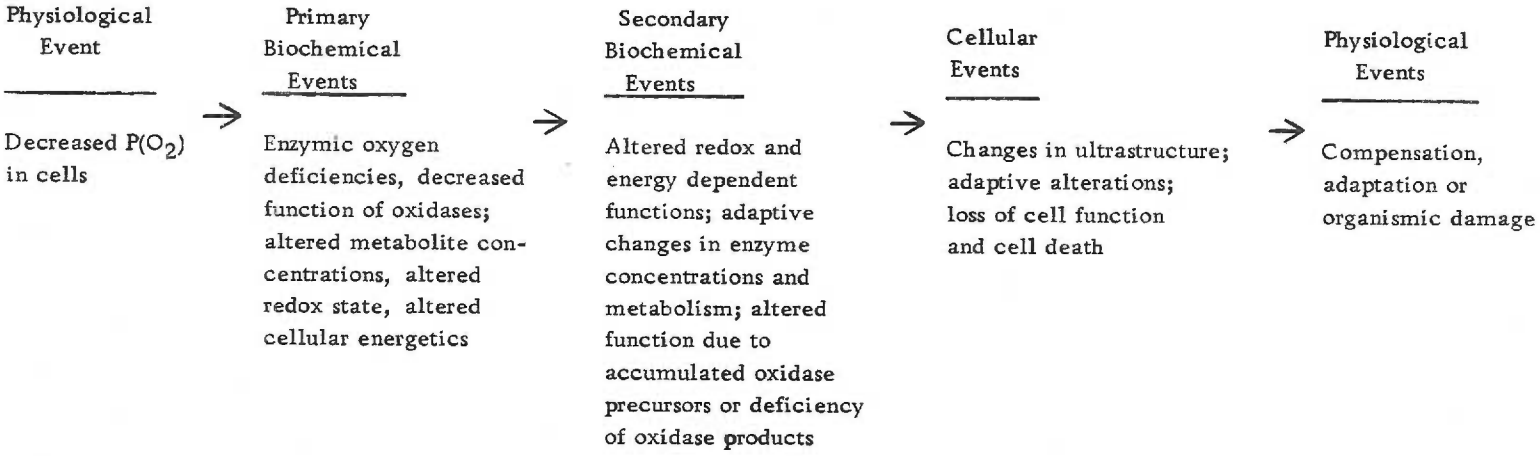
Physiological Event
Decreased $P(O_2)$ in cells
Primary Biochemical Events
Enzymic oxygen deficiencies, decreased function of oxidases; altered metabolite concentrations, altered redox state, altered cellular energetics
Secondary Biochemical Events
Altered redox and energy dependent functions; adaptive changes in enzyme concentrations and metabolism; altered function due to accumulated oxidase precursors or deficiency of oxidase products
Cellular Events
Changes in ultrastructure; adaptive alterations; loss of cell function and cell death
Physiological Events
Compensation, adaptation or organismic damage

is reduced from normal (see Figure I-3; Kessler et al., 1973; Losse et al., 1973; Lubbers, 1973; Schuchhardt, 1973; Vaupel, Braunbeck and Thews, 1973; Vaupel et al., 1973; Whalen, 1973).

Oxygen tension is not always measurable, and in such cases one must rely upon physiological or biochemical changes as criteria for hypoxia. Since changes occur only as a consequence of decreased oxygen to an oxidase, the affinity of the oxidase for oxygen will determine the degree of hypoxia under which the change is elicited (see Section I.B.4.). Thus, functional changes dependent upon different oxidases will occur at different oxygen tensions. These changes are defined by the primary oxidase affected; for example, an altered rate of norepinephrine synthesis due to oxygen insufficiency to dopamine β-hydroxylase is termed dopamine β-hydroxylase hypoxia. This usage defines explicitly the biochemical system and condition. It requires that the tissue oxygen tension is subnormal and that oxygen dependence is not zero order. It does not reflect in any way whether the condition is beneficial, innocuous, or harmful.

Two terms for operationally defining the oxygen dependence of different systems are critical oxygen tension and half maximal oxygen tension (Chance, 1957; Chance et al., 1962; Cohen, 1972; Gurdjian, Stone and Webster, 1944; Hill, 1948; Jobsis, 1964; Stainsby, 1966). Critical oxygen tension means here the oxygen tension at which the first observable biochemical change occurs in an

oxygen-dependent system as the oxygen tension is lowered from an oxygen-independent range, i.e., the oxygen tension at which a zero to first order oxygen dependence transition begins. This definition is more general than that usually stated (for instance, see Cohen, 1972, or Jobsis, 1964), since it allows definition of a critical oxygen tension for each oxygen dependent function rather than simply for the overall respiration rate. The half maximal oxygen tension is the oxygen tension at which a half maximal change occurs in an oxygen dependent function. This term can be used to describe metabolite changes, enzyme activities, or other biological parameters. It is NOT synonymous with $Km(O_2)$; it is a more general term which encompasses $Km(O_2)$ values and may be used as an apparent $Km(O_2)$ only under conditions where an enzyme activity can be measured directly as a function of oxygen tension. The use of critical oxygen tensions and half maximal oxygen tensions allow comparison of hypoxic changes in a semiquantitative fashion without regard to reaction sequences or mechanisms and can be used to relate both primary and secondary hypoxias.

Other terms often used to describe hypoxic conditions are hypoxemia, anoxia, anoxemia, anaerobiasis, cyanosis, and ischemia. Hypoxemia is a subnormal oxygen content in the blood, usually the arterial blood. Anoxia is an absence of oxygen, and anoxemia is the corresponding state of blood. Anaerobiasis is complete absence of

oxygen and is generally applied to in vitro conditions. Cyanosis is a clinical term for the bluish coloration of skin as in response to hypoxemia or to decreased capillary circulation in the skin or mucous membranes. Ischemia refers to partial or total cessation of blood flow to a tissue or organ due to mechanical obstruction.

A classification of medically important hypoxias based upon Barcroft's original classification of anoxemias (Barcroft, 1920) is given in Table I-A. He proposed three types according to the physiological cause: 1) low oxygen pressure in the blood (anoxia type), 2) reduced functional hemoglobin (anemic type), and 3) insufficient blood supply to the tissues (stagnant type). Peters and Van Slyke (1932) proposed a fourth type in which cells are supplied with sufficient oxygen but are unable to utilize it because the cells are poisoned (histotoxic type). Peters and Van Slyke modified their definition of anoxia (hypoxia) to include this by defining anoxia as "any condition which retards the oxidation processes in the tissues." This definition has not been accepted in subsequent literature, but the use of "histotoxic hypoxia" continues (Dittmer and Grebe, 1958; Van Liere and Stickney, 1963) because the symptoms caused by certain poisons are similar to the symptoms of some hypoxias. The use of "histotoxic hypoxia" should be abandoned for several reasons: 1) It is not a true hypoxia. 2) It provides the misleading impression that poisoning of a cellular component results in an oxygen insufficiency such as

Table I-A. Physiological classification of hypoxias.[1]

Type (A)	Cause (B)	Mechanism (C)	Clinical or experimental state (D)
		Hypoxic Hypoxia	
Ambient	Dilution of oxygen	Lowered $P(O_2)$ in inspired air	Fire damp, black damp
	Rarified atmosphere		Mountain sickness, high altitude blackout
	Selective reduction O_2		In experimental studies, anesthesia accidents
Respiratory	Ventilatory insufficiency	Lowered $P(O_2)$ in alveolar air	Obstructive lesions, emphysema, respiratory tract obstruction, strychnine poisoning.
			Space-occupying lesions; e.g., pneumothorax. CNS depression from drugs, anesthetics, CNS lesions.
	Alveolar wall block	Impaired alveolo-capillary diffusion	Fibrosis or edema of alveolar wall; infection, mitral stenosis, left ventrical failure.
	Physiologic intra-pulmonary shunt	Blood passage through non-ventilated segments of lung.	Certain consolidations, incomplete bronchial obstruction.
	Pulmonary arterio-venous shunt	Shunt of unoxygenated blood around normal alveoli.	Pulmonary hemangioma or arterio-venous shunt.
		Hemic Hypoxia	
Anemic	Reduction in total circulating hemoglobin	Decreased concentration of oxygen in whole blood	Anemias of blood loss, deficiency state, hemolysis or bone marrow depression.
Toxic	Reduction in functional circulating hemoglobin	Conversion of Hb into COHb, metHb or sulfHb	Toxicity of CO, nitrites, chlorates, various coal tar derivatives; rare congenital metabolic disorders
		Circulatory Hypoxia	
Volumetric	Blood volume loss		Shock associated with hemorrhage, burns, trauma or infection.
	Volume capacity increase	Low circulating blood flow	Peripheral vascular collapse, states with sequestration of blood.

(Continued on next page)

Table I-A. (Continued)

Type (A)	Cause (B)	Mechanism (C)	Clinical or Experimental state (D)
Cyanotic congenital cardiac	Anomalous inflow or outflow routes of the heart	Routing of venous blood into left atrium or aorta	Anomalous vena caval drainage, transposition of great vessels, persistent truncus arteriosus.
	Absence of one or more cardiac chambers	Mixing of bloods in common cardiac chamber	Cor biloculare, cor triloculare biatriatum.
	Abnormal communication between lesser and greater circulations	Ejection of venous blood into left heart or into aorta (right to left shunt)	Fallot type: pulmonary or tricuspid stenosis, or atresia with interatrial or interventricular communication. Eisenmenger type: pulmonary hypertension with "reverse" shunt through atrial septal defect, ventricular septal defect or persistent ductus arteriosus
Minute flow discrepancy	Myocardial fault	Low cardiac output resulting from diseased myocardium	Heart failure, myocardial infarction, myocarditis.
	Constrictive lesion of heart	Low cardiac output resulting from poor diastolic filling	Cardiac tamponade, constrictive pericarditis, arrhythmia, thoracic wall deformity.
	Obstructive lesion of heart	Low cardiac output resulting from high resistance to flow	Heart valve lesions, increased pulmonary or systemic vascular resistance.
	Relative minute flow insufficiency	Oxygen demands of tissue in excess of minute flow supply	Beriberi, thyrotoxicosis, arterio-venous fistula.
Peripheral vascular	Arterial obstruction	Distal ischemia	Coarctation of aorta, atherosclerosis, thrombosis, embolism, arteritis, arteriolitis; laceration, division, extrinsic pressure on artery.
	Venous statis	Peripheral congestion	Congestive heart failure, venous obstruction, venous valve incompetence.
	Lymph stasis	Low capillary blood flow as a result of high tissue tension	Chronic infection of lymphatics, general edematous states, idiopathic.
	Vasospastic states	Distal ischemia resulting from abnormal degree of angiospasm	Raynaud's disease, arterial or venous spasm, certain cold injuries

(Continued on next page)

Table I-A. (Continued)

Type (A)	Cause (B)	Mechanism (C)	Clinical or experimental state (D)
		Pseudohypoxia	
Metabolic	Metabolic oxidase inhibition	Failure of oxidase function	Monoamine oxidase inhibitor administration SFK 525A administration
Bioenergetic	Oxidase inhibition	Failure of oxidase function	Cyanide poisoning
	ATP depletion	Adenine trapping	Ethionine administration
	ATP depletion	Uncoupling oxidative phosphorylation	Arsenic poisoning
Genetic	Inherited oxidase disorders	Loss of oxidase function	Phenylketonuria, alkaptonuria
Imbalance	Water and electrolyte imbalance	Distorted cellular chemistry	Hyponatremic states

[1] Modified from Dittmer and Grebe (1958). Contributors for original were S. A. Wesolowski, R. Bruce, C. A. Finch, A. Selzer, and J. C. Stickney.

would occur if a tissue oxygen carrier were inhibited (Longmuir and McCabe, 1965); no such hypoxia has been demonstrated (however, see Burns and Burtner, 1973; Gurtner and Burns, 1973). 3) Non-specific metabolic inhibitors may affect respiration by mechanisms quite unrelated to primary events in hypoxia. Thus, although some characteristics of inhibition are similar to hypoxia, the remaining metabolism is not.

A more appropriate term for metabolic disturbances similar to hypoxia caused by specific inhibitors of oxidases is pseudohypoxia. For inhibitors which have a low or unknown specificity the name of the inhibitor is used as an adjective, e.g., cyanide pseudohypoxia. If the inhibitor is known to be highly specific or if the inhibition of a specific enzyme is being considered, the name of the enzyme is used as an adjective in analogy to the naming of enzyme-specific hypoxias, e.g., dopamine-β-hydroxylase pseudohypoxia (DβH pseudohypoxia).

I.B.2. Systemic Effects of Hypoxia

Hypoxia is a major factor in the pathophysiology of most circulatory and respiratory defects. These defects have a high incidence of morbidity and mortality as shown in Tables I-B and I-C.

The U.S. National Center for Health Statistics reported that over 57% of the deaths in 1973 were due to respiratory and circulatory causes. The Metropolitan Life Insurance Company reported that in

Table I-B. Deaths for selected causes with possible hypoxic involvement in United States, 1968-1973. From Monthly Vital Statistics Report, 1974.

Cause of death	Number					
	1973	1972	1971	1970	1969	1968
All causes	1,977,000	1,962,000	1,927,542	1,921,031	1,921,990	1,930,082
Major cardiovascular diseases	1,937,460	1,028,560	1,017,145	1,007,984	1,013,015	1,023,399
Diseases of heart	754,460	752,450	743,368	735,542	739,265	744,653
Active rheumatic fever and chronic rheumatic heart disease	13,580	14,090	14,644	14,889	15,432	16,338
Hypertensive heart disease	7,810	7,570	7,860	8,413	8,976	9,811
Hypertensive heart and renal disease	5,390	5,550	6,190	6,578	7,310	7,337
Ischemic heart disease	682,910	683,100	674,292	666,665	669,829	675,747
Acute myocardial infarction	348,010	357,350	357,714	357,241	361,583	364,610
Other acute and subacute forms of ischemic heart disease	4,380	4,400	4,027	4,246	4,677	4,691
Chronic ischemic heart disease	330,440	320,950	312,351	304,962	303,362	300,226
Angina pectoris	130	160	200	216	207	230
Chronic disease of endocardium and other myocardial insufficiency	4,870	5,330	6,132	6,705	7,475	7,336
All other forms of heart disease	39,900	36,810	34,250	32,293	30,243	28,019
Hypertension	8,010	7,680	7,837	8,273	8,426	9,063
Cerebrovascular diseases	214,650	210,050	209,092	207,166	207,197	211,390
Cerebral hemorrhage	34,270	36,580	38,563	41,329	43,303	27,002
Cerebral thrombosis	56,260	56,460	57,229	57,845	58,748	60,331
Cerebral embolism	940	890	954	884	1,005	1,136
All other cerebrovascular diseases	123,180	116,120	112,346	107,058	104,123	102,921
Arteriosclerosis	33,430	32,820	31,521	31,682	33,063	33,568
Other diseases of arteries, arterioles, and capillaries	26,910	25,560	25,327	25,321	25,082	24,720
Acute bronchitis and bronchiolitis	810	1,080	1,154	1,310	1,286	1,437
Bronchitis, emphysema, and asthma	30,280	28,750	30,284	30,889	31,144	33,078
Chronic and unqualified bronchitis	5,810	5,360	5,591	5,846	5,843	6,203
Emphysema	22,540	21,310	22,539	22,721	22,939	24,135
Asthma	1,930	2,090	2,154	2,332	2,362	2,688
Certain causes of mortality in early infancy						
Birth injury, difficult labor, and other anoxic and hypoxic conditions	17,790	18,940	20,992	22,801	21,939	22,132

Table I-C. Disability from hypoxic or related causes. Data represent incidence of disability lasting eight days or more among personnel of the Metropolitan Life Insurance Company. From Statistical Bulletin, 1974.

Cause of disability	New cases per 1,000							
	Males, at ages				Females, at ages			
	17-64	17-24	25-44	45-64	17-64	17-24	25-44	45-64
			1973					
All causes	101.4	71.7	76.7	141.5	178.8	110.0	168.5	246.6
Diseases of respiratory system	13.6	13.9	11.5	16.0	50.2	32.3	43.3	72.0
Diseases of circulatory system	15.9	3.2	5.8	32.5	11.0	2.1	8.5	20.9
Diseases of heart	10.4	0.4	2.6	23.4	2.7	-	1.1	6.6
			1972					
All causes	95.1	70.9	71.6	133.4	177.6	122.8	163.7	239.0
Diseases of respiratory system	12.6	10.8	10.2	16.4	51.5	36.2	46.0	70.3
Diseases of circulatory system	14.5	2.4	6.1	29.1	10.5	2.5	4.7	23.2
Diseases of heart	8.7	1.4	2.6	19.0	3.0	0.2	0.7	7.6

discussions of physiological responses to hypoxia are available (Kronenberg et al., 1972; Tenney and Lamb, 1965; Van Liere and Stickney, 1963). If physiological adaptations are inadequate to supply the tissues with sufficient oxygen, muscular weakness, headache, vomiting, incoordination, mental confusion, hearing problems, visual problems and coma or death may occur (Van Liere and Stickney, 1963). The survival times of individual tissues during hypoxia offer an indication of the extreme variability of the sensitivity of different tissues to hypoxia. Ultimately, the survival of the entire organism is dependent upon the individual components, and under various conditions, different tissues may be the "weakest link." Tenney and Lamb (1964) list the maximum length of time that various tissues can be revived following acute anoxia. The brain cortex is revivable for only 5 minutes, while the medulla is revivable up to 15 minutes. The heart may survive 10 minutes of anoxia and the liver and kidney about an hour. Skeletal muscle is highly resistant to anoxia and can survive in the resting state for 8 hours. Thus, in acute anoxia, the brain is the most susceptible tissue.

The hope of hypoxia research is to identify the susceptible cell types under the various clinical conditions and to provide a complete pedigree of causality for hypoxic tissue damage. This knowledge of sites and mechanisms of hypoxic damage is an essential prerequisite

for a rational approach to therapy to minimize the morbidity and mortality.

I.B.3. Cellular Oxygen Supply

Function of oxygen utilizing systems depends upon the oxygen tension available to these systems (see Section I.B.4.c.). Determination of tissue oxygen tensions and the factors affecting them are consequently important to understanding the function of these systems. Oxygen tension is a balance between consumption and supply.

Oxygen consumption rates have been determined for many tissues (Altman and Dittmer, 1971; Dittmer and Grebe, 1958). Representative values are found in Table I-D. The rates vary greatly between tissues and within the same tissue during periods of different functional activity. Skeletal muscle oxygen consumption during exercise may increase 20-fold over resting values (37°C) of 0.25-1.0 ml O_2/100 gm/min (0.11-0.45 mM/min assuming specific gravity = 1; Kunze, 1968). Gastrointestinal values parallel digestive functions (Grim, 1965). Kidney $Q(O_2)$[1] rises with blood flow because increased energy is required for absorption (Deetjen, 1968). In contrast, the brain oxygen consumption is relatively constant (Lubbers, 1968).

[1] $Q(O_2)$ means oxygen consumption rate per unit tissue. The standard physiological unit for oxygen consumption has been ml O_2/100 gm tissue/min, which has been retained in this discussion. However, concentration units, as recommended by IUB, are included where practicable.

Table I-D. Tissue oxygen supply parameters. A great variety of methodology was used in these determinations and cannot be summarized here. The references in parentheses are listed below this table.

Animal	Tissue	$Q(O_2)$ (ml/min/ 100 gm)	Blood flow (ml/min/ 100 gm)	Blood volume (ml/100 gm)	Maximum diffusion distance (μm)	$P(O_2)$ (torr)	Krogh's diffusion constant x 10^5	Capillary length (mm/mm^3)
Man	Brain	3.3-3.9	50-64		18-20			750-1000
		(21)	(2)		(23)			(2)
	Heart	8-10	70		9-10			3340-3740
		(9)	(22)		(23)			(2)
	Kidney	6.24	320					
		(7)	(8)					
	Liver	4.6	82					
		(9)	(4)					
	Skeletal muscle	0.17 (rest)	4.5			21-30		
		(9)	(25)			(18)		
	Spleen							
	Thyroid		400					
			(6)					
Dog	Brain	4.4	41	1.1	22	25-35		670
		(15)	(15)	(12)	(23)	(21)		(2)
	Heart	7-10	72-85	6.6		15		
		(9)	(11)	(12)		(20)		
	Kidney	9.7	400	8.1		50		
		(9)	(2)	(12)		(26)		
	Liver	4.3	86	14.7				
		(9)	(2)	(12)				
	Skeletal muscle	0.2-1.3	6.9	1.1		25		780
		(9)	(13)	(12)		(26)		(2)
	Spleen		70	51				
			(28)	(12)				
	Thyroid	9.3	355					
		(9)	(9)					

(Continued on next page)

Table I-D. (Continued)

Animal	Tissue	$Q(O_2)$ (ml/min/ 100 gm)	Blood flow (ml/min/ 100 gm)	Blood volume (ml/100 gm)	Maximum diffusion distance	$P(O_2)$ (torr)	Krogh's diffusion constant x 10^5	Capillary length (mm/mm^3)
Rat	Brain	18.6 (cortex) (9)		3.3 (10)	16-18 (23)		2.1 (27) 2.7 (14)	1160 (2)
	Heart	15.8 (9)		26.2 (10)	7-11 (23)		1.9 (27) 15.4 (19)	2700 (2)
	Kidney	19 (cortex) (9)	734 (1)	12.8 (10)	16 (cortex) (29)	75 (17)	6.3 (19)	
	Liver	13 (5)	79 (3)	27.0 (10)	12-25 (estimate)	25 (16)	16.4 (19)	
	Skeletal muscle	1.6 (slice) (9)		2.6 (10)	16 (red) 29 (white) (23)			1250 (red) 370 (white) (2)
	Spleen	2.4 (9)		17.0 (10)				
	Adrenal	9.2 (9)	190 (24)	23.8 (10)				

(1) Altman, 1959
(2) Altman and Dittmer, 1971
(3) Birnie and Grayson, 1952
(4) Bradley et al., 1945
(5) Brauer et al., 1963
(6) Catchpole and Gersh, 1947
(7) Clark and Barker, 1951
(8) Crosley et al., 1956
(9) Dittmer and Grebe, 1958
(10) Everett et al., 1956
(11) Foltz et al., 1950
(12) Gibson et al., 1946
(13) Green et al., 1944
(14) Grote, 1960
(15) Halley et al., 1958
(16) Kessler et al., 1973a
(17) Kessler et al., 1973b
(18) Kunze, 1968
(19) Longmuir and Bourke, 1960
(20) Losse et al., 1973
(21) Lubbers, 1968
(22) Moret, 1971/72
(23) Reivich, 1971
(24) Sapirstein and Goldman, 1959
(25) Selkurt, 1971
(26) Sinagowitz et al., 1973
(27) Thews, 1968
(28) Vaupel et al., 1973a
(29) Vaupel et al., 1973b

Intraorgan variations in $Q(O_2)$ are difficult to determine, and consequently less data are available. Variations have been detected between working muscle fibers and Purkinje fibers in the heart (Fabel, 1968), grey matter and white matter in brain (Opitz and Schneider, 1950), cortex and medulla in kidney (Deetjen, 1968), and cortex and medulla in adrenals (Sourkes and Heneage, 1952). Oxygen consumption also may differ either qualitatively or quantitatively in cells according to their relationship to the capillary circulation. Mitochondrial shape in hepatic parenchymal cells is dependent upon intralobular location (Copenhaver et al., 1971). This suggests a functional variance which is of particular importance since most analyses of tissue oxygenation assume homogeneous oxygen consumption. Likewise, oxygen consumption is usually considered to be continuous with time; however, cyclical changes in mitochondrial or cellular oxygen consumption in intact cells cannot be excluded (Aschoff and Pahl, 1970; Jobsis, 1972). Delivery of oxygen to cells is influenced by rate of blood flow, capillary density, capillary flow patterns, and diffusion properties of the tissue.

Tables of blood flow rates to various tissues in different organisms are available (Altman, 1959; Altman and Dittmer, 1971). Measurement of tissue blood flows and factors affecting them are treated in detail in recent symposia (Bain and Harper, 1967; Lubbers et al., 1968) and in three volumes entitled "Circulation," edited by

W.F. Hamilton (1965) and will not be discussed here. A selected list of blood flow measurements is given in Table I-D.

As with oxygen consumption, blood flow varies between tissues. This variation does not parallel oxygen consumption differences, indicating that for some tissues blood supply to the tissue is not strictly dependent upon oxygen consumption. Blood supply to different parts of an organ also can vary, as evidenced by differences in medullary and cortical flows in the kidneys (Selkurt, 1971). Blood flow to a given tissue may be highly variable or relatively constant. Flow to the liver may double during digestion or fall to 50% of normal during exercise (Shoemaker and Elwyn, 1969). Blood flow to the brain is remarkably constant (Opitz and Schneider, 1950).

Local heterogeneity of flow in skeletal muscle has been suggested by Van Liew (1963), based upon regional variations in $P(O_2)$ and $P(CO_2)$ measurements. Lubbers (1973) measured capillary flow on the surface of guinea pig brain and found local values to vary from 41 to 200 ml/100 gm/min. Assuming homogeneous cellular respiration, differences in blood flow could result in major differences in tissue oxygen tensions.

Capillary density is a second factor in determining delivery of oxygen to cells. Different expressions of capillary densities in tissues have been used (Altman and Dittmer, 1971): blood volume/tissue mass, number of capillaries/mm^2, length of capillaries/mm^3,

and intercapillary distance (often expressed as maximum diffusion distance = 1/2 intercapillary distance). Values for blood volumes, capillary length/volume and maximum diffusion distances are given in Table I-D. Blood volumes are crude estimates of capillary density because of the rapid dilatations and constrictions which can occur. Some organs, such as the spleen and liver, have a blood storage function and consequently contain a disproportionate amount. Estimates of the number of capillaries/cross sectional area have been made for cardiac or skeletal muscle in some organisms; human cardiac muscle has about 3350 capillaries/mm^2 (Altman and Dittmer, 1971). Resting skeletal muscle has about 750/mm^2 (Stainsby and Otis, 1964). Capillary length/volume and maximum diffusion distance data are easier to use for mathematical treatments and therefore are preferred. Values for brain, heart, and skeletal muscle are given in Table I-D. These values are merely averages and do not reflect tissue variations. Lockard (1973) lists average intercapillary distances for several portions of the brain ranging from 21 to 86 micrometers. A frequency distribution of intercapillary distances for rat kidney cortex is given in Figure I-2 (Vaupel et al., 1973). This shows that intercapillary distances range from less than 20 to over 45 micrometers in the same tissue.

Total capillary length/mm^3 does not provide data for individual capillary length. Individual capillary length is important because the

Figure I-2. Frequency distribution of intercapillary distances and length of capillaries of renal cortex. From Vaupel et al. (1973).

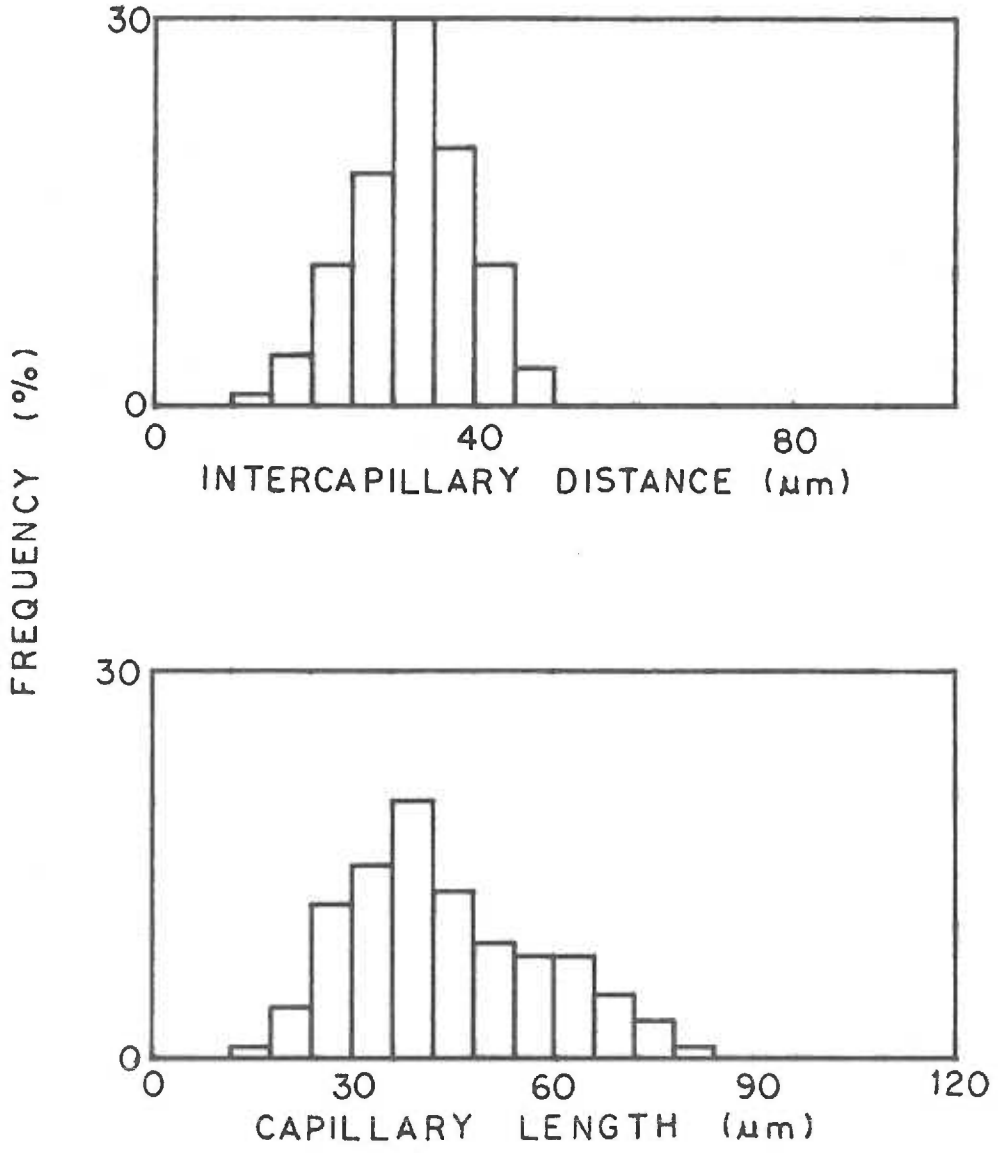
30
0
0
40
80
INTERCAPILLARY DISTANCE (μm)
FREQUENCY (%)
30
0
0
30
60
90
120
CAPILLARY LENGTH (μm)

diffusion of oxygen out of the blood as it passes through the capillary results in a lower $P(O_2)$ at the venous end rather than at the arterial end (Borg, 1969). Measures of capillary length provide a frequency distribution of lengths as shown in Figure I-2 (Vaupel et al., 1973). Average capillary length in rat renal cortex is about 42 μm with a range from about 20 to over 70 μm.

The liver and spleen have modified capillaries called sinusoids or sinuses. All parenchymal cells in the liver have at least one contact surface with a sinusoid (Copenhaver et al., 1971); therefore, the average intercapillary distance is between the diameter, 25 μm, and twice the diameter, 50 μm.

Average intercapillary distances or capillary lengths do not provide a complete model for capillary geometry or blood flow patterns. Different proposals for capillary geometry and flow pattern are reviewed briefly by Bruley (1973). The primary model, a capillary passing through a tissue cylinder, was introduced by Krogh and treated mathematically by Erlang. This model is still of fundamental importance in understanding oxygen diffusion in tissues; a recent treatment is given by Boag (1969). The single capillary model has been extended to multicapillary systems and analyzed with assymetric, concurrent, and countercurrent flow patterns. Bruley feels these models need to be critically analyzed and tested for validity by comparison to experimental measurements. More accurate

anatomical and physiological parameters are needed, including consideration of statistical distribution of capillary dimensions, metabolic rate and hemodynamic characteristics.

Relatively few measurements of oxygen diffusion through tissue have been made (see Table I-E). With the exception of data by Longmuir and Bourke (1960) the values are in reasonable agreement. The mechanism of oxygen diffusion in tissues is still unresolved. Wittenberg (1970) proposed the role of myoglobin in facilitating oxygen diffusion in muscle. Longmuir and coworkers (1971) proposed the role of cytochrome P-450 in the facilitation of oxygen diffusion in the liver. Hills (1970) analyzed tissue as a heterogeneous diffusion medium and concluded that "the concept of tissue as cells of irregular shape suspended in a continuous extracellular phase of much greater permeability would appear to be consistent with data on the steady-state assimilation of oxygen." More extensive studies of diffusion in tissue are necessary to establish the validity of these proposals.

Data concerning the factors affecting tissue oxygen tensions are currently too incomplete to allow a description of oxygen tension in these terms. The best available assessment of oxygen supply conditions is a direct measure of tissue oxygen tensions. Microelectrodes (< 10 μm tip; see Section I.A.) have been used to measure tensions in a variety of tissues. These values are normally

Table I-E. Diffusion coefficients,[1] O_2 in tissue.

Species	Tissue	Diffusion coefficient ($\times 10^5$) (cm^2/sec)	Krogh's constant ($\times 10^5$) ($cm^2/min/atm$)	Reference
Human	aorta, intima	0.8	1.1	Kirk and Laursen, 1955
	aorta, media	1.0	1.3	"
Rabbit	cerebral cortex	1.4	1.9	Greven, 1960
	corneal stroma	0.67		Takahashi et al., 1967
Guinea pig	liver	0.8	1.1	Greven, 1960
Rat	cerebral cortex	1.6	2.1	Thews, 1960
	cerebral cortex		2.7	Grote, 1960
	heart	1.5	1.9	Grote and Thews, 1962
	heart		15.4	Longmuir and Bourke, 1960
	kidney		6.3	"
	liver		16.4	"
Frog	skeletal muscle	1.3	1.6	Krogh, 1919

[1] Diffusion coefficient is a proportionality constant relating flux through a unit area to the concentration gradient of the diffusing substance.

expressed as histograms, which show the frequency distribution of oxygen tension measurements. Histograms for a variety of tissues are presented in Figure I-3. Tensions vary over a wide range for all tissues. The distributions of the frequencies are similar for brain (Lubbers, 1973), liver (Kessler et al., 1973), kidney (Kessler et al., 1973), skeletal muscle (Sinagowitz et al., 1973), and spleen (Vaupel et al., 1973) except for a variation in the median. Heart muscle (Losse et al., 1973; Schuchhardt, 1973), skeletal muscle with subnormal arterial $P(O_2)$ (Sinagowitz et al., 1973), and tumors (Vaupel et al., 1973) have a frequency distribution skewed toward zero oxygen tension.

Oxygen tension is not randomly distributed in tissues but occurs as a gradient. Highest values must occur adjacent to the arteriolar end of the capillaries. Visual representation of oxygen gradients based upon various models are available (Grunwald, 1973; Hutton, 1973; Mutzger, 1973). It must be emphasized that these are only theoretical constructs. Actual measures of oxygen tension fields have been determined by insertion of microelectrodes into tissues (Lubbers, 1968, 1973). A trace of oxygen tension as a function of distance in cat brain cortex is given in Figure I-4. The remarkable feature is the great variation in oxygen tension over such small distances. Other measurements corroborate such large fluctuations (Bicher, 1973).

Figure I-3. Histograms of tissue oxygen measurements.
a. guinea pig brain (Lubbers, 1973)
b. dog heart (Losse et al., 1973)
c. beating guinea pig heart (Schuchhardt, 1973)
d. rat liver (Kessler et al., 1973)
e. kidney (Kessler et al., 1973)
f. renal cortex (Vaupel et al., 1973)
g. dog skeletal muscle, resting
h. dog skeletal muscle with arterial hypoxemia (Singawotz et al., 1973)
i. spleen (Vaupel, Braunbeck and Thews, 1973)
j. cat carotid body (Whalen, 1973)

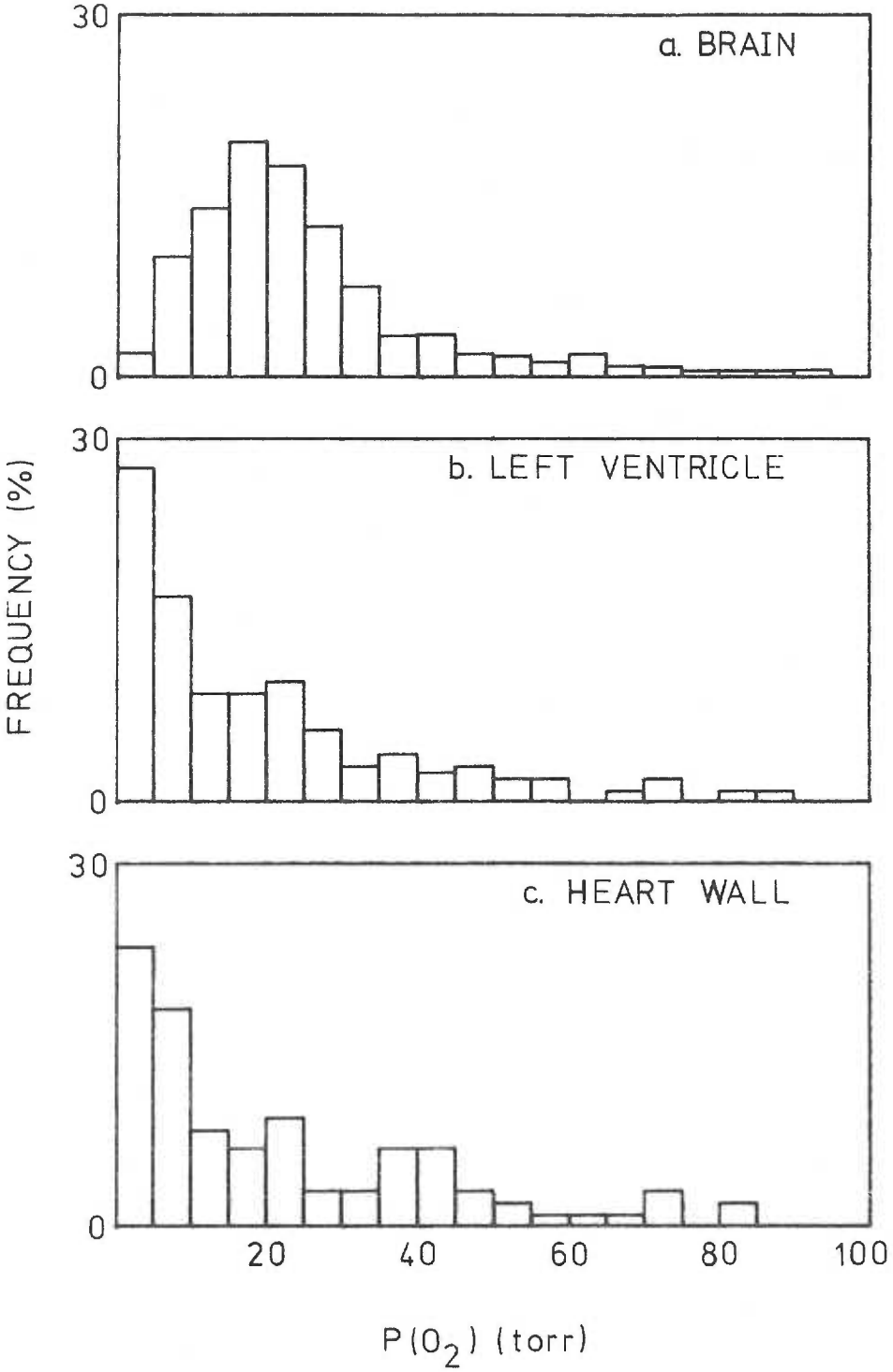
30
a. BRAIN
0
30
b. LEFT VENTRICLE
0
30
c. HEART WALL
0
FREQUENCY (%)
20
40
60
80
100
P(O2) (torr)

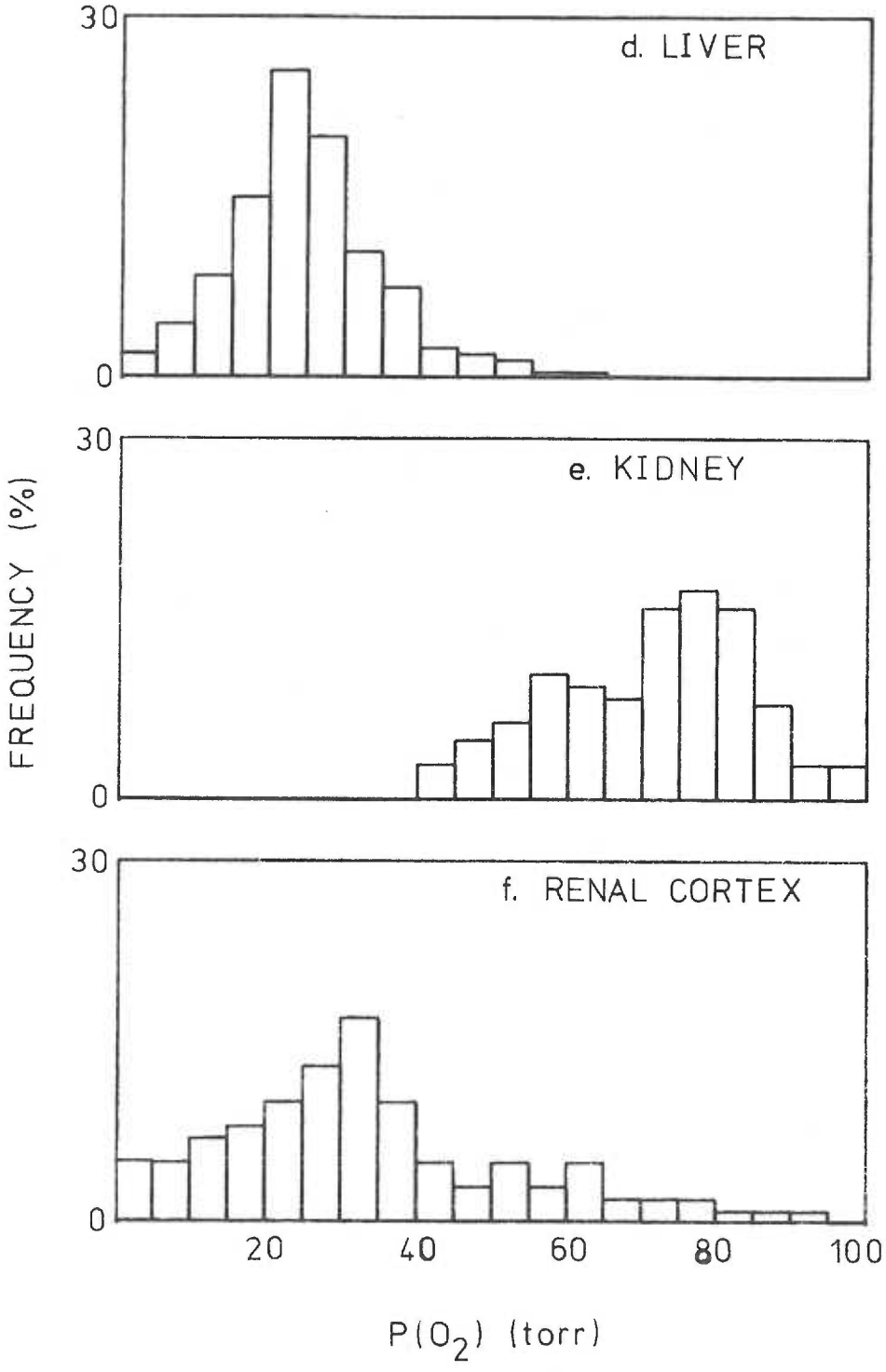
30
d. LIVER
0
30
e. KIDNEY
0
FREQUENCY (%)
30
f. RENAL CORTEX
0
20
40
60
80
100
P(O2) (torr)

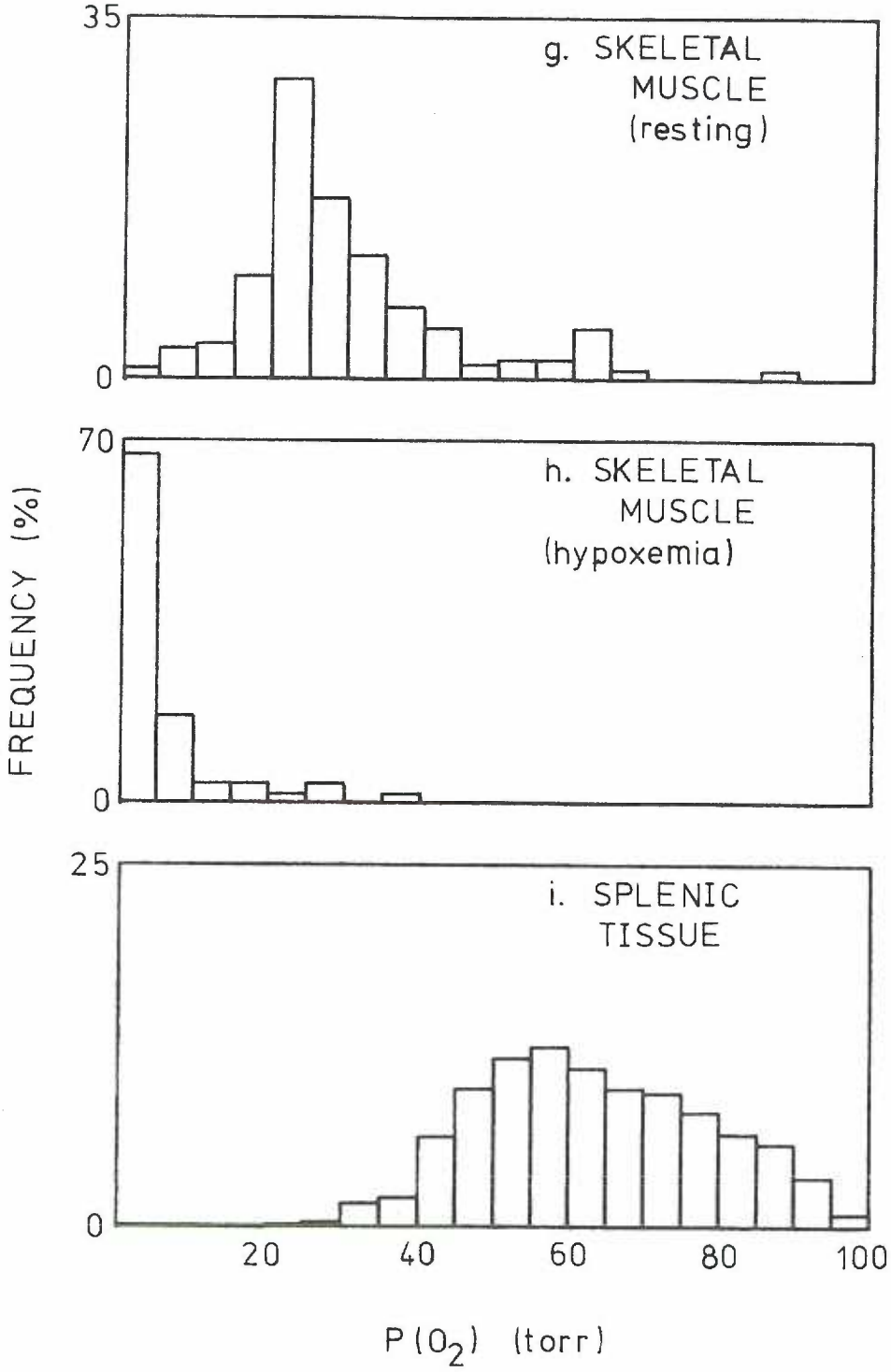
35
g. SKELETAL MUSCLE (resting)
0
70
h. SKELETAL MUSCLE (hypoxemia)
0
FREQUENCY (%)
25
i. SPLENIC TISSUE
0
20
40
60
80
100
P(O2) (torr)

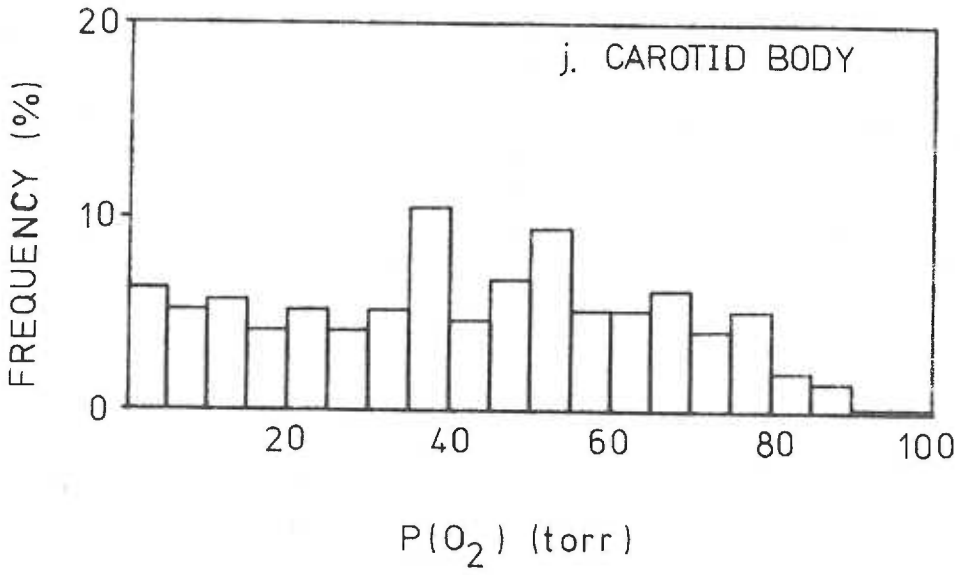
j. CAROTID BODY
FREQUENCY (%)
20
10
0
20
40
60
80
100
P(O2) (torr)

Figure I-4. Oxygen tension field in the cat brain. The oxygen tension field was measured by insertion of a platinum needle electrode perpendicularly into the brain. The solid line represents measurements taken every 50 microns. From Lubbers (1973).

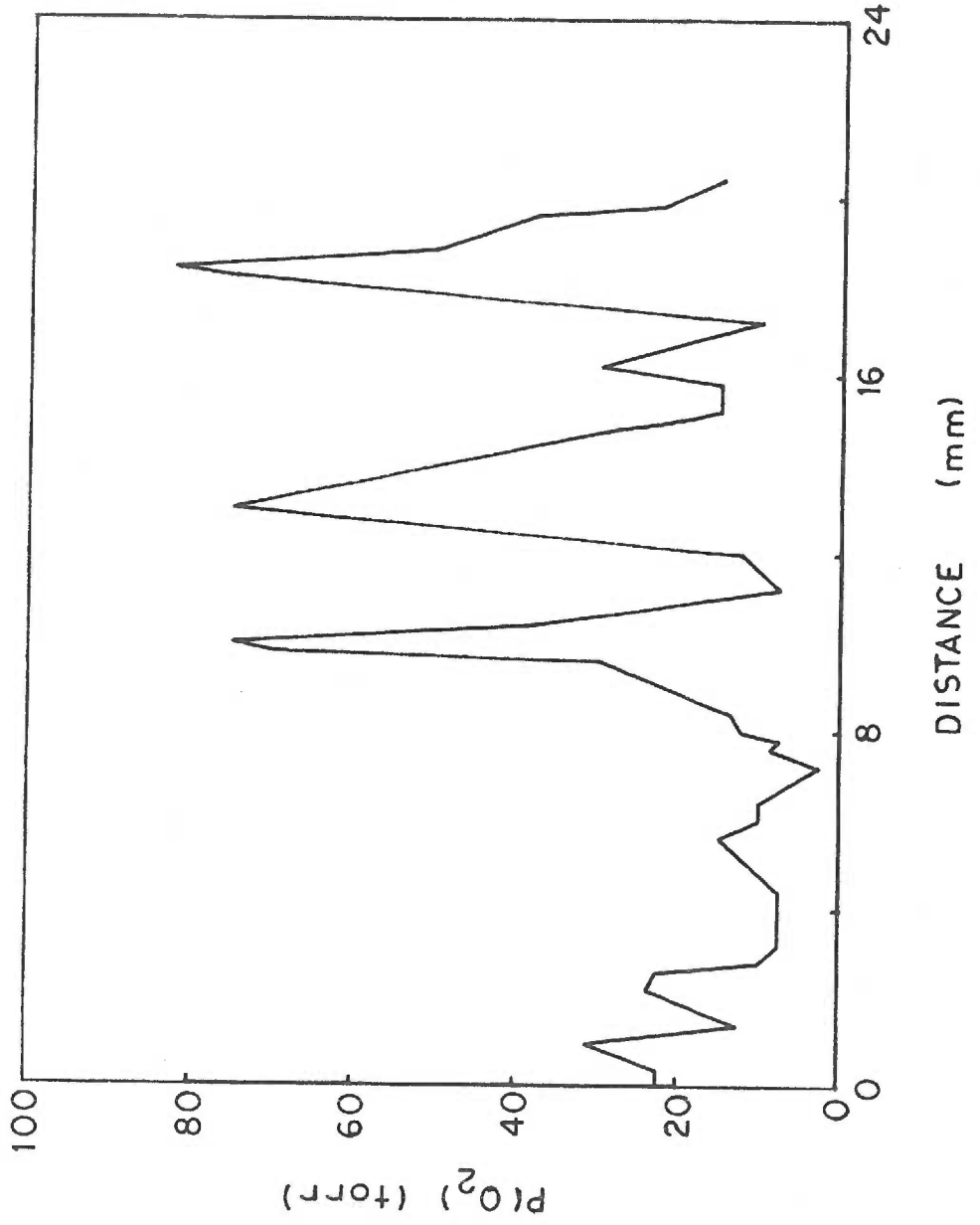
100
80
60
40
20
0
$P(O_2)$ (torr)
0
8
16
24
DISTANCE (mm)

I. B. 4. Cellular Metabolism of Oxygen

The metabolic function of oxygen is discussed in most introductory biochemistry texts (Mahler and Cordes, 1971; White, Handler and Smith, 1973). More specific discussions with regard to hypoxia have been written by Chance (1957, 1965), Cohen (1972), and Jobsis (1964, 1972, 1974). Enzymatic reactions utilizing oxygen also have been extensively reviewed (Gunzalus et al., 1975; Hayaishi, 1968, 1969, 1974; Hayaishi and Nozaki, 1969; Mason, 1957, 1965). The present discussion is limited to 1) primary events of hypoxia in mammalian metabolism, 2) enzymatic reactions secondarily dependent upon oxidase function, and 3) a theoretical treatment of the functional dependence of metabolic pathways on oxygen. Experimental studies of metabolism during hypoxia are treated in the following section.

Oxidases: The primary events of hypoxia are probably enzymatic oxygen deficiencies. Biological reactions of molecular oxygen are catalyzed by enzymes known as oxidases (Mason, 1957).[2] A list

---

[2] Hayaishi (1974) reserves the term "oxidases" for electron transfer oxidases of Mason's nomenclature (see text) and terms oxygen transferring enzymes "oxygenases." With regard to hypoxia, a general term for all oxygen dependent enzymes is needed. The definition of "oxidases" given by Mason fits this requirement and will be used in this discussion. The author feels the unfortunate discrepancy in terminology may be resolved by defining oxidases as enzymes for which oxygen is a substrate and oxygenases as a subclass of oxidases in which one or two atoms of molecular oxygen are transferred

of mammalian oxidases and the reactions they catalyze is given in Table I-F. They have been classified according to the reactions catalyzed (Mason, 1957): electron transferases catalyze the reduction of molecular oxygen to water or hydrogen peroxide, mixed function oxidases transfer one atom of oxygen to substrate and reduce the other atom to water, and oxygen transferases catalyze the transfer of a molecule of oxygen to substrate.

The mechanism by which a primary hypoxia may affect metabolism is determined by the oxidases involved. If the oxidase catalyzes only incorporation of molecular oxygen into a metabolite, the failure of its function can only result in secondary hypoxia as a consequence of substrate buildup or product deficiency. Many of the oxygen transferases, such as tryptophan pyrrolase and homogentisate oxidase, catalyze this type of reaction. If an oxidase requires both oxygen and reducing equivalents for oxygen transfer to a substrate, then reduced function can result in secondary hypoxic changes either as a consequence of substrate or product changes or as a consequence of cellular redox changes as reflected in the $NADH:NAD^+$ ratio or the $NADPH:NADP^+$ ratio. This type of reaction is catalyzed by many mixed function oxidases, such as by the cytochrome P-450

---

to substrate (see Gunzalus et al., 1975). Oxygenases may then be further divided into reactions in which only one atom is transferred to substrate and the other reduced to water (mixed function oxidases or monooxygenases) and reactions in which both atoms are transferred to substrate (oxygen transferases or dioxygenases).

Table I-F. Functions of mammalian oxidases.

Oxidase	Function
Amino acid metabolism	
Phenylalanine hydroxylase	phenylalanine degradation, tyrosine synthesis
p-Hydroxyphenylpyruvate oxidase	tyrosine degradation
Homogentistic acid oxidase	tyrosine degradation
Tyrosine 3 hydroxylase	catecholamine synthesis
Tyrosinase	melanogenesis
Tryptophan pyrrolase	tryptophan degradation, nicotinic acid synthesis
Kynurenine 3 hydroxylase	tryptophan degradation, nicotinic acid synthesis
3-Hydroxyanthranilate oxidase	tryptophan degradation, nicotinic acid synthesis
Tryptophan 5' mono-oxygenase	seratonin synthesis
Cysteine oxidase	cysteine degradation
Cysteamine oxidase	taurine synthesis
L-amino acid oxidase	L-amino acid degradation
D-amino acid oxidase	D-amino acid degradation
Protocollagen proline hydroxylase	collagen synthesis
Protocollagen lysine hydroxylase	collagen synthesis
E alkyllysinase	E alkyllysine → lysine
D aspartate oxidase	aspartate degradation
Sarcosine oxidase	sarcosine → glyoxylate
Amine oxidation	
Monoamine oxidase	catecholamine, monoamine degradation
Diamine oxidase	histamine, other diamine degradation
Spermine oxidase (plasma amine oxidase)	spermine, spermidine degradation
Dopamine-β-hydroxylase	norepinephrine and epinephrine synthesis
Carbohydrate metabolism	
L-gulonolactase oxidase	ascorbate synthesis
Meso-inositol oxidase	inositol → glucose
Nucleic acid metabolism	
Xanthine oxidase	purine catabolism
Uricase (not in man)	purine catabolism
Lipid metabolism	
Fatty acid desaturase	desaturation of fatty acids
Glyceryl ether oxidase	glyceryl ether → glyceryl ester
Fatty acid ω-oxidase	drug and fatty acid oxidation
Squalene epoxidase	cholesterol synthesis
Sterol demethylase	cholesterol synthesis
Steroid 7α-hydroxylase	bile acid synthesis
Steroid 12α-hydroxylase	bile acid synthesis
Steroid 16α-hydroxylase	bile acid synthesis

(Continued on next page)

Table I-F. (Continued)

Oxidase	Function
Cofactor metabolism	
α Heme oxidase	heme catabolism
γ Butyrobetaine hydroxylase	carnitine synthesis
β Carotene 15-15' oxygenase	retinal formation
Pyridoxamine phosphate oxidase	pyridoxamine phosphate → pyridoxal phosphate
Hormone metabolism	
Steroid 11β hydroxylase	cortisol synthesis
Steroid 17α hydroxylase	androgen synthesis
Steroid 21 hydroxylase	deoxycorticosterone synthesis
Steroid 18 hydroxylase	aldosterone synthesis
Steroid 20α hydroxylase	pregnenolone synthesis
8, 11, 14 eicosatrienoic acid oxidase	prostaglandin synthesis
Detoxification	
Sulfite oxidase	cysteine degradation
Aryl 4-hydroxylase	analine hydroxylation
Other cytochrome P-450 related oxidases	drug detoxification
Miscellaneous	
Cytochrome oxidase	terminal respiration
Glycollate oxidase	glycollate → glycoxylate
Aldehyde oxidase	aldehydes → acids
Ceruloplasmin	p-diphenol → p-quinone

system which requires an external source of reducing equivalents in addition to substrate and oxygen. If the reaction catalyzed is a transfer of electrons to oxygen, such as occurs with electron transfer oxidases, the effect on metabolism is characteristic of the specific substrates and products involved. For instance, if the electron donor is an electron carrier, reduced function may affect the redox state of the cell. If this electron transfer is coupled to oxidative phosphorylation, as with cytochrome oxidase, both the redox state and ATP synthesis can be affected. If the electron donor is a small metabolite, such as an aldehyde substrate for aldehyde oxidase, metabolic affects may occur as a consequence of substrate buildup. If the product of the electron transfer to oxygen is hydrogen peroxide, metabolism may be affected as a consequence of lack of substrate for peroxidases. Thus, primary hypoxia can secondarily affect metabolism in three ways: altered substrate and product levels, altered redox state, and altered phosphorylation state.[3] If the primary events affect substrate and product levels, the condition is

---

[3] Phosphorylation state is a non-rigorous term used in this discussion to indicate the relative availability of acid labile phosphate in tissue (i.e., phosphates which may be hydrolyzed with 1N acid for 7 min at 100°C). It is used in contexts where a general term is required in place of more specific quantitative terms which are not mathematically equivalent yet represent the same phenomenological change, i.e., decreased [ATP] ≠ decreased adenylate energy charge ≠ decreased phosphorylation state potential, but all represent a decreased availability of acid labile phosphate and are thus described adequately by decreased phosphorylation state.

termed metabolic hypoxia. If the energy charge is affected, it is bioenergetic hypoxia. An altered redox state can occur with either a metabolic hypoxia or a bioenergetic hypoxia and therefore is discussed as the redox component of either type.

I.B.4.a. Primary Oxygen Dependence. Many enzymatic systems may be affected by primary hypoxia as a result of the occurrence of oxidases in these pathways; some of these systems will now be discussed.

Primary Metabolic Oxygen Dependence: The biological functions of oxygenases have been reviewed by Hayaishi (1968, 1969, 1974) and Hayaishi and Nozaki (1969). These discussions must be used with some caution with regard to mammalian systems because many of the enzymes discussed are not present in mammals. Oxidases occur in many metabolic pathways in mammals, but vary between organisms and cell types. The consideration that many of these enzymes are important remains teleological; however, genetic defects and metabolic inhibitor studies indicate that the function of some are critical. Mental retardation in humans has been reported to be associated with enzymatic defects in sulfite oxidase (Irreverre, 1967; Mudd et al., 1967), p-hydroxyphenylpyruvate oxidase (Gentz et al., 1965), phenylalanine hydroxylase (Kauffman and Fisher, 1974), and possibly with tryptophan pyrrolase (Tada et al., 1963). A reduced kynurenine-3-hydroxylase activity was reported in a case with an unusual

scleroderma (Price et al., 1967). Xanthine oxidase deficiency was found in a woman suffering from phaeochromocytoma and heart failure (Watts et al., 1964). Deficiency of α-oxidation of phytanic acid was found in tissue cultures from patients with Refsum's disease, a disease characterized by atypical retinitis pigmentosa, peripheral polyneuropathy and cerebellar ataxia (Herndon, Skinberg and Uhlandorf, 1969). Disorders of adrenal steroid biogenesis are reviewed by Bongiovanni et al. (1967). They discuss a variety of disorders including 11β-, 17- and 21-hydroxylase deficiencies. Lack of 11β-hydroxylase activity is associated with virilization and hypertension. 17-Hydroxylase deficiency occurs with hypertension and lack of sex hormone production. 21-Hydroxylase deficiency is associated with virilization and salt loss.

Therapy with monoamine oxidase inhibitors for treatment of mental depression is associated with increases in brain norepinephrine and dopamine and can potentiate hypertensive episodes with ingestion of dietary catecholaminic agents such as tyramine (Horowitz et al., 1964; Jarvik, 1965; Thompson and Cummins, 1970). Administration of metyrapone, a cytochrome P-450 inhibitor, reduces cortisol production by inhibition of adrenal 11β-hydroxylation and may induce acute adrenal insufficiency in patients with reduced adrenal secretory capacity (Travis and Sayers, 1965). Administration of α-methyltyrosine, a tyrosine hydroxylase inhibitor, results in

behavioral depression, apparently due to a decrease of catecholamine pools (Moore and Dominic, 1971). Allopurinol treatment of gout patients inhibits xanthine oxidase activity and results in a beneficial decrease in serum uric acid concentration (Bywater and Glynn, 1970), but must be used with caution because of its toxicity.

The relatively innocuous consequences of alkaptonuria, a genetic defect of homogentisate oxidase, indicates that deficient function of this enzyme is not nearly as critical as those mentioned above (Milne, 1970). Albinism, a defect in tyrosinase, may increase susceptability to UV irradiation, but is otherwise non-debilitating. Consequently, mere presence of an oxidase in a metabolic pathway is no indication that deleterious effects will result from reduced function.

The following discussion of the role of oxidases in metabolism is done without regard to whether these roles are critical. It is intended to provide a basis for a further understanding of the biochemistry of hypoxia by identifying those reactions which are possible sites of primary hypoxia.

Biogenic Amines: Oxygen is a required substrate for reactions involved in the synthesis, interconversion, and inactivation of biogenic amines. In a review of the biochemistry of catecholamines, Molinoff and Axelrod (1971) list five oxidases involved in dopamine, norepinephrine, and epinephrine metabolism (Figure I-5). Synthesis

Figure I-5. Oxidases in calecholamine metabolism. Enzymes involved in catecholamine metabolism are

1. phenylalanine hydroxylase
2. tyrosine hydroxylase
3. L-amino acid decarboxylase
4. dopamine-β-hydroxylase
5. phenethanolamine-N-methyltransferase
6. monoamine oxidase
7. catechol-O-methyl transferase
8. alcohol dehydrogenase
9. aldehyde oxidase

Enzymes 1, 2, 4, 6 and possibly 9 are oxidases.
(From Molinoff and Axelrod, 1971, and Duncan, 1972.)

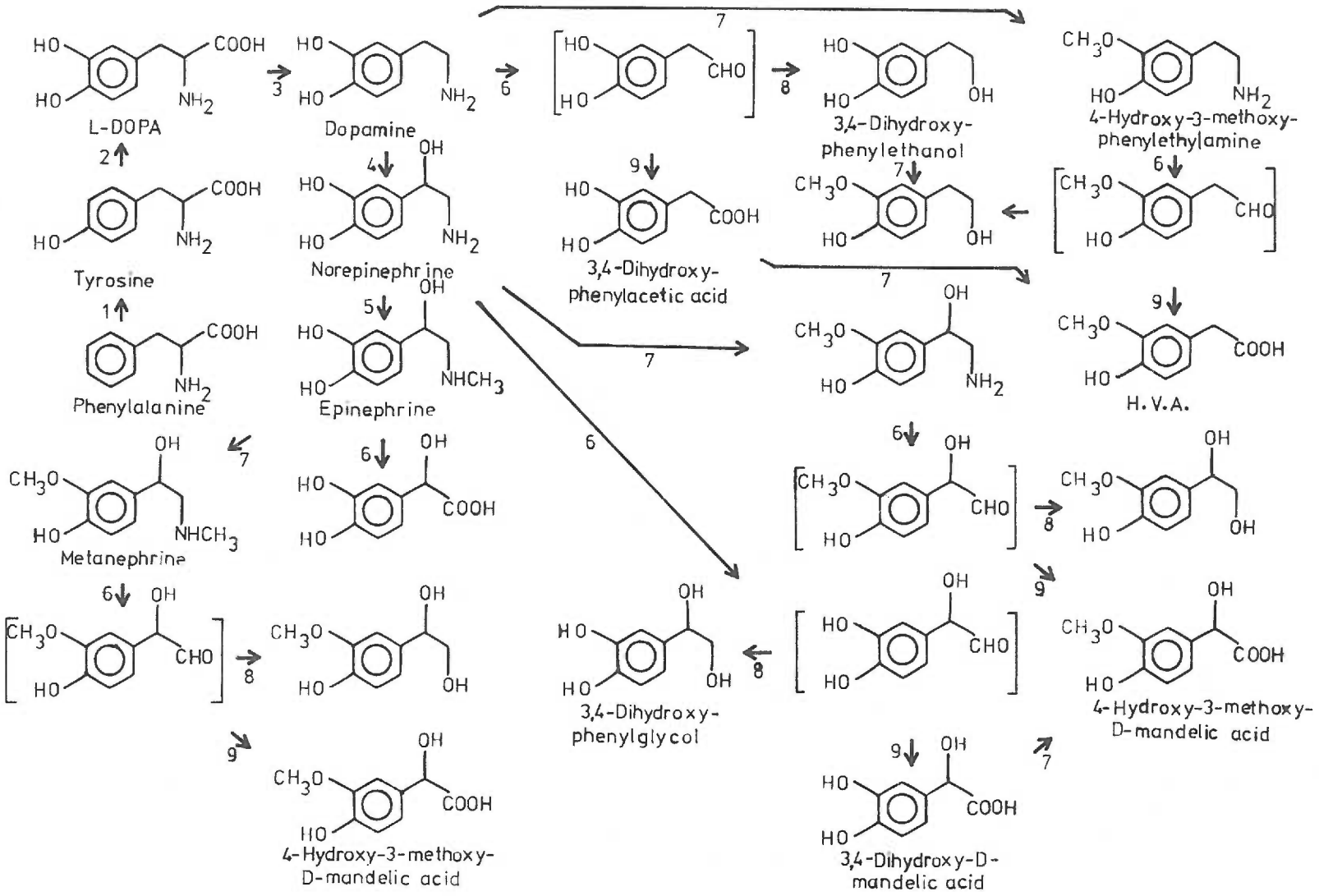
L-DOPA
Dopamine
3,4-Dihydroxy-phenylethanol
4-Hydroxy-3-methoxy-phenylethylamine
Tyrosine
Norepinephrine
3,4-Dihydroxy-phenylacetic acid
Phenylalanine
Epinephrine
H.V.A.
Metanephrine
3,4-Dihydroxy-phenylglycol
4-Hydroxy-3-methoxy-D-mandelic acid
4-Hydroxy-3-methoxy-D-mandelic acid
3,4-Dihydroxy-D-mandelic acid

of dopamine occurs primarily by o-hydroxylation of tyrosine to 3, 4-dihydroxylphenylalanine and decarboxylation to dopamine. The hydroxylation is catalyzed by a pterin-requiring oxidase, tyrosine hydroxylase (Kaufman and Fisher, 1974). Dopamine may also be formed from tyrosine by decarboxylation to tyramine and subsequent hydroxylation by an NADPH requiring microsomal oxidase system. Norepinephrine formation from dopamine is catalyzed by a copper containing oxidase, dopamine-β-hydroxylase. Epinephrine is formed from norepinephrine by methylation, and thus the synthesis of both is dependent upon oxygen. The physiological activity of catecholamines is apparently initiated by release of these agents from storage granules and terminated by uptake into presynaptic nerve endings. Chemical inactivation of the molecules occurs by two reactions, oxidation of the amine by monoamine oxidase or 0-methylation by catechol-0-methyltransferase. Either reaction may be followed by further oxidation. The aldehyde product of monoamine oxidase may be oxidized to the corresponding acid by an aldehyde oxidase. The 0-methylated amines may be oxidized by monoamine oxidase.

The biosynthesis and degradation of serotonin is remarkably similar to that of catecholamines (Sirek and Sirek, 1970). Serotonin is synthesized from tryptophan by hydroxylation to form 5-hydroxytryptophan and subsequently decarboxylated to 5-hydroxytryptamine (serotonin). The hydroxylase is a pterin-requiring

oxidase similar to tyrosine hydroxylase (Kaufman and Fisher, 1974). Serotonin is degraded primarily by two successive oxidations to 5-hydroxyindoleacetic acid. These reactions, like those for catecholamine inactivation, are catalyzed by monoamine oxidase and aldehyde oxidase.

Serotonin is also the source of melatonin (N-acetyl-5-methoxytryptamine) by N-acetylation and 0-methylation (White, Handler and Smith, 1973). Melatonin is rapidly metabolized by liver microsomes to 6-hydroxymelatonin and conjugated with either sulfate or glucuronic acid.

Steroids: The role of oxygenases in steroid metabolism has been reviewed (Hamberg et al., 1974; Hayano, 1962) and will only be summarized here. Reviews of cholesterol synthesis (Good, 1970), steroid hormone metabolism (McKerns, 1968; Solomon et al., 1967) and bile acid synthesis (Danielsson, 1973; Danielsson and Sjovall, 1975) are available.

At least two reactions in cholesterol synthesis are catalyzed by oxidase systems. Cyclization of squalene is initiated by an NADPH dependent microsomal mixed function oxidase, squalene epoxidase (Sano and Granick, 1961). C-4 demethylation is also catalyzed by a microsomal system requiring both NADPH and oxygen; C-14 demethylation is thought to be analogous (Hamberg et al., 1974).

Cholesterol is utilized for steroid hormone and bile acid synthesis. Both of these reaction networks involve numerous oxidases. Steroid hormone biosynthesis occurs in the adrenal cortex, corpus luteum, ovary, placenta and testis (Hamberg et al., 1974). These tissues contain systems capable of hydroxylating at the 11β, 17α, 18, 19 and 21 positions. A 20α, 22-R dihydroxylating system is also present. In addition, mixed function oxidases catalyze oxygen dependent side chain cleavage in the C-17 and C-20 lyase and C-20 and C-22 lyase reactions. A microsomal mixed function oxidase, placental aromatase, is involved in the aromatization of androstenedione (Thompson and Siiteri, 1974). The liver contains oxidases for metabolism and elimination of steroids from the body. Different steroids can by hydroxylated at different positions. The reactions include hydroxylations at the 1β, 2α, 2β, 6α, 6β, 7α, 7β, 15α, 15β, 16α and 18 positions.

Bile acids are synthesized in the mammalian liver by a series of reactions involving hydroxylations at the 6β, 7α, 12α, 24α and 26 positions (Hamberg et al., 1974). These reactions are carbon monoxide inhibited and therefore thought to be cytochrome P-450 dependent. Bjorkheim and Gustafsson (1974) showed ^{18}O incorporation during ω-hydroxylation of the cholesterol side chain by rat liver mitochondria.

Prostaglandins: The rapid progress in prostaglandin research has been reviewed frequently (Bergstrom, Carlson and Weeks, 1968;

Hinman, 1972; Pickles, 1969; Ramwell and Shaw, 1970; Samuelsson et al., 1975). Oxygen is required in synthesis and possibly in degradation of these potent humoral agents. The first and rate limiting reaction in the synthesis of prostaglandins from the essential fatty acids appears to be an incorporation of both atoms of molecular oxygen into the substrate (Samuelsson, 1969). The reaction involves formation of an 11-peroxy-compound and transformation into an endoperoxide with formation of a 5-carbon ring. A second molecule of oxygen is required for hydroxylation at the C-15 position.

Prostaglandin degradation occurs primarily in the liver by β-oxidation and ω-hydroxylation (Hamberg, Israelsson and Samuelsson, 1971). The β-oxidation occurs in the mitochondria (Hamberg, 1968) and may be similar to β-oxidation of fatty acids which do not require oxygen. The ω-hydroxylation occurs in the microsomal fraction (Israelsson et al., 1969) and is likely to be similar to the oxygen dependent ω-hydroxylation of fatty acids (Robbins, 1968).

Amino Acids and Protein: The numerous oxygenases involved in the metabolism of tryptophan have been reviewed by Hayaishi (1974). The use of tryptophan as a precursor for serotonin and melatonin has been discussed. Tryptophan is also a precursor for nicotinic acid through a series of reactions involving three oxidases. The first reaction is catalyzed by tryptophan pyrrolase, a dioxygenase which cleaves the pyrrole ring with insertion of two atoms of molecular

2-oxoglutarate coupled dioxygenases such as prolyl hydroxylase and lysyl hydroxylase (Abbott and Udenfriend, 1974). Homogentisate oxidase requires ferrous ion and a reducing agent for maximal in vitro activity (Nozaki, 1974). Maleylacetoacetic acid is subsequently metabolized to tricarboxylic acid cycle intermediates.

Cysteine metabolism occurs primarily by two pathways containing oxidases (Yamaguchi et al., 1973). An NADPH and oxygen dependent enzyme, cysteine oxidase, catalyzes the formation of cysteinesulfinic acid which is rapidly desulfinated or decarboxylated. Desulfination produces sulfite which is oxidized to sulfate by sulphite oxidase. Decarboxylation produces hypotaurine which is utilized for taurine and subsequently taurocholic acid synthesis. Hypotaurine can also arise from cysteine by initial decarboxylation followed by oxidation of cysteamine by cysteamine oxidase.

Two 2-oxoglutarate coupled dioxygenases are involved in the synthesis of collagen (Abbott and Udenfriend, 1974). These enzymes, prolyl hydroxylase and lysyl hydroxylase, act only upon amino acid residues which are found in polypeptide chains. The two activities have been separated and further characterized. Both require ferrous ion, reducing agent, 2-oxoglutarate, polypeptide substrate and oxygen. One atom of oxygen is incorporated into substrate and the other into 2-oxoglutarate.

Degradation of D-amino acids occurs in the liver and kidney catalyzed by D-amino acid oxidases. These enzymes have low specificity with regard to D-amino acids and a relatively high enzymatic activity. L-amino acid oxidases also occur in these tissues but have a lower relative activity. Both L- and D-amino acid oxidases are flavoproteins which catalyze a deamination with oxidation and produce the corresponding 2-oxoacids and hydrogen peroxide.

Carbohydrates: Most of the central pathways of monosaccharides do not directly require oxygen. There are no oxidases in the glycolytic, gluconeogenic, or pentosephosphate pathways. The glucuronate-gulonate pathways (Mahler and Cordes, 1971; Figure I-6) contain two oxidases, myoinositol oxidase and L-gulonolactone oxidase. Myoinositol oxidase catalyzes the non-aromatic ring cleavage of myoinositol to D-glucuronate. L-gulonolactone oxidase catalyzes the oxidation of L-gulonolactone to the 2-oxo derivative in the synthesis of ascorbate. This enzyme is not present in man, rendering him incapable of ascorbate synthesis. Ascorbate oxidation is catalyzed by a serum protein, ceruloplasmin (Osaka, Walter and Frieden, 1963), but the physiological meaning of this reaction, if any, is not known.

Fatty Acids: Oxidase catalyzed reactions of lipids and lipid derived substances have been reviewed (Hamberg et al., 1964;

Figure I-6. Glucuronate-gulonate pathways. Myoinositol oxidase catalyzes the oxidation of myoinositol to glucuronate, and l-gulonolactone oxidase catalyzes the oxidation of l-gulonolactone to 2-keto-l-gulonolactone in the synthesis of ascorbic acid. l-Gulonolactone oxidase does not occur in man. (From Mahler and Cordes, 1971.)

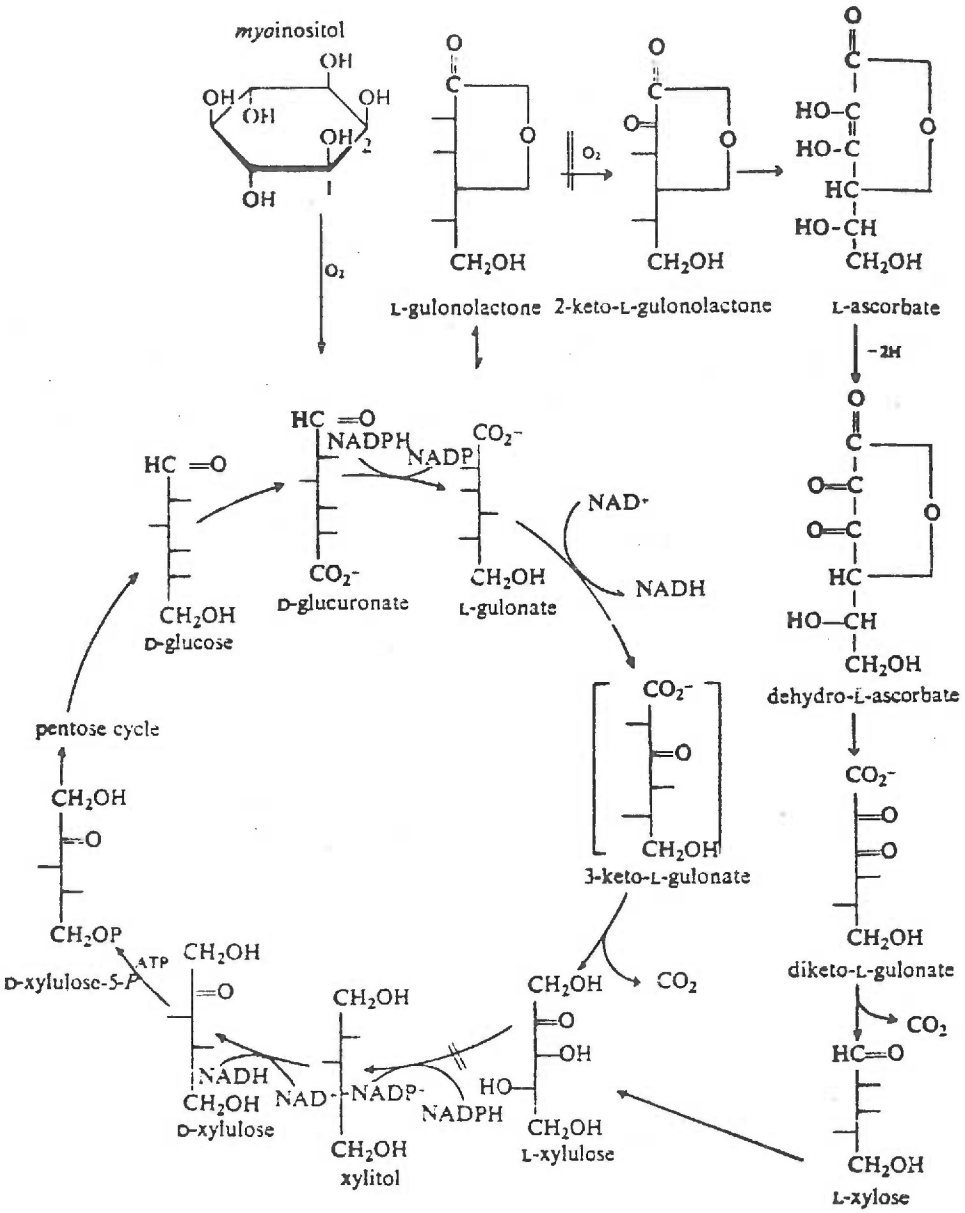
myoinositol
L-gulonolactone
2-keto-L-gulonolactone
L-ascorbate
dehydro-L-ascorbate
diketo-L-gulonate
L-xylose
D-glucose
D-glucuronate
L-gulonate
3-keto-L-gulonate
L-xylulose
xylitol
D-xylulose
D-xylulose-5-P
pentose cycle
NADPH
NADP
NAD
NADH
ATP
CO2

Hayano, 1962); cholesterol synthesis, bile metabolism, steroid metabolism, and prostaglandin metabolism, have already been discussed. Saturated fatty acid metabolism is similar to the central reactions of carbohydrate metabolism in that no oxidases are directly involved. However, important oxidase catalyzed α-oxidations, ω-oxidations and desaturations, are known. A rat liver mitochondrial NADPH dependent mixed function oxidase catalyzes the α-oxidation of phytanic acid (Tsai, Avigan and Steinberg, 1969). A different α-oxidase is found in the microsomal fraction from brain. ω-Oxidation of medium chain fatty acids was shown by Robbins (1968), and later found for other lipid substances (Hamberg et al., 1974). This reaction requires NADPH and oxygen and occurs in the microsomal fraction. Desaturation of stearyl CoA is a mixed function oxidation thought to be important in the synthesis of unsaturated fatty acids in mammals.

Nucleotides and Nucleic Acids: In mammals, two oxidases occur in the degradative pathway of purines. One of these, uric acid oxidase, is not found in man. The other, xanthine oxidase, is a flavoprotein which catalyzes two successive reactions: hypoxanthine to xanthine and xanthine to uric acid. Both reactions require oxygen and produce hydrogen peroxide and superoxide.

Cofactors and Prosthetic Groups: The requirement of oxygen for NAD and ascorbate synthesis has already been mentioned. Oxygen

is also a substrate for reactions involved in heme metabolism, carnitine formation, and vitamins A and D metabolism. An enzyme thought to be involved in heme synthesis was partially purified by Sano and Granick from beef liver mitochondria (Sano, 1966; Sano and Granick, 1961). The enzyme, coproporphyrinogen oxidase, has a marked specificity for coproporphyrinogen III and requires oxygen. the initial reaction in heme degradation is catalyzed by an hepatic microsomal mixed function oxidase, heme oxygenase (Tenhunen et al., 1969). The reaction is thought to be rate limiting in heme catabolism. The ferriprotoporphyrin ring is cleaved at the α-methylene bridge and the α-bridge carbon is oxidized to carbon monoxide. The product, bilirubin, is nearly stoichiometrically recovered from parenterally administered hemoglobin, indicating that this is the primary pathway of degradation.

Carnitine is an important component of fatty acid metabolism as a consequence of its role in fatty acid transport across the mitochondrial membrane. Carnitine is synthesized in vivo from γ-butyrobetaine by an oxygen dependent hydroxylation (Abbott and Udenfriend, 1974; Lindstadt et al., 1967). The enzyme requires ferrous ion, a reducing agent and 2-oxoglutarate.

Dietary β-carotene is an important source of vitamin A through an oxygen dependent cleavage to retinal (Goodman et al., 1967). The enzyme is found in the intestines and liver. A dioxygenase mechanism

has been proposed in which molecular oxygen reacts with the two central carbon atoms of β-carotene and results in the cleavage of this bond to produce two molecules of retinal.

1, 25-Dihydroxycholecalciferol has recently been found to be a highly active form of vitamin D. It is formed in the renal cell mitochondria by a mixed function oxidase, 25-hydroxycholecalciferol-1-hydroxylase (Ghazarian, Schones and DeLuca, 1973). It is NADPH dependent and inhibited by carbon monoxide. The sensitivity of this inhibition to monochromatic light of varying wavelengths was studied by Henry and Norman (1974). Maximal sensitivity was observed at 450 nm, from which they concluded that cytochrome P-450 was involved. This interpretation was corroborated by inhibitor and kinetic studies (Ghazarian et al., 1974).

Drugs: The role of cytochrome P-450 catalyzed mixed function oxidations in hydroxylation of drugs and other compounds foreign in mammals has been reviewed (see Section V). These reactions occur in the endoplasmic reticulum and require NADPH. Introduction of hydroxyl groups increases the polarity of these compounds and facilitates renal elimination.

Primary Bioenergetic Oxygen Dependence: Cytochrome oxidase (Lemberg, 1969; Nicholls and Chance, 1974; Pullman and Schatz, 1967) is an unique oxidase because its function is necessary for electron flow in the mitochondrial electron transport pathway, to

which is coupled the chemical energy conserving process known as oxidative phosphorylation (for reviews see Lardy and Ferguson, 1969; Lehninger, 1971; Pinchot, 1965). Cytochrome oxidase is the primary means by which reducing equivalents are removed from cells, and oxidative phosphorylation is the primary source of ATP. Continual synthesis of ATP from ADP and inorganic phosphate is essential to maintain a normal phosphorylation state within cells. Phosphorylation state is expressed quantitatively by the phosphorylation state potential ([ATP] /[ADP][Pi]) or by Atkinson (1968) as the adenylate energy charge (energy charge = [ATP] + 1/2[ADP] /[ATP] +[ADP] + [AMP]). The primary consequence of diminished cytochrome oxidase functions are increase in reduced: oxidized forms of electron carriers (Chance et al., 1962) and a decrease in energy charge and phosphorylation state potential. Decreased cytochrome oxidase function therefore results in a bioenergetic hypoxia.

I. B. 4. b. Secondary Oxygen Dependencies. As discussed above, primary hypoxia may result in alterations in substrate and product levels, redox state, and energy charge. These changes may in turn cause secondary hypoxic changes. Without regard to whether these changes are metabolic or bioenergetic, or deleterious or compensatory, some types of changes can be identified:

1. Substrate deficiencies for other enzymatic reactions and metabolic functions. Failure of ATP dependent functions such as

muscle contraction during prolonged anoxia are well known. Decreased serotonin levels have been proposed to play a role in the functional affects of mild oxygen deprivation in the brain (Davis et al., 1973).

2. Intermediate accumulations resulting in metabolic interference with other processes. Inability to inactivate dopamine by oxygen dependent processes within ischemic areas has been proposed to potentiate the physiological effects of dopamine (Zervas et al., 1974). NADH accumulation perturbs the pyruvate: lactate relationship resulting in increased lactate and a concomitant acidosis (Huckabee, 1958).

3. Allosteric activation or inactivation. Increased ADP and decreased ATP are stimulatory on the phosphofructokinase reaction since ADP is an activator and ATP is an inhibitor of this reaction.

Predicting secondary affects of hypoxia is more difficult than predicting sites of primary hypoxia. Knowledge of allosteric effectors and physiological competitive inhibitors is incomplete. Substrate and product changes during metabolic hypoxia are largely unknown. In spite of this, many possible sites of secondary affects of hypoxia may be predicted as a consequence of their dependence on redox potential, energy charge, or hydrogen peroxide.

Most redox dependent enzymes utilize NADH or NADPH as electron donors or NAD^+ or $NADP^+$ as electron acceptors. Other

cofactors are utilized, such as lipoate and pteridine. These systems appear to be coupled to either the $NADH:NAD^+$ or $NADPH:NADP^+$ pair by specific oxido-reductases and therefore are probably dependent upon these ratios. The transfer of electrons between the $NADH:NAD^+$ pair and the $NADPH:NADP^+$ pair is an isoenergetic reaction catalyzed by an extra-mitochondrial transhydrogenase. The mitochondrial membrane offers a barrier to NADH diffusion. Systems for transfer of reducing equivalents across the mitochondrial membrane have been postulated (Grunnet, 1974; Parilla et al., 1974; Scholz, Hansen and Scholz, 1973; Simpson and Estabrook, 1968; Thurman and Scholz, 1969, 1973; Williamson et al., 1969, 1972), but the rate of transfer may be less than consumption or production and therefore steady state ratios may not be achieved (van Dam and Meyer, 1971). Intraorganelle redox states are doubtlessly important in control of intraorganelle metabolism, yet methodology permits direct measurement of only certain total cellular components (Chance et al., 1962, 1965). Ratios of reduced to oxidized forms have been estimated from equilibrium constants for dehydrogenase catalyzed reactions and measurements of oxidized and reduced cosubstrates for the reactions (Williamson, Lund and Krebs, 1967). Analysis of reactants of systems localized primarily in the mitochondria and primarily in the cytoplasm show a striking disparity in ratios. Consequently, redox changes in one part of the cell may be much more

dramatic than in other parts. However, because of the carrier systems, an altered redox state in one part of the cell is likely to affect the state in other parts of the cell. Unraveling electron transfer is under active study and is of great importance in the biochemistry of hypoxia.

Lists of reactions which require pyridine nucleotides are available (Barwin, 1969; Enzyme nomenclature, 1965, 1972; Mahler and Cordes, 1971). Some of these reactions require oxygen for mixed function oxidations and thus appear in Table I-F. The function of these enzymes either may be dependent on redox potential or alter the redox state as a consequence of their function (Moldeus et al., 1974).

Energy requiring processes in cellular metabolism are also numerous, diverse, and essential for normal function. ATP plays a central role in this metabolism, both directly as a substrate and indirectly through coupling with other high energy compounds. Lists of reactions which require high energy intermediates are available (Atkinson and Martin, 1960; Mahler and Cordes, 1971).

Many reactions are dependent upon either ATP concentration or phosphoryl potential ($[ADP][P_i] / [ATP]$), and some appear to be dependent upon ATP, ADP, and AMP, and are related quantitatively by the energy charge (Atkinson, 1968). ATP, ADP and AMP all act as allosteric effectors; consequently reactions of enzymes which

require none of these as substrates may be affected by alterations in energy charge.

Peroxidases are enzymes which require hydrogen peroxide as substrate (Paul, 1963). Hydrogen peroxide is thought to arise in vivo from a two electron reduction of oxygen catalyzed by electron transfer oxidases (Wolff, 1970) or dismutation of superoxide to peroxide and oxygen by superoxide dismutase (Klebanoff, 1974). Peroxidases have a limited distribution in mammals (White, Handler and Smith, 1973), yet are thought to be involved in important metabolic processes. For example, myeloperoxidase is associated with an antimicrobial system in polymorphonuclear leukocytes (Klebanoff, 1974) and thyroid peroxidase is involved in the iodination of tyrosyl residues of thyroglobulin in the synthesis of triiodothyronine and thyroxin (Taurog, 1970).

Tricarboxylic Acid Cycle[4]: Four dehydrogenases are involved in the tricarboxylic acid cycle (Table I-G). Succinate dehydrogenase

---

[4]This thesis is not intended to provide a comprehensive discussion of intermediary metabolism, but only to point out some of those reactions which may be secondarily affected by hypoxia and to emphasize the breadth and complexity of this dependence. In the following discussion of reactions dependent upon redox state or high-energy phosphate intermediates no references are given because these reactions are discribed in secondary textbook sources (Larner, 1971; Lehninger, 1975; Mahler and Cordes, 1971; Stryer, 1974; White, Handler and Smith, 1973). Some of the pioneering discoveries are cited in Section I-A; further information may be obtained from contemporary reviews: TCA cycle (Lowenstein, 1967; van Dam and Meyer, 1971); Amino acids (Felig, 1975; Truffa-Bachi and

requires FAD and the others require NAD^+. Isocitrate and 2-oxoglutarate dehydrogenase-catalyzed reactions are essentially irreversible due to subsequent decarboxylations. The introduction of substrate from the glycolytic pathway is by the oxidative decarboxylation of pyruvate and conjugation with coenzyme A to acetyl CoA in a complicated series of steps requiring NAD^+. A second means of pyruvate entry into the TCA cycle is by the reductive carboxylation of pyruvate to malate requiring NADH. Pyruvate may also be carboxylated to oxaloacetate in a two-step reaction requiring ATP and acetyl CoA.

Adenylates are not required for other reactions in the TCA cycle. However, citrate synthetase, isocitrate dehydrogenase and pyruvate dehydrogenase are all controlled by energy charge.

Carbohydrate Metabolism: Adenylates and pyridine nucleotides are either substrates or allosteric modulators for several reactions involving carbohydrates (Table I-G). In glycolysis, ATP is a substrate for the important control enzyme phosphofructokinase. The activity of this enzyme is modulated by energy charge and citrate concentration. ADP is a substrate for both phosphoglycerate kinase

---

Cohen, 1973); Lipids (Fulco, 1974; Gatt and Barenhol, 1973; McMurray and McGee, 1972; Stoffel, 1971; Van den Bosch, 1973; Volpe and Vagelos, 1973); Hormones, cofactors, etc., (Danielsson and Sjovall, 1975; Hinman, 1972; Samuelsson et al., 1975; Wasserman and Corradino, 1971; Wasserman and Taylor, 1972); Nucleotides (Tso, 1970).

Table I-G. Selected redox and phosphorylation state-dependent reactions of intermediary metabolism.

Pathway	Enzyme	Redox (R) or phosphorylation state (P) dependence
Tricarboxylic acid cycle		
	Isocitrate dehydrogenase	R
	2-Oxoglutarate dehydrogenase	R
	Succinate dehydrogenase	R
	Malate dehydrogenase	R
	Pyruvate carboxylase	P
	Malic enzyme	R
	Citrate synthetase	P
	Isocitrate dehydrogenase	P
	Pyruvate dehydrogenase	P
Carbohydrate metabolism		
	Phosphofructokinase	P
	Phosphoglycerate kinase	P
	Pyruvate kinase	P
	Glyceraldehyde-3-phosphate dehydrogenase	R
	Lactate dehydrogenase	R
	Phosphoenolpyruvate carboxykinase	P
	Glucose-6-phosphate dehydrogenase	R
	6-Phosphogluconate dehydrogenase	R
Lipid Metabolism		
	Thiokinase	P
	Fatty acyl-S-CoA dehydrogenase	R
	β-Hydroxyacyldehydrogenase	R
	Acetyl-S-CoA-carboxylase	P
	β-Hydroxyacyldehydrogenase	R
	Enoyl reductase	R
Amino acid, protein metabolism		
	Glutamate dehydrogenase	R
	Cysteine reductase	R
	Isovaleryl CoA dehydrogenase	R
	Piperidine-2-carboxylic acid reductase	R
	Isobutyryl CoA dehydrogenase	R
	β-Hydroxyisobutyric acid dehydrogenase	R
	Carbamyl phosphate synthesis	P
	Phosphoribosyl pyrophosphate-ATP-pyrophosphorylase	P
	Glutamine synthetase	P

and pyruvate kinase. NAD^+ is electron acceptor for the glyceraldehyde-3-phosphate dehydrogenase reaction; this reaction is stoichiometrically balanced during anaerobic metabolism by the NADH dependent reduction of pyruvate catalyzed by lactate dehydrogenase.

In gluconeogenesis, the pyridine nucleotide dependent reactions are simply reversed. The pyruvate kinase reaction is replaced by an ATP dependent carboxylation of pyruvate to oxaloacetate which is subsequently decarboxylated and phosphorylated in a GTP dependent reaction, to phosphoenol pyruvate.

A second pathway of carbohydrate catabolism and interconversion is the pentose shunt pathway. This pathway is an important source of cytoplasmic reducing equivalents through two $NADP^+$ dependent reactions. Glucose 6-phosphate dehydrogenase catalyzes an energetically favorable electron transfer reaction allowing substrate entry into the pathway. An essentially irreversible oxidative decarboxylation with concomitant $NADP^+$ reduction is catalyzed by 6-phosphogluconate dehydrogenase.

Other bioenergetic dependent reactions occur throughout carbohydrate metabolism but will not be discussed here. These include reactions in the biosynthesis of oligo- and polysaccharides such as hyaluronic acid, chondroitin sulfate, and heparin, and monosaccharide conversions such as ascorbic acid synthesis.

Lipid Metabolism: As with carbohydrate metabolism, lipid metabolism is highly dependent upon pyridine nucleotide reduction states and upon adenylate concentrations (Table I-G). Fatty acids provide acetyl CoA for mitochondrial ATP production through the β - oxidation pathway. ATP is required for the cytoplasmic thio-kinase catalyzed conversion of fatty acid to coenzyme A derivatives. These are subsequently oxidized and cleaved in the mitochondrion by a repetitive reaction sequence to the two-carbon acetyl CoA units. Two dehydrogenase reactions are involved, FAD dependent fatty acyl-S-CoA dehydrogenase and NAD^+dependent β-hydroxyacyl dehydrogenase.

Fatty acid synthesis occurs from acetyl Coenzyme A by a separate system in the cytoplasm. ATP is required for citrate and biotin dependent carboxylation of acetyl-S-CoA to malonyl-S-CoA. After transfer to an acyl carrier protein, the malonyl unit condenses with the acyl carrier protein derivative of either acetyl CoA or the growing fatty acid and simultaneously decarboxylates. Reduction occurs in two NADPH dependent reactions for each two-carbon addition.

Synthesis of triglycerides, phospholipids, and sphingolipids requires oxidation-reduction reactions and high energy intermediates. Desaturation of fatty acids requires NADPH and molecular oxygen. Numerous steps in cholesterol synthesis require NAD^+, NADPH, or

ATP. These reactions will not be discussed; however, it should be clear that lipid metabolism is highly dependent upon the redox state and high energy intermediates in the cell.

Amino Acids, Proteins: The biosynthesis of nonessential amino acids consists of largely energy independent reaction pathways interconnected with carbohydrate metabolism (Table I-G). Some of the pathways have NADH dependent steps and most are indirectly dependent on NADH through transamination with glutamate. Glutamate is formed from 2-oxoglutarate and ammonia by an NADH dependent reaction catalyzed by glutamate dehydrogenase. Histidine and arginine both require ATP for synthesis; arginine synthesis is part of the urea cycle, illustrating that urea synthesis is also an energy requiring process. Glutamine is an important storage molecule for ammonium; it is synthesized from glutamate by glutamine synthetase in an ATP requiring reaction.

Degradation of non-essential amino acids occurs primarily by the reversal of the synthetic pathways, resulting in formation of carbohydrate intermediates. Degradation of essential amino acids occurs by fairly specific nonreversible reaction pathways resulting in lipid intermediates. The role of 2-oxoglutarate for transamination in a variety of amino acid degradation pathways must be emphasized. Thus, the NADH-NAD^+ dependent interconversion of 2-oxoglutarate and glutamate is an important control of amino acid degradation.

Other deamination reactions are possible, especially the oxygen dependent amino acid oxidase and the amine oxidases which act on the decarboxylation products of amino acids.

Protein synthesis requires high energy intermediates for several reactions but apparently has no direct dependence upon the redox state of the cell.

Nucleotides and Nucleic Acids: Both purine and pyrimidine nucleotides are synthesized by highly energy consuming reaction pathways. NAD^+ is required by dihydroorotate dehydrogenation in pyrimidine synthesis and for inosinate dehydrogenation in guanylic acid synthesis. NADPH is required for the conversion of the ribotyl derivatives to the deoxyribotyl derivatives. NADPH is also required for the dihydropyrimidine dehydrogenation in cytosine and thymine degradation.

Nucleic acid synthesis is dependent upon the energy state of the cell as a consequence of the direct utilization of nucleotides in this synthesis.

Hormones, Cofactors, etc.: The important role of pyridine nucleotides in cholesterol synthesis has already been mentioned. NADPH, NAD^+ and $NADP^+$ are also cofactors for numerous reactions in androgen and estrogen metabolism and in corticosteroid metabolism. Bile acid synthesis and conjugation with glycine or taurine requires both NADPH and ATP. Synthesis of prostaglandins requires NADPH

for microsomal hydroxylations. NAD^+ and Coenzyme A both require ATP for synthesis. Heme degradation depends on NADPH.

The complete extent to which metabolism depends on the redox state and/or chemical energy availability in cells is not currently understood, and indeed, is one of the major questions in the study of hypoxia. The importance of the function of cytochrome oxidase is obvious from the many metabolic processes which are secondarily dependent upon it. The study of cytochrome oxidase function during hypoxia does not provide a complete understanding of hypoxia, however, since many other primary changes may occur. For a complete understanding of the function of a pathway during hypoxia, the primary and secondary hypoxic events must be understood.

I. B. 4. c. Functional Dependence of Metabolic Pathways upon Oxygen. A metabolic pathway may have a primary dependence upon oxygen as a consequence of the presence of an oxidase in the pathway. It may have a secondary dependence as a consequence of substrate or cofactor deficiency, competitive inhibition, non-specific inhibition or allosteric regulation. In addition, modified synthesis or degradation rates of enzymes may secondarily affect pathways. Given this varied list of possible affects, it is not possible to predict the function of a pathway during hypoxia. However, if the discussion is limited to primary metabolic hypoxia and the redox and phosphorylation state components of bioenergetic hypoxia, it is possible to consider in a

general sense the types of changes to be expected in a pathway during hypoxia.

Rates of oxidase-catalyzed reactions are functions of oxygen concentration. A convenient means for comparing oxygen dependencies of oxidases is the Michaelis constant with respect to oxygen ($Km(O_2)$) when other substrate concentrations are saturating. A list of $Km(O_2)$ values for isolated oxidases is given in Table I-H. These values vary over a wide range of oxygen tension and indicate that some oxidases may function in vivo at an oxygen-limited velocity. As oxygen decreases, the activities of those oxidases with high $Km(O_2)$'s are likely to be affected first. Cytochrome oxidase has a low $Km(O_2)$ relative to other oxidases and therefore is likely to be one of the last affected during hypoxia. Tryptophan hydroxylation decreases before redox state or adenylate energy charge as oxygen tension is lowered in rat brain (Davis et al., 1973). The change in redox state precedes the change in adenylate energy charge (Ballard, 1971; Davis et al., 1973). Thus, at varying degrees of hypoxia, systems will be differentially affected as a consequence of the $Km(O_2)$ values of oxidases in those pathways, and their dependency upon redox state or phosphorylation state. To illustrate this, an hypothetical pathway containing an oxidase with $Km(O_2)$ of 20 torr, a mixed function oxidase with $Km(O_2)$ of 5 torr, an NAD^+ coupled reductase and an ATP dependent

Table I-H. $Km(O_2)$ for mammalian oxidases.

Enzyme	Km (M)	$P(O_2)$ (torr)	Reference
Oxidative degradation of amino acids			
Tryptophan pyrrolase (rat liver)	1.6×10^{-4}	122	Tanaka and Knox, 1959
Kynurenine 3-hydroxylase (rat liver)	1.8×10^{-5}	10	Schmeling et al., 1969
3-Hydroxyanthranilate oxygenase (bovine kidney)	3.1×10^{-4}	230	Ogasawasa et al., 1966
3-Hydroxyanthranilate oxygenase (rat liver, ox liver)	1.2×10^{-4}	91	Iaccarino et al., 1961
Phenylalanine hydroxylase (rat liver)	3.6×10^{-6}	2.7	Fisher and Kaufman, 1972
Phenylalanine hydroxylase (rat liver)	3.1×10^{-4}	236	Bublitz, 1969
p-Hydroxyphenylpyruvate oxidase (rat liver)	1.0×10^{-4}	76	Fellman et al., 1972
Homogentisic acid oxidase (beef liver)	1.0×10^{-3}	760	Flamm and Crandall, 1963
Tyrosine hydroxylase (bovine adrenal medulla)	7.4×10^{-5}	56	Ikeda et al., 1966
Tyrosine hydroxylase (bovine adrenal medulla)	1.0×10^{-5}	7.6	Fisher and Kaufman, 1972
	1.5×10^{-4}	114	Poillon, 1974
D-amino acid oxidase (hog kidney)	1.8×10^{-4}	145	Dixon and Kleppe, 1965
D-amino acid oxidase (pig kidney)	1.3×10^{-4}	99	Massey et al., 1964

(Continued on next page)

Table I-H. (Continued)

Enzyme	Km (M)	$P(O_2)$ (torr)	Reference
D-amino acid oxidase (pig kidney)	2.0×10^{-4}	122	Tanaka and Knox, 1959
Oxidative degradation of amines			
Monoamine oxidase (pig brain mitochondria)	2.34×10^{-4}	152	Miyake et al., 1960
Amine oxidase (beef plasma)	3.3×10^{-5}	25	Ichiyama and Nakamisa, 1970
Spermine oxidase (beef plasma)	6.7×10^{-5}	5.1	"
Oxidation degradation of carbohydrates			
L-gulonolactone oxidase (rat liver)	2.0×10^{-4}	152	Ishewood et al., 1960
Oxidation degradation of nucleic acid metabolism			
Xanthine oxidase (bovine milk)	2.4×10^{-4}	180	Ackerman and Brill, 1962
Xanthine oxidase (bovine milk)	2.4×10^{-5}	18	Fridovich and Handler, 1962
Xanthine oxidase (bovine milk)	8.2×10^{-5}	62	Fridovich, 1964
Others			
Ceruloplasmin (human serum)	10×10^{-6}	7.6	Osaki et al., 1966
NADPH oxidase (rat liver microsomes)	1.5×10^{-4}	114	Staudinger and Zubzycki, 1963

(Continued on next page)

Table I-H. (Continued)

Enzyme	Km (M)	$P(O_2)$ (torr)	Reference
Aldehyde oxidase (rabbit liver)	2.3×10^{-5}	17.5	Handler et al., 1964
P-450	10^{-7}	0.076	Estabrook, 1964
P-450	2×10^{-6}	1.5	Kerekjarto and Staudinger, 1966
P-450	28×10^{-6}	21	"
P-450	7×10^{-6}	5.3	"
P-450	0.7×10^{-6}	0.53	"
Cytochrome oxidase (rat liver cells)	0.5×10^{-6}	0.38	Longmuir, 1957
Cytochrome oxidase (rat liver mitochondria)	0.8×10^{-6}	0.5	Handler et al., 1964
Cytochrome oxidase (pig heart)	0.2×10^{-7}	0.01	Longmuir, 1954
Cytochrome oxidase (Keilen Hartree particles)	1.0×10^{-6}	0.76	Chance, 1957
Protocollagen proline hydroxylase (chick embryo)	3×10^{-5}	23	Hutton et al., 1967
Steroid-β-hydroxylase	9.0×10^{-6}	6.8	Ando and Horie, 1971

kinase may be considered:

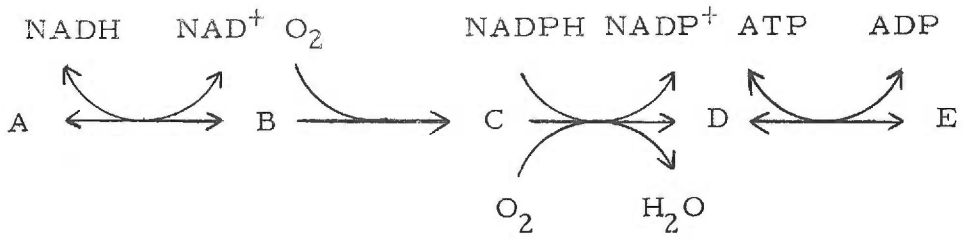

One can assume the system functions normally at 40 torr. When the tissue $P(O_2)$ is lowered to 20 torr, the velocity of the reaction catalyzed by the oxidase with a $Km(O_2)$ of 20 torr will be 50% of normal. A lowered level of C, D, and E and an increased level of A and B are expected. At 5 torr, the mixed function oxidase activity is reduced to 50% while the activity of the other oxidase is reduced even more substantially. Thus, crossover points exist now at both B → C and C → D. At 2 torr, the redox state is changed due to bioenergetic hypoxia. A crossover will be seen at the reductase reaction and possibly a reverse crossover at the mixed function oxidase reaction. Finally, at 1 torr the phosphorylation state of the cell is decreased and a crossover occurs at the kinase reaction.

For any actual pathway, kinetic information such as Michaelis constants for oxygen, redox cofactors, and pyridine nucleotides are necessary to predict whether crossovers will indeed occur. Allosteric affects must be taken into account. In addition, altered metabolite concentrations do not necessarily indicate an altered flux through

the pathway. For two substrate reactions functioning at submaximal substrate concentrations, a decrease in one metabolite may be compensated by an increase in the other so that a nearly constant reaction velocity is maintained.

Finally, with regard to the importance of biochemical changes during hypoxia, it is currently unclear which changes are causally involved in hypoxia damage. A priori, there is no reason to suspect one reaction or pathway over another. There is no indication which perturbation would be irreversible or whether a change has an evolutionarily protective or regulatory function. Consequently, the function of different metabolic pathways must be examined under varying degrees of hypoxia to provide a foundation for an understanding of hypoxia tissue damage.

I.B.5. Biochemical Studies of Hypoxia

No simple biochemical explanation of hypoxic tissue damage is possible. Hypoxia is not a unique single state but a series of continuous states of decreased oxygen availability and their consequences (I.B.1.). It may be systemic, or organ specific (I.B.1.). Tissues are affected differently as a consequence of variations in oxygen supply (I.B.3.). Cells within a tissue are affected differently due to oxygen tension fields (I.B.3.), and intracellular organelles within single cells may be exposed to different oxygen tensions as a

consequence of intracellular gradients. Numerous physiological responses (I. B. 2.) and biochemical responses (I. B. 4.) may attenuate hypoxia. Most biochemical systems are dependent primarily or secondarily upon oxygen (I. B. 4.). Oxidase dependent systems have different patterns of responses (e.g., crossover points) due to the relative affinities of the enzymes for O_2, pyridine nucleotides, adenylates, etc. (I. B. 4.). The time course of oxygen deprivation may range from acute to chronic, and the onset of pathology may be insidious or acute. Biochemical, physiological and pathological changes may be reversible or irreversible. Certain tissues have specific metabolic vulnerabilities to oxygen deprivation (I. B. 2.). These and other complications require 1) a thorough knowledge of normal metabolic function, 2) extensive experimentation on different tissues under varying degrees of oxygen deprivation, and 3) testable hypotheses to guide experimentation attempting to relate biochemical consequences of oxygen deprivation to hypoxic damage.

Experimental studies of hypoxia are described from two aspects: 1) methods used in the study of hypoxia, and 2) experimental studies of hypoxia in individual organs. Theories of hypoxic damage are treated in Section I. B. 6.

I. B. 5. a. Methods for Studying Hypoxia. Study of hypoxia has been approached on different levels of organization ranging from whole organisms to subcellular fractions. Each of the levels has

inherent advantages and disadvantages; studies on all levels are essential to understanding hypoxia.

Intact Organisms: Early studies of hypoxia were performed on intact animals under conditions of reduced oxygen inspiration. Various techniques have been developed to produce hypoxia in intact organisms (van Liere and Stickney, 1963). The most common methods are: 1) dilution of oxygen with an inert gas, 2) reducing air pressure below atmospheric, and 3) continuous air rebreathing from a vessel containing a carbon dioxide absorbant.

Intact organism studies have an advantage over other approaches in that the functional interactions of the complete organism are retained. Cells retain their location-function relationship. Physiologic oxygen gradients exist. Few special preparations are required so that the experimental model is minimally perturbed. Because of the interacting systems, however, it is difficult to study just one component. Other than hemic parameters, most functions cannot be studied continuously. Tissue samples can be taken only at the termination of the experiment. Single experiments are thus time-consuming and expensive. Stopping metabolism rapidly in specific tissues is also difficult. Oxygen supply to specific tissues may be measured polarographically and controlled by altering inspiratory $P(O_2)$ (Davis et al., 1973).

Perfused Organs: Elimination of most humoral and neurogenic interactions is attained by studying isolated organs supplied with nutrients and oxygen by perfusion. The perfusion may involve either single passage of perfusate through the tissue or continuous recycling. Techniques are available for many different organs (Diczfalusy and Diczfalusy, 1971). Perfusion systems allow selective control of individual components, such as oxygen tension. Metabolites can be monitored continuously in the perfusate; rates of metabolism can be calculated by measurement of rate of flow and initial and final concentrations of metabolites. Cellular values are obtainable only at the conclusion of the experiment.

With perfusion, cells are not exposed to equal oxygen tensions due to the oxygen gradients within the organ. On the other hand, normal location-function relationships of cells are retained.

Tissue Slices: The merits of tissue slices for study of hypoxia, anoxia and ischemia are discussed by Cohen (1973). A general description of this approach is available (DeLuca and Cohen, 1964). Cohen (1973) cites avoidance of sampling difficulties, more stringent controls, reduction of experimental variables, and shorter time per experiment as the chief attributes of this approach over perfusion techniques. Whether there is an actual reduction of experimental variables or whether the variables are merely different is not obvious. In the tissue slice procedure a large and variable fraction of the cells

is destroyed by the slicing. Oxygen gradients within the tissues exist, but unlike the organ perfusion techniques, these gradients are no longer similar to the normal physiological gradients.

Cell Suspensions: Cell suspensions have been used to study metabolism as a function of oxygen tension for unicellular organisms (Chance, 1957) and ascites tumor cells (Chance, 1965). This approach has been of limited applicability until recently to normal mammalian tissues for two reasons: lack of techniques to produce intact isolated cells from normal tissue and to provide constant oxygen supply at different oxygen tensions, but recent developments have obviated these problems (Sections II and III, respectively).

The major advantage of cell suspensions over intact organisms, perfusion or tissue slices in the study of hypoxia is that all cells have uniform exposure to oxygen and other metabolites. Metabolite entry into cells is limited only by transport across the plasma membrane; uptake of metabolite can thus be assumed to be uniform for all cells. The advantage of this system over subcellular systems is the integrity of cellular metabolism and retention of possible intracellular oxygen gradients. The most serious uncertainty in use of cell preparations in metabolic studies arises from possible changes due to the isolation procedure (Section II.C.). Studies with cell suspensions share with tissue and subcellular systems the advantage of rapid quenchability, that is, rapid metabolic immobilization. Continuous monitoring is

possible by physical techniques such as absorption spectroscopy or by sequential sampling. Intracellular concentrations may be obtained by direct measurement or indirectly by measuring concentration in suspending medium and in total incubation.

Subcellular Fractions. The subcellular fractions most extensively utilized in studies of oxygen utilization are mitochondria, microsomes, and purified oxidases. Studies of these preparations provide information on the function of individual components free from interactions with other cellular components. Individual reactions may be studied more directly and control parameters examined. The major difficulty with this approach is that information obtained on isolated systems may not reflect the true intracellular situation. Thus, results of studies on isolated systems must be interpreted with caution with relation to hypoxic effects at cellular or tissue levels until it is confirmed that the function is unchanged in intact cells and tissues.

I.B.5.b. Hypoxic Effects. As indicated by survival times (Section I.B.2.), different organs have different susceptibilities to hypoxia due to intrinsic differences in O_2-dependent functions and metabolism. The present review is limited to biochemical changes in tissues in the context of primary and secondary hypoxia. It is intended to serve as a basis for a re-evaluation of hypoxic processes in this newly defined framework with the hope of ultimately yielding a better understanding of the pathology of hypoxia. The nervous system,

heart, and liver are discussed in some detail, and kidneys and other tissues are briefly discussed.

Hypoxia of the Central Nervous System: The basis for functional changes of the central nervous sytem during hypoxic, anoxic and ischemic conditions has received intensive study as a consequence of its clinical importance. Nevertheless, an attitude still too frequently maintained is that "the higher psychic functions are associated with biochemical changes so subtle and complex as to render any attempt to describe them in terms of mere oxygen utilization no more adequate than to predict the fidelity of a radio by its power requirements" (Kety and Schmidt, 1948). This is the challenge of research of the biochemistry of hypoxia--to provide an explanation for those changes of higher psychic functions in terms of oxygen utilization. It requires an understanding of enzymatic oxygen utilization and of the dependence of metabolism on oxygen tension. The first requirement is characterization of those enzymes with primary oxygen dependencies, i.e., the oxidases. Secondly, the function of these enzymes with regard to oxygen tension must be determined. Thirdly, the secondary dependencies upon oxygen tension must be examined, e.g., changes related to redox and phosphorylation state changes. Finally, control and supraenzymatic processes must be examined with regard to the above changes. Hypoxia must be regarded as a continuum between normoxia and anoxia; studies of the direct normoxic-anoxic transitions

such as those involving arterial ligation are of limited value in understanding the complexities of hypoxia. Rather, metabolism must be examined when the other factors, such as blood flow and metabolite supply, are controlled while oxygen tension is selectively reduced.

Techniques have been introduced for such study of brain metabolism, which I believe mark a turning point in the study of hypoxia in the brain. Especially important in this regard is the methodology of Salford, Plum and Siesjo (1973). They introduced quantitative control to the model of Levine (1960), which uses carotid artery ligation to control cerebral blood pressure, and controlled inspiratory gas to control arterial $P(O_2)$. In this manner, they could control the degree of hypoxia and separate any ischemic effects. With the intentional oversight of studies not examining metabolism as a function of oxygen tension, I will proceed to devote this discussion to hypoxia of the brain in terms of primary and secondary dependencies on oxygen and the use of controlled oxygen tension in the study of brain hypoxia. This approach is partially rationalized by the fact that an excellent review of the "Biochemistry of Cerebral Anoxia, Hypoxia and Ischemia" was recently written by Cohen (1973).

At the outset it must be recognized that the brain is a heterogeneous system with regard to cell type, oxygen tension, oxygen consumption, blood supply, metabolic function, etc. This is of utmost importance in examination of hypoxia, since minimum perturbations

have been sought to identify those "first" affects of oxygen deprivation. If one considers the complexity of the neural system, the variability between organisms, and experimental sampling problems, the sensitivity of analysis of various parameters is likely to be no better than ± 5%. Thus, for change consequent to hypoxia to be detectable and experimentally significant, it must be on the order of 5%. However, since the tissue is heterogeneous, this change is not likely to reflect a 5% change in all cells, but rather a larger change in a smaller number of cells. Thus a 5% total change may reflect a 10% change in 50% of the cells or a 50% change in 10% of the cells. A 10% change in 10% of the cells or a 100% change in 1% of the cells would be undetectable. The consequences of this are quite significant with regard to in vivo response to hypoxia since strategically located "sensor" cells could trigger responses to hypoxia without detectable changes in the entire organ. One must be aware, therefore, that measured metabolic changes as a consequence of arterial $P(O_2)$ are only minimally detectable changes.

Several oxidases found in the brain have been identified and are listed in Table I-J. The small number by comparison to liver and kidney may reflect the differences in function of the tissues or may be a consequence of biochemists' preference for those tissues which may be removed quickly and easily. If the latter is the case, the search for oxidases in the brain may be fruitful in supplying a further

Table I-J. Oxidases in the mammalian brain.

Cytochrome oxidase
Phenylalanine hydroxylase
Tyrosine hydroxylase
Dopamine β hydroxylase
Monoamine oxidase
Tryptophan hydroxylase
D-amino acid oxidase
Protocollagen proline hydroxylase
Squalene epoxidase
C-4 demethylase
Fatty acid α-oxidase

understanding of both normal function and changes consequent to hypoxia.

Of the oxidases known to occur in the brain, cytochrome oxidase is the most widespread (Lubbers, 1968; Ridge, 1967). Estimates have been made from studies using respiratory inhibitors that it consumes 90-95% of the total oxygen; however, this may be an overestimation because of nonspecificity of the inhibitors. The central importance of cytochrome oxidase in the cellular requirement for oxygen was expounded by Chance (1957). Since that time, he and coworkers have expanded this study to cytochrome oxidase function at low oxygen tensions. They developed a sensitive procedure (reviewed by Jobsis, 1972) for measuring the fluorescence of protein bound NADH and NADPH in the brain as a function of inspiratory oxygen. They also measured the oxygenation of hemoglobin spectrophotometrically so that the capillary oxygen tension could be estimated from a standard hemoglobin saturation curve. The percent reduction of pyridine nucleotides as estimated from the fluorescence is redrawn in Figure I-7 as a function of capillary oxygen tension as estimated from the absorbance change and a standard hemoglobin saturation curve (Marshall and Wyche, 1972). The capillary oxygen tension providing half maximal change in this estimation of redox state can be calculated to be approximately 12-13 torr, and the critical capillary oxygen tension can be estimated to be about 27 torr.

Figure I-7. Pyridine nucleotide reduction and lactate-to-pyruvate ratio in brain as a function of oxygen tension.

a. Change in fluorescence of protein-bound NADH plus NADPH in rat brain cortex as a function of capillary $P(O_2)$. Redrawn from Chance et al. (1965).

b. Lactate to pyruvate ratio in rat brain at measured tissue and arterial $P(O_2)$. Tissue data from Schmal et al. (1968); $P(O_2)$ values represent rat cortex surface $P(O_2)$. Arterial and venous data from MacMillan and Siesjo (1971); arterial $P(O_2)$ values were measured and venous $P(O_2)$ estimated from arterial value.

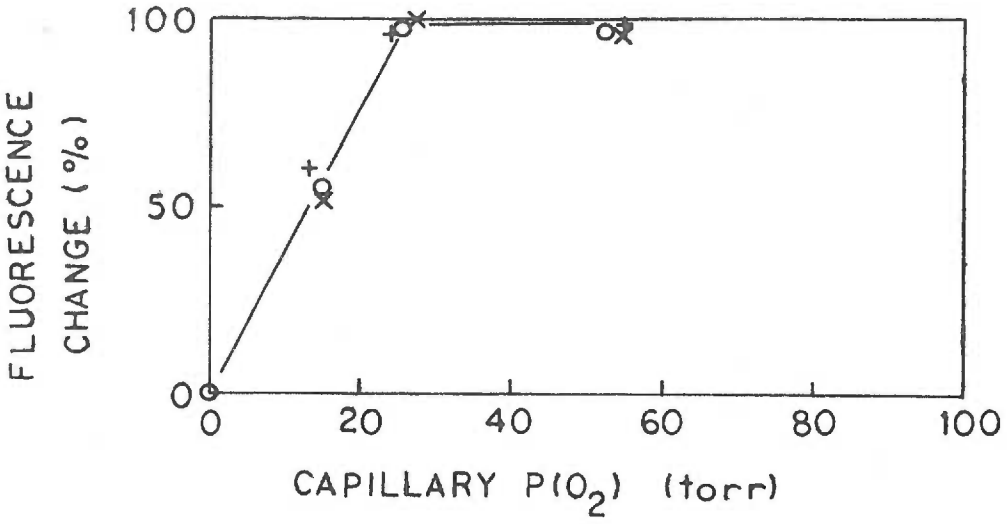
FLUORESCENCE CHANGE (%)
100
50
0
0
20
40
60
80
100
CAPILLARY P(O2) (torr)

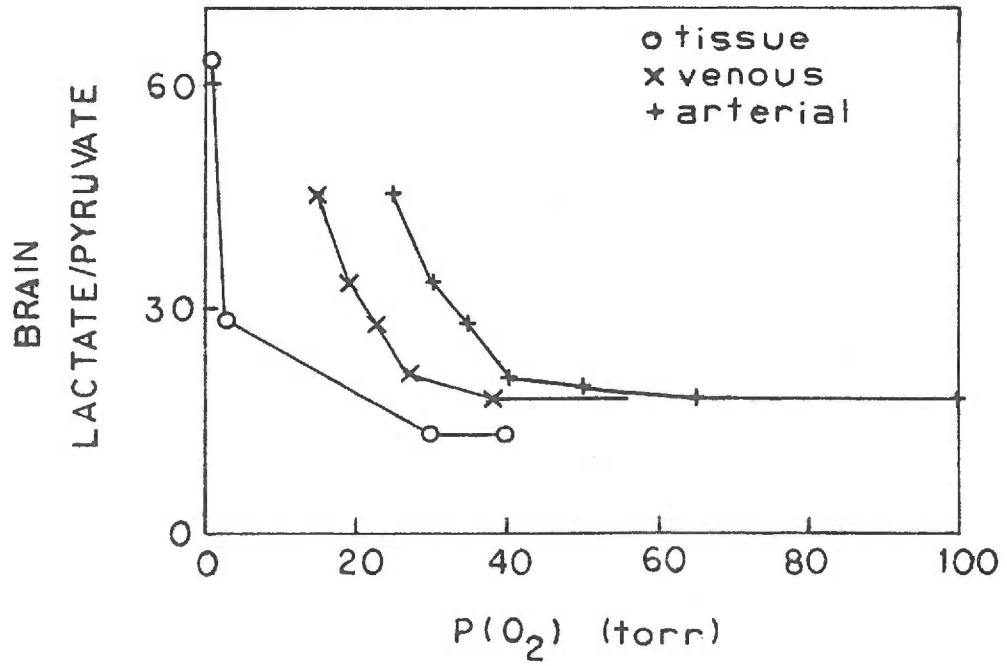
BRAIN LACTATE/PYRUVATE
60
30
0
o tissue
x venous
+ arterial
0
20
40
60
80
100
P(O2) (torr)

A different approach to the estimation of intracellular redox state was developed by Williamson et al. (1967) relying on enzyme maintained equilibrium of oxidation-reduction reactions involving pyridine nucleotides. In the cytoplasm, lactic dehydrogenase catalyzes the $NADH:NAD^+$ coupled reversible oxidation-reduction of the lactate-pyruvate pair. If this reaction is sufficiently rapid and the cytoplasmic lactate and pyruvate pools can be measured, an estimate of $NADH:NAD^+$ can be made. Schmahl et al. (1968) measured the lactate:pyruvate in cat brain cortex while the animals inspired low oxygen gas mixtures. The cortex surface $P(O_2)$ was measured polarographically with a special multiple point electrode. The results are given in Figure I-7 and show that the critical $P(O_2)$ is less than 30 torr. MacMillan and Siesjo also measured the lactate and pyruvate in the cerebrum after maintenance at constant arterial $P(O_2)$ for 30 min. The lactate:pyruvate ratios as a function of arterial and venous $P(O_2)$ which were reported are shown in Figure I-7. They estimated that the critical arterial $P(O_2)$ for these changes was about 50 torr. This corresponds to a critical venous $P(O_2)$ of about 35 torr. The calculation of $NADH:NAD^+$ from lactate:pyruvate is complicated by the fact that the pH may change during hypoxia. MacMillan and Siesjo (1971) proposed from estimates of intracellular pH that the cytoplasmic $NADH:NAD^+$ ratio does not necessarily change even at a venous $P(O_2)$ as low as 10 torr. They concluded (MacMillan and

Siesjo, 1971b) that the measured increase in the lactate:pyruvate was "due to an effect of acidosis on the LDH equilibrium and not hypoxia per se." This conclusion does not indicate what the biochemical basis for the lactate:pyruvate changes really is and does not fit with the direct observations of Chance et al. (1964) that the reduction of pyridine nucleotides increases half maximally at capillary $P(O_2)$ of about 12 torr. Coupled with the inherent difficulty of intracellular pH determination, these results suggest that the contention that lactate: pyruvate change is due solely to acidosis is not warranted. I do not reject the importance of pH changes during hypoxia, but rather suggest that pH changes are a consequence of primary hypoxia. Similarly, lactate:pyruvate change is a secondary event of hypoxia. The primary event is altered oxidase function. In this case, the most important oxidase is very probably cytochrome oxidase. When the function of this oxidase is diminished due to oxygen limitation, an alteration in mitochondrial $NADH:NAD^+$ is likely to occur. This alteration will affect the cytoplasmic redox state in addition to possible changes in mitochondrial pH and cytoplasmic pH. The altered redox state will be reflected in the cytoplasmic $NADH:NAD^+$. The alterations in this ratio and in the pH can increase the ratio of lactate to pyruvate. In addition, increased glycolysis will result in an increase in pyruvate production so that the observed increase in both pyruvate and lactate concentrations during hypoxia can be explained (Salford et al.,

1973). This fact cannot be easily explained simply by a change in pH.

Another primary affect of diminished oxygen supply to cytochrome oxidase is a change in cellular phosphorylation state. ATP is synthesized from ADP in the process known as oxidative phosphorylation. The transfer of electrons to molecular oxygen catalyzed by cytochrome oxidase is essential for this function. When oxygen tension is decreased to a level which affects this function, ATP synthesis will be diminished, and ATP concentration will decrease. Other parameters of cellular energetics such as ATP:ADP, phosphorylation state potential (Wilson, 1974) and adenylate energy charge (Adkinson, 1968) will also reflect a decrease in ATP synthesis. The adenylate energy charge in rat brain after maintenance at constant arterial $P(O_2)$ for 30 min was measured by Davis et al. (1973) as shown in Figure I-8. The critical arterial $P(O_2)$ was about 35 torr. ATP:ADP as a function of brain surface $P(O_2)$ (Schmahl et al., 1968) is also shown in Figure I-8. A critical $P(O_2)$ cannot be obtained from these data, but detectable change occurs at 2 to 3 torr.

Another parameter of cellular energetics that has been measured during hypoxia is phosphocreatine content. The results determined by Schmahl et al. (1968) as a function of brain surface $P(O_2)$ and of MacMillan and Siesjo (1971b) as a function of arterial and venous $P(O_2)$ are given in Figure I-8. The critical arterial $P(O_2)$ for a decline in phosphocreatine was about 35 torr.

Figure I-8. ATP:ADP and phosphocreatine content in brain as a function of oxygen tension.

a. Adenylate energy charge as a function of arterial $P(O_2)$ (Davis et al., 1973).

b. ATP:ADP ratio as a function of brain surface $P(O_2)$ (from Schmahl et al., 1968).

c. Phosphocreatine content of brain as a function of brain surface $P(O_2)$ (Schmahl et al., 1968) and arterial $P(O_2)$ (MacMillan and Siesjo, 1971).

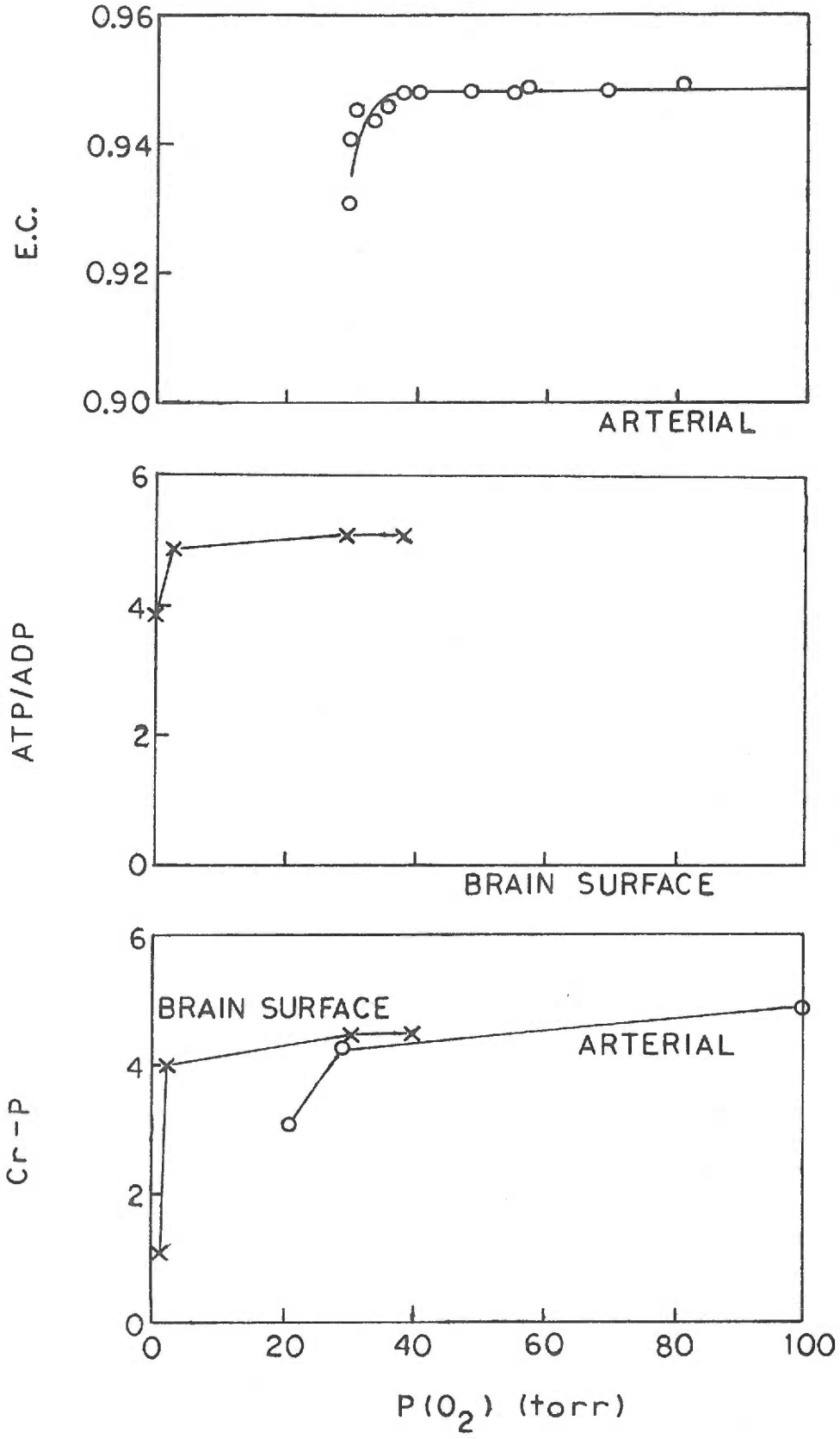
0.96
0.94
0.92
0.90
E.C.
ARTERIAL
6
4
2
0
ATP/ADP
BRAIN SURFACE
6
4
2
0
Cr-P
BRAIN SURFACE
ARTERIAL
0
20
40
60
80
100
P(O2) (torr)

The question of what the tissue oxygen tensions are when changes in metabolism due to hypoxia are observed is a matter of much discussion and conjecture.[5] Chance and coworkers proposed and have maintained that since redox and energetic changes are related to cytochrome oxidase function, the in vivo mitochondrial oxygen tension under conditions giving altered redox and energetic properties is related to in vitro mitochondrial respiration as a function of oxygen tension (see, for instance, Sugano et al., 1974). Consequently, they measured the apparent $Km(O_2)$ for isolated respiring mitochondria and submitochondrial particles, which they found to be 0.02-0.05 μM (Chance, 1965). They consequently proposed that there exists a 1000-fold oxygen tension gradient between the capillary and the mitochondrion (Sugano et al., 1974). This idea was based upon the assumption that the conditions for study of isolated mitochondria adequately simulated in vivo conditions so that metabolism and control were not grossly perturbed. However, Petersen et al. (1974) showed that the apparent $Km(O_2)$ for mitochondrial respiration is dependent upon the ratio of ATP:ADP. They showed that in the presence of high ATP:ADP the apparent $Km(O_2)$ is increased over the uncoupled state 3 value.

---

[5] This general discussion of cellular oxygen tensions and tissue oxygen tension gradients is applicable to all tissues. It is included here because most of the data concerning intact tissues are for the brain (presented above). The research on isolated mitochondria by Chance and others indicates a similarity between mitochondria from various sources.

Thus, data measured on isolated mitochondria do not necessarily reflect *in vivo* function unless appropriate conditions are chosen. Values of 0.25 mM ADP and no ATP do not reflect the 0.5 mM ADP and 2 mM ATP normally found *in vivo*, and thus the $Km(O_2)$ values measured by Chance and coworkers should not be used to predict *in vivo* tissue gradients.

Other approaches are possible to estimate *in vivo* oxygen gradients in a semiquantitative fashion without assumptions about the *in vivo* affinity of cytochrome oxidase for oxygen. An estimation of an "average" oxygen tension gradient from capillaries to tissues can be made by subtracting the mean capillary oxygen tension from the mean tissue oxygen tension. The mean capillary oxygen tension is not the arithmetic mean of the arterial and venous tensions because of the nature of the oxygen dissociation curve. Rather, the mean capillary oxygen tension is more closely approximated by the oxygen tension at which one-half of the difference in arterial and venous oxygen content has been released. This can be estimated to be about 57 torr using an arterial $P(O_2)$ of 90 torr, a venous $P(O_2)$ of 43 torr, pH 7.4, and the oxygen dissociation curve of Marshall and Wyche (1972). The mean tissue $P(O_2)$ in the grey matter can be estimated from the results of Lubbers (1973) to be about 22 torr. Thus, an "average" gradient may be considered to be about 35 torr.

A second estimation of the average oxygen gradient between capillaries and tissue can be obtained from the independent studies of the tissue metabolite changes as a function of arterial or venous $P(O_2)$ and of tissue $P(O_2)$. Lactate/pyruvate measured as a function of arterial, venous and tissue surface $P(O_2)$ is presented in Figure I-7. From this one can estimate that the "average" capillary to tissue oxygen gradient is 25-35 torr.

A third estimation can be obtained from theoretical models using measured values for intercapillary distance, capillary length, blood flow rate, arterial $P(O_2)$, venous $P(O_2)$ diffusion constant in tissue, and oxygen consumption rate. Thews' (1967) treatment based upon the Krogh model allows an estimate of the average capillary tissue $P(O_2)$ difference of about 15 to 20 torr.

Two additional points need to be mentioned with regard to the meaning of capillary-tissue gradients. The first is that "average" gradients are probably more meaningful than "maximal" gradients when measuring metabolite levels as a function of oxygen tension since the metabolite levels are also "average" tissue measurements (i.e., a 100% change in 1% of the tissue is usually undetectable, see above). Secondly, the above estimates say nothing about intracellular or intramitochondrial oxygen tensions. Thus, in spite of the aforementioned problem with the approach of Chance and coworkers, there is little other data for these estimations.

Primary hypoxia has been demonstrated in the brain for the tryptophan hydroxylation reaction in serotonin synthesis. Davis et al. (1973) measured the accumulation of cerebral 5-hydroxytroptophan after decarboxylase inhibition in rats maintained at fixed arterial oxygen tensions. They found a decreased accumulation of this metabolite below 60 torr (Figure I-9) and concluded that this decrease was due to a decreased activity of the tryptophan hydroxylase because of limiting oxygen. They proposed that this substrate deficiency for a metabolic oxidase may be responsible for behavioral changes of mild hypoxia. This report provides an important but incomplete analysis of the affect of mild hypoxia on serotonin metabolism. Serotonin is a substrate for monoamine oxidase, and at least some of this metabolite is thought to be oxidized by this enzyme in vivo (Sirek and Sirek, 1970). Thus, diminished $P(O_2)$ might also result in decreased degradation of serotonin and counteract an affect of decreased synthesis.

Primary hypoxia also occurs in catecholamine metabolism in the brain. Two oxidases are involved in epinephrine and norepinephrine synthesis, and one oxidase is involved in degradation. Tyrosine is the primary metabolic precursor for dopamine as demonstrated by ^{18}O incorporation into the 3 position of homovanillic acid (Mayevsky et al., 1973). Dopamine is hydroxylated to norepinephrine by dopamine β-hydroxylase in central noradrenergic neurons which

Figure I-9. Brain tryptophan hydroxylation as a function of arterial $P(O_2)$. Accumulation of 5-hydroxytryptophan after maintenance of arterial $P(O_2)$ at designated values for 30 min in the presence of a 5-hydroxytryptophan decarboxylase inhibitor (from Davis et al., 1973).

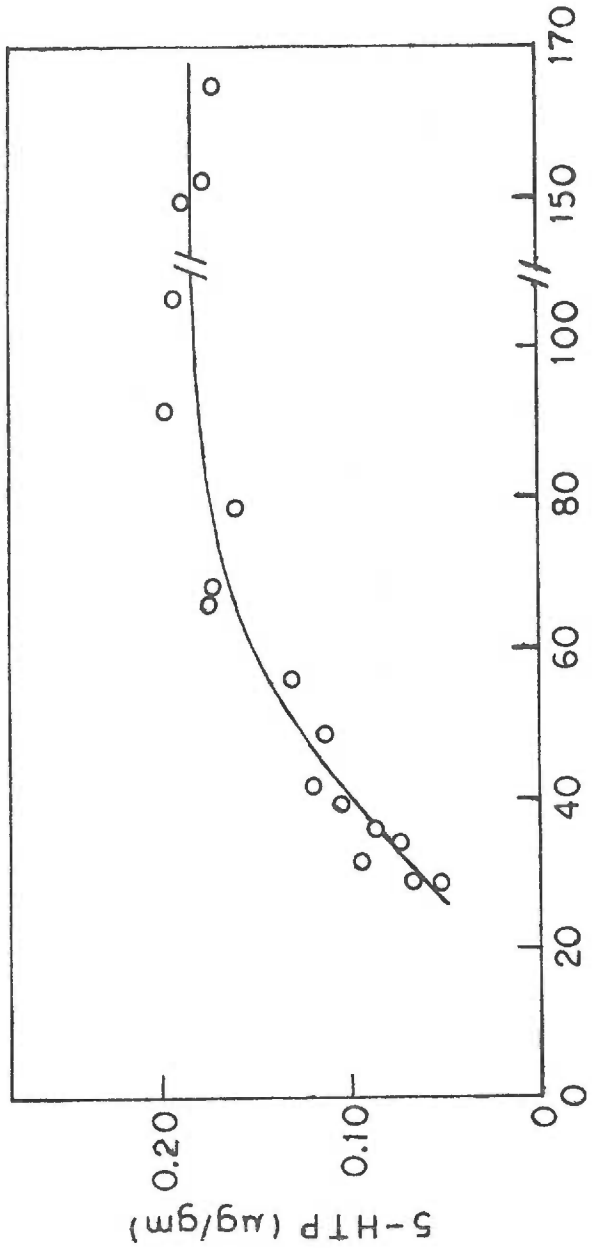
5-HTP (μg/gm)
0.20
0.10
0
0
20
40
60
80
100
150
170
ARTERIAL ($P(O_2)$)
(torr)

innervate cerebral arteries and arterioles (Hartman, 1973). Norepinephrine and its methylated product, epinephrine, are oxidized by monoamine oxidase, a reaction thought to terminate its physiological response in the brain (Krishner, 1968; Wurtman and Zervas, 1974). Zervas et al. (1974) showed that brain dopamine was significantly reduced and norepinephrine was moderately reduced 24 hours after carotid ligature in gerbils. Davis and Carlsson (1973) observed a decreased accumulation of noradrenaline and dopamine in rat brain following 1 hour exposure to 5.6% oxygen and a monoamine oxidase inhibitor. The indication is that a decreased availability of oxygen to oxidases involved in this metabolism is responsible for these changes. If this is true, then the general interpretation of the role of monoamine transmitters following injury to the central nervous system as described by Wurtman and Zervas (1974) must be expanded to include these important biochemical events. Thus, in addition to a decrease in uptake and oxidative deamination of monoamines, there could be decreased synthesis. This is an important point with regard to overall monoamine metabolism during oxygen limiting conditions.

Although information on other oxidases in the central nervous system is limited, there are sufficient data to speculate on other primary hypoxias which deserve further investigation. Lipid constitutes 30% of the wet weight of brain white matter (Davison, 1968) and is therefore likely to play an important role in cerebral function.

Decreased unsaturated fatty acids in the brain of a patient after severe hypoxia (Gerstl, 1963) could be a direct consequence of decreased desaturation activity due to oxygen limitation to a microsomal (mixed function oxidase) desaturase. Cholesterol synthesis has been shown to occur in the brain (Nicholas and Aexel, 1967) and is known to involve at least two oxidases (see Section I.B.4.). Therefore, this synthesis could be impaired during hypoxia. Prostaglandins are lipophilic hormones which are normal constituents of nervous tissue (Hinman, 1972), suggesting that synthesis and/or metabolism may occur in nervous tissue. Since oxygen dependent reactions are known to be involved in both synthesis and metabolism of prostaglandins, this metabolism may also be sensitive to decreased $P(O_2)$.

In addition to the amino acid oxidases mentioned above, a D-amino acid oxidase activity has been measured in the diencephalon part of the brain (Yagi, Nagatsu and Ozawa, 1956), and phenylalanine hydroxylation in the brain in vivo has been reported (Bagchi and Zarychi, 1970). Protocollagen proline hydroxylase activity has also been measured (Cutroneo, Guzman and Sharawy, 1974). These oxidases and other primary oxygen dependent functions may be important in understanding the complex and perplexing biochemical changes in hypoxia.

Secondary effects of hypoxia are too numerous to consider in this brief discussion; however, data illustrative of the type of

information valuable to understanding these changes are given in Figure I-10. These metabolic changes are dependent upon oxygen tension only secondarily through the redox state or phosphorylation state and may have additional indirect effects of great importance. An example may be seen in the indirect effect of oxygen tension on the level of γ-aminobutyrate (GABA), a possible neurotransmitter, in the brain. GABA concentration was found to be increased in the brain following anoxia (Wood, 1967; Wood and Watson, 1969). The precursor, glutamate, was also elevated. Glutamate may be formed from 2-oxoglutarate by reductive amination, a reaction which is sensitive to the NADH to NAD^+ ratio. Thus, decreased $P(O_2)$ resulting in elevated NADH:NAD^+ could shift the glutamate dehydrogenase equilibrium toward increased glutamate. The increased glutamate concentration may then result in increased decarboxylation and an increase in tissue GABA concentration.

Heart: "Anoxic damage to myocardial cells alone causes 20 to 25% of all deaths in industrialized nations (Robbins and Angell, 1971). This statement reveals the medical importance of unraveling the primary events in myocardial hypoxia so that appropriate therapy based upon these changes in the affected tissue might be instituted (Jennings, 1969). Most anoxic damage to the myocardium in man results from ischemia, a reduction in blood flow by occlusion of the coronary artery (Opie, 1971/72; Robbins and Angell, 1971).

Figure I-10. Secondary metabolic changes during hypoxia. Metabolite concentration (millimoles/kg wet weight) in the brain as a function of arterial $P(O_2)$ (from Salford et al., 1973).

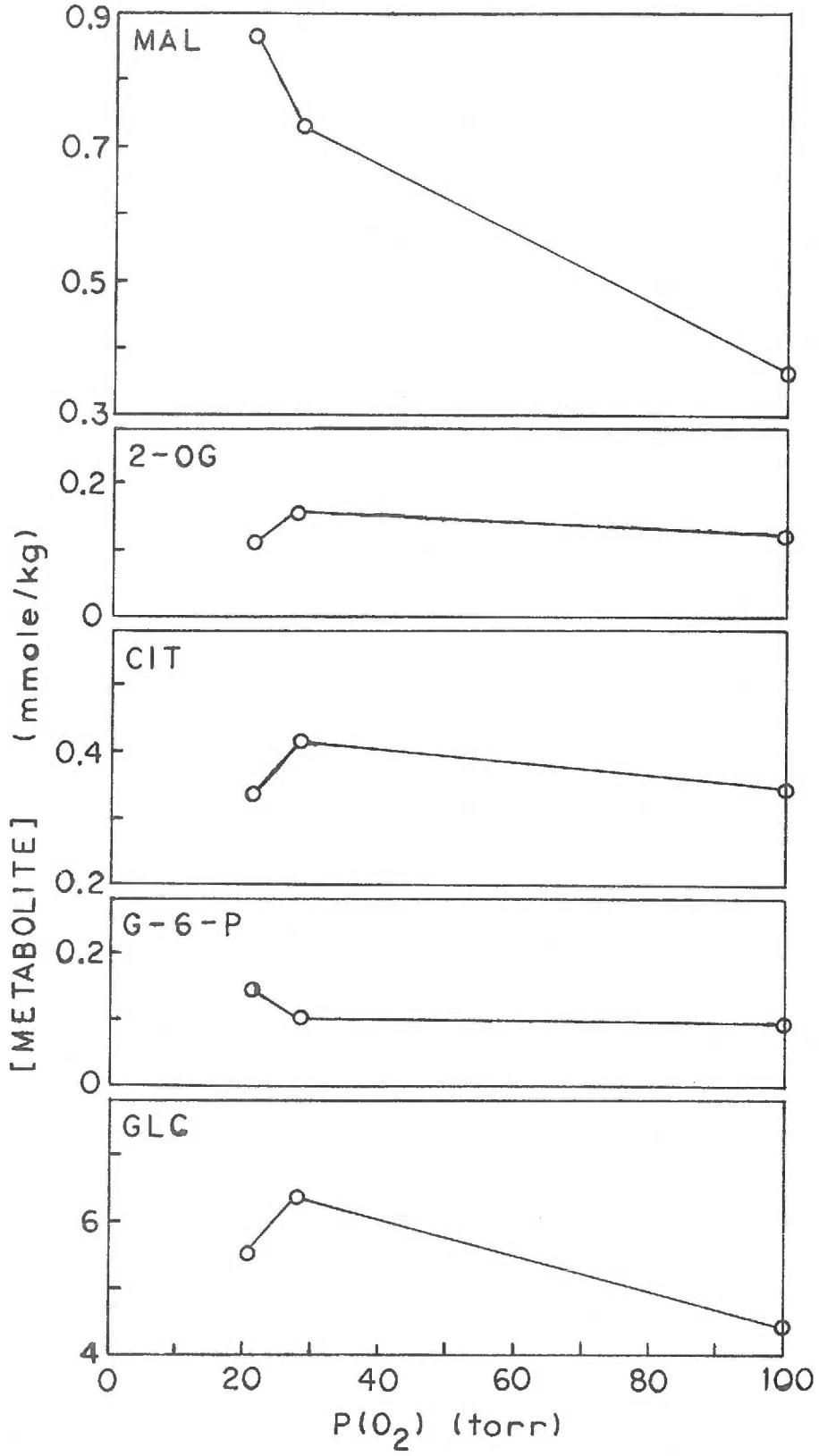
MAL
2-OG
CIT
G-6-P
GLC
0.9
0.7
0.5
0.3
0.2
0
0.4
0.2
0.2
0
6
4
0
20
40
60
80
100
[METABOLITE] (mmole/kg)
P(O2) (torr)

Interpretation of metabolic changes during ischemia are complicated by the reduction in blood flow which alters substrate supply and product removal in addition to oxygen supply. Yet oxygen deficiency is thought to be the primary metabolic disturbance (Case, Nasser and Crampton, 1969; Jennings, 1969). Most biochemical and pathological studies on myocardial hypoxia use coronary occlusion as an experimental model. As previously stated, the normoxic-anoxic transition is of limited value in unraveling the complex events of oxygen deprivation. In the ischemic model, the problem is further complicated by perturbations in substrate supply and product removal. Biochemical studies on the heart with graded hypoxia while blood flow is normal are needed to eliminate the ambiguities of the ischemic model.

An important review of metabolism in the hypoxic myocardium was written by Scheuer (1967). He proposes that when oxygenation is impaired, "the primary biochemical lesion occurs at the oxidation of cytochrome A." This view is consistent with that expounded by Chance (1957) and Jobsis (1964). Changes in adenylate concentrations and in redox state are adequately discussed in either of these papers; however, Scheuer's review deals most directly with myocardial hypoxia. Quantitation of these changes in the myocardium as a function of the degree of oxygen deprivation have not been made.

Two major mechanisms control myocardial contractility, tonic and phasic control (Katz, 1975). Tonic control is a slow adaptation involving synthesis of new protein and resulting in altered ATPase activity of myosin. Six hour exposure of rats to 4-5% O_2 resulted in no discernible changes in myosin or myosin synthesis (Aschenbrenner et al., 1971), suggesting that tonic control is of minimal importance in acute hypoxia. Phasic control involves control of flow of calcium to the contractile proteins and is a rapid, beat-to-beat control. It may be affected by biogenic amines and other adenylate cyclase activators. Neurogenic and humoral controls of heart rate and ventricular contractility have been related to hypoxia of the central nervous system and the adrenals (Downing, 1966). Increased release of norepinephrine by the heart of rats breathing 6% O_2 compared to 21% O_2 was postulated to be due to reflex stimulation (Goldman and Harrison, 1970). Specific metabolic alterations within the heart related to enzymic oxygen deficiencies may also occur. Decreased catecholamine synthesis may occur due to tyrosine hydroxylase hypoxia or DβH hypoxia. Potentiation of catecholaminic action can occur as a consequence of MAO hypoxia, i.e., decreased physiologic inactivation of catecholamines. Prolonged stimulation by prostaglandins or steroid hormones may occur by similar mechanisms.

Ischemia or anoxia cause rapid loss of contractility of the myocardium (Scheuer, 1967). Under aerobic conditions, fatty acids

are the preferred substrate for energy production. This metabolism is exclusively aerobic; the myocardium has an abundant supply of mitochondria (Stenger and Spiro, 1961) and high concentrations of cytochromes (Biorick, 1956). Lipid accumulates during anoxia (Jennings and Ganote, 1974; Wartman et al., 1956) as glycolysis takes over energy production. Chronic hypoxia increases succinate dehydrogenase activity and is related to a more efficient mitochondrial function; acute, severe hypoxia (4-5% O_2) causes increased degradation of mitochondrial components (Aschenbrenner et al., 1971).

Depletion of creatine phosphate begins within seconds after initiation of anoxia and is followed by a slower decrease in ATP (Feinstein, 1962). As ATP supplies become limiting, electrocardiographic and hemodynamic abnormalities occur (Scheuer, 1967). The electrical activity requires ATP-dependent pumping of sodium and potassium to maintain transmembranal gradients. Contractile proteins (actin and myosin) require ATP for interaction.

Increased glycolysis during hypoxia results in reversal of the normal lactate uptake by the heart (Krasnow et al., 1962) and in depletion of glycogen (Jennings and Garote, 1974). Adenosine is released from the cells, perhaps as a consequence of increased ATP breakdown, and is thought to be a mechanism of coronary vascular autoregulation (Kukovetz, 1972).

Scheuer (1967) reports that electrocardiographic changes in isolated ischemic rat hearts may occur even in the presence of normal ATP and creatine phosphate levels. This observation suggests that cytochrome oxidase function may not supply a complete explanation of myocardial hypoxia and that other primary biochemical lesions may be important.

Any oxygen dependent enzyme in the heart may be considered a possible site for a primary biochemical lesion during hypoxia, but few have been specifically identified. The sensitivity of the heart to catecholamines (Downing, 1966) and prostaglandins (Bergstrom, 1967) suggests that synthesis and/or metabolism of these agents may be important. Other oxidases involved in steroid, cholesterol, fatty acid and amino acid metabolism are likely to have critical functions in the heart. Protocollagen prolyl hydroxylase and lysyl hydroxylase are known to be required for collagen maturation and must function properly for repair of hypoxic myocardial damage.

The heart is somewhat unique among tissues in its requirement for oxygen. The histogram of $P(O_2)$ values measured in a beating heart (Figure I-3) shows that much of the tissue has a relatively low oxygen tension under normal conditions. Some measurements of $P(O_2)$ are lower than the critical $P(O_2)$ for mitochondria (Fabel, 1968). Thus, the heart appears to be extremely susceptible to oxygen limitation. In addition, a decrease in arterial oxygen tension

necessitates an increased heart function to supply sufficient oxygen to other tissues, such as the brain. Thus, during hypoxia, the heart's oxygen requirement actually increases. Measurements of function of the heart during oxygen limitation have been performed on recirculating perfused hearts (Harris and Gloster, 1971/72; Opie and Mansford, 1970; Scheuer and Stezoski, 1972), however, these studies have used hemoglobin free perfusates. The omission of hemoglobin in the perfusate greatly increases oxygen gradients and alters calibration curves for tissue oxygen tensions relative to arterial $P(O_2)$. In the absence of these calibrations, suitable comparisons of the results cannot be made.

Liver: The broad spectrum of metabolic function of the liver is reflected in the large number of oxidase activities which have been observed in this tissue (Table I-K). The apparent $Km(O_2)$ has been measured for many of these enzymes and are given in Table I-H. Since many of these values occur in the range of normal liver $P(O_2)$ (Figure I-3), one can assume that this may be a fruitful tissue for examining metabolic function during hypoxia.

The functions of hepatic oxidases have been discussed (Section I.B.4.). It is of interest to briefly review metabolic changes during hypoxia which have been observed in these pathways. Changes in amine metabolism and tissue response to amines during hypoxia have been primarily studied in nervous tissue and muscle and has been

Table I-K. Oxidases in mammalian liver.

D-amino acid oxidase	Kynurenine 3-hydroxylase
L-amino acid oxidase	Monoamine oxidase
Aryl 4-hydroxylase	Phenylalanine hydroxylase
Aldehyde oxidase	Protocollagen proline hydroxylase
α Butyrobetaine hydroxylase	Sarcosine oxidase
β Carotene 15-15' oxygenase	Squalene epoxidase
Cysteine oxidase	Steroid 7α-hydroxylase
Cysteamine oxidase	Steroid 12α-hydroxylase
Diamine oxidase	Steroid 2β-hydroxylase
Fatty acid ω-hydroxylase	Steroid 6β-hydroxylase
Fatty acid desaturase	Steroid 6ξ-hydroxylase
Glyceryl ether oxidase	Steroid 16-hydroxylase
Glycollate oxidase	Sterol demethylase
Gulonolactone oxidase	Sulfite oxidase
α Heme oxidase	Tryptophan pyrrolase
Homogentisic acid oxidase	Tryptophan 5'-monooxygenase
3-Hydroxyanthranilate oxidase	Xanthine oxidase
p-Hydroxyphenylpyruvate oxidase	

discussed above. Metabolism of amino acids is a primary function of the liver (Bloxam, 1971) and thus numerous oxidases involved in this metabolism are found in the liver. The $Km(O_2)$ values for these oxidases range from 2.7 to 760 torr, suggestive of in vivo oxygen dependent function. Increases in alanine, glutamate, leucine, phenylalanine and tyrosine were reported during hypoxia in the rat brain (Tews et al., 1963). These increases may be a result of increased protein degradation during hypoxia as has been reported in the heart (Aschenbrenner et al., 1971); however, increased protein synthesis during hypoxia has also been reported (Smialek and Hamberger, 1970). A careful overall study of protein synthesis, protein degradation, amino acid pools and amino acid degradation during hypoxia will be required to ascertain the importance of oxidative metabolism of amino acids during oxygen limitation.

The impaired function of tryptophan metabolism (tryptophan pyrrolase, kynurenine-3-hydroxylase) in the synthesis of nicotinic acid, required for maintenance of the pyridine nucleotide pools, is suggested by the observation that administration of nicotinic acid protects rats from hypoxic damage (Calder, 1948). Taurine is synthesized in the liver from cysteine in a pathway involving cysteamine oxidase (Yamaguchi et al., 1973). Interruption of this pathway during hypoxia may play a role in the observed disturbance of bile metabolism during hypoxia (van Liere and Stickney, 1963) since taurine is

an important metabolite for formation of secreted forms of bile acid such as taurocholic acid. Another possible mode for interruption of bile metabolism during hypoxia is through the mixed function oxidations required for synthesis of these compounds from cholesterol (see Section I. B. 4.). In this regard, a disturbance in cholesterol metabolism is apparent from the increased level of cholesterol found during hypoxia (van Liere and Stickney, 1963). Heme metabolism during hypoxia has been frequently studied due to the importance of heme in oxygen transfer and mitochondrial respiration, the first reaction in heme catabolism is oxygen dependent (Tenhunen, Marver and Schmid, 1969) and may play an important role in hypoxic changes.

Disturbances of fatty acid metabolism have been observed during hypoxia (van Liere and Stickney, 1963). While many of these changes are likely to be a result of secondary hypoxic changes, a primary hypoxic affect might occur through the mixed function oxidases which desaturate, demethylate and hydroxylate fatty acids (see Section I. B. 4.). In addition, transfer of fatty acids across the mitochondrial membrane occurs by a carnityl carrier. Since carnitine is formed through a pathway containing the oxygen dependent γ-butyrobetaine hydroxylase, a decreased level of this carrier and subsequently a depressed lipid mobilization could result from a chronic hypoxia.

The numerous detoxification reactions catalyzed by the microsomal cytochrome P-450 system, which are so essential in an

organism's encounter with its environment, may also be impaired during hypoxia (Sanvordeker and Lambert, 1974). This is of particular importance in the clinical administration of drugs, since excretion of many of these compounds is dependent upon hepatic hydroxylation. Thus, the pharmacologic activity of a drug may be altered in an hypoxic patient. Alterations in metabolism or threshhold response have been reported as a consequence of hypoxia for pentobarbital (Buemel et al., 1970) and sulfadiazine, isoniazid and p-aminopropiophenone (Mustala and Azarnoff, 1969).

The anatomical structure of the liver has been discussed by Block (1970) and Goresky (1973). Unlike other tissues, nearly all cells in the liver are directly exposed to the blood supply. This limits the average capillary-to-tissue gradients, but does not eliminate the danger due to oxygen limitation since much of the hepatic blood supply is from the portal vein which contains less oxygen than arterial blood. Hepatic failure usually occurs during complex hypoxic crises in the clinical setting (Schaffner, 1970). This has been simplified experimentally by use of the isolated perfused liver (Brauer et al., 1965; Tygstrup, 1975). The critical venous $P(O_2)$ for respiration, ATP:ADP, and adenylate energy charge, for such a preparation is about 30 torr (Tygstrup, 1975). Galactose elimination capacity was found to have a critical venous $P(O_2)$ of about 20-25 torr (Tygstrup, 1975). The mitochondrial NAD^+:NADH and adenylate

energy charge in intact liver of rats respiring various $P(O_2)$ gases were studied by Ballard (1971). This preparation is not as simple as the isolated liver because of the interaction with other hypoxic tissues, and it does not provide a direct measure of hepatic oxygenation. Cytoplasmic and mitochondrial NAD^+:NADH were estimated according to the method of Williamson et al. (1967) and are reproduced along with the adenylate energy charge in Figure I-11. All of these parameters are indirect indicators of cytochrome oxidase function. The most important observation is that the critical $P(O_2)$ values for each of these parameters approximates atmospheric $P(O_2)$. Thus, respiratory function in the intact rat liver may be oxygen dependent under normoxic conditions. The physiological and pathological significance of this observation is unclear. Perhaps it reflects a reserve of respiratory function under conditions of metabolic stress to allow additional ATP synthesis or electron removal. Further research is necessary to clarify this point. Changes in cytosol NAD^+/NADH roughly parallel mitochondrial NAD^+/NADH but both decrease at higher $P(O_2)$ than adenylate energy charge.

Other Tissues: All mammalian tissues are susceptible to hypoxic tissue damage, but medical importance and/or ease of developing an experimental model have resulted in an abundance of studies on the previously mentioned tissues but relatively fewer studies on others. Based upon a bioenergetic explanation of hypoxia,

Figure I-11. Hepatic NAD^+:NADH and adenylate energy change in intact rats at various inspired oxygen (from Ballard, 1971). In all experiments animals were exposed to the particular atmosphere for 5 min before injection and 15 min after injection of 100 μM of lactate (a and b) or 20 μM L-aspartate (c, d and e). Redox values were calculated as described by Williamson et al. (1967).

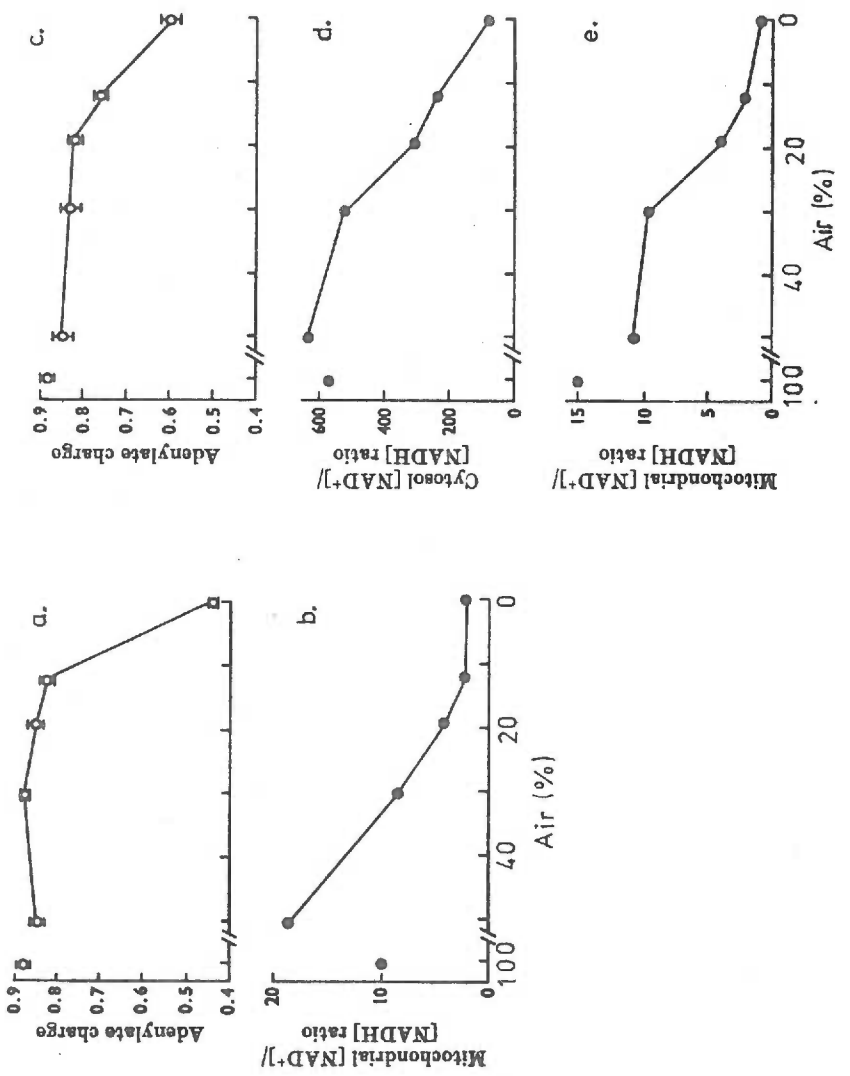
a.
Adenylate charge
0.9
0.8
0.7
0.6
0.5
0.4
b.
Mitochondrial [NAD+]/
[NADH] ratio
20
10
0
100
40
20
0
Air (%)
c.
Adenylate charge
0.9
0.8
0.7
0.6
0.5
0.4
d.
Cytosol [NAD+]/
[NADH] ratio
600
400
200
0
e.
Mitochondrial [NAD+]/
[NADH] ratio
15
10
5
0
100
40
20
0
Air (%)

this is acceptable for all tissues which rely largely upon mitochondrial respiration for maintenance of the energy supply and redox state. However, if one considers hypoxia in terms of the metabolic oxidases, tissues with different oxidases will have different primary hypoxias. Thus, the complicated affect of hypoxia on adrenal cortex and adrenal medulla functions (van Liere and Stickney, 1963) may in part be due to the different oxidases present in these tissues. This same generalization may be applied to other specialized functions in other tissues. Lack of fertility at high altitudes (van Liere and Stickney, 1963) may be a consequence of primary hypoxic lesions in steroid hormone metabolism in gonads. Decreased thyroid function during hypoxia (Van Middlesworth and Berry, 1951) may be a consequence of a secondary oxygen requirement for thyroid peroxidase activity (Section I. B. 4.). The role of oxygen tension in wound healing has been studied (Brighton and Krebs, 1972; Hunt and Pai, 1972; Lundgren and Zederfeldt, 1969; Niinikoski and Hunt, 1972; Silver, 1968), and the maturation of collagen partially related to proline hydroxylation (Chvapil, Hurych and Ehrlichova, 1968) and lysine oxidation to allysine (Grant and Prockop, 1972b).

Renal tissue is similar to liver in that numerous metabolic functions are present. A list of some of the oxidases is given in Table I-L. The critical $P(O_2)$ for respiration of isolated kidney cells is 16.5 torr (Weiss,

Table I-L. Oxidases in mammalian kidney.

Cytochrome oxidase
E alkyl lysinase
D aspartate oxidase
Cytochrome P-450
Aldehyde oxidase
Monoamine oxidase
p-Hydrophenylpyruvate hydroxylase
Glycollate oxidase
Urate oxidase
3-Hydroxyanthranilate oxidase
Meso-inosotol oxidase
Homogentisate oxidase
L-amino acid oxidase
D-amino acid oxidase

1968). Functions of individual oxidases during hypoxia have not been studied in renal tissue, however Vogt and Farber (1968) concluded from a study of renal ischemia that neither ATP nor lactate levels could be correlated with the irreversibility of changes. Thus, function of other oxidases may be important in this pathology.

Carotid bodies are of interest because they contain arterial chemoreceptors and thus play a role in cardiodynamics. They have a high catecholamine content although the role of these amines in the chemoreceptor mechanism is unclear. Mills and Slotkin (1975) measured the catacholamine content of cat carotid bodies after exposure of animals to 8-40% oxygen (60.8-304 torr) for one hour. Catecholamine content increased with oxygen tension, which they interpreted to indicate increased release at lower oxygen tensions. By analogy to brain studies, they excluded decreased synthesis as a possible explanation. Further studies will be required to validate this interpretation, since both decreased synthesis and metabolism of catecholamines occur in the brain during hypoxia. Long-term studies are needed to determine if steady-state hypoxic catecholamine contents are identical to normal values.

I.B.6. Theories of Hypoxic Damage

Hypoxic damage is frequently explained in terms of decreased available energy for maintenance of cellular functions or structural

and metabolic denaturation due to decreased pH (Cohen, 1972, 1973; Jennings, 1969; Sobel, 1974; Vogt and Farber, 1968). Decreases in ATP and pH during hypoxia are well documented and can be explained in terms of altered mitochondrial and glycolytic function (see references above). The primary biochemical lesion for these changes is decreased available oxygen to cytochrome oxidase (Chance, 1957). These theories do not supply a total explanation of hypoxic changes since altered function of other oxidases during hypoxia has been observed Chvapil et al., 1968; Davis et al., 1973). In addition, experimental depletion of ATP in the liver and kidney does not duplicate the rapid irreversible changes of hypoxia (Farber, 1971, 1973; Vogt and Farber, 1968). Lack of a direct relationship of lactate and pH with irreversible hypoxic changes is clear from the discussion by Cohen (1972). Further doubt is cast upon the acidosis theory of hypoxic damage by the recent observation that acidosis protects renal and cardiac tissues from anoxic damage (Bing, Brooks and Messer, 1973; Penttila and Trump, 1974).

Mason (1964) proposed that the affects of anoxia should be interpreted in terms of oxidase systems in addition to the mitochondrial system. This proposal forms the basis for a new theory of hypoxic tissue damage: that primary biochemical events of hypoxia are enzymatic oxygen deficiencies (Figure I-1). These enzymatic deficiencies result in decreased conversion of substrate to product

and result in secondary changes due to substrate accumulation and product deficiency. These secondary changes are adaptive or non-adaptive and affect metabolism, ultrastructure, and functional chemistry producing the characteristic lesions of hypoxia.

I.C. Statement of the Problem

The present research develops a system for the study of hypoxia on a cellular level and uses this system to study metabolism at low $P(O_2)$. Isolated rat hepatocytes (Berry and Friend, 1969) were chosen for the biological system because 1) metabolism in isolated cells compares favorably to metabolism in intact liver (Krebs et al., 1974), 2) oxygen diffusion problems associated with tissues are eliminated (Berry and Friend, 1969), 3) a useful quantity of cells can be obtained in a couple of hours, 4) metabolism can be rapidly interrupted and stopped, 5) uptake of substrates and metabolites is uniform and measurable (Moldeus et al., 1974; Quistorff et al., 1973), 6) intracellular concentrations can be estimated, and 7) cultured mammalian cells have altered oxidative metabolism. An apparatus was designed to provide a constant, desired oxygen tension in a suspension of respiring cells. This apparatus was used to examine drug metabolism by the cytochrome P-450 system, tyrosine degradation, adenylate concentrations, and cytoplasmic $NADH/NAD^+$ as a function of oxygen tension. These studies provide a basis for comparison of oxidative

metabolism on subcellular systems with that observed on intact tissues and organisms. In addition, the research provides information on the relative sensitivities to oxygen limitation of different oxidase systems and tests the feasibility of the theory that the function of oxidases other than cytochrome oxidase may be important in the pathological lesions of hypoxia.

II. EXPERIMENTAL

II.A. Materials

II.A.1. Reagents

All chemicals were reagent grade unless otherwise indicated. The following were obtained from Sigma Chemical Company: 2-oxoglutaric acid, monosodium salt; homogentisic acid, grade 2; tyrosine HCl; semicarbazide HCl; glycine HCl; NAD^+, grade III; NADH, disodium salt, grade III; $NADP^+$, sigma grade; ATP, disodium salt, sigma grade; ADP, sodium salt, sigma grade; AMP, sodium salt, type III; phospho-(enol)pyruvate trisodium salt, hydrate; pyruvic acid, sodium salt, type II; L(+) lactic acid, hemi-calcium salt, Grade L-IV; pyridoxal-5' phosphate; p-hydroxyphenylpyruvic acid; p-hydroxyphenylacetic acid; DL-p-hydroxyphenyllactic acid; PL-b-phenyllactic acid; o-hydroxyphenylacetic acid; b-phenylpyruvic acid, type I, sodium salt; p-hydroxycinnamic acid; L-glutamic acid, sigma grade; L-ascorbic acid, sodium salt; hexobarbital; bis (trimethylsilyl) trifluoroacetamide (BSTFA); 2,5-diphenyloxazole (PPO); desiccated firefly lanterns; keto-enol tautomerase; glutamic dehydrogenase, type II; lactic dehydrogenase, type I; pyruvate kinase, type II; myokinase, grade III; collagenase, type I; hyaluronidase, type I; 3-methylcholanthrene. Phenol red and trypan blue were obtained from

Allied Chemical. Phenyramidol HCl was prepared by Mallinckrodt Chemical Works, Pharmaceutical Products Division, St. Louis, Mo., and obtained as a gift from Dr. N. Gerber. Ethyl acetate (spectrophotometric grade) and toluene (scintillation grade) were obtained from Mallinckrodt. p-Hydroxybenzoic acid and 1-nitroso-2-napthol were obtained from Eastman Organic Chemicals. N, N, N', N'-tetramethyl-P-phenylene-diamineDI HCl was from K & K Laboratories. n-Hexane was procured from Merck. Lubrol WX was procured from I.C.I. Organics, Inc. Medium 199 was obtained from DIFCO. NCS tissue solubilizer, L-[3, 5 ^{3}H] tyrosine (49 Ci/mmole), and L-[U ^{14}C] tyrosine (483 mCi/mole) were purchased from Amersham-Searle. Alprenolol HCl and [^{3}H] alprenolol HCl (527 mCi/mmole) were a gift from Hassle. [2-^{14}C] hexobarbital (8.58 mCi/mmole) was purchased from New England Nuclear. p-Hydroxyphenyl-[carboxy-^{14}C]-pyruvate was kindly provided by Dr. J.H. Fellman. bis-(Trimethylsilyl)acetamide (BSTA) was obtained from Aldrich Chemical Co. L-cysteine HCl was purchased from the California Foundation for Biochemical Research. p-bis-[2-(5-Phenyloxazolyl)]-benzene (POPOP) was from Research Products International Corporation. Lab-trol protein standard was obtained from Dade. Phenobarbital ("Luminal") was purchased from Winthrop Labs. Sodium pentobarbital ("Nembutal")was purchased from Abbott. Sodium chloride for biological work was obtained from Merck. All other chemicals were common laboratory reagents.

Pyruvic acid, lactic acid, NAD^+, NADH, $NADP^+$, NADPH, ATP, ADP, AMP, POP, firefly lanterns, collagenase, hyaluronidase, pyridoxal phosphate and pHPP were stored desiccated at -20°C. Homogentisate, 2-oxoglutarate, phenylpyruvate, BSTFA and BSTA were stored, desiccated, at 4°C. GDH, LDH, PK, MK and keto-enol tautomerase were stored at 4°C.

II.A.2. Solutions

Distilled and deionized water was used throughout. Solutions were prepared fresh for each experiment with the exception of phosphate buffers, Hank's solution, 2% Trypan Blue, and solutions for protein determinations by the Lowry method. Phosphate buffers were prepared from 0.2 M monobasic and 0.2 M dibasic sodium phosphate. Calcium and glucose free Hank's medium (modified Hank's medium) was prepared fresh for each preparation from stock solutions maintained at 4°C containing 1 ml chloroform/liter. Fifty ml stock A (160 gm NaCl, 8 gm KCl, 4 gm $MgSO_4$) plus 50 ml stock B (0.96 gm Na_2HPO_4, 1.2 gm KH_2PO_4, 7.0 gm $NaHCO_3$) were diluted to one liter with distilled water then bubbled with 95% oxygen, 5% CO_2 for at least 30 minutes to remove the chloroform and to adjust the pH. A stock solution of 2% trypan blue in 150 mM phosphate buffer (pH 7.0) was maintained at 4°C. Solutions for protein determination by the Lowry method (see Section II.B.1.) were maintained at room

temperature with the exception of the phenol reagent, which was stored at 4°C.

II. A. 3. Gases

Chemically pure carbon monoxide was obtained from Matheson Gas Products. All other gases were obtained from Liquid Air, Inc. Gases used for the oxystat ranged from 95% O_2, 5% CO_2 to 95% N_2, 5% CO_2. Ninety-five percent O_2, 5% CO_2 was used for equilibration of Hank's solution and liver perfusion. One hundred percent O_2 was used in the preparation during the second incubation and also for assay of homogentisic acid oxidase. Air and 1.98% O_2 were used as standards for electrode calibration.

II. A. 4. Biological Materials

Male Sprague-Dawley rats, 200-300 gm, were used for all hepatocyte preparations. The rats were maintained at least one week under constant conditions by the University of Oregon Health Sciences Center Animal Care prior to use for experimentation. Care was taken to prevent exposure to antibiotics, pesticides, and disinfectants. Animals were fed ad libitum and maintained in a constant day-night cycle.

Beef heart was obtained fresh from a local slaughterhouse. Baker's yeast was a commercial variety purchased locally.

II. B. Assays

II. B. 1. Total Protein

Total protein was estimated by the method of Lowry et al. (1951) on the acid precipitable fraction. Protein was precipitated by addition of 0.3 ml H_2SO_4/ml protein solution, and centrifuged. The precipitate was solubilized by addition of an accurate volume of 1 NaOH, using a volume to give a final protein concentration of about 3 mg/ml. Samples (10 µl) were then diluted to 0.2 ml with distilled water and protein standards (10-100 µl) were prepared in 0.2 ml volume. Solution B (1 ml 1% $CuSO_4 \cdot 5H_2O$) was then mixed with 1 ml solution C (2.6% sodium potassium tartrate$\cdot 4H_2O$) and 1 ml of this mixture rapidly stirred into 50 ml solution A (2% $NaCO_3$ in 0.1 N NaOH) to give solution D. Solution D (1.0 ml) was then added to each tube containing 0.2 ml standard or sample; the tubes were mixed on a vortex mixer and allowed to stand 10 min at room temperature before addition of 0.1 ml phenol reagent (1 M). After incubation for 45 min at room temperature, optical density was read at 700 nm. Protein in unknowns was then expressed relative to the Labtrol standard.

II. B. 2. Adenylates

Quantitation of Adenylates. Adenylates were measured by a modification of the luciferase assay of Stanley and Williams (1969) or

by the fluorometric method of Williamson and Corkey (1969). Aliquots were deproteinated by addition of ice cold 2N H_2SO_4 (0.3 ml/2 ml sample) and centrifugation. These samples were then frozen in liquid nitrogen until the day of assaying, when they were thawed and neutralized with 1 N NaOH.

ATP was measured by the luciferase assay by addition of 50 µl samples to 1 ml 67 mM arsenate buffer containing 26 mM $MgSO_4$ and crude luciferase (prepared by homogenizing firefly tails, 10 tails/30 ml, directly into buffer and centrifuging 20 min at 16 K in a Sorvall RC2B). Light emission was measured at 560 mM after 60 sec, in an Aminco spectrophotofluorometer.

ADP was determined by measuring ATP resulting from pyruvate kinase conversion of ADP to ATP in the presence of phosphoenolpyruvate (PEP). Five hundred µl neutralized sample was incubated one hour with 100 µl of 250 mM glycylglycine buffer (pH 7.4) containing 0.6 mM $MgSO_4$, 14 mM KCl, 1.75 mg PEP/ml and 75 µg pyruvate kinase/ml. Five hundred µl of the incubate was mixed with 500 µl H_2O, added to 1 ml arsenate buffer, and light emission of the ATP luciferase reaction was measured as above. ADP was quantitated by subtracting the ATP in the sample (as determined above) from the measured ATP + ADP. AMP was determined by converting all adenylates to ATP with pyruvate kinase, myokinase, and PEP, and measuring with luciferase as above. ATP and ADP values were

subtracted from total adenylates to give the AMP level. AMP and ADP were converted to ATP by incubating under the same conditions as for the ADP alone, except that myokinase (20 µl/incubation) was added.

The fluorometric assay utilized the same enzymes for conversion of AMP and ADP to ATP as for the luciferase assay. The assay was performed by mixing 10-50 µl samples, 2 ml of 50 mM glycylglycine buffer (pH 7.4) containing 10 mM $MgCl_2$ and 5 mM EDTA, 10 µl of 1 M glucose solution, and 10 µl of $NADP^+$ solution (10 mg/ml). The fluorescence was then measured (excitation wavelength, 340 nm; emission wavelength, 465 nM) to serve as blank. Five microliters of the enzyme solution was then added (hexose, 2 mg/ml; glucose-6-phosphate dehydrogenase, 0.2 mg/ml). The fluorescence change was then observed until it stabilized (3-4 min) and recorded. Quantitation was obtained from a standard curve.

To test for the completeness of conversion, standard mixtures of ADP and AMP were incubated and assayed as above. As a further test for complete conversion and to check the purity of standards, samples were assayed by thin-layer chromatography according to the method of Randerath and Randerath (1967). Samples were spotted on PEI cellulose 300 plates (Brinkman Instruments) and run for two hours in 1 N LiCl and 1 N acetic acid, then examined under ultraviolet light.

Adenylates were quantitated spectroscopically using the millimolar extinction of 15.4 at 259 nm (Bock et al., 1956) on a Cary 14 recording spectrophotometer.

II. B. 3. Lactic Acid

The enzymatic assay of lactic acid described by Loomis (1961) was used. This assay is based upon the reduction of NAD^+ to the fluorescent NADH by lactate dehydrogenase in the presence of lactate. Deproteinated samples and standards were added to 20 ml tubes and brought to 0.1 ml volume. One milliliter 0.1 M glycine buffer (pH 10.5) containing 50 mg semicarbazide/ml, 0.5 mg lactate dehydrogenase/ml, and 2.0 mg NAD^+/ml was added to each tube with mixing and allowed to stand at room temperature for 90 min. Fifteen milliliters of 20 mM NaOH containing 0.1 mM EDTA was then added to each tube and read in an Aminco Spectrophotofluorometer at 360 nm excitation and 450 nm emission.

II. B. 4. Pyruvic Acid

Pyruvic acid was measured by the method of von Korff (1969). Deproteinated and neutralized sample (0.1 to 0.5 ml) was added to 0.3 ml phosphate buffer (100 mM, pH 7.4) plus 0.1 ml NADH solution (4 mg/ml), and sufficient water to give 2.99 ml. Optical density at 340 nm was then recorded. Ten µl phosphate buffer (100 mM, pH 7.4) containing lactic dehydrogenase (1 mg/ml; at least 100 I.U./mg) was then added and the change in absorbance at 340 nm observed. The pyruvate concentration in the samples was then calculated relative

to similarly run pyruvate standards. A pyruvate standard approximately 1 mM was used.

II.B.5. Tyrosine and Tyramine

Tyrosine and tyramine were assayed by the fluorometric method of Waalkes and Udenfriend (1957). For tyrosine, deproteinated samples were diluted to 1 ml with water. One milliliter of 0.1% 1-nitroso 2 naphthol in 95% ethanol and 1 ml nitric acid reagent (24.5 ml of 1:5 nitric acid + 0.5 ml 2.5% $NaNO_2$) were added. The tubes were mixed and incubated at 55°C for 30 min. Ten milliliters of ethylene dichloride was added to each tube to extract the unchanged nitrosonaphthol. The tubes were shaken and centrifuged. The aqueous supernates were decanted and assayed in an Amino-Bowman spectrophotofluorometer with an activation wavelength of 460 nm and emission wavelength of 570 nm. Quantitation was made against tyrosine standards in the range of 0.35-15 μg. Tyramine was initially extracted into 10 volume isoamyl alcohol after adjusting the pH of the sample to 0.6 as described by Udenfriend and Cooper (1952). The tyrosine was then returned to an aqueous phase for assay by adding an equal volume of n-hexane to the isoamyl alcohol and shaking with 0.2 N HCl.

II. B. 6. Gas Chromatography of Phenolic Acids

Cell incubations were deproteinated by addition of 0.15 ml 2 N H_2SO_4/ml incubate followed by centrifugation. Phenolic acids were extracted with three washes of 2 volumes ethyl acetate. The ethyl acetate was dried with anhydrous sodium sulfate. The solvent was then evaporated with a flash evaporator until only about 1 ml remained. This volume was transferred to a small test tube along with two 1-ml washes of the round bottom flask. The remaining solvent was then evaporated under a stream of nitrogen gas. Silylation was then performed by addition of 100-200 µl bis(trimethylsilyl) trifluoroacetamide (BSTFA) directly to the residue and heating for 30 min at 60°C.

Suitable aliquots were chromatographed on an F & M model 810 DR-12 instrument equipped with a 12' SE 30 column and a hydrogen flame detector. Column temperature was programmed to increase 4°/min from 140°C to 210°C. Quantitation was done relative to known standards and corrected for losses during extraction by addition of p-hydroxyphenylacetic acid as an internal standard to the initial acidified sample.

II. B. 7. p-Hydroxyphenylpyruvic Acid (pHPP)

pHPP was assayed by gas chromatography as described above and by the method of Diamondstone (1966). The method of

Diamondstone is based upon the conversion of p-hydroxyphenylpyruvic acid to p-hydroxybenzaldehyde in strong alkali. pHPP is extracted from acidified sample with two washes of 2 volumes ethyl acetate. pHPP is then returned to the aqueous phase by shaking the organic phase with 200 mM phosphate buffer (pH 8.0); 0.1 ml NaOH is added to 1 ml of sample and allowed to stand 30 min at room temperature. The strongly absorbing p-hydroxybenzaldehyde is then measured at 331 nm. The working millimolar extinction, 19.9, of Diamondstone was used for quantitation. Assay of standard pHPP and correspondence of this method with the gas chromatographic method confirmed this value.

II.B.8. Homogentisic Acid (HG)

Homogentisic acid was assayed by gas chromatography as described above and by the colorimetric assay of Fellman et al. (1972). This assay measures the chromophoric thiazine produced by the reaction of p-quinones with cysteine.

Homogentisic acid was extracted from incubations by two washes with 2 volumes ethyl acetate. Homogentisate was then returned to the aqueous phase by shaking the ethyl acetate with 200 mM potassium phosphate buffer (pH 8.0). The ethyl acetate was discarded and 0.2 ml of 1 M KBH_4 was added to a 1-ml aliquot of the aqueous phase. After 10 min, excess KBH_4 was destroyed by addition of

0.1 ml of 5 M acetic acid. The chromophoric 1, 4-thiazine was then formed by the addition of 0.2 ml of 200 mM cysteine and 3 ml of 500 mM potassium phosphate (pH 12.0). After 15 min the optical density at 390 nm was read. Quantitation was done relative to homogentisate standard.

II. B. 9. Glutamic Acid

Glutamic acid was measured by the fluorometric method of Williamson and Corkey (1969). This assay is based upon the glutamic dehydrogenase catalyzed oxidative deamination of L-glutamate to 2-oxoglutarate and NH_4^+ which is coupled to the reduction of NAD^+ to NADH. Buffer (1.9 ml; 0.1 M tris base, 0.4 hydrazine hydrate, 10 mM $MgCl_2$, 5 mM EDTA, pH 8.5) plus 0.1 ml deproteinated sample and 10 µl NAD^+ (80 mg/ml) was mixed in fluorometric cuvette and fluorescence emission at 450 nm was recorded using 360 nm excitation. Glutamic dehydrogenase (20 µl; 10 mg/ml, 3 U/mg) was then added and increase of fluorescence recorded. After attaining a constant reading (5-10 min) an additional 20 µl glutamic dehydrogenase was added to allow for correction of increased fluorescence due to binding of NADH to the enzyme. After a constant reading was again attained, 10 µl standard glutamate solution (0.5 mM) was added, and glutamate concentration in the sample was calculated relative to the standard.

II. B. 10. 2-Oxoglutarate

2-Oxoglutarate was measured by the method of Williamson and Corkey (1969) based upon the reversible glutamic dehydrogenase catalyzed oxidative deamination of l-glutamate to 2-oxoglutarate and NH_4^+ coupled to the reduction of NAD^+ to NADH. Buffer (1.9 ml; 100 mM potassium phosphate, pH 7.0), 100 µl deproteinated sample, 10 µl NADH (1 mg/ml) and 5 µl $(NH_4)SO_4$ (5 M) were mixed in a cuvette and fluorescence was recorded at 450 nm, with 360 nm excitation. Ten microliters of glutamic dehydrogenase (20 mg/ml, 3 U/mg) was then added and fluorescence decrease recorded. After reaching a constant fluorescence, 10 µl of glutamic dehydrogenase was added to allow for correction of fluorescence due to binding of NADH to the enzyme. 2-Oxoglutarate standard (1-10 µl; 0.1 mM) was added and fluorescence recorded. 2-Oxoglutarate concentration in the sample was calculated relative to the standard.

II. B. 11. Hexobarbital (5-(1-cyclohexen-1-yl)-1,5-dimethylbarbituric acid)

Hexobarbital metabolism was measured by the radiochemical method of Gerber et al. (1971). ^{14}C hexobarbital (8.58 mCi/mmole) was diluted just prior to use to 61 µCi/mmole with hexobarbital at a final concentration of 20.5 mM sodium phosphate, pH 11.3. Aliquots of this stock were then added to incubations to provide the desired

hexobarbital concentration. Hexobarbital is readily soluble under these conditions at room temperature but insoluble at 0°C. Autoxidation, followed by decrease in absorbance at 245 nm, was found to occur under these conditions at 0.78%/hour, thus necessitating fresh hexobarbital for each experiment. Radiochemical purity of ^{14}C hexobarbital was determined to be 99% by thin-layer chromatography on precoated silica gel plates in 9:1 (v/v) chloroform/acetone (Kupfer and Rosenfeld, 1973). Partitioning of the radiolabel between 1-chlorobutane and 100 mM phosphate buffer (pH 6.8) was found to be 9.0.

Amount of hexobarbital converted to polar products was measured by scintillation counting of aliquots of the aqueous phase after extraction of the polar substrate with 1-chlorobutane. Two to 4 ml incubation samples were quenched by pipetting into 50 -ml extraction tubes containing 10 ml 1-chlorobutane plus sufficient 100 mM phosphate buffer, pH 6.8, to give a 1:1 volume ratio of organic to aqueous phase. Following vigorous shaking for 1 min, the tubes were centrifuged and 6 ml of the organic phases transferred to a second series of tubes containing 6 ml 100 mM phosphate buffer (pH 6.8). The remaining 1-chlorobutane was aspirated away and 10 ml fresh 1-chlorobutane was added per tube for a second washing. Both series of tubes were shaken vigorously, centrifuged, and re-extracted in a similar fashion. The resultant aqueous phase contained polar

products with 99.9% of the unreacted substrate removed, and the resultant 1-chlorobutane phase contained unreacted substrate with 99.9% of the products removed (Gerber et al., 1971). From each, 0.1 ml of aqueous phase was added to 0.5 ml NCS tissue solubilizer (Amersham-Searle) and 10 ml toluene-PPO-POPOP in a scintillation vial, and similarly 4.0 ml of each 1-chlorobutane phase was added to 10 ml toluene-PPO-POPOP in a scintillation vial. Samples were counted in a TriCarb Scintillation Counter. Counting efficiency was determined by addition of ^{14}C toluene standards and by automatic efficiency ratio determination using quenched ^{14}C toluene standards. Counting efficiency for aqueous samples was 92.0% and for 1-chlorobutane samples was 86.5%. Corrections for metabolite and substrate partitioning during the washes was made by utilizing partition coefficients, 9.0 for hexobarbital and 0.09 for ketohexobarbital (Gerber et al., 1971).

II.B. 12. Phenyramidol (2-(β-hydroxyphenethylamine)pyridine)

The metabolism of phenyramidol hydrochloride was measured by the method of Gerber et al. (1974). Phenyramidol hydrochloride (0.20 ml, 4.0 mM) was added to 8.0 ml cell suspension ($2-3 \times 10^6$ cells/ml) and incubated for desired period of time (0-50 min). Samples (1.0 ml) were then pipetted into 50 ml extraction tubes containing 9 ml 100 mM phosphate buffer (pH 6.8) plus 10 ml

1-chlorobutane. Tubes were shaken vigorously for 1 min, centrifuged, and 9 ml of the organic phase transferred to an additional series of tubes containing 2 ml 0.1 N HCl. The tubes were shaken vigorously for 1 min, centrifuged and the aqueous phase examined spectrophotometrically between 330 and 280 nm in a Cary 14 spectrophotometer. The absorption maximum of phenyramidol at 308 nm has a millimolar extinction of 6.59 (Gerber, 1974). The amount metabolized was calculated relative to a zero time control with this extinction value; 90.9% of the unreacted drug was recovered in the acid fraction as determined by zero time controls.

II. B. 13. Alprenolol (1-(2-allyl-phenoxy)-3-isopropylaminopropanol)

The metabolism of alprenolol was determined by the method of Moldeus et al. (1974). ^{3}H alprenolol (0.53 Ci/mmole) was diluted to 1.8 mCi/mmole at a final concentration of 1.4 mM just prior to each experiment. This stock (0.2 ml) was added to 6.0 ml incubation mixture to give a final concentration of alprenolol equal to 45 μM. After incubation, 4.0 ml was pipetted into 1.0 ml 2.5 N NaOH and stirred on a vortex mixer. Ten milliliters n-hexane was then added, the tubes shaken vigorously for 1 min and then centrifuged. One milliliter of the n-hexane phase was then added to a scintillation vial containing 10 ml toluene-PPO-POPOP cocktail and counted.

Ninety-five percent of the alprenolol was extracted as determined by zero time controls. Alprenolol metabolized was calculated by substrate loss relative to zero time samples.

II. B. 14. Lactic Dehydrogenase

Lactic dehydrogenase activity was determined spectrophotometrically by the method of Kornberg (1955). Samples were homogenized and maintained on ice until assay. A suitable aliquot to give a change in optical density of 0.02 to 0.05 per minute was added to a 3-ml cuvette containing 0.1 ml of 10 mM sodium pyruvate, 0.1 ml of 2 mM NADH, 1.0 ml of 100 mM phosphate buffer (pH 7.4) and water to make a total volume of 2.0 ml. The rate of change of OD_{340} was determined on a Cary 14 recording spectrophotometer and the activity expressed as the specific activity (units/mg protein) where a unit of activity is the amount which causes a change of OD_{340} of 6.2/min at room temperature.

II. B. 15. Tyrosine Aminotransferase

Tyrosine aminotransferase activity was measured spectrophotometrically by the method of Lin and Knox (1958). Homogenized sample (50 µl) was mixed with 3 ml 0.67 M borate buffer (pH 8.0) containing tyrosine (3.5 mM), diethyldithiocarbamate (3 mM), and keto-enoltautomerase (0.5 U/ml). 2-Oxoglutarate (7 mM) was added.

Homogenized and centrifuged sample (50-100 µl) was mixed and the rate of increase in optical density at 310 nm due to the formation of the borate enol complex of p-hydroxyphenylpyruvate was recorded. The rate of formation of pHPP was then determined using 9850 as the molar extinction coefficient for this complex.

II. B. 16. p-Hydroxyphenylpyruvic Acid Oxidase

This enzyme was assayed by two methods of Fellman et al. (1972). The radiochemical assay based upon the evolution of $^{14}CO_2$ from p-hydroxy (carboxy-^{14}C)phenylpyruvic acid was performed using 1.25 mM 2, 6-dichloroindophenol and 26 mM GSH as activators. Aliquots of homogenized cells were incubated for 5 min at 37°C with activators in 1.5 ml volume in a specially stoppered single-arm Warburg vessel. The stopper was embedded with a 1.5 cm pin holding an 11 mm diameter disk of Whatman #4 filter paper moistened with 0.25 ml hyamine hydroxide in methanol. p-Hydroxy(carboxy-^{14}C)phenylpyruvate (0.5 ml, 2 mM) was then tipped in from the side arm. The mixture was incubated for 10 min at 37°C and 0.3 ml 2 N H_2SO_4 was added. Ten minutes were allowed for equilibration and the discs were transferred to scintillation vials containing 19 ml Buhler's solution for counting. The amount of $^{14}CO_2$ evolved was then used to calculate the activity of pHPP oxidase in the cells. Homogentisic acid production from p-hydroxyphenylpyruvic acid was

assayed by a method based upon the reaction of p-quinones with cysteine to produce a chromophoric thiazine. Cells or tissue were homogenized in 100 mM phosphate buffer (pH 7.3). The pH was then adjusted to 5 with 5 M acetic acid to destroy homogentisate oxidase activity and readjusted to pH 7.3. The enzyme was then activated by addition of ascorbate to a final concentration of 3.2 mM 5 min prior to assay. Suitable aliquots of the homogenate were then diluted to give 1.5 ml volumes and 0.5 ml of 2 mM pHPP was added immediately prior to incubation at 37°C. After 10 min 0.5 ml 0.8 M sulfosalicyclic acid was added to each tube to stop the reaction and deproteinate the incubation. The tubes were centrifuged to remove protein, and 1 ml of each was transferred to 15 ml extraction tubes for two extractions each with 2 volumes of ethyl acetate. The extracts were combined and 1 ml 0.2 M potassium phosphate buffer (pH 8.0) was added with shaking. The ethyl acetate was discarded and 0.2 ml of 1 M KBH_4 was added. After 10 min, excess KBH_4 was destroyed by addition of 0.1 ml of 5 M acetic acid. The chromophoric 1, 4-thiazine was then formed by the addition of 0.2 ml of 200 mM cysteine and 3 ml of 500 mM potassium phosphate (pH 12.0). After 15 min the optical density was read at 390 nm against optical density zero time blanks. Quantitation was done relative to homogentisic acid standards.

II. B. 17. Homogentisic Acid Oxidase

Homogentisic acid oxidase activity was determined by following production of maleylacetoacetate. The increase in absorbance at 330 nm upon addition of homogentisic acid (13 mM, 100% O_2, 200 mM phosphate buffer, pH 7.2) was measured. The molar absorbance coefficient of 1.4×10^4 was used (K. Adachi et al., 1966).

II. B. 18. Glucose Synthesis from Pyruvate

Rats were starved for 24 hours to deplete the livers of glycogen; cells were prepared in the normal manner as described below. Cell suspensions were incubated for 40 min at 37°C in modified Hank's medium containing bovine serum albumin (15 mg/ml) and 10 mM pyruvate. Controls were run without pyruvate. The synthesis was stopped and the suspension deproteinated by addition of 0.15 ml 2 N H_2SO_4/ml, then centrifuged. One milliliter of the suspension was added to 8.0 ml of 0.2 M K_2HPO_4 and neutralized with 10% NaOH. The volume was then adjusted to 10 ml with water. Glucose was determined polarographically with glucose oxidase (1 mg/ml) and catalase (0.1 mg/ml) or fluorometrically by coupling the reduction of $NADP^+$ to glucose content with hexokinase and glucose-6-phosphate dehydrogenase (see Quantitation of Adenylates, p. 133).

II.C. Preparations

II.C.1. Isolated Hepatocytes

Isolated hepatocytes have been prepared for biochemical studies for many years (Anderson, 1953; Branster and Morton, 1957; Jacob and Bhargava, 1962; Kaltenback, 1954; Longmuir and Rees, 1956), but perturbed morphology and metabolism limited their experimental use. Improvements in methodology, primarily the selection of suitable enzymes for cellular dispersal and hydrolysis of connective tissue (Howard et al., 1967; Lasfargues, 1957) and introduction of these enzymes by vascular perfusion (Berry and Friend, 1969) allowed isolation of cells which retain most metabolic functions present in perfused organs and in vivo. The enzymes collagenase and hyaluronidase are introduced by continual reperfusion until the liver cells can be readily dispersed with a blunt spatula. The improved cell preparation has instilled confidence in the use of isolated hepatocytes for metabolic studies (Krebs et al., 1974). Within five years of the publication of the improved method (Berry and Friend, 1969), the isolated cells had been used for studies of respiration and energy metabolism (Berry, 1971; Quistorff et al., 1973; Wilson et al., 1974), gluconeogenesis (Berry, 1974; Berry and Kun, 1972; Williamson et al., 1974), protein synthesis (Ingebratsen and Wagle, 1972; Schreiber and Schreiber, 1972; Weigard et al., 1971), drug

metabolism (Moldeus et al., 1974), lipid metabolism (Berry and Werner, 1974; Goodridge, 1973), hormone response (Johnson et al., 1972), and membranal permeability (Quistorff et al., 1973).

Hepatocytes are complex and fragile; during isolation, they undergo perturbations due to mechanical, chemical, thermal and enzymatic insults. Consequently, stringent tests must be applied to determine their functional integrity, and criteria must be established to compare preparations from different laboratories. As previously stated, hepatocytes compare very well to tissue preparations. Different laboratories have obtained consistent findings for a variety of parameters. The properties which have received widest application for characterization include 1) trypan blue exclusion, 2) respiratory rate, 3) gluconeogenic rate, and 4) lactic dehydrogenase content. These criteria are not comprehensive, yet they provide at least minimal characterization of the metabolic integrity of a preparation.

I.C.1.a. Preparation. Two methods of cell preparation were tested. The recirculating perfusion method was found to be superior to the cell slice method and therefore used in all metabolic studies.

The recirculating perfusion method of Berry and Friend (1969) was used for cell preparation. Male Sprague-Dawley rats (200-300 gm) were maintained in a constant environment and fed ad libitum for at least one week prior to use. Cell preparations were routinely begun between 9 and 10 a.m. Rats were anesthetized with ether; the

peritoneal cavity was opened, and the portal vein was cannulated. Perfusion (10 ml/min) was begun immediately with a Sigmamotor Pump using two tubes through the pumping mechanism with pulsations out of phase so that pressure fluctuations were eliminated. The perfusion medium, modified Hank's buffer, was equilibrated with 95% O_2-5% CO_2 by continual bubbling through the solution contained in a beaker held at 37°C in a closed container. The chest was rapidly opened and the inferior vena cava cut in order to prevent excessive pressure in the liver. The inferior vena cava was ligated just above the level of the renal veins. The liver was transferred to a beaker containing the perfusion medium so that the perfusate was returned to the beaker and allowed an "open" recirculating system. This method was preferred over a closed system since only one cannulation was required. The volume of buffer was adjusted to about 100 ml and 50 mg collagenase (Type I, Sigma) and 100 mg hyaluronidase (Type I, Sigma) were added. The perfusion was continued for 30 min with constant bubbling of the solution with 95% O_2-5% CO_2. The liver was transferred to another beaker containing 50 ml fresh enzyme solution, readily dispersed into a cell suspension with a blunt spatula, transferred to an Erlenmeyer flask and incubated for 15 min at 37°C under 100% oxygen in a Gyrotory shaking incubator. The suspension was filtered through two layers of nylon mesh, centrifuged at 50 g for 3 min, and the pellet was resuspended in ice cold enzyme free

buffer. The cells were recentrifuged twice; the final suspending media was that desired for further studies.

Special precautions were required for removal of hemoglobin from cells for spectral work. Clotted blood was carefully removed from the liver after perfusion, and the liver washed externally with buffer before dispersal. Portions of the liver which appeared inadequately perfused as judged by a "reddish" color were discarded. Care was taken not to transfer buffer from the perfusion to the 50 ml incubation. Red blood cells normally pellet on top of hepatocytes, so following each centrifugation the top portion of the pellet was carefully removed with a spatula and discarded to eliminate red blood cells which may have remained. These precautions usually provided hepatocytes free from detectable hemoglobin as measured by the Hb CO minus Hb O_2 absorbance difference at 418 nm.

In the cell slice method (Goodridge, 1973), male Sprague-Dawley rats (200-400 gm) were fed ad libitum for at least one week prior to use. Cell preparations were routinely begun between 9 and 10 a.m. Rats were knocked unconscious and weighed. The peritoneal cavity was opened and the inferior vena cava cut. The liver was perfused through the spleen with 6 ml ice cold modified Hank's buffer equilibrated with 95% O_2-5% CO_2, and containing hyaluronidase (1 mg/ml), collagenase (0.5 mg/ml) and streptomycin sulfate (0.1 mg/ml). The liver was removed, weighed and placed in ice cold modified

Hank's buffer until sliced into 0.75 mm sections (not more than 5 min). The slices were placed into 50 ml Erlenmeyer flasks (2-3 gm/flask) containing 10 ml of the enzyme solution used in the perfusion. The flasks were flushed with 95% O_2-5% CO_2, sealed loosely, and placed in a Dubnoff incubator (120 shakes/min) at 37°C. After 20 min, the flasks were flushed with 100% O_2 (the CO_2 produced during the incubation is sufficient to maintain buffer below pH 7.4). After incubating a total of 40 min, the flasks were placed on ice. The tissue was gently dispersed with a glass rod, filtered through two layers of nylon mesh and centrifuged at 500 x g. The pellet was resuspended in ice cold modified Hank's buffer by gentle agitation with a glass rod. The cells were recentrifuged and washed in this manner a total of three times. The final pellet was resuspended in 10 ml of the buffer used in subsequent experiments, transferred to a tared tube for weighing (to obtain an accurate final volume) and maintained on ice until use.

Isolation of hepatocytes by the perfusion method became "routine" only after about 15 preparations were attempted. The simpler tissue slice method was attempted a few times and considered an inferior preparation for the reasons discussed below. However, perfusion preparations had aberrant characteristics about 5% of the time: low cell viabilities, low cell yields, slow centrifugation at 50 g, massive cell debris which continually aggregated upon storage

on ice, and rapid loss of cell viability upon storage on ice. The cause was not clear. These preparations were discarded.

The routine preparation took about 2-2 1/2 hours from anesthetizing the animal to obtaining isolated and washed cells. All materials and equipment were prepared in advance, usually the day before, with the exception of temperature and gas equilibration. The greatest difficulty in preparation was cannulation of the portal vein, especially in the phenobarbital and 3-methylcholanthrene treated rats. This step was simplified by obtaining assistance from other lab members for tying the cannula in the vein. On occasions when cannulation of the portal vein was unsuccessful or not possible, cannulation of the inferior vena cava and ligation of the inferior vena cava superior to the renal vein was used. This method was as successful as the other in cell yield and viability, but generally resulted in greater hemoglobin contamination.

Inclusion of phenol red and streptomycin sulfate in the perfusion and incubation medium were found to be nonessential if care was taken in pH control and in surgery. Perhaps most important in surgery was avoidance of piercing the digestive tract and careful washing of liver with buffer prior to incubation.

II.C.1.b. Characterization of Hepatocytes. Initial characterization of isolated hepatocytes was performed to determine that preparations were similar to those reported in the literature and that

properties from different preparations were consistent. A sample data sheet for this characterization is given in Appendix II. Results are given in Table II-A. A comparison of characteristics of cells prepared by the two procedures is given in Table II-B.

Light Microscopy: Cells prepared by the perfusion method previously described were suspended in Kreb's Ringer phosphate buffer (pH 7.4) containing 0.2% trypan blue. The cell concentration was about 10^6 cells/ml, since higher concentrations led to rapid aggregation of the microscope slide. Micrographs were taken on a Zeiss light microscope equipped with a 35 mm camera, at 64X magnification (Figure II-1). Cells rapidly aggregated when illuminated for photography, apparently due to the heat from the lamp.

Electron Microscopy: Isolated hepatocytes were prepared as previously described. The final pellet of isolated cells was suspended in 70 mM cacodylate buffer (pH 7.4, $0^{\circ}C$) containing 1.4% glutaraldehyde, 1% para-formaldehyde, 3% glucose and 25 mg% $CaCl_2$, and allowed to stand on ice for 15 min with occasional gentle swirling. Cells were allowed to settle, the supernatant was decanted, and cells were washed in 50 mM cacodylate buffer (pH 7.4, $0^{\circ}C$) containing 4.5% glucose. The supernatant was decanted and the cells were fixed for 1 hour in the same buffered glucose solution containing 1% osmium tetroxide. The supernatant was removed and the cells dehydrated stepwise with 50, 70, 90 and 100% ethanol. Cells were

Table II-A. Characterization of hepatocyte preparation.

Characteristic	N	Mean	1 S.D.	Range
Cell yield	26	2.03×10^8	$\pm 1.83 \times 10^8$	$0.69\text{-}6.93 \times 10^8$
% Excluding trypan blue	26	90.6%	± 2.87%	83.3-95.1
Protein content	28	1.59 mg/10^6 cells	± 0.13	1.36-1.75
$Q_{O_2}^{cell}$ at 37°C in modified Hank's buffer	6	20.1 µl O_2/10^6 cells/hr	± 3.4	16.0-23.7
		(0.9 µmoles/10^6 cells/hr)	(± 0.15)	(0.714-1.06)
$Q_{O_2}^{pro}$ at 37°C in modified Hank's buffer	6	13.8 µl O_2/mg pro/hr	± 1.2	12.4-16.0
		(0.62 µmoles/mg pro/hr	(± 0.05)	(0.554-0.714)

Table II-B. Comparison of liver cells isolated by the liver slice and liver perfusion techniques. (Values ± 1 standard deviation; number of samples in parentheses.)

Criterion	Slice method	Perfusion method
Cell yield	$5.36 \pm 3.00 \times 10^7$ (5)	$2.03 \pm 1.93 \times 10^8$ (26)
Excluding trypan blue (% viability)	65.4 ± 5.5 (5)	90.6 ± 2.9 (26)
Protein/10^6 cells	1.51 ± 0.18 (5)	1.59 ± 0.13 (28)
$Q_{O_2}^{cell}$ at 37°C in GLC-free Hank's buffer + BSA (15 mg/ml) (μl O_2/10^6 cells/hr) (μmole O_2/10^6 cells/hr)	18.1 ± 4.1 (4) (0.808 ± 0.183)	20.1 ± 3.4 (6) (0.9 ± 0.15)
$Q_{O_2}^{pro}$ (same conditions as above) (μl O_2/mg pro/hr) (μmole O_2/mg pro/hr)	11.8 ± 3.2 (4) (0.527 ± 0.143)	13.8 ± 1.2 (6) (0.62 ± 0.05)
ATP (mmoles/kg wet wt, assuming 7.25 mg wet wt/10^6 cells) (as isolated)	0.0032 ± 0.0038 (5)	2.28 ± 0.46 (4)
Adenylate energy charge (as isolated)	0.76 (average) (2)	0.91 (average) (3)
Lactate dehydrogenase activity (units/mg protein) (as isolated)	4.6 (average) (2)	10.7 ± 2.7 (4)
Lactate dehydrogenase activity, % retained in cells after 1 hr	77.6 (average) (2)	92.6 ± 3.1 (4)

Figure II-1. Light micrographs of hepatocytes. Cells suspended in modified Hank's medium containing 0.2% trypan blue. (X300)

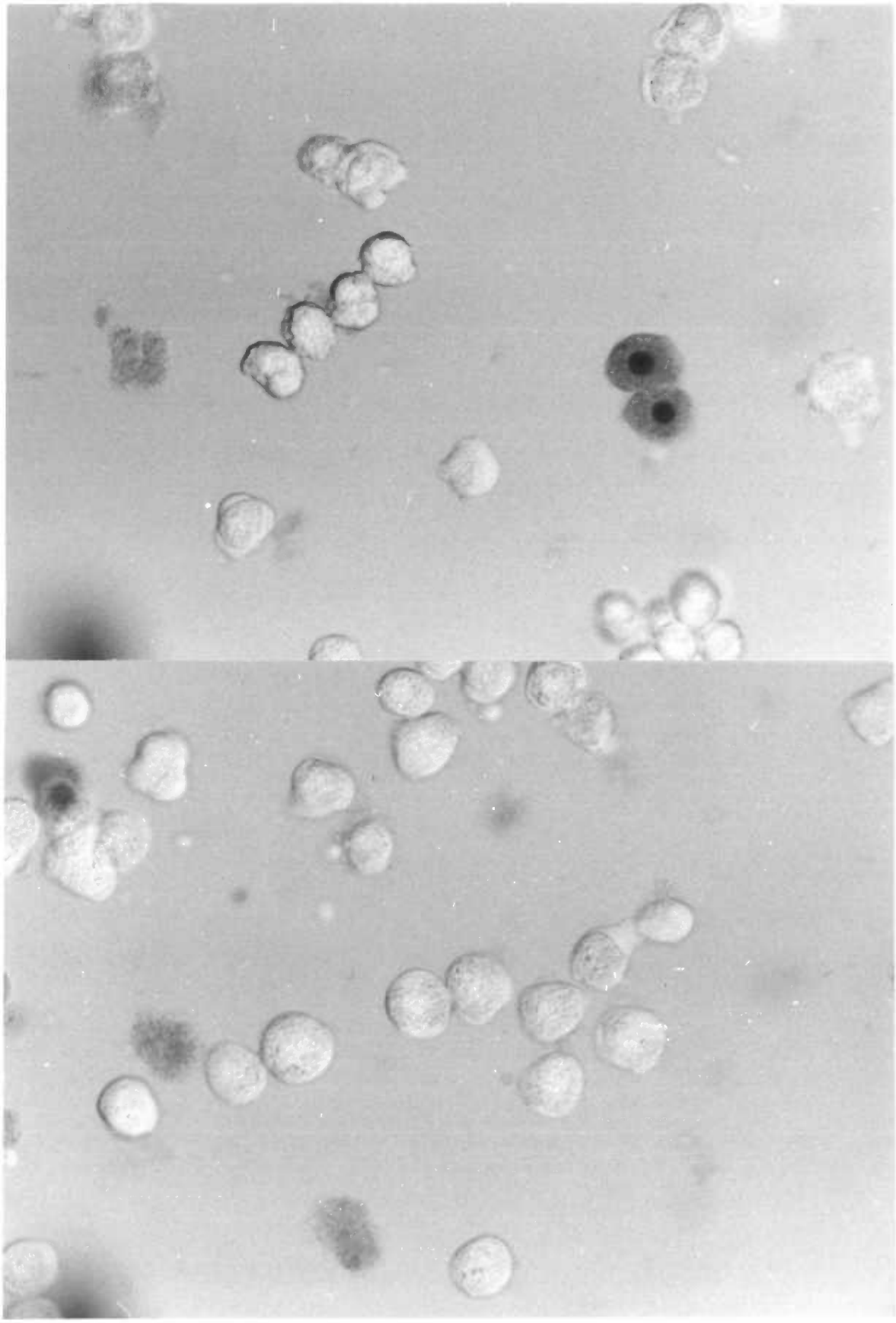

infiltrated with 100% propylene oxide overnight, and Epon 812 was added in steps to give a 50% Epon mixture for 1 hour, a 75% Epon mixture for 3 hours, and finally 100% Epon overnight. Cells were centrifuged to form a pellet and heated at 60°C for 1 week. Thick sections were cut on a LKB Ultratome with glass knives for examination by light microscopy. Thin sections were cut with glass knives as above or with a diamond knife on a Porter-Blum microtome. Thin sections were mounted on 200 mesh copper grids, stained with 1% uranyl acetate, and lead citrate, and studied on a RCA EMU 3-G electron microscope and a Phillips 200 electron microscope (Figure II-2).

The preparation yielded almost entirely parenchymal cells; there was less than 1% contamination by other cell types. Approximately 92% (385/418) of the cells quantitated were intact as judged by cytoplasmic density and membranal integrity (92.9% excluded trypan blue for this preparation). Damaged cells had disrupted membranes, distorted organelles and low cytoplasmic density. Of the intact cells, 9% had small regions of contact with other cells. In intact cells there were no apparent breaks in the plasma membrane. The mitochondria, nuclei, lysosomes, Golgi apparatus and endoplasmic reticulum appeared intact. Occasional dilatation of Golgi complex and small periferal vacuoles were present.

Figure II-2. Electron micrographs of isolated hepatocytes. Cells were prepared for examination as described in text. (X6800)

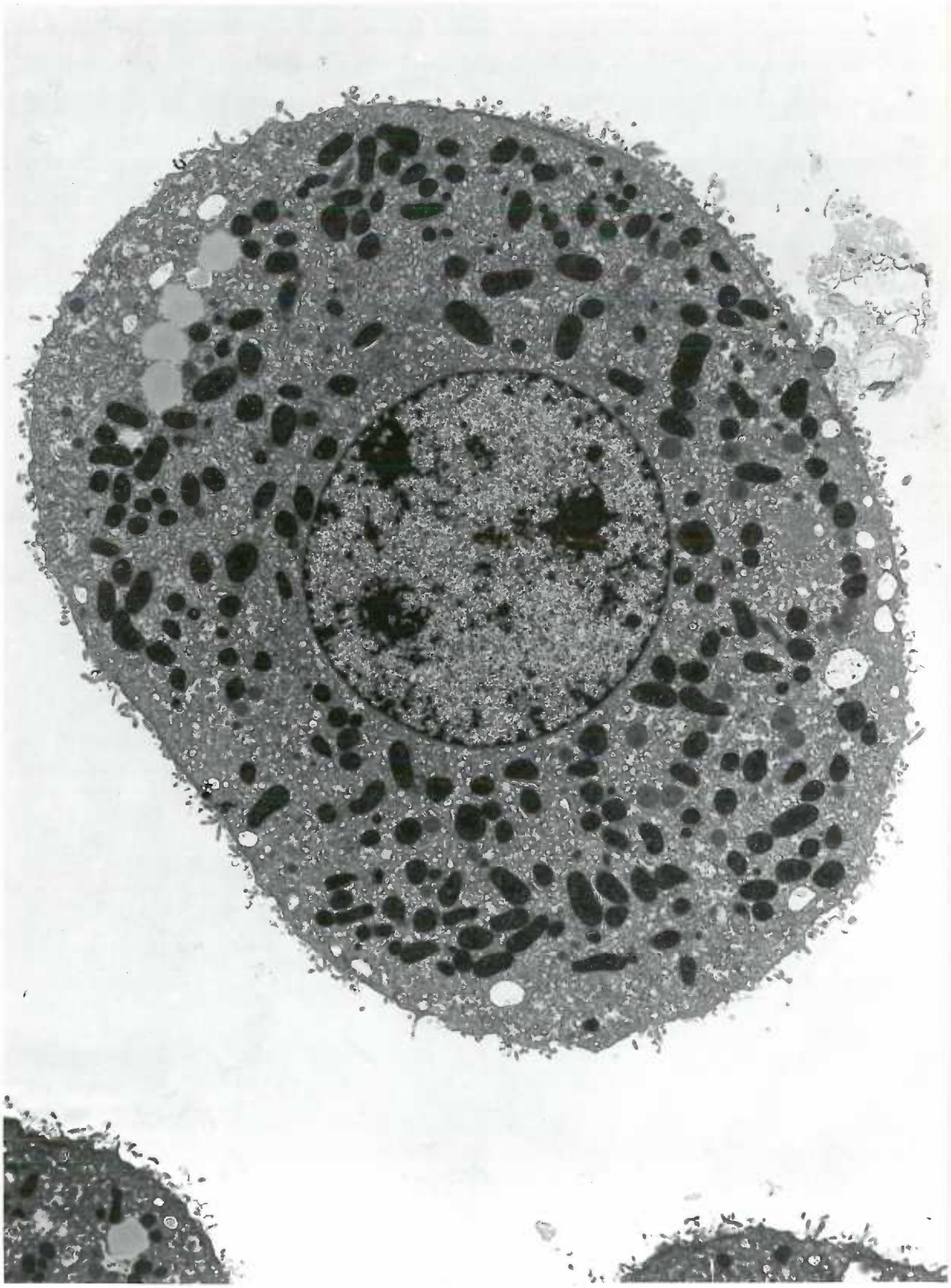

Cell Quantitation and Viability: Total cell number was obtained by counting on a hemocytometer in the presence of 0.2% trypan blue or 0.1% toluidine blue. The percentage of cells excluding the vital dye, trypan blue, is used as an indicator of cell "viability."

Cell yield for the perfusion method calculated for 26 cell preparations was 2.03×10^8 cells/liver. The range of cell yields was 6.90×10^7/liver to 6.93×10^8 cells/liver. The yield was routinely greater than 10^8 cells/liver after selective removal of unperfused lobes before dispersal and of red blood cells during the three washings with modified Hank's solution. Greater yields could be effected by more vigorous dispersal or by elimination of the steps for removal of red blood cell contamination. However, these changes resulted in a more heterogeneous preparation. Cell yield by the tissue slice method was $5.36 \pm 3.00 \times 10^7$ cells for five preparations, and was usually contaminated with hemoglobin even though the livers were perfused with buffer and externally washed prior to preparation. The range was $1.20\text{-}6.60 \times 10^7$ cells/liver.

Trypan blue exclusion was always tested within an hour after after preparation and usually done as soon as the cells were prepared. The attrition rate of cells stored on ice was found to be 2%/hour. The percent of cells excluding trypan blue for cells prepared by the perfusion technique was 90.6 ± 2.9 for 26 preparations. The range was from 83.3% to 95.1%. Initial viability of 88.0% was the cutoff

value for use of cell preparations for metabolic studies. The percent of cells excluding trypan blue for the tissue slice method was 65.4 ± 5.5 for five cell preparations, with a range of 60-74%.

The protein content of the isolated hepatocytes was measured by the method of Lowry et al. (1951) on the acid precipitable fraction (see Section II. B. 1.). The determination of protein on the acid precipitable fraction eliminates many of the acid soluble metabolites which also give a color reaction with the phenol reagent. In addition, solubilization with NaOH eliminates errors in pipetting due to the presence of particulate matter in the sample. The protein content of hepatocytes isolated by the perfusion method for 28 cell preparations was 1.59 ± 0.13 mg/10^6 cells with a range of 1.36-1.75 mg/10^6 cells. The protein content for five cell preparations using the tissue slice method was 1.51 ± 0.18 mg/10^6 cells with a range of 1.33 to 1.76 mg/10^6 cells.

Lactic Dehydrogenase Content: Leakage of cytoplasmic enzymes is characteristic of mechanically damaged cells (Berry and Friend, 1969). The specific activity of lactic dehydrogenase in hepatocytes from four preparations by the perfusion method was 10.7 ± 2.7 units/mg protein (Kornberg, 1955). After incubation at 37°C for 1 hour the cells contained 92.6 ± 2.1% of the original LDH content.

Glucose Synthesis: A more stringent test for metabolic integrity

is the synthesis of glucose from pyruvate (Hems et al., 1966) in hepatocytes prepared from 24 hour starved rats. Cells isolated by the perfusion method were found to synthesize glucose at the rate of 0.314 μ gm/10^6 cells/min (1.74 mmole/10^6 cells/min).

Respiratory Rate: The respiration rate is an important criterion for characterization of hepatocytes and for experimental work at fixed oxygen tensions. The Q_{O_2} for hepatocytes (see Table II-B) at 37°C in modified Hank's solution for six preparations (perfusion method) was 20.1 ± 3.4 μl O_2/10^6 cells/hr (0.90 ± 0.15 μmole/10^6 cells/hr). The range was 16.0 to 23.7 μl O_2/10^6 cells/hr (0.714 to 1.06 μmole/10^6 cells/hr). Calculated according to protein content the Q_{O_2} was 13.8 ± 1.2 μl O_2/mg protein/hr (0.62 ± 0.05 μmole/mg protein/hr) with a range of 12.4 to 16.0 μl O_2/mg protein/hr (0.554 to 0.714 μmole/mg protein/hr). The Q_{O_2} for four cell preparations under the same conditions prepared by the tissue slice method (Table II-B) was 18.1 ± 4.1 μl O_2/10^6 cells/hr (0.808 ± 0.183 μmole/10^6 cells/hr) or 11.8 ± 3.2 μl O_2/mg protein/hr (0.527 ± 0.143 μmole/mg protein/hr).

Integrity of the glycolytic pathway was examined by measuring the effect of added pyruvate on respiration. The reasoning was that a disturbance of this pathway may be reflected by a decreased substrate for oxidative phosphorylation (see Berry and Friend, 1969). No stimulation of respiration was observed upon addition of 10 mM pyruvate to cells prepared by the perfusion method. The intactness

of the cellular membrane and respiratory system is further suggested by the fact that addition of 0.5 mM ADP did not stimulate oxygen consumption.

Isolated hepatocytes from animals starved or treated with phenobarbital or 3-methylcholanthrene were prepared as above. Food was removed from rats 24 hours prior to cell preparation to starve the animals. Phenobarbital induced animals received injections (100 mg phenobarbital (Luminol)/kg) daily at 5 p.m. for four consecutive days followed by a day with no injection and preparation of cells at 9 a.m. on the subsequent day. Thus, the final injection was 40 hours prior to cell preparation. 3-Methylcholanthrene induction was performed similarly with three daily injections (25 mg 3-methylcholanthrene in corn oil (12.5 mg/ml)/kg).

Extensive characterization of hepatocytes isolated from rats starved or treated with phenobarbital or 3-methylcholanthrene was not performed. A comparison of cell yields, viabilities, and protein content of cells from rats given these various treatments is given in Table II-C. Average cell yields were 25 to 40% below the average for fed, non-treated rats. Cell viabilities were comparable for starved and phenobarbital induced, but slightly lower for 3-methylcholanthrene treated rats. The protein content for cells from 3-methylcholanthrene and phenobarbital treated rats was higher than for fed, non-treated rats, while that for cells from starved rats was lower.

Table II-C. Viability and yield of hepatocytes from variously treated animals.

Treatment	Yield	% Excluding trypan blue	Protein (mg/10^6 cells)
None	$2.03 \pm 1.93 \times 10^8$ (26)	90.6 ± 2.9	1.59 ± 0.13
Starvation	1.48×10^8 (1)	91.5	1.40
3-Methylcholanthrene induced	1.21×10^8 (3)	88.5	1.72
Phenobarbital induced	1.39×10^8 (3)	92.0	1.96

II.C.2. Microsomes

Microsomes were prepared essentially by the method of Omura and Sato (1964). Rats were sacrificed by a blow on the head. The inferior vena cava was cut and the liver perfused with a 6-ml ice cold normal saline. The liver was removed, washed in isotonic KCl and minced in four volumes KCl with scissors. The mince was homogenized with a Teflon pestle homogenizer and centrifuged 25 min at 10,000 x g in a Sorvall centrifuge. The supernatant was then centrifuged at 100,000 x g in a Spinco Model 2 ultracentrifuge. The pellet was resuspended in isotonic KCl by homogenization and re-pelleted as above. The pellet was resuspended, diluted 1:10 in 50 mM phosphate buffer (pH 7.5), containing 25% glycerol and 1% Lubrol WX, and frozen in liquid nitrogen until needed.

II.C.3. Beef Heart Submitochondrial Particles

Submitochondrial particles containing cytochrome oxidase were prepared by a combination of techniques of Smith (1955) and King (1967). Fresh beef heart was obtained from a local slaughterhouse, minced, and washed six times in cold tapwater. Mince (400 gm) was further washed with 2 liters 0.1 M phosphate buffer (Sorenson's type), pH 7.4, for 1 hour at 4^{o}C and subsequently with 4 liters deionized water. Mince was then homogenized in a Waring blender for 7 min in

1 liter 0.05 M phosphate buffer (pH 7.4). Homogenate was centrifuged 20 min at 2000 x g in a refrigerated centrifuge. The supernatant was decanted and adjusted to pH 5.6 with 10% acetic acid and centrifuged at 1500 x g for 30 min. The pellet was suspended in 50 mM Tris sulfate (pH 8.0) containing 0.66 M sucrose and 1 mM histidine, and centrifuged at 78,000 x g for 10 min. The pellet was resuspended and centrifuged twice before freezing in liquid nitrogen. Particles were maintained at -20°C until needed and then thawed and diluted 1:10 in 50 mM phosphate (pH 7.5) containing 25% glycerol and 1% Lubrol WX.

II.D. Uptake and Partitioning of Metabolites

Because of the numerous biological functions of liver, isolated parenchymal cells can be used in diverse research areas. Many involve affects of added substances upon cellular metabolism as measured by metabolite levels or product formation. For interpretation of results three basic factors must be considered: kinetics of uptake of added substances, kinetics of release of metabolites and other products, and possible multiplicity of pathways involved. As an example, consider the relationship of cellular [pyruvate] to cellular [alanine]. Alanine can be formed from pyruvate by transamination; glutamate is the amine donor and 2-oxoglutarate is the product. Cells may be incubated in media containing varying concentrations of pyruvate, and alanine concentration can be measured after a fixed time.

The results would probably reveal little about the relationship of interest because of factors illustrated by the following equations:

$$[\text{alanine}]_{\text{total}} = [\text{alanine}]_{\text{cellular}} + [\text{alanine}]_{\text{extracellular}}$$

$$[\text{pyruvate}]_{\text{total}} = [\text{pyruvate}]_{\text{cellular}} + [\text{pyruvate}]_{\text{extracellular}}$$

Measured alanine in the suspension would represent the total and not the cellular alanine. Cellular [pyruvate] is not likely to be equal to the added extracellular [pyruvate] due to cell permeability limitations. Further, the intracellular concentration may not have a linear relationship to added [pyruvate]. Therefore, the kinetics of uptake must be investigated to determine the time required for the intracellular and extracellular pools to stabilize (i.e., approach equilibrium or steady state). In addition, the relationship of the cellular to extracellular pools must be determined. This may be accomplished by centrifugation (Quistorff et al., 1973) or by special sampling techniques (Meijer and Williamson, 1974; Wilson et al., 1974).

Finally, even after the intracellular relationship between [pyruvate] and [alanine] is determined, the interpretation of this relationship in terms of kinetics of the transaminase reaction may not be simple. Exogenous [pyruvate] may be enzymatically converted to oxalacetate or acetyl CoA, both of which are substrates for the tricarboxylic acid cycle and thus can alter the 2-oxoglutarate level. Since 2-oxoglutarate is also a reactant in the transaminase reaction,

added pyruvate could have an indirect affect by this pathway. Thus, in a complex system such as isolated cells, studies of kinetics of specific reactions or reaction sequences must be considered in relationship to the overall metabolism.

In the present work, exogenous substrates were limited to hexobarbital, alprenolol, phenyramidol and tyrosine. The three drugs are relatively hydrophobic and rapidly equilibrate between cells and suspending media (Section V). Tyrosine is not as permeable and therefore uptake measurements were required. Radiolabeled tyrosine was added to isolated hepatocytes at 37°C and incubated for varying lengths of time before sampling (Section VI.C.). Two methods were used to separate cells from the incubating medium, rapid filtration on millipore filters and centrifugation. Neither method was totally satisfactory. Millipore filters had a small capacity for cells and a background count due to the inclusion volume of the filter. Centrifugation was slow, allowing a minimal time point of three minutes.

Partitioning of metabolites between cells and incubating medium was determined by two methods: centrifugation and filtration. For centrifugation, isolated cells (3×10^6 cells/ml) were incubated under air at 37°C. The initial tyrosine concentration was 0.25 mM in Ringer-phosphate buffer (pH 7.4). After 30 min the suspension was transferred to a centrifuge tube and cooled to 0°C in ice. The samples were then centrifuged at 50 x g for 3 min. The supernatant

was decanted, and both supernatant and pellet assayed for tyrosine, pHPP, HG, ATP, lactate, pyruvate, 2-oxoglutarate, and glutamate, as described (Section II. B.).

A special filtration capsule was designed for rapid separation of cells from incubation medium so that metabolite concentrations in cells could be estimated from the difference between the total incubation and suspending medium metabolite levels. The requirement that the cells be removed completely and rapidly (1-2 sec) without damage was met by the capsule shown in Figure II-3 after testing a series of designs.

A 6-ml monoject disposable syringe (Sherwood Medical Industries, Inc.) was cut off at the 4 ml mark. Two glass fiber filters (ReeveAngel, grade 934ah) were cut into discs with a diameter of 1.3 cm and inserted into the bottom of the syringe. A loose pack of glass wool was added to fill to the 3 ml mark. The rubber disc from the syringe plunger was removed from the plunger and a small hole cut in the center so that a 20 gauge syringe needle (12 cm long) could be inserted. The rubber disc with needle was then inserted into the syringe and another 20 gauge needle (1-5 cm long) placed on the other end (in the normal position).

The capsule is used as follows: the short syringe needle is inserted through a serum cap on the test tube or vial in which the sample is to be collected. An aspirator is connected to the test tube

Figure II-3. Filtration capsule design. See text for description of construction.

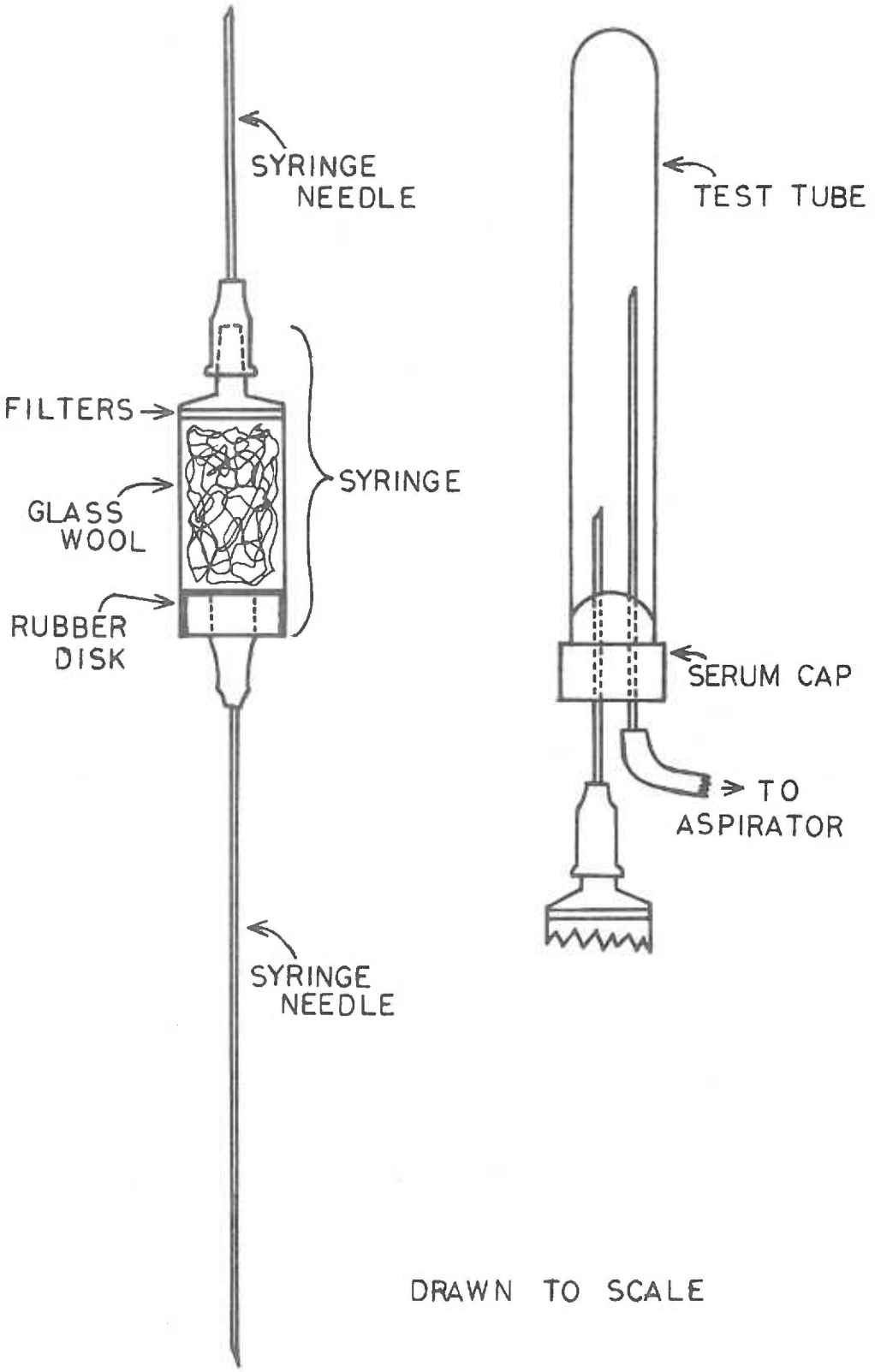

DRAWN TO SCALE

to create a negative pressure in the tube for pulling in a sample. The long syringe needle is inserted into the gas phase of the incubation vessel and finally into the liquid phase. About 2 ml of the medium is collected in the test tube, and the tube is removed and placed in an ice bath. A measured sample is then transferred to another tube and acidified with 2 N H_2SO_4. A sample of the incubation containing both cells and medium is also taken so that the concentration in the cells can be calculated.

II. E. Optical and ESR Spectroscopy

Isolated cells offer the opportunity for spectroscopic study of many oxidation-reduction reactions in their normal cellular environment. Isolated mitochondria and microsomes have received extensive optical and ESR investigation. Their study in hepatocytes is difficult because of interference of other chromophores and low attainable concentrations. Optical spectroscopy is further complicated by increased light scattering and sedimentation of cells.

Spectral work with isolated hepatocytes has been limited to use of optical changes for measurement of specific metabolic properties. Moldeus et al. (1974) used the spectrum of cytochrome P-450 drug complexes to follow cellular drug uptake. Wilson et al. (1974) used change in absorbance in the difference, $OD_{550}-OD_{540}$, as a measure

of cytochrome c reduction. The validity of these methods is indicated by correlation with properties of isolated subcellular fractions.

Optical Spectroscopy: A room temperature difference spectrum (dithionite reduced minus air oxidized) of isolated cells is given in Figure II-4. Cells were solubilized in 50 mM phosphate buffer (pH 7.0) containing 25% glycerol and 1% Lubrol WX, and concentration adjusted to 2.3 mg protein/ml. A baseline from 650 to 400 μm was recorded on a Cary Model 14 recording spectrophotometer. A few crystals of sodium dithionite were added to the sample cuvette, and the contents were mixed gently with a Teflon stirring rod. After 6 min the spectrum was recorded. A mixture of mitochondrial and microsomal chromophores is apparent. The 605 nm absorbance maximum is the α region of cytochrome $\underline{a} + \underline{a}_3$ (Vanneste, 1966). The absorbance between 550 and 560 nm represents the α-regions of cytochrome $\underline{b}_5$ (556 nm; Estabrook et al., 1972), P-450 (55 nm; Ichikawa and Yamano, 1970), $\underline{c}$ (550 nm; Chance and Hagihara, 1963), and $\underline{c}_1$ (554 nm; Chance and Hagihara, 1963). The β absorbances of cytochromes b_5, c and c_1 occur as a broad band at about 520 nm. The Soret band of cytochrome $\underline{a} + \underline{a}_3$ is at 445 nm. The Soret bands of cytochromes b, b_5, c, c_1 and P-450 appear as one peak in the 420-430 nm region.

Spectral examination of <u>intact</u> hepatocytes at room temperature was difficult because of light scattering and settling of cells from

Figure II-4. Room temperature difference spectrum (dithionite-reduced minus air oxidized) of isolated hepatocytes. See text for details.

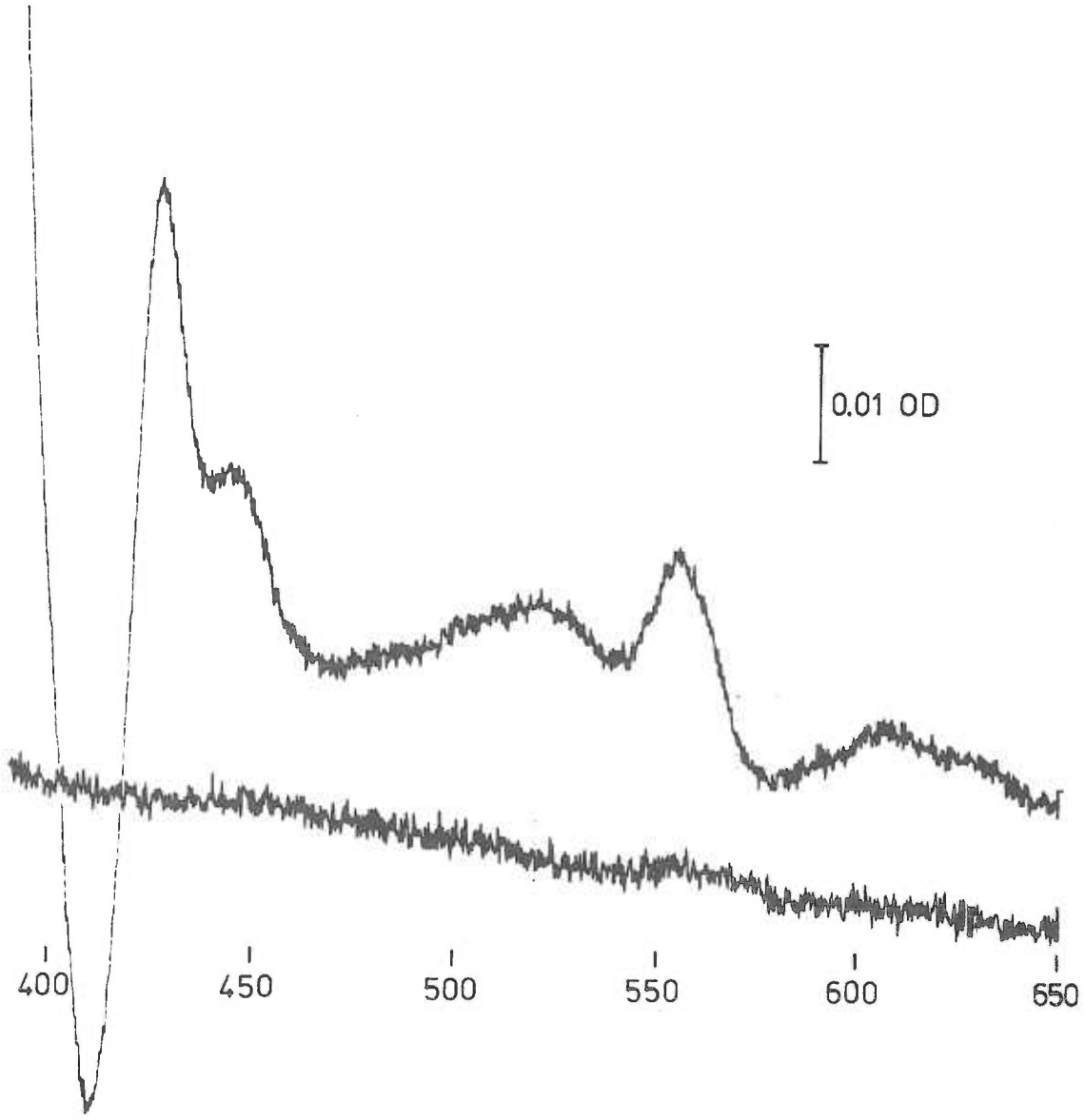
0.01 OD
400
450
500
550
600
650

suspension. The scattering problem was alleviated by use of a scattered transmission accessory for the Cary 14 spectrophotometer. Settling of cells was eliminated by using an isopycnic suspending medium (modified Hank's medium containing 25% Ficoll 400; a comparison of cells suspended for 1 hour in modified Hank's medium with and without 25% Ficoll 400 showed that it does not alter survival rate as judged by trypan blue exclusion). Under these conditions a relatively flat baseline was attained, and difference spectra (dithionite minus air, anaerobic minus aerobic) were recorded. However, both anaerobicity and dithionite caused cellular aggregation so that reliable spectra were not obtainable. The qualitative features were identical to Figure II-4 when recordings were made immediately after reduction.

Increased resolution of absorbance maxima was attained by observing cells frozen in liquid nitrogen (77°K). Cells (9 mg protein/ml) were pipetted into low-temperature cuvettes (3.2 mM, lucite windows) maintained in a T-cuvette holder. A few crystals of dithionite were added to the sample cuvette and a crystal of potassium ferricyanide was added to the reference cuvette. The contents were mixed by inversion and frozen immediately in liquid nitrogen. The cuvette holder was transferred to a Dewar flask equipped with optical windows and filled with liquid nitrogen. Spectra were recorded from 650 to 450 nm (Figure II-5). Baselines were obtained similarly

Figure II-5. Low temperature difference spectrum (dithionite-reduced minus ferricyanide-oxidized) of isolated hepatocytes. See text for details.

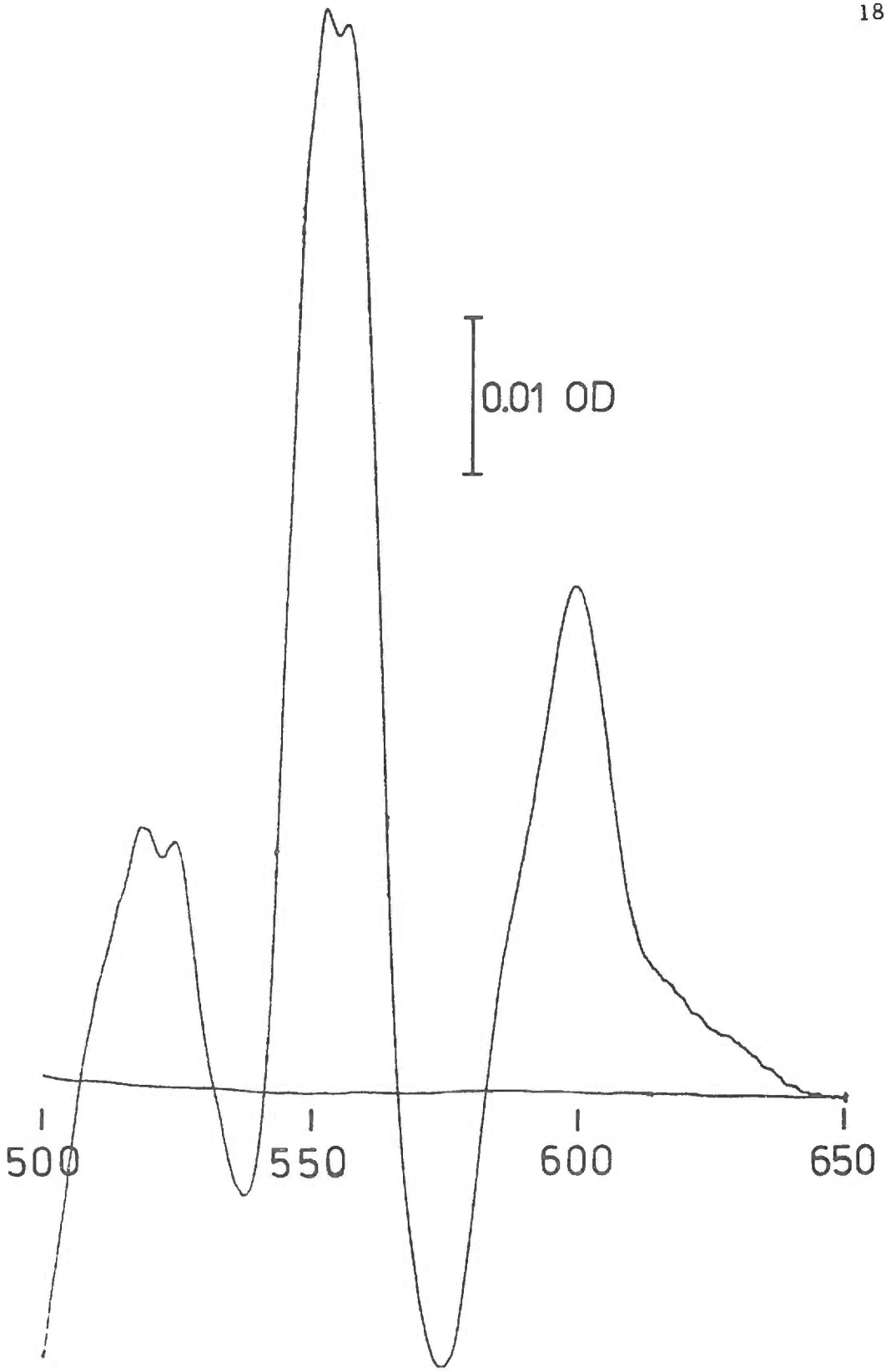
0.01 OD
500
550
600
650

without addition of oxidizing and reducing agents. The results reveal the individual chromophores more clearly and allows resolution of the α-band of cytochrome c_1 from cytochromes b_5 and P-450. Cytochrome c is apparent only as a shoulder on the cytochrome c_1 peak. In a cell, the measure used for cytochrome c oxidation-reduction (Wilson et al., 1974) may be affected by rather large contribution from cytochrome b_5 due to proximity of absorbance maxima. This complication requires that application of spectroscopic methods to the complex system of isolated hepatocytes be applied conservatively. A comprehensive study of redox and substrate dependent optical changes will be essential to determine optimum conditions for measurement of specific chromophores with minimal interference from others.

ESR Spectroscopy: Preliminary ESR spectroscopy was performed to determine the feasibility of observing oxygen dependent spectral changes. The low concentration of chromophores in intact cells necessitated high cell concentrations. The concentration of packed cells ($\sim$20 x g, 5 min) is about 4.3×10^7 cells/ml. However, these cells cannot be transferred between vessels. The maximum concentration of cells that can be transferred accurately and without damage to the cells is about 2.3×10^7 cells/ml. At this concentration between 20 and 37°C oxygen consumption due to respiration is so rapid that cells become anaerobic within a few seconds. Consequently,

aerobic samples must be cooled prior to concentration. Anaerobic samples can be prepared easily by raising the temperature of cells in an anaerobic EPR tube to 37°C for 5 min; however, the usual precaution of serial evacuation and flushing (6 x) with ultra-pure argon (Matheson Gas Products, 99.999%) was performed. Aerobic and anaerobic spectra (Figure II-6) were recorded with a Varian V-4502 spectrometer at -165°C. Conditions were: modulation amplitude, 8.0 gauss; microwave power, 25 mW; microwave frequency, 9.15 GH_z; time constant, 1 sec.

The aerobic spectrum had several peaks, including g = 2.24 and Sm = 2.43 characteristic of oxidized, low spin cytochrome P-450 (Ichikawa and Yamano, 1969). An absorbance at g = 1.93 may represent either g = 1.91 of cytochrome P-450 (Ichikawa and Yamano, 1969) or g = 1.93 of non-heme iron proteins (Orme-Johnson et al., 1973). This signal remains after cells are made anaerobic, whereas the g = 2.24 and Sm = 2.43 signals are greatly diminished, suggesting that a large portion of this signal is not due to cytochrome P-450. A large signal at g = 2.00, present in both aerobic and anaerobic samples, is due to free radicals. Other smaller absorbances occurring in both aerobic and anaerobic cells were at g = 2.03, g = 2.08, g = 2.14, and g = 2.17. After reduction with sodium dithionite, absorbances remained at g = 1.92, g = 2.08, g = 2.13 and g = 2.16. Spectra of modified Hank's medium had none of these absorbances.

Figure II-6. EPR spectra of isolated hepatocytes. Cells were suspended in modified Hank's medium (2.3×10^7 cells/ml) equilibrated with 95% O_2, 5% CO_2 and frozen immediately in liquid nitrogen for aerobic sample. Anaerobic sample was serially evacuated and flushed with ultrapure argon prior to freezing. Temperature was $-165^{\circ}C$.

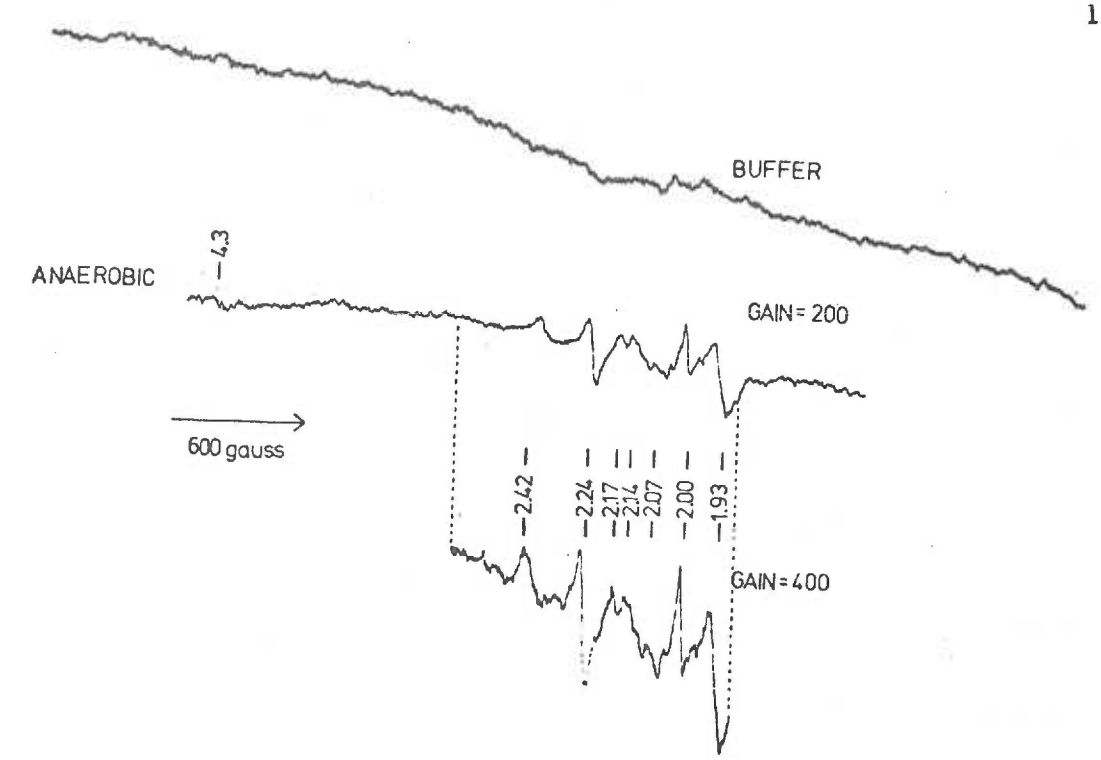
BUFFER
ANAEROBIC
4.3
GAIN = 200
600 gauss
2.42
2.24
2.17
2.14
2.07
2.00
1.93
GAIN = 400

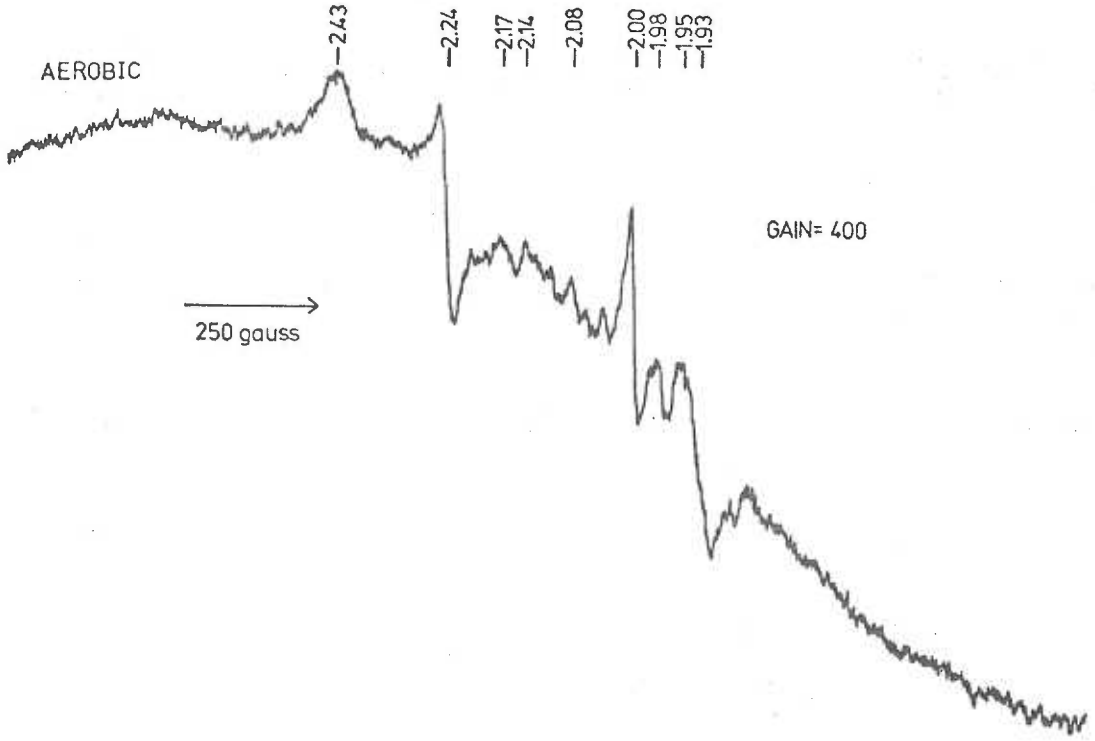
AEROBIC
2.43
2.24
2.17
2.14
2.08
2.00
1.98
1.95
1.93
GAIN= 400
250 gauss

II. E. 1. Cytochrome Oxidase Determination in Submitochondrial Particles

Submitochondrial particles were suspended by homogenization in 50 mM phosphate buffer (pH 7.5) containing 25% glycerol and 1% Lubrol WX. The protein concentration was adjusted to about 2 mg/ml and 3 ml aliquots added to matched 1 cm cuvettes. A baseline was recorded for the wavelength span 650 to 580 nm on a Cary model 14 recording spectrophotometer. A few crystals of dithionite was added to the sample cuvette, and a few crystals of ferricyanide added to the reference cuvette. Both were stirred gently with a cuvette stirring bar and the spectrum from 650 to 580 nm was recorded. Heme *a* content was calculated using the extinction value 13.8 mM^{-1} cm^{-1} (Vanneste, 1966).

Cytochrome a_3 was determined from the carbon monoxide difference spectrum of the dithionite reduced particles. Particles were suspended in the Lubrol solution as above; 3 ml aliquots were placed in each of two cuvettes and a baseline recorded from 470 nm to 400 nm. Carbon monoxide was then bubbled through the sample cuvette for 1 min followed by addition of a few crystals of dithionite to both sample and reference cuvettes. The spectrum was recorded and the cytochrome a_3 content estimated from the extinction coefficient 136 mM^{-1} cm^{-1} for the 428.5-445 nm absorbance difference (Vanneste, 1966).

II.E.2. Cytochrome P-450 Determination in Microsomes

Washed microsomes were suspended by homogenization in 50 mM phosphate buffer (pH 7.5) containing 25% glycerol and 1% Lubrol WX, to a final protein concentration of about 0.5 mg/ml. Three ml aliquots were placed in matched 1 cm cuvettes and a baseline recorded from 500 nm to 400 nm. Carbon monoxide was then bubbled through the sample cuvette for 1 min, and a few crystals of dithionite were added to each cuvette. The spectrum was then recorded from 500 to 400 nm. The cytochrome P-450 content was estimated with the extinction value of 91 mM^{-1} cm^{-1} (Omura and Sato, 1964) for the 450-490 nm wavelength pair.

II.E.3. Hemoglobin

Contamination of preparations by hemoglobin was examined by absorption spectroscopy. The difference spectrum of carbon monoxyhemoglobin minus oxyhemoglobin has an absorption maximum of 418 nm (Estabrook et al., 1972), and can be observed without interference from cytochrome $\underline{a}_3$-CO or cytochrome P-450-CO if no reducing agent is added. Thus, 3 ml aliquots of microsome, submitochondrial particles, or cells, were placed in each of two cuvettes, and a baseline recorded (450-400 nm). Carbon monoxide was then bubbled through the sample cuvette and the spectrum again recorded.

With care in preparation, negligible contamination by hemoglobin was attained.

II. E. 4. Cytochrome $\underline{a}_3$ and Cytochrome P-450 Determination in Isolated Hepatocytes

II. E. 4. a. Cytochrome $\underline{a}_3$. Cytochrome $\underline{a}_3$ content in isolated hepatocytes was determined from the carbon monoxide difference spectrum of the reduced compound using a method of additions. Beef heart submitochondrial particles were prepared as described above and solubilized by homogenization in 50 mM phosphate buffer (pH 7.5) containing 25% glycerol and 1% Lubrol WX. Cytochrome $\underline{a}_3$ content was determined from the CO difference spectrum of the reduced form on a Cary model 14 spectrophotometer (extinction coefficient of Vanneste, 1966). Cells were solubilized in the same manner as the submitochondrial particles and brought to a final concentration of 1.3-1.5 mg protein/ml containing additions of submitochondrial particles to give 0-0.5 nmoles cytochrome $\underline{a}_3$/ml. Three ml samples were transferred to sample and reference cuvettes. The sample cuvette was bubbled with CO for 1 min and 25 µl ascorbate (1 M, pH 7.0) and 30 µl TMPD (15 mM) added to both sample and reference cuvettes. After 30 min, the difference spectrum was recorded from 500 to 400 nm. The X- intercept of a plot of $\Delta OD_{428.5-445}$ as a function of mitochondrial additions gives a direct measure of cytochrome $\underline{a}_3$ content in isolated hepatocytes.

II.E.4.b. Cytochrome P-450; Method of Additions with Submitochondrial Particles. Using the cellular cytochrome $\underline{a}_3$ concentration determined above, the contribution of cytochrome $\underline{a}_3$ to the $\Delta OD_{450-490}$ (CO·dithionite minus dithionite difference spectrum) was determined by extrapolation to zero cytochrome $\underline{a}_3$. Cells and submitochondrial particles were prepared; after bubbling the sample cuvette with CO for 1 min, a few crystals of dithionite were added to each cuvette. Spectra were recorded after 15 min from 500 to 420 nm; $\Delta OD_{450-490}$ was plotted as a function of cytochrome $\underline{a}_3$ addition and extrapolated to zero cytochrome $\underline{a}_3$ to give a corrected $\Delta OD_{450-490}$ for cytochrome P-450. This corrected $\Delta OD_{450-490}$ was then used with Omura and Sato's extinction coefficient of 91 mM^{-1} cm^{-1} to give the concentration of cytochrome P-450 in the cells.

A simplified approach without the method of additions was devised for the rapid determination of cytochrome P-450 using a minimal amount of material, based upon the selective reduction of cytochrome $\underline{a}_3$. One milliliter of solubilized cells (1.5-2.0 mg/ml protein) was pipetted into 1 ml sample and reference cuvettes. Carbon monoxide was bubbled through the sample cuvette for 1 min followed by additions of 10 µl ascorbate (1 M, pH 7.0) and 10 µl TMPD (15 mM) to both cuvettes. After 30 min the spectrum was recorded from 500 to 420 nm. A few crystals of dithionite were then added to each cuvette and after 15 min the spectrum was again

recorded. The $\Delta OD_{450-490}$ for the first spectrum was then subtracted from that for the second spectrum. This "corrected ΔOD" was then used with the extinction of 91 mM^{-1} cm^{-1} to give cytochrome P-450 content.

II.E.4.c. Cytochrome P-450 (Ghazarian et al., 1974). This method is based upon the selective reduction of cytochrome $\underline{a}_3$ with ascorbate + TMPD in the presence of cytochrome P-450, in the reference cuvette. The cytochrome $\underline{a}_3$ + CO is subtracted from the cytochrome P-450 + CO + cytochrome $\underline{a}_3$-CO formed in the sample cuvette upon the addition of dithionite resulting in a difference spectrum largely due to CO·cytochrome P-450. To test this assay for quantitation of cytochrome P-450 in isolated hepatocytes, the method of additions was used with both washed microsomes and submitochondrial particles.

Cytochrome P-450 content of washed microsomes was determined by the method of Omura and Sato (1964). Cells were solubilized and suspended to a final concentration of approximately 0.5 mg protein/ml containing added microsomes to give 0, 0.65, 1.3 or 1.95 μM P-450. CO was bubbled through both sample and reference cuvettes. Additions of 25 μl ascorbate (1 M, pH 7.0) and 30 μl TMPD (15 mM) were made to the reference and sample cuvettes, followed by a few crystals of dithionite to the sample cuvette. Spectra were recorded after 30 min from 500 to 400 nm (Ghazarian et al., 1974). The

X-intercept of a plot of $\Delta OD_{450-490}$ as a function of known microsomal cytochrome P-450 additions gives the cellular cytochrome P-450 content. The effective extinction coefficient for cytochrome P-450 using this assay in isolated hepatocytes was 76 mM^{-1} cm^{-1} for $\Delta OD_{450-490}$.

II.F. Oxygen Tension and Respiration Rate

Oxygen tension was measured polarographically with a Clark-type oxygen electrode (Beckman Polarographic Oxygen Sensor used in conjunction with the Model 777 Oxygen Analyzer). The gold cathode and silver anodes were washed thoroughly with household cleanser approximately every two weeks of operation. Beckman oxygen electrolyte gel and Teflon membrane (#77948) were used for charging. The electrode was "zeroed" with prepurified nitrogen (O_2 less than 8 ppm), dithionite, or ascorbate plus copper sulfate. Calibration was performed at 37°C routinely with distilled water equilibrated with air and with distilled water equilibrated with 1.98 $\pm$ 0.01% O_2, balance N_2 (Industrial Air Products, certified grade). Complete calibration over the operating range 0-150 torr was performed by initially equilibrating distilled water with prepurified nitrogen followed by additions of aliquots of distilled water equilibrated with air with a Hamilton gas-tight syringe.

Oxygen tensions are routinely expressed in terms of the partial pressure of oxygen (1 torr = 1 mm mercury) with which the incubation is equilibrated at 37°C. Using the Bunsen solubility value for oxygen at 37°C of 0.0239 (Umbreit et al., 1964), 100% O_2 = 760 torr = 760 mm mercury = 0.0239 ml O_2/ml = 1.07 mM O_2. Therefore, $P(O_2)$ values determined at 37°C expressed in torr can be readily converted to oxygen concentration: $1.07 \times 10^3 \times P(O_2)(\text{torr})/760 = O_2$ (μM).

The respiration rate was obtained from the slope of a polarographic tracing of oxygen tension against time at 37°C in modified Hank's solution containing bovine serum albumin (15 mg/ml) unless otherwise indicated. Rates were obtained immediately after preparation of cells (about 90 min after start of preparation). Cell concentration was about 2-4 x 10^6 cells/ml. Rates are expressed as $Q_{O_2}^{cell}$ (μl O_2 uptake/10^6 cells/hr) or as $Q_{O_2}^{pro}$ (μl O_2 uptake/mg protein/hr). The affect of pyruvate (10 mM) and ADP (0.5 mM) on respiration was determined by adding the substrates to the incubation media. The affect of CO_2 evolution on the pH during determination of the oxygen consumption was monitored by using a double electrode cell containing both a pH electrode and an oxygen electrode.

Respiration rate as a function of oxygen tension was determined using the above polarographic system connected on-line through an analog-digital converter to a PDP-11 computer (Digital Electronics Corporation). Oxygen tension recordings were registered

at 10 sec^{-1} with 10 point averaging to give 1 sec^{-1} data. The rate was then determined from consecutive O_2 values to give O_2/sec and plotted with an 11 point smoothing routine (see below) as a function of $P(O_2)$.

II. G. Computer Analyses

All computer analysis of data was performed on a PDP-11 computer (Digital Electronics Corporation) with Focal 11 programming. Pertinent programs for on-line determination of respiration rate, linear least squares, data plotting, curve smoothing, mean and standard deviation, and double reciprocal plots are given in Appendix IV. Curve smoothing was done according to Savitzky and Golay (1964).

III. THE OXYSTAT

III. A. Basis for Design

A number of different approaches to the study of metabolism as a function of oxygen tension has been made. A simple method has been suspension of O_2-consuming material in a vessel in which the liquid is in continual equilibrium with the gas phase. A specific metabolite accumulation or loss is measured as a function of time at different constant oxygen tensions to give metabolic rates as functions of $P(O_2)$. The necessary conditions for this technique to be effective are that the rate of oxygen consumption (R) be small relative to the rate of oxygen transfer (v_t) from the gas to the liquid, and the oxygen content of the gas and R must not vary markedly during the measurement. This method is used most widely for kinetic studies on isolated enzymes and can suitably be performed with a Warburg apparatus (Umbreit et al., 1964).

A second method is a continuous polarographic recording of oxygen tension as a function of time for a closed, oxygen consuming system. The continuous slope of this tracing is then plotted for the oxygen tension at which the slope was measured to provide the rate as a function of oxygen tension. The requirements for this method are that the oxygen consumption must occur primarily by one system and that the polarograph response must be rapid enough to reflect the true

oxygen tension within the time course of measurement. This method has received greatest application to the study of cytochrome oxidase in whole cells (Longmuir, 1964) and mitochondrial preparations (Chance, 1957; Chance et al., 1964), and cytochrome P-450 in microsomes (Choi, 1971; Kerekiarto and Staudinger, 1966).

An improved approach to study of mitochondrial respiratory pigments at low oxygen tensions essentially in steady state conditions has been developed by Degn and Wohlrab (1971), namely, a respirograph for providing a gas mixture linearly increasing in $P(O_2)$ with time. When this flow is applied to a reaction vessel equipped with a polarographic electrode and optical windows, relative oxidation states of respiratory pigments as a function of oxygen tension can be measured. The major difficulty is that only rapidly responding systems are in steady state and the condition of steady state cannot be established by a linear decrease in oxygen tension. The respirograph has been applied only to purified enzymes and mitochondrial preparations (Degn and Wohlrab, 1971) although application to study of spectral changes in intact cells appears possible.

None of these methods are generally applicable to the study of cellular metabolism under hypoxic conditions because of one or more limitations. The first method requires that R is small relative to v_t or that R remain relatively constant. Incubations of isolated hepatocytes at sufficient concentrations to allow metabolite assay

respire too rapidly to permit equilibration across the gas-liquid interface. In addition, because of cellular attrition, R continually decreases. The second and third methods do not allow steady state oxygen tension in solution to be maintained for slowly responding systems so that metabolism at a specific oxygen tension can be measured. Consequently, a new apparatus was required to allow the desired experimentation.

The basic requirement for maintenance of constant oxygen concentration in an oxygen consuming system is that rate of oxygen supply be equal to rate of oxygen consumption. This may theoretically be achieved either by addition of a solution containing oxygen (analogous to the manner in which a chemostat supplies nutrients) or by introduction of sufficient oxygen into the gas phase. The high oxygen consumption rate of hepatocytes would require significant dilution during an experiment and introduce uncontrollable variables. Therefore, the introduction of oxygen through the gas phase was chosen for further consideration.

An open system with continuous flow of oxygen containing gas through the system was preferred over a closed system into which oxygen gas is injected, because carbon dioxide would accumulate in the closed system. In an open system, gas pressure can be maintained at one atmosphere, and under constant conditions a steady state oxygen concentration in solution can be attained which is

described by

$$C_f = \frac{k_1 C_g - R}{k_2} \qquad \text{(III-1)}$$

(Myers and Matsen, 1955) where C_f is concentration of oxygen in solution (µl/ml), C_g is concentration of oxygen in gas (µl/ml), k_1 and k_2 are rate constants for transfer of oxygen into and out of solution (ml/min), and R is the respiration rate (µl/ml/min). Under steady state conditions, the rate of oxygen consumption must be equal to the rate of oxygen entry into solution, $R = v_t$, where v_t is the rate of oxygen entry in µl/ml/min. Equation III-1 can be rearranged to

$$R = k_1 C_g - k_2 C_f . \qquad \text{(III-2)}$$

By definition, k_1/k_2 is the Bunsen solubility constant, α, so that the right-hand side can be rearranged to

$$R = (\alpha C_g - C_f) k_2 \qquad \text{(III-3)}$$

or

$$R = (C_g - C_{f/\alpha}) k_2 \alpha . \qquad \text{(III-4)}$$

C_g and $C_{f/\alpha}$ can be converted to $P(O_2)_g$ and $P(O_2)_f$, respectively, by multiplication by 760 torr/1000 µl/ml. The expression, $k_2\alpha$ can be redefined as a constant (K), and the steady state equation written

$$R = K[P(O_2)_g - P(O_2)_f] . \qquad \text{(III-5)}$$

K is the oxygen transfer constant (Degn and Wohlrab, 1971) and is

dependent upon surface area, volume, temperature, stirring rate and composition of the liquid phase. It can be determined directly for a vessel under specified conditions with a solution of known R under fixed $P(O_2)_g$ by measuring steady state of $P(O_2)_f$. Alternatively, the rate of oxygen transfer, v_t, can be measured for solution where R = 0 according to the equation

$$v_t = K[P(O_2)_g - P(O_2)_f] \qquad \text{(III-6)}$$

(Degn and Wohlrab, 1971). Deoxygenated distilled water is most convenient since $P(O_2)_f$ is initially zero. Gas of known oxygen content can be introduced and the oxygen tension in solution measured polarographically as a function of time. The initial slope is then equal to v_t when $P(O_2)_f$ is zero, and K is equal to $v_t/P(O_2)_g$.

From Equation III-5, one can see that sequential studies at different $P(O_2)_f$ could be performed by systematically changing R, K or $P(O_2)_g$. R can be changed by varying cell concentration, however, extensive controls would be required to determine if variation in cell concentration over a relatively large range would have any affect on measured metabolism. K can be varied by changing surface area to volume ratio or by changing stirring rate. Changing the surface area to volume ratio can be done simply by altering the volume if the vessel is an elliptic cylinder and the surface area is constant. However, this does not provide sufficient change in K to allow control of $P(O_2)_f$ over a large range. Variation of the stirring rate cannot be used for control

of K because of the relatively small range which will allow adequate mixing without excessive damage to the cells. Variation of $P(O_2)_g$ is the easiest and most suitable method for controlling $P(O_2)_f$.

The oxygen tension in an incubation of isolated hepatocytes (3×10^6 cells/ml) exposed to constant $P(O_2)_g$ is given in Figure III-1. For an oxygen consuming system, a steady state solution oxygen tension will occur when oxygen consumption and supply are balanced. However, isolated hepatocytes die at a rate high enough to significantly affect the oxygen consumption rate and consequently with constant $P(O_2)_g$ the solution $P(O_2)$ continually increases (Figure III-1). Thus, an instrument is required to regulate $P(O_2)_g$ to maintain constant $P(O_2)_f$. Preliminary studies showed that control of $P(O_2)_g$ by manual regulation of flow of high $P(O_2)$ and low $P(O_2)$ gases through a flow-meter was difficult and not very accurate. A system was developed to provide control of $P(O_2)_g$ automatically so that a desired $P(O_2)_f$ could be maintained in a respiring system.

II. B. Components of the Oxystat

An oxystat was designed to maintain specified oxygen tensions in systems with high oxygen consumption rates. Commercially available oxygen controlling systems (e.g., Dissolved Oxygen Controller, New Brunswick Corp.) were found to be constructed for large volume industrial or microbiological incubations and did not

Figure III-1. Oxygen tension in respiring hepatocyte preparation with constant O_2 input. Isolated hepatocytes were incubated in the special vessel at 4.12×10^6 cells/ml in 8 ml total volume. The temperature was 37°C and a hydrated gas mixture initially containing 53.5% O_2 was passed over the aqueous phase at a flow rate of 34 ml/min. Oxygen tension was recorded polarographically as a function of time.

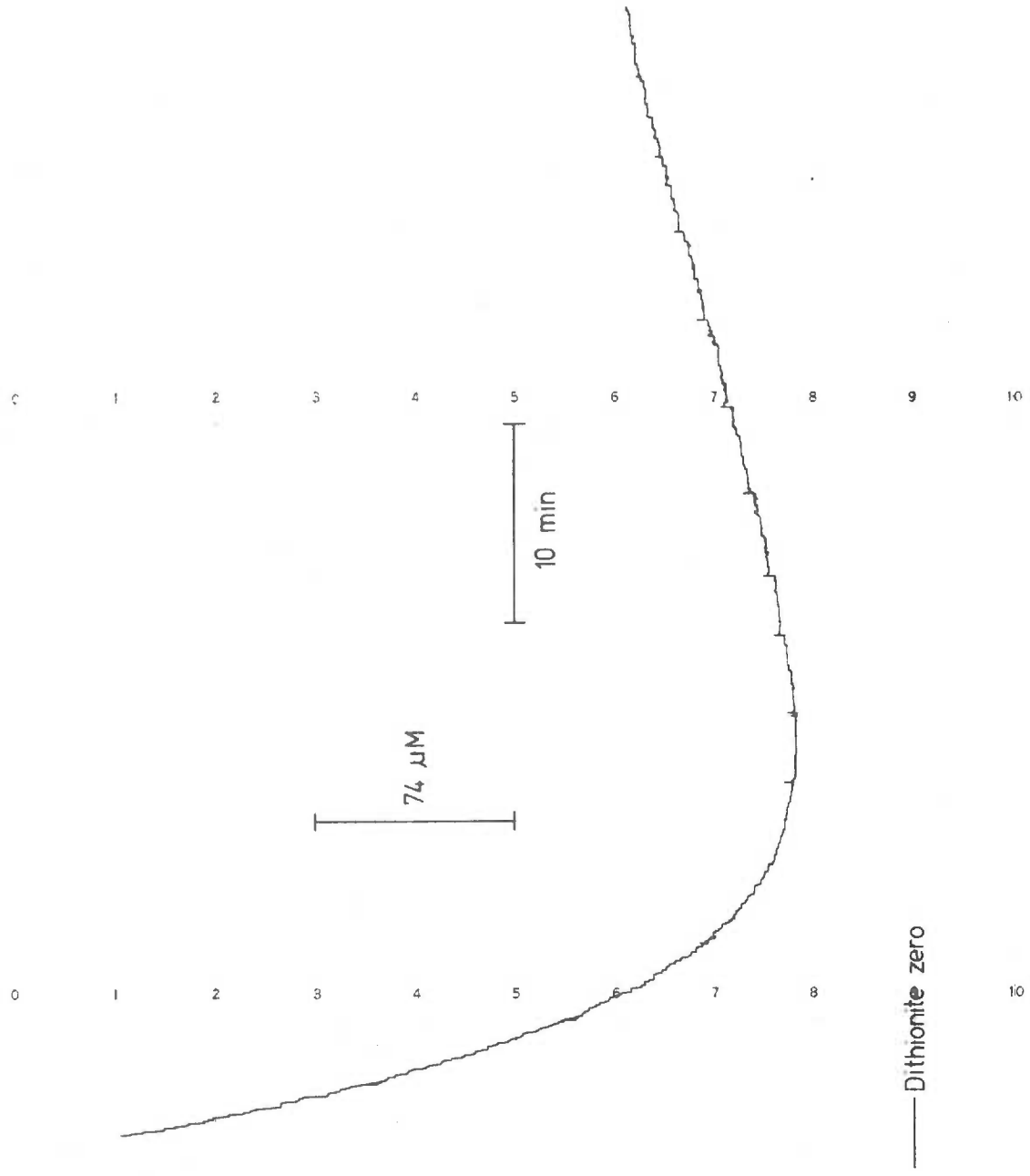
0
1
2
3
4
5
6
7
8
9
10
10 min
74 µM
Dithionite zero

Figure III-2. Schematic design of the oxystat.

A. thermostatted incubation vessel (see Figure III-4)
B. oxygen electrode (Beckman Polarographic Oxygen Sensor)
C. amplifier (Beckman, Model 777 Oxygen Analyzer)
D. recorder (Texas Instruments Servoriter, Model MWS)
E. millivolt transmitter (Rochester Instrument Systems, Model SC-1306)
F. controller (The Hays Corp., Universal Electronic Controller Model 854)
G. needle valve (Hoke, Model 1666 with electro-mechanical valve actuator #012F2E)
H. carrier gas
I. controlled gas
J. gas hydrating towers
K. gas flowmeter (Matheson, Models 600 and 601) and mixer (Matheson, Model 665)

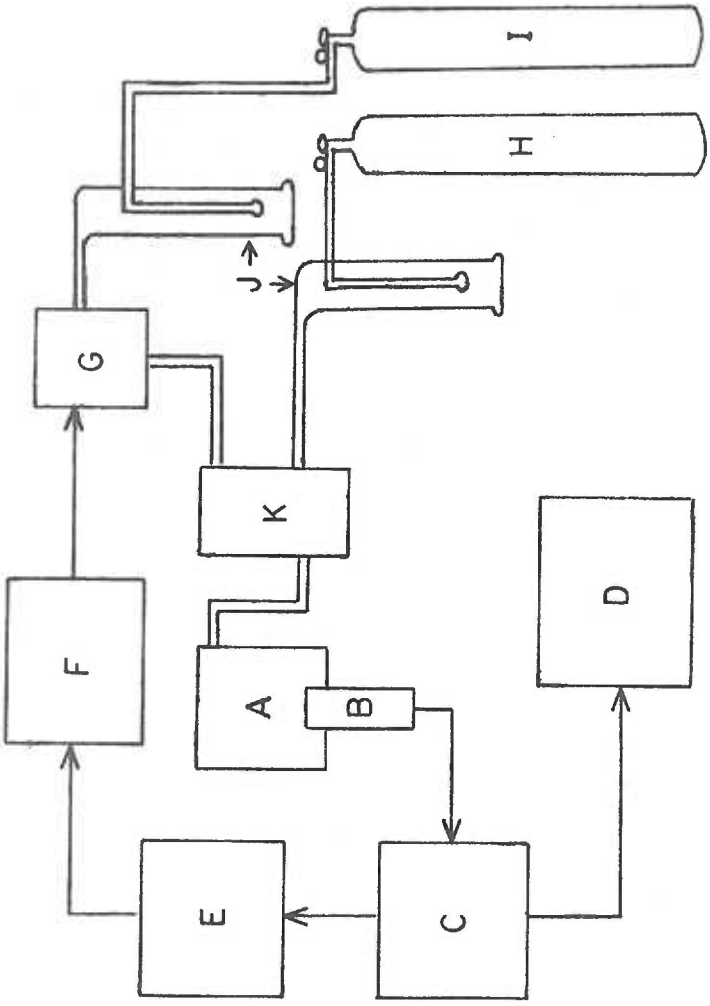
I
H
J
G
K
F
A
B
D
E
C

an oxygen electrode, have a suitable mode for continual gentle mixing, have a gas phase with inlet and outlet, have an easily accessible sampling port, and be temperature controlled. Two flask constructions with different modes of stirring were studied to determine which was less destructive to cells. A tonometer equipped with an oxygen electrode was considered. The tonometer swirling rate was adjusted to 108 rpm (approx. 2 sec mixing time) and 92 rpm (approx. 3 sec mixing time) for measuring the death rate of isolated hepatocytes. Hepatocytes (8 ml, 3×10^6 cells/ml) in modified Hank's medium were pipetted into a 50 ml round bottom flask and swirled at 37°C under 95% O_2, 5% CO_2 for 10, 20, and 30 min. The percentage of cells excluding trypan blue were measured initially and after each time interval as shown in Figure III-3. At 108 rpm, hepatocyte attrition was 13.5%/30 min and at 92 rpm it was 10.8%/30 min. These values were considered too high for experiments requiring 15-20 min; however, slower mixing rates would not provide adequate agitation for polarograph function. A vessel utilizing magnetic stirring was therefore preferred.

The death rate of cells using magnetic stirring was examined. Cells (8 ml, 3×10^6 cells/ml) were incubated at 37°C with stirring under 95% O_2, 5% CO_2 in a 25 ml Erlenmeyer flask. Stirring was adjusted to give complete mixing in 3 sec with a 1.0 cm cylindrical stirring disc (Radiometer, #D4030). The death rate was found to be

Figure III-3. Attrition of hepatocytes during incubation in tonometer and special incubation vessel. Eight milliliters of isolated suspension (3×10^6 cells/ml) was incubated at 37°C under 95% O_2, 5% CO_2 in the vessels described. The suspension medium was modified Hank's solution. Cells were examined in 0.2% trypan blue after varying periods of incubation, and results are expressed as percent excluding trypan blue as a function of time.

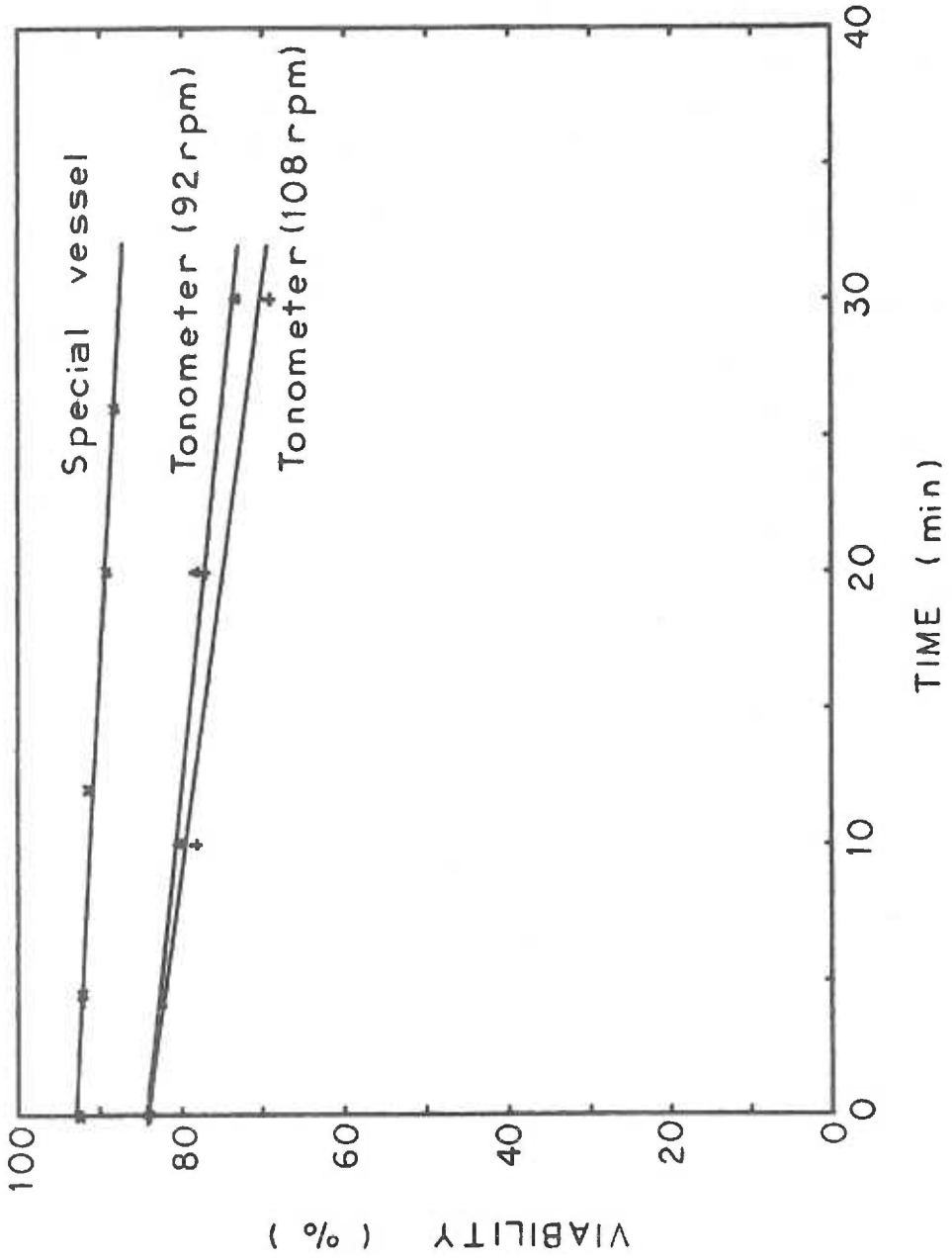
Special vessel
Tonometer (92rpm)
Tonometer (108rpm)
VIABILITY (%)
100
80
60
40
20
0
0
10
20
30
40
TIME (min)

significantly less, 4.8%/30 min and to be within a tolerable range. Details of the design were refined with the collaboration of Mr. Gunther Weiss (Portland, Oregon), the glassblower who constructed the vessel. The design is shown in Figure III-4. Stirring was accomplished with Micro-V magnetic stirrer (Cole, Parmer, Chicago), modified by attachment of a circular magnet extended vertically 4.4 cm above internal stirring mechanism. The sampling port was the screw cap portion of a 13 x 100 culture tube. A 1 mm hole was drilled into the screw cap, and the Teflon cap liner was replaced with a gas chromatograph septum (Hewlett-Packard, part #5080-5022). The temperature was controlled at 37°C with a Haake type F circulating temperature control unit.

The vessel was mounted with an Aeroseal clamp on a firm support so that movements during incubations did not occur, yet the vessel could be readily removed if necessary. The opening for the oxygen electrode was selected so that the electrode would fit tightly with appropriate O-rings. The gas inlet and outlet were equipped with stopcocks to allow sealing off the vessel when required. The inlet was connected to the gas supply by a gas-tight ball joint (12/2) containing an O-ring and secured with a Thomas ball joint clamp (#12 A).

Figure III-4. Design of thermostatted polarographic incubation vessel. Drawn to scale. See text for details.
A. front view
B. right side view

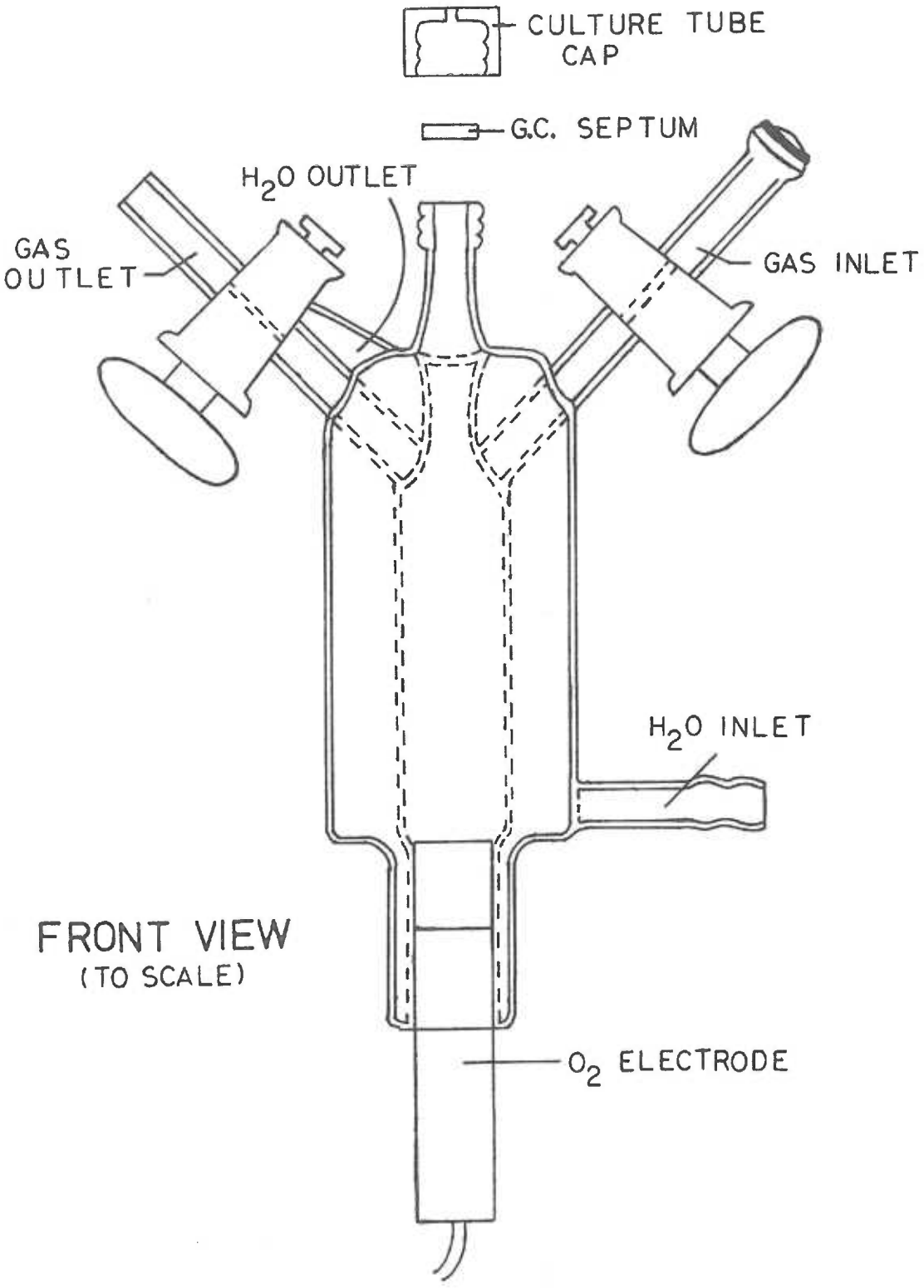
CULTURE TUBE CAP
G.C. SEPTUM
H_2O OUTLET
GAS OUTLET
GAS INLET
H_2O INLET
FRONT VIEW
(TO SCALE)
O_2 ELECTRODE

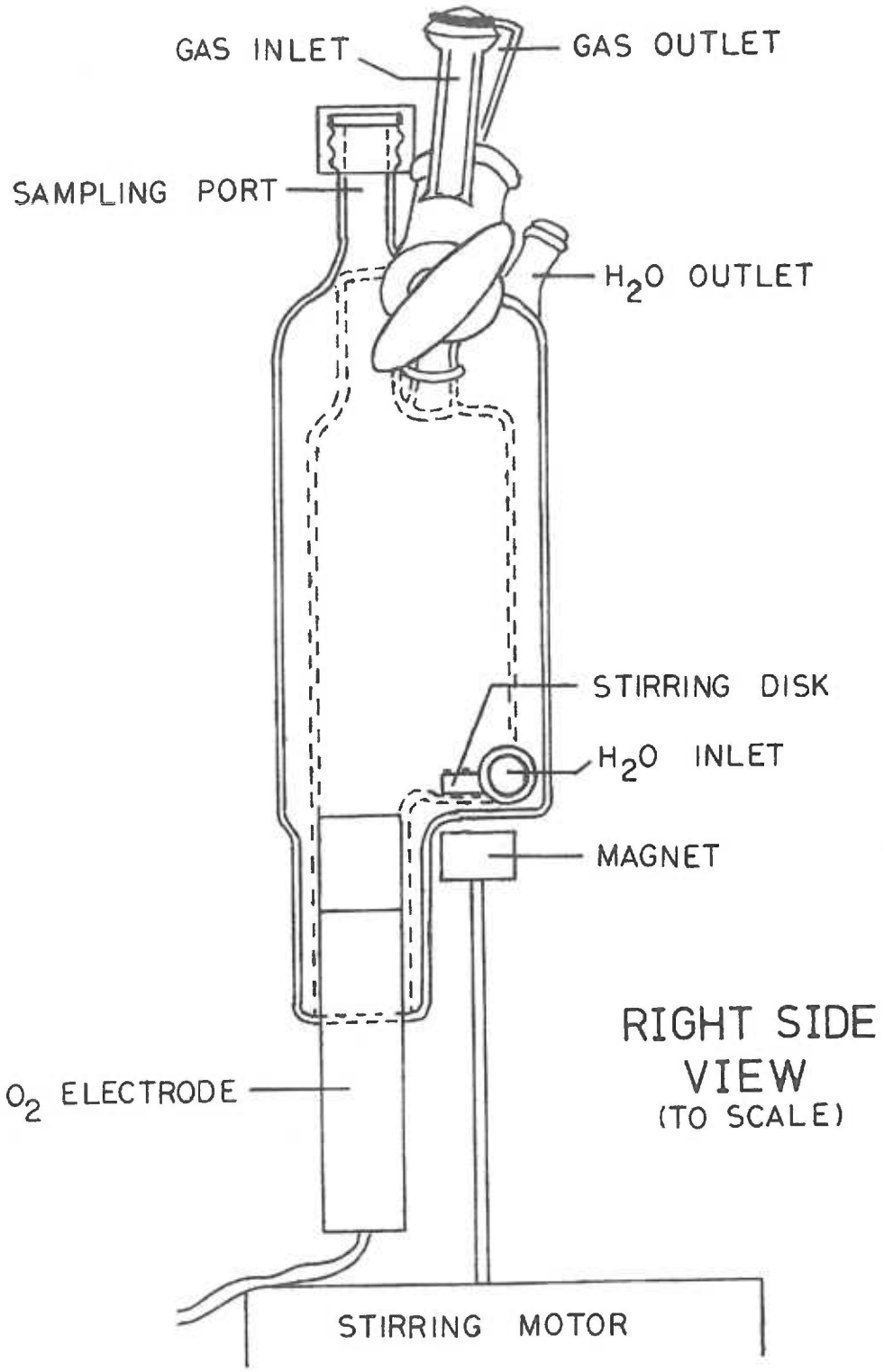
GAS INLET
GAS OUTLET
SAMPLING PORT
H_2O OUTLET
STIRRING DISK
H_2O INLET
MAGNET
O_2 ELECTRODE
STIRRING MOTOR
RIGHT SIDE VIEW
(TO SCALE)

III.B.2. Oxygen Analyzer

The oxygen analyzer was a polarographic system with a Clark-type oxygen electrode (Beckman Polarographic Oxygen Sensor used in conjunction with the Model 777 Oxygen Analyzer). The gold cathode and silver anodes were washed thoroughly with household cleanser approximately every two weeks of operation. Beckman oxygen electrolyte gel and Teflon membrane (#77948) were used for charging. Routine calibration of the oxygen electrode was performed at 37°C with distilled water equilibrated with air or 1.98% O_2, 98.02% N_2. Complete calibration over the operating range 0-150 torr was performed by initially equilibrating distilled water with prepurified nitrogen followed by additions of aliquots, with a Hamilton gas-tight syringe, of distilled water equilibrated with air (Figure III-5). Sodium dithionite, ascorbate plus copper sulfate, or prepurified nitrogen (O_2 less than 8 ppm) was used to obtain a "zero." A continuous recorder tracing was obtained with a Texas Instrument Servoriter recorder (Model PWS). Additional amplification of signal from the oxygen analyzer was attained by a Variable Recorder Amplifier (Instruments and Communications, Inc., Wilton, Conn.). Optimum performance was obtained after the entire polarographic system was equilibrated for 3 hours. A signal to noise ratio of at least 50 was maintained above 10 torr. At oxygen tensions below

Figure III-5. Oxygen electrode calibration. Distilled deionized water was boiled 30 min, then cooled under prepurified nitrogen gas. Nitrogen was bubbled through continuously for 6 hours. A 2.5 ml volume was transferred to a polarographic vessel which had been flushed with nitrogen. The transfer was made through butyl-rubber tubing with a syringe needle on each end using pressure from N_2 in the bubbling flask to provide a positive pressure for flow. Aliquots of distilled water equilibrated with air at 25°C were then added and the electrode response recorded. The calibration with air at 37°C relative to the dithionite zero is also shown.

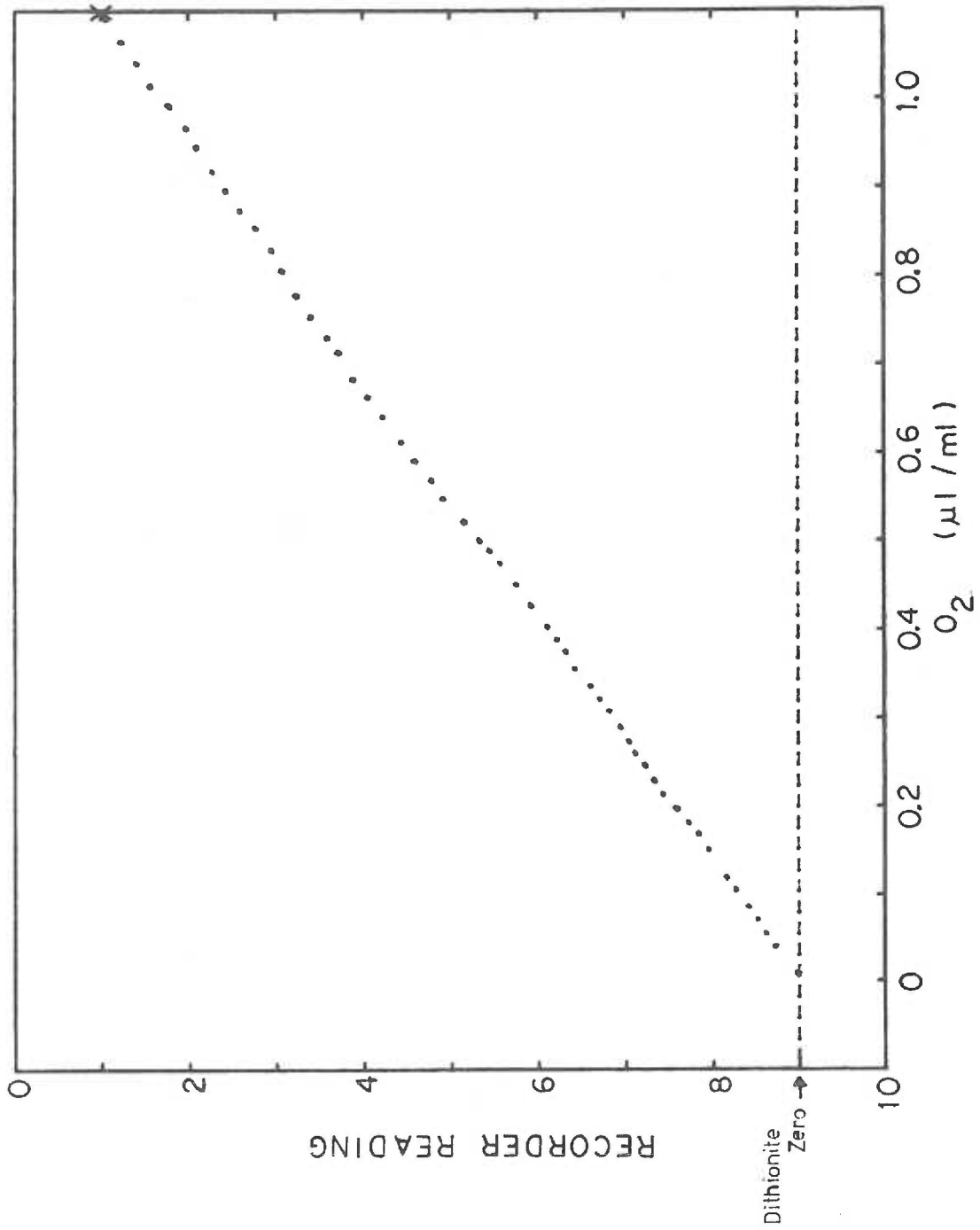
RECORDER READING
0
2
4
6
8
10
Dithionite
Zero
0
0.2
0.4
0.6
0.8
1.0
O_2 (µl / ml)

10 torr noise was about 0.2 torr. The electrode noise is included in the more useful term, % fluctuation, for analysis of oxystat function (see below).

III. B. 3. Oxygen Controller

The 0-50 mV output from the oxygen analyzer was converted to a 1-5 mA signal with a millivolt transmitter (Model SC-1306, Rochester Instrument Systems, Inc., Rochester, N. Y.) to be compatible with the controller, a Universal Electronic Controller (Model 854, The Hays Corporation, Michigan City, Indiana) with three mode control. The output from the controller signaled the position of the gas controlling valve (Hoke, Model 1666 series micromite metering valve) through a Hoke Electromechanical valve actuator (#012F2E).

III. B. 4. Oxygen Supply System

Variable O_2:N_2 mixtures containing 5% CO_2 were obtained commercially. For a given experiment, two tanks were chosen with O_2 contents as described by calibration curves to allow control of oxygen tension in solutions over the range of 0-150 torr. Both gases passed through three hydrating towers and a water droplet trap at 37°C prior to mixing. The gas flow from the tank with the lower oxygen content, termed "carrier gas," was regulated and monitored by a Matheson flowmeter, model #600. The gas flow from the other

tank, the "controlled gas," was initially set with a Matheson flowmeter, model #601, with the valve completely open, and controlled by the valve. The gases were mixed in a model 665 gas proportioner (Matheson Gas Products), then passed into the incubation vessel. All tubing was low oxygen permeability butyl rubber (Fisher Scientific Cat. #14-168A) thermally insulated with mylar tape.

Flowmeter calibration was performed by measuring volume displacement of water as a function of time at various flowmeter settings. The results for the controlled gas flowmeter (#601) are shown in Figure III-6a, and the results for the carrier gas flowmeter (#600) are shown in Figure III-6b. The calibration of flow through the Hoke valve at different valve settings is given in Figure III-7. The valve makes 18 1/2 full turns from open to closed. With valve completely open a flow rate was measured. Then the valve was closed successively 10% of the full range as measured on the controller valve setting indicator and flow again measured.

III. C. Characterization

III. C. 1. Incubation Vessel Characteristics

The total volume of the incubation vessel is 24 ml, and the liquid volume can range from 3 to 20 ml. The primary limit to volume is maintenance of adequate mixing time without excessive

Figure III-6. Flowmeter calibration curves. Flowmeters were calibrated for operating conditions involving a minimal pressure differential across the flowmeter. Gas flow at given flowmeter settings was measured by volume displacement of water.
a. controlled gas flowmeter (Matheson #601)
b. carrier gas flowmeter (Matheson #600)

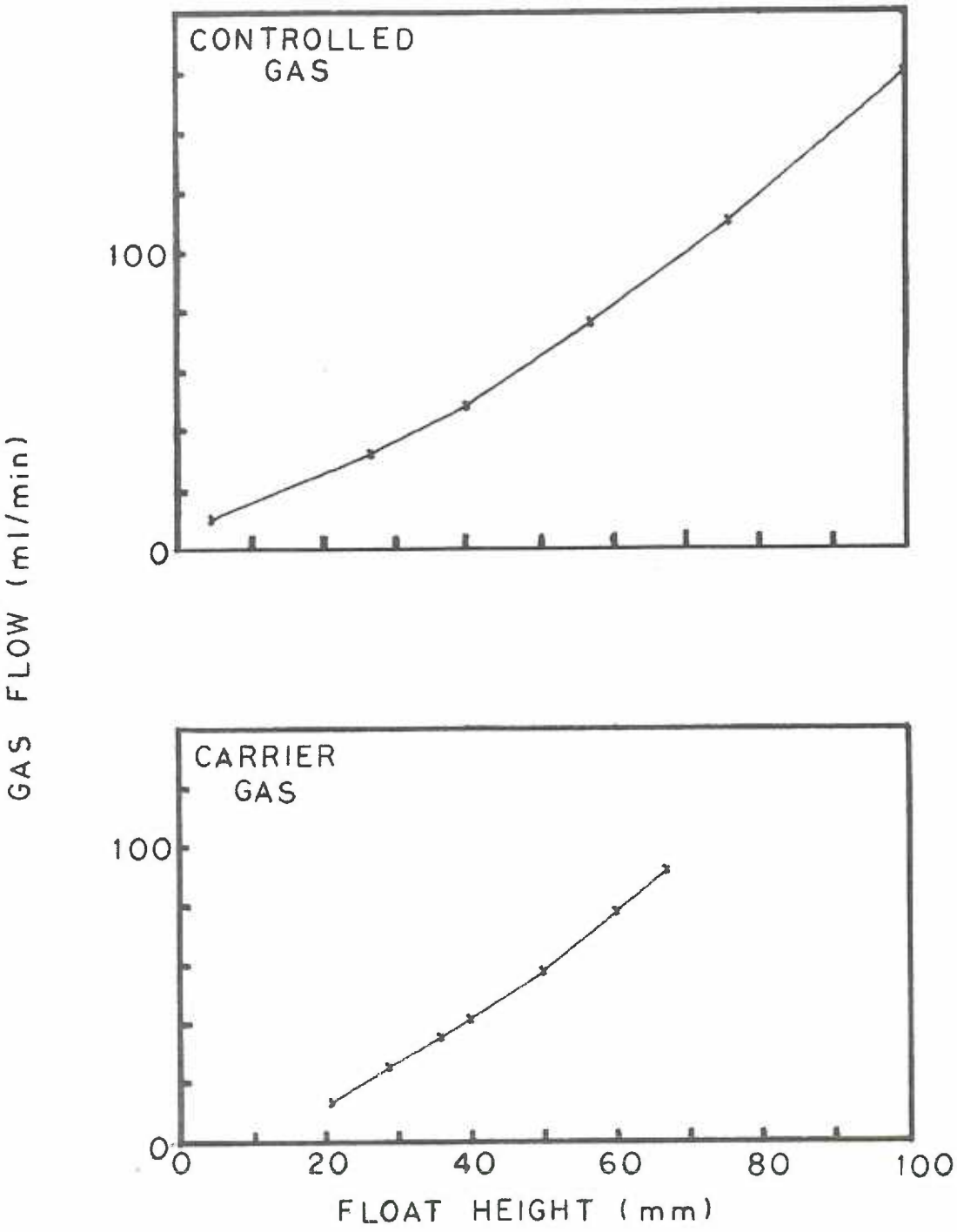
CONTROLLED
GAS
100
0
CARRIER
GAS
100
0
0
20
40
60
80
100
GAS FLOW (ml/min)
FLOAT HEIGHT (mm)

Figure III-7. Gas flow as a function of valve setting. Initial gas flow with valve completely open was set to 94, 60 and 35 ml/min. Valve was closed successively 10% of the full range for each of the initial flow rates, and the flows determined from Figure III-6a or measured by volume displacement of water.

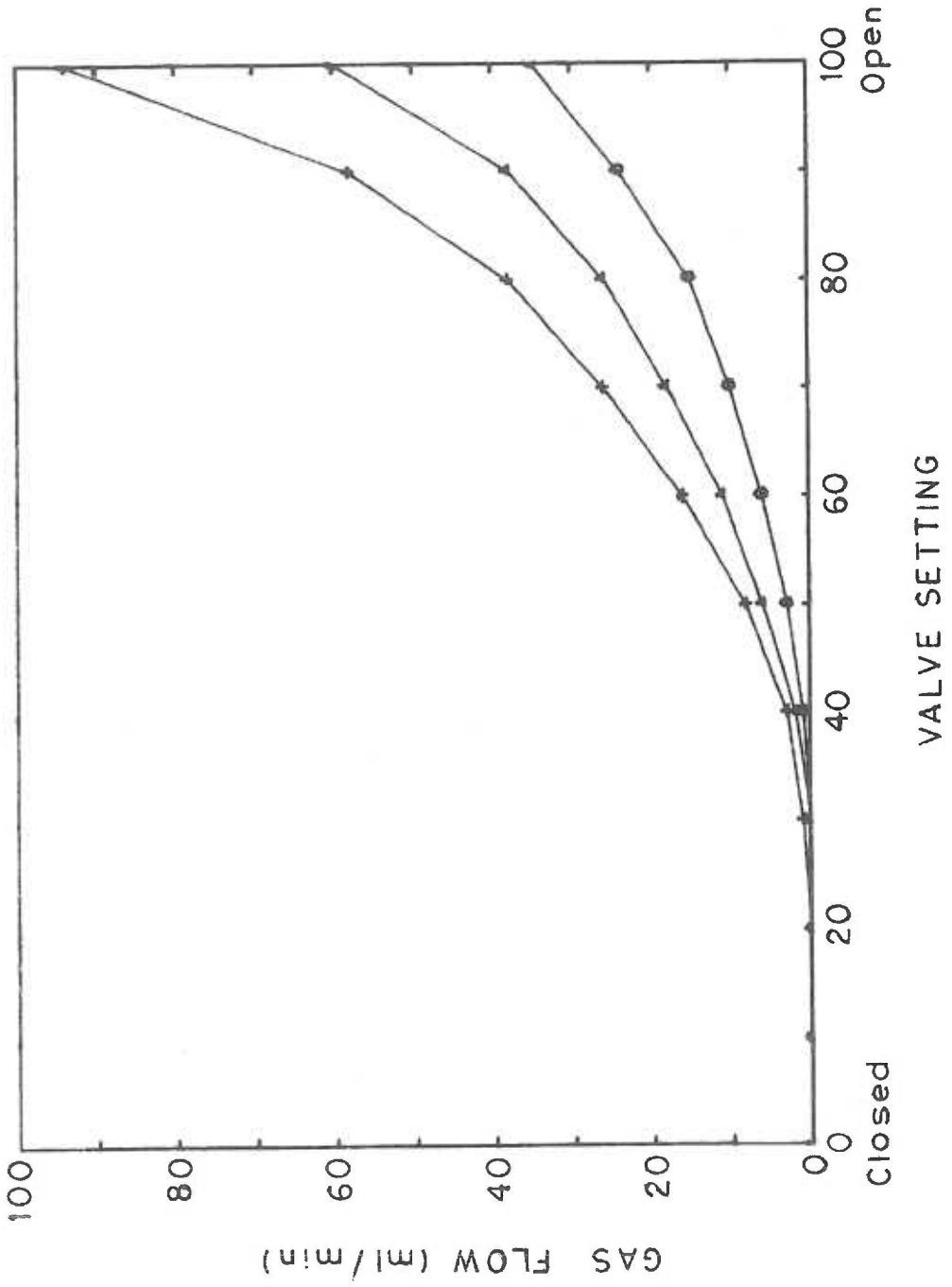
GAS FLOW (ml/min)
100
80
60
40
20
0
0
Closed
20
40
60
80
100
Open
VALVE SETTING

Figure III-10. Oxygen transfer constant at different solution volumes. Modified Hank's solution (4, 6, 8 or 10 ml) was placed in the incubation vessel at 37°C with stirring rate adjusted to give about a 2 sec mixing time. Through the vessel was passed 95% N_2, 5% CO_2 until the solution $P(O_2)$ was near zero. Then 20% O_2, 5% CO_2, 75% N_2 was passed through the vessel and the oxygen tension in solution measured as a function of time. The initial slope, known $P(O_2)_g$ and measured initial $P(O_2)_f$ were used to calculate K (see text). Calculated values for K are expressed as a function of liquid volume in the incubation vessel.

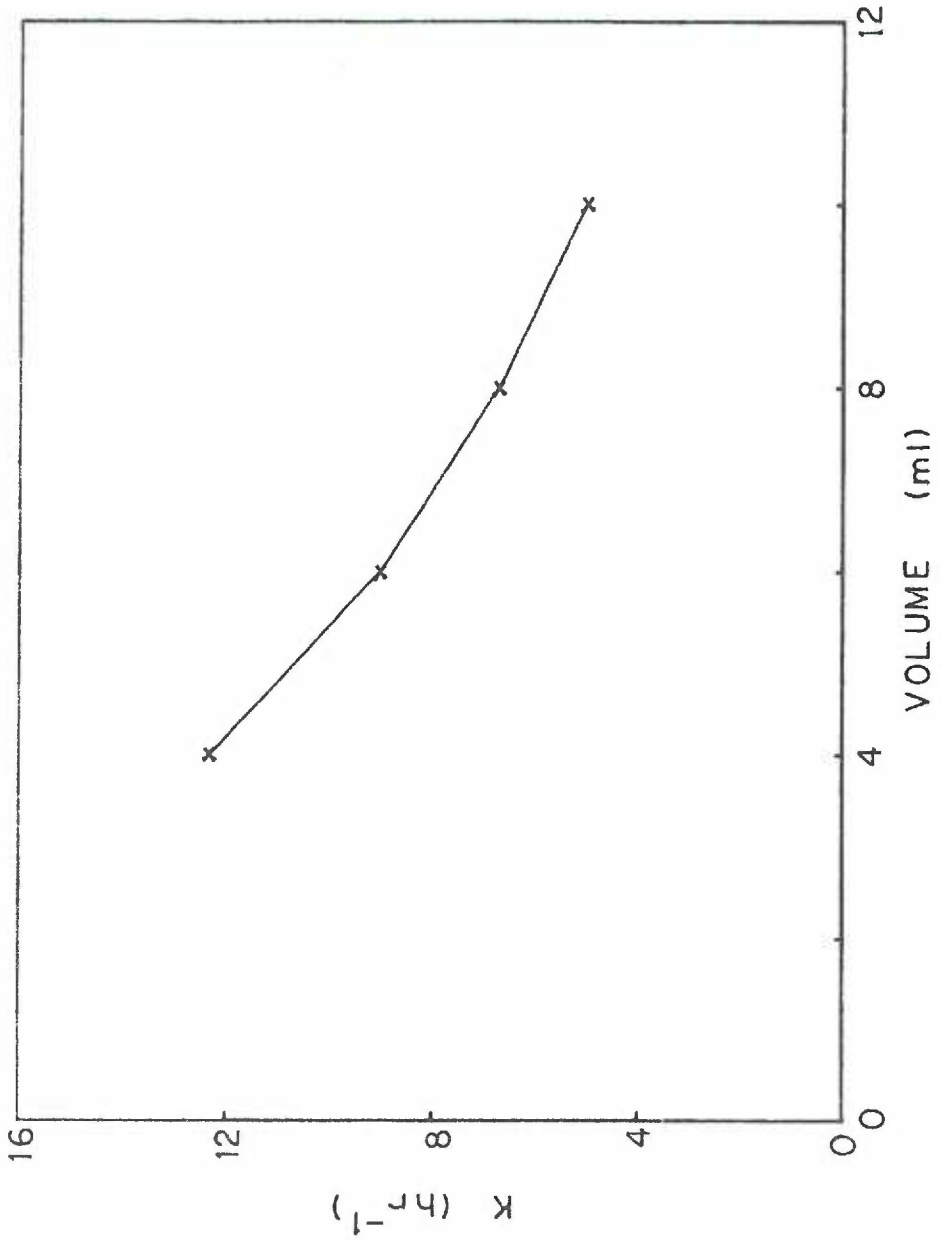
16
12
8
4
0
κ (h⁻¹)
0
4
8
12
VOLUME (ml)

was found to have no effect on K. Variations in stirring rate also had no effect over the narrow tolerable range of stirring rates.

III. C. 3. Steady State Oxygen Tensions in Solution

As a check of the oxygen transfer constant and a further characterization of the incubation vessel, yeast solutions with known respiratory rates were incubated under constant input percent oxygen and the steady state oxygen tension in solution measured. Dry baker's yeast (0.8 gm) was dissolved in 50 ml 100 mM sodium phosphate buffer (pH 7.0) containing 10 mM glucose. Oxygen consumption was measured polarographically at 37°C after 6 x dilution in additional buffer and found to be 12.3 µl O_2/mg dry weight/hr (0.55 µmole O_2/mg hr). Dilutions of the stock yeast solution were then made so that solutions with respiration rates from 10 to 70 µl O_2/ml/hr (0.45-3.13 mM/hr) were obtained. Eight milliliter aliquots were placed in the incubation vessel and gas of known percent oxygen passed through the vessel. The results are shown in Figure III-11 along with the theoretical steady state solution oxygen tensions using the measured rate constant and Equation III-5.

Experiments were performed with constant dilutions of yeast of known respiratory rate as above to determine the steady state solution oxygen tension as a function of input percent oxygen. Steady state solution oxygen tensions were measured polarographically at known

Figure III-11. Steady state oxygen tension in respiring yeast solutions as a function of respiration rate at fixed input percent oxygen. Yeast solutions with respiration rates between 10 and 70 μl O_2/ml/hr (0.45-3.13 mM/hr) were placed in the incubation vessel and equilibrated to 37°C. Incubating medium was 100 mM sodium phosphate buffer (pH 7.0) containing 10 mM glucose. Total aqueous volume was 8 ml. For each incubation, a gas mixture containing 24, 33, 42, or 52% oxygen (182, 250, 319 or 395 torr) was passed through the vessel. The oxygen tension in solution was measured polarographically. After about 15 min, a steady state solution oxygen tension was attained. This value is expressed in the figure as a function of the respiration rate and according to the input percent oxygen. The solid lines are theoretical lines drawn from the equation $R = K \times (P(O_2)_g - P(O_2)_f)$ using the measured value of K and the fixed input $P(O_2)_g$ values.

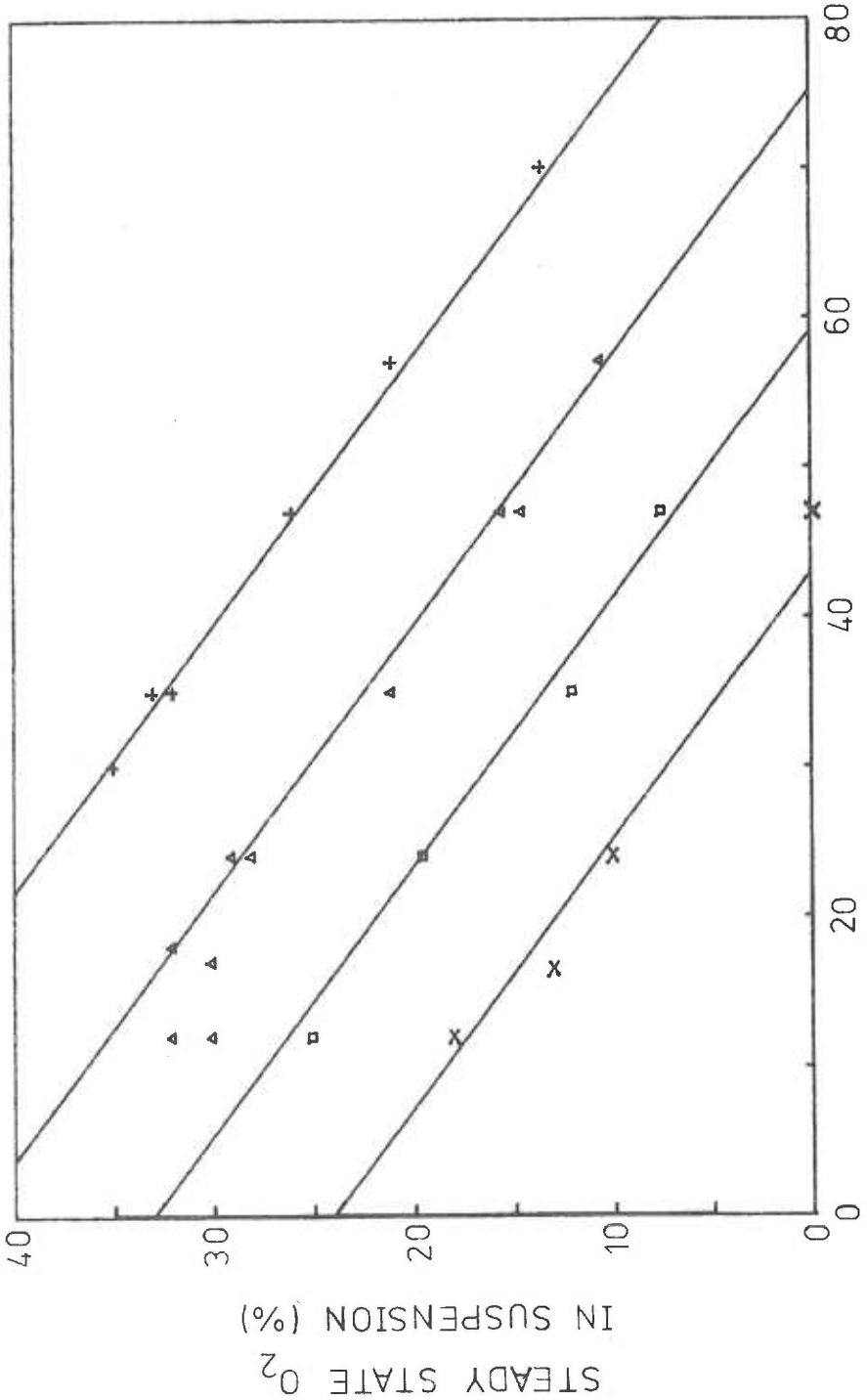
STEADY STATE O_2
IN SUSPENSION (%)
40
30
20
10
0
0
20
40
60
80
RESPIRATORY RATE
($\mu l\ O_2/ml/hr$)

percent oxygen in the gas phase. The results are shown in Figure III-12. Results are consistent with measured rate constant and Equation III-5 as demonstrated by theoretical curves drawn for the respiratory rates used.

III.C.4. Input $P(O_2)$

To achieve optimal control of oxygen tension in solution a minimum difference in percent of oxygen between the carrier and controlled gases is required. The minimum difference is limited by the range of solution oxygen tensions desired and the rate of oxygen consumption in solution. The percent oxygen input to give a desired solution oxygen tension at a specified respiration rate is given below. Once the desired range of input percent oxygen is determined, Figure III-13 can be used to determine the valve position required to give a desired input percent oxygen at preset carrier and controlled gas flow rates. Curves in Figure III-13 were calculated from the gas flow as a function of valve position for the controlled gas given in Figure III-7, the known percent oxygen in the controlled gas, the flow rate for the carrier gas, and the known percent oxygen in the carrier gas.

The measured oxygen transfer constant can be used with the Equation III-5 to calculate the required input percent oxygen to give a desired solution oxygen tension at a specified respiration rate. A

Figure III-12. Steady state oxygen tension in respiring yeast solutions as a function of input percent oxygen. Conditions are the same as Figure III-11 except that R is fixed to 17.7, 30, 46.6 or 80 μl O_2/ml/hr (0.79, 1.34, 2.08 or 3.57 mM/hr) and input $P(O_2)$ varied by mixing 100% N_2 and 100% O_2.

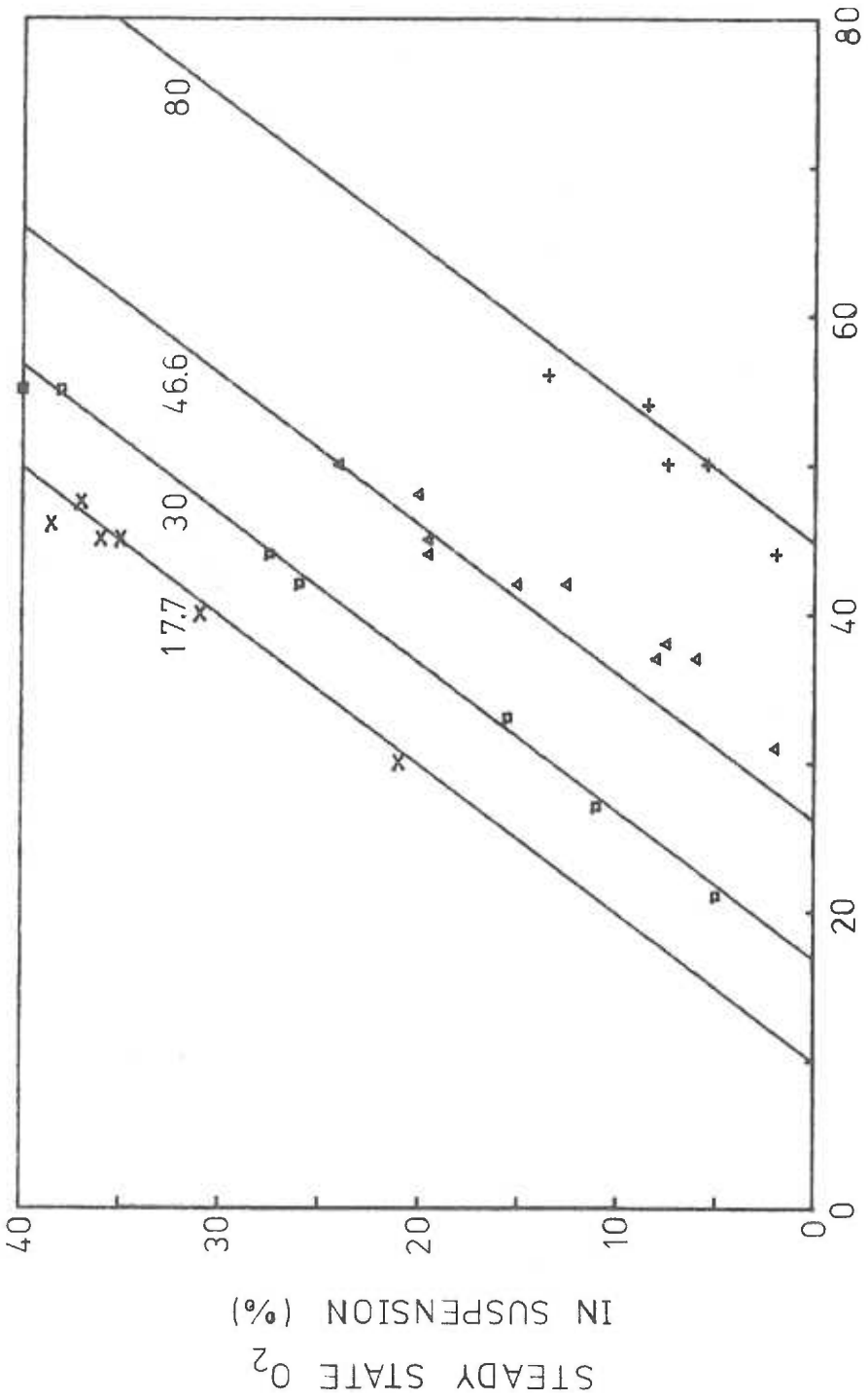
80
46.6
30
17.7
0
20
40
60
80
O_2 INPUT (%)
0
10
20
30
40
STEADY STATE O_2
IN SUSPENSION (%)

Figure III-13. Percent oxygen in mixed gas as a function of valve position for various controlled and carrier gases. Points were calculated from the defined percent oxygen in the controlled and carrier gases, the flow rate for the carrier gas, and the flow rate of the controlled gas as a function of valve position (Figure III-12) according to the equation:

$$\%\ O_2 \text{ mixed} = \frac{(\%\ O_2 \text{ carrier}) \times (\text{flow rate carrier}) + (\%\ O_2 \text{ controlled}) \times (\text{flow rate controlled})}{(\text{flow rate carrier}) + (\text{flow rate controlled})}$$

A. 30% O_2 carrier gas (20 ml/min), 95% O_2 controlled gas (94 ml/min)

B. 20% O_2 carrier gas (20 ml/min), 70% O_2 controlled gas (94 ml/min)

C. 20% O_2 carrier gas (30 ml/min), 70% O_2 controlled gas (60 ml/min)

D. 0% O_2 carrier gas (30 ml/min), 70% O_2 controlled gas (60 ml/min)

E. 0% O_2 carrier gas (20 ml/min), 35% O_2 controlled gas (94 ml/min)

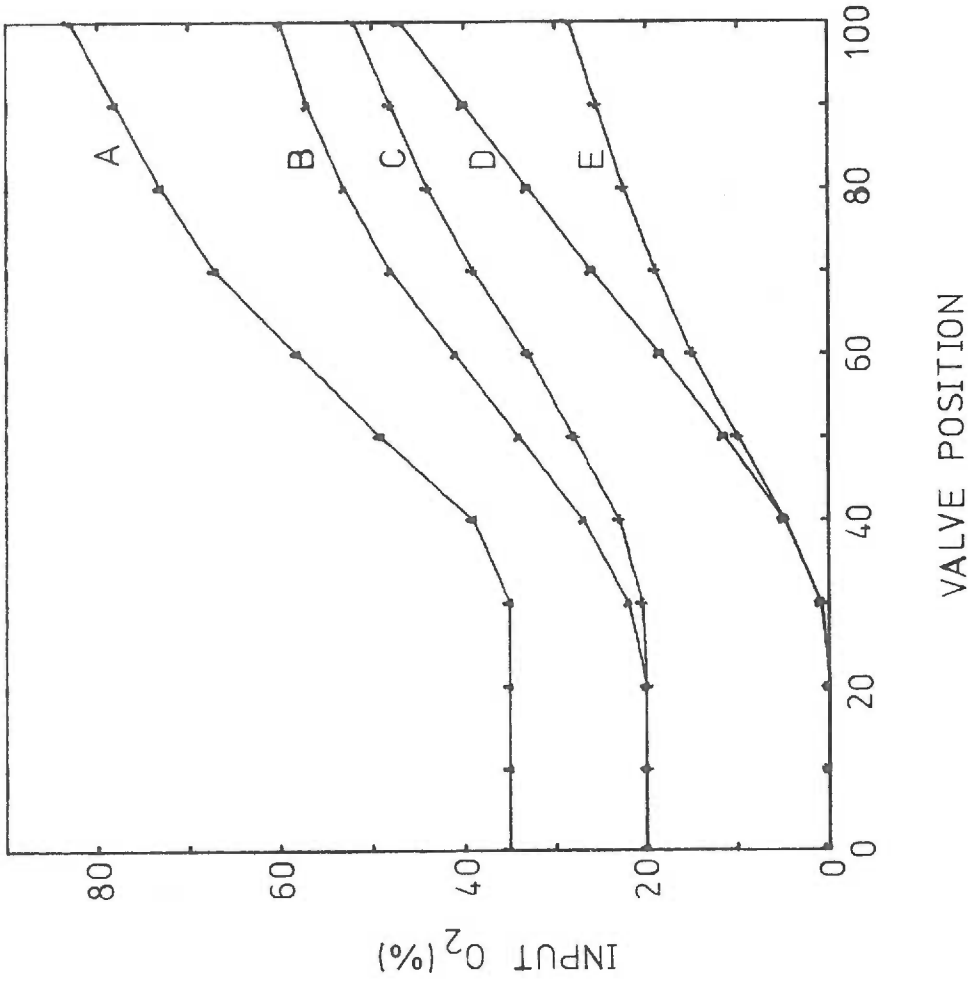
A
B
C
D
E
0
20
40
60
80
100
0
20
40
60
80
VALVE POSITION
INPUT O_2 (%)

typical relationship is shown in Figure III-14. Thus, if one has a suspension consuming oxygen at a rate of 60 μl/ml/hr (2.9 mM/hr) and desires to control the oxygen in the range of 0-20% (0-152 torr) solution oxygen, the percent oxygen input must be controlled between 35 and 55% oxygen. One can then choose carrier and controlled gases with oxygen tensions that span this range, e.g., carrier gas = 20% O_2, controlled gas = 70% O_2. Using Figure III-13, gas flow can be set so that the controller will function over the desired range.

Since oxygen transfer content can be varied by manipulating sample volume, it is of interest to examine the control parameters as a function of K. The percent of oxygen in the gas phase required to maintain a solution oxygen tension of 38 torr at constant rates of oxygen consumption as a function of K is given in Figure III-15. In Figure III-16, the percent oxygen in the gas phase which is required to give solution oxygen tensions of 152, 76, 38, 7.6 and 0 torr, at a respiration rate of 60 μl O_2/ml/hr (2.9 mM/hr) is given as a function of K. From the graphs one can see that the lower the rate of oxygen consumption, the lower the acceptable oxygen transfer constant. The oxygen consumption rates of interest for this work were in the range of 40-80 μl O_2/ml/hr (1.79-3.57 mM/hr). Thus, a transfer constant of 5 or larger is adequate. The percent oxygen input required to maintain solution $P(O_2)$ of 38 torr as a function of oxygen consumption rate for the vessel with an oxygen transfer constant of 6.71 is shown

Figure III-14. Calculated input percent oxygen required to give a desired solution oxygen tension at a specified respiration rate. This series of curves was computer drawn according to the equation III-5. K was set equal to 6.71 hr^{-1}. $P(O_2)_f$ was set equal to 0, 2, 5, 10 or 20% (0, 15.2, 38, 76, or 152 torr), and $P(O_2)_g$ calculated as a function of R and expressed in terms of percentage O_2. R was assumed to be independent of $P(O_2)_f$.

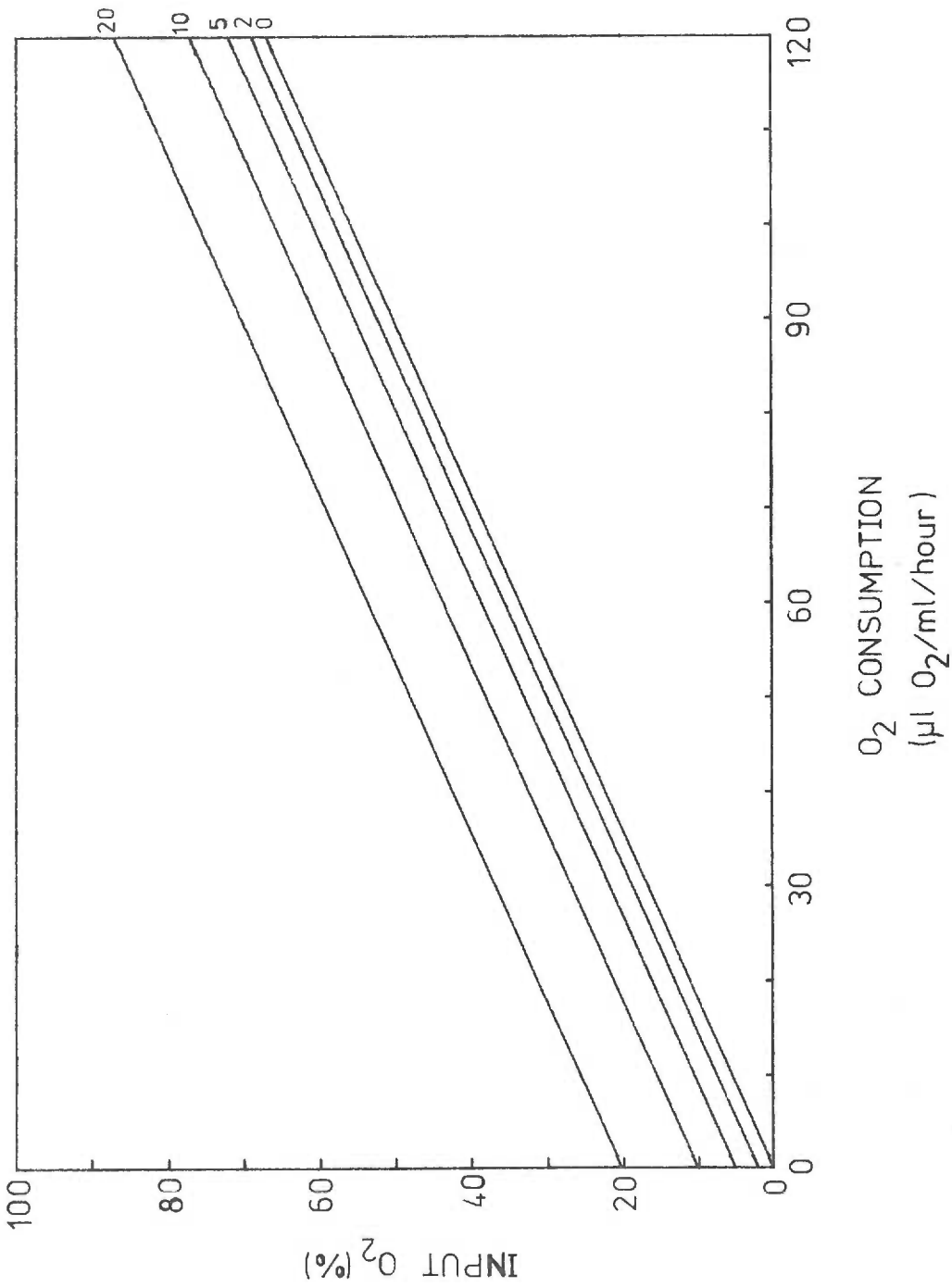
INPUT O_2 (%)
100
80
60
40
20
0
0
30
60
90
120
O_2 CONSUMPTION
(µl O_2/ml/hour)
20
10
5
2
0

Figure III-15. Percent oxygen input required to maintain solution $P(O_2)$ equal to 38 torr as a function of oxygen transfer constant at fixed respiration rates. This series of curves was computer drawn according to the Equation III-5. R was fixed at 20, 40, 60, or 80 µl O_2/ml/hr (0.89, 1.79, 2.68, or 3.57 mM/hr). $P(O_2)_f$ was set at 5% O_2 (38 torr). $P(O_2)_g$ was calculated as a function of K between 0 and 15 hr^{-1}.

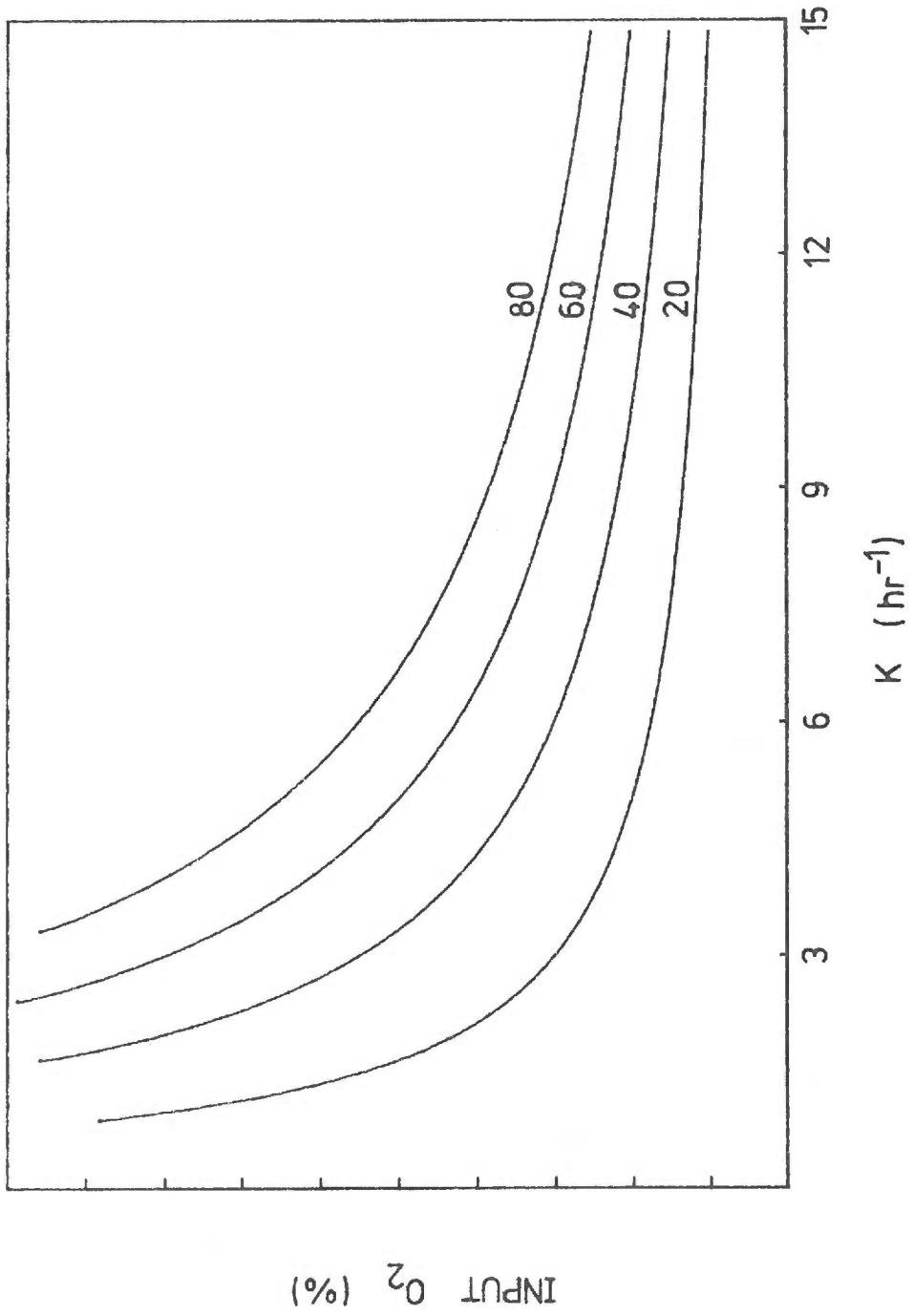
80
60
40
20
3
6
9
12
15
K (hr^{-1})
INPUT O_2 (%)

Figure III-16. Percent oxygen input required to give 0-20% oxygen in a respiring suspension at different values of the oxygen transfer constant. This series of curves was computer drawn to 60 μl O_2/ml/hr (2.68 mM/hr). $P(O_2)_f$ was set at 0, 1, 5, 10, or 20% O_2 (0, 7.6, 38, 76, or 152 torr). Percent oxygen in gas phase was calculated as a function of K from 0 to 15 hr^{-1}.

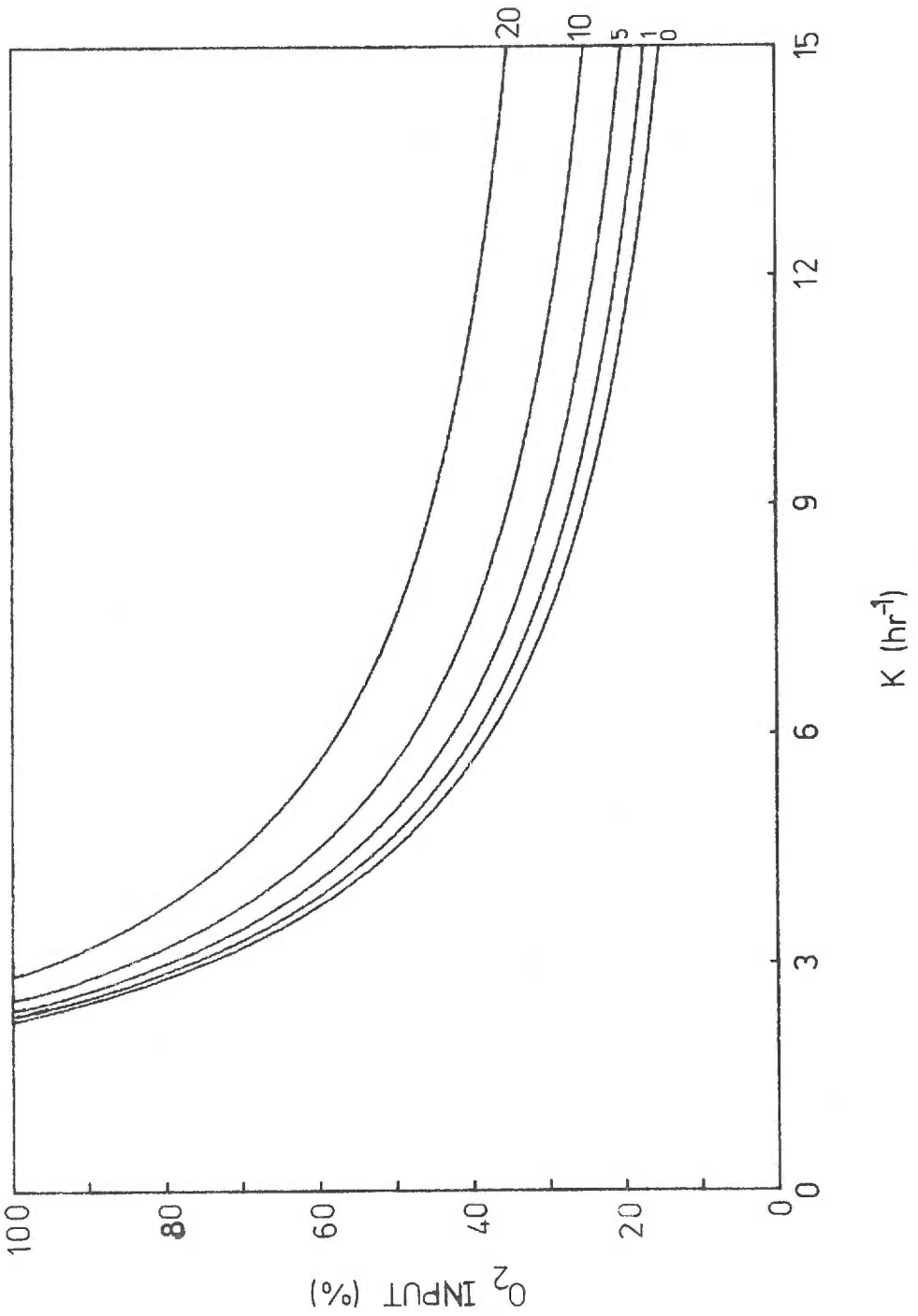
20
10
5
1
0
100
80
60
40
20
0
0
3
6
9
12
15
O_2 INPUT (%)
K (hr^{-1})

in Figure III-17. Curves for other values of K are also given, and used in conjunction with Figure III-10, allow calculation of the maximal incubation volume for the incubation vessel at a known rate of oxygen consumption. Figure III-18 shows the percent oxygen in solution as a function of percent oxygen input at defined values of K and 60 μl O_2 consumption/ml/hr (2.9 mM/hr). Using this graph, corrections can be made during an experiment for errors in respiration rate estimation to adjust control into the desired solution oxygen tension range. For example, if an error were made in estimation of oxygen consumption rate such that the oxystat was equilibrated with carrier and controlled gases which could not provide control at the desired solution $P(O_2)$, the simplest correction is to use this graph to determine a value of K which will provide control and then use Figure III-10 to determine the appropriate aqueous volume. This approach can also be used to extend the oxygen tension range over which solution oxygen tension control can be achieved at constant oxygen consumption rate without changing carrier or controlled gases.

III.D. Operation

Detailed operation instructions for the oxystat are given in Appendix III. The determination of proper controller settings is described in the Hays model 854 Universal Solid State controller instruction manual. Determination of optimum settings requires

Figure III-17. Percent oxygen input required to maintain a solution $P(O_2)$ of 38 torr as a function of respiration rate. This series of curves was computer drawn using the Equation III-5. K was set equal to 3, 6.71, 12 or 24 hr^{-1}. $P(O_2)_f$ was set equal to 38 torr. Percent O_2 input was calculated as a function of O_2 consumption rate over the range 0-100 µl O_2/ml/hr (0-4.46 mM/hr).

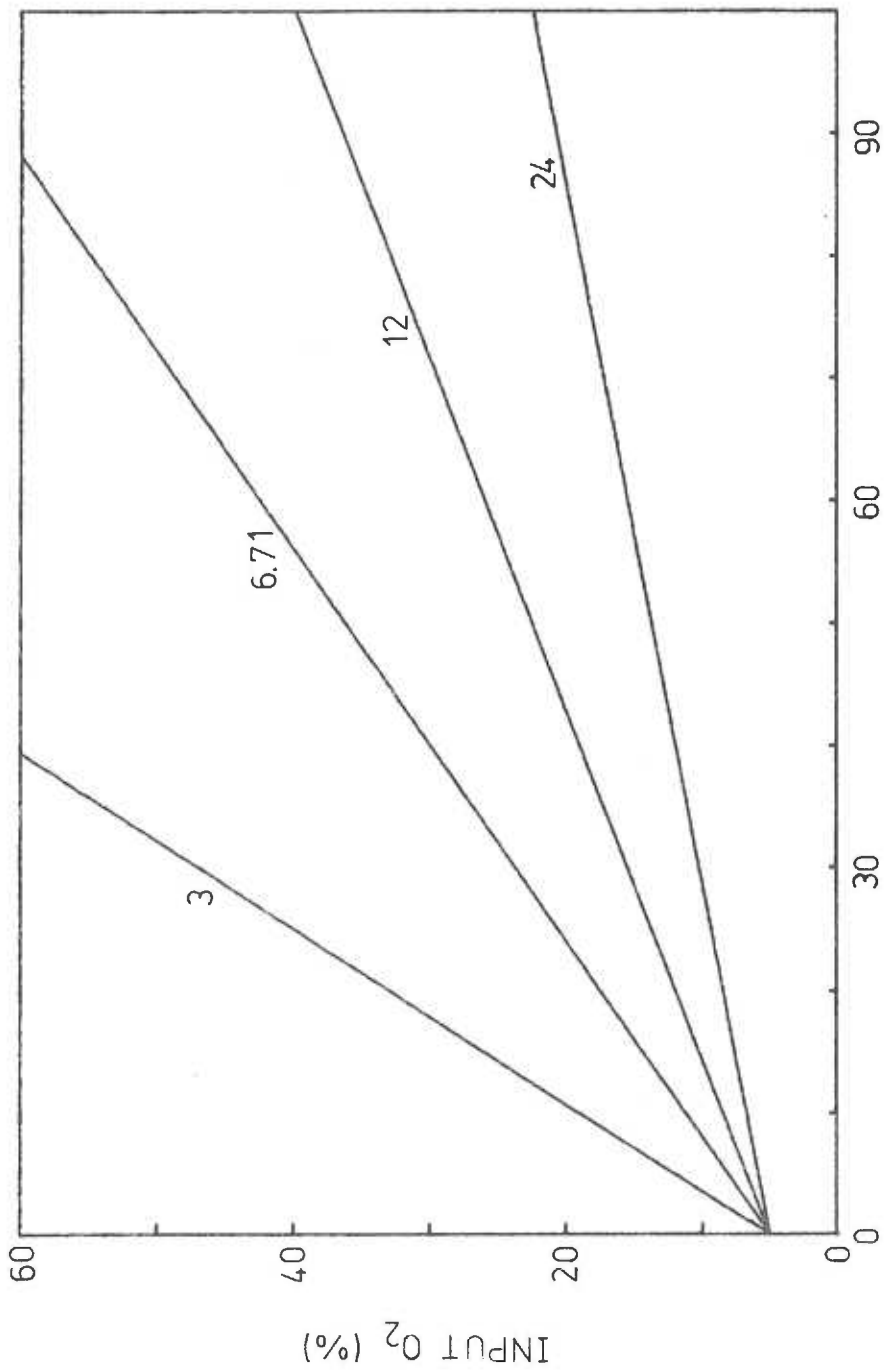
INPUT O_2 (%)
60
40
20
0
0
30
60
90
O_2 CONSUMPTION RATE
(µl/ml/hr)
3
6.71
12
24

Figure III-18. Percent oxygen in solution as a function of percent oxygen input at various values of K. This series of curves was calculated using the Equation III-5. R was set at 60 µl O_2/ml/hr (2.68 mM/hr). K was set equal to 3, 6.71, 12, 24 hr^{-1} or infinity. $P(O_2)_f$ was calculated as a function of $P(O_2)_g$. R was assumed independent of $P(O_2)_f$.

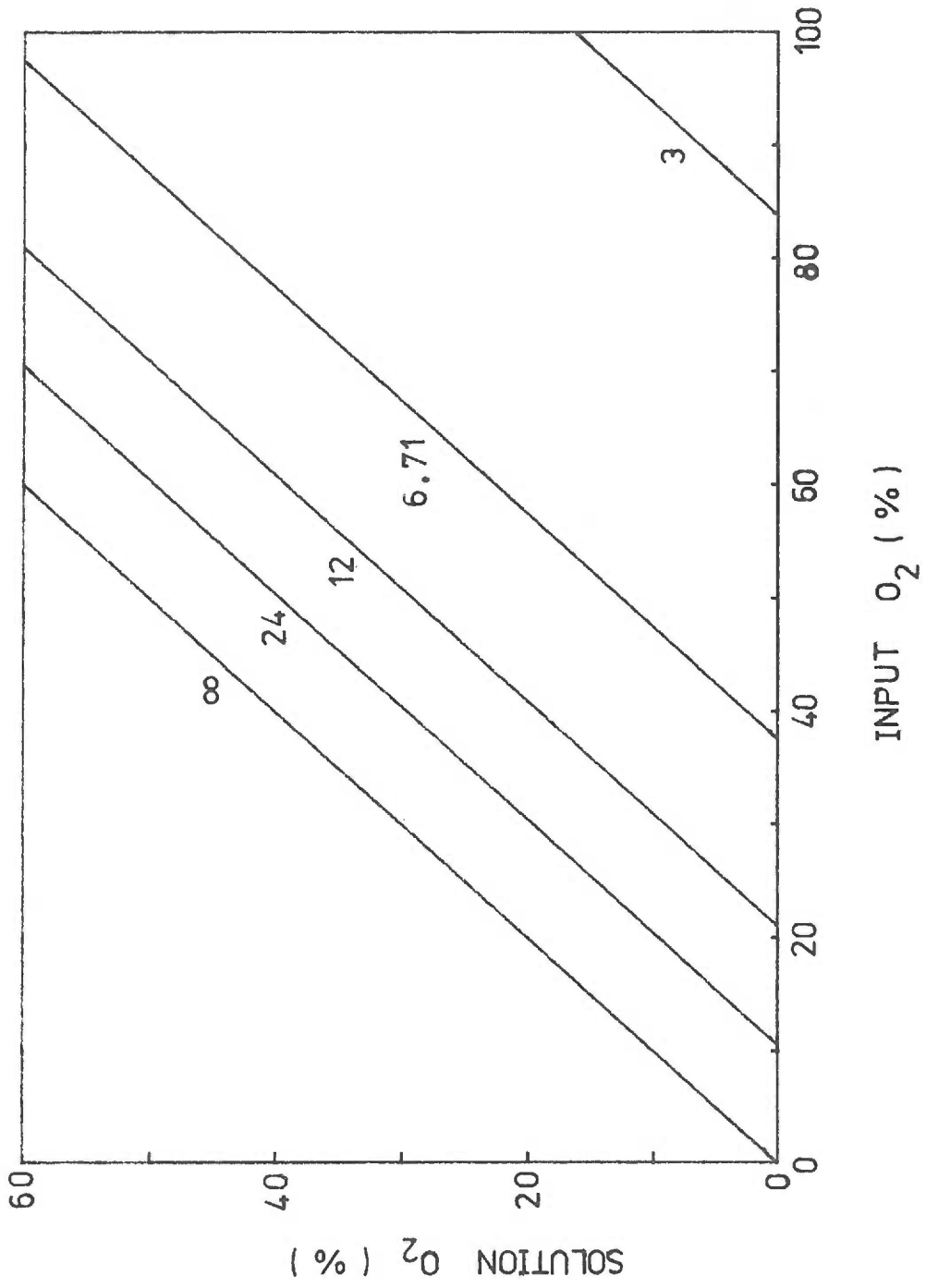
SOLUTION O_2 (%)
0
20
40
60
INPUT O_2 (%)
0
20
40
60
80
100
3
6.71
12
24
∞

obtaining a balance between speed of response and accuracy of response. The proportional band, expressed as a percent of the full oxygen range, determines the amount the valve will move for a given deviation from the desired oxygen tension. Greatest accuracy is attained at high proportional band settings; however, these high settings have the poorest speed of response. For short term experiments (e.g., less than 1 hr), a sacrifice must be made in accuracy to provide rapid control. The rate control is an anticipation factor which examines the first derivative of approach to set point. The system did not have a large lag in response and this control was not needed. Reset controls the rate of valve position change as determined by the proportional band. It is expressed in repeats per minute. The highest possible setting which does not produce oscillations gives the fastest system response. Settings which provide optimum response and optimum control for a system with an oxygen transfer constant of 6.71 hr^{-1}, an oxygen consumption rate of 40-70 µl O_2/ml/hr (1.79-3.13 mM/hr), and a solution oxygen tension of 1-150 torr (1.4-210 µM) were as follows: proportional band at 500%, rate off, and reset at 0.1 rpm. Dead band was adjusted to the minimum possible value. These settings were obtained empirically starting with rate and reset off and proportional band at 70%. The proportional band was then increased stepwise until oscillations ceased. The oxygen tension in solution under such conditions would attain a

constant value; however, this value did not necessarily approach the set point, so reset was introduced stepwise until oscillations again appeared. Then the reset was reduced one step to give the optimal setting.

The controller was tested to determine its ability to maintain a constant solution $P(O_2)$ for different rates of oxygen consumption using the above settings. The results are given in Figure III-19 for two different sets of carrier and controlled gases. The set point in either case was 76 torr (106 μM). Control of $P(O_2)_f$ is approximately ± 7% as long as the valve is operating 60-90% open even over the broad range of oxygen consumption rates shown. Drift in solution $P(O_2)$ occurs at lower rates of oxygen consumption and oscillations occur at higher rates of oxygen consumption.

Oxygen control experiments reported in Sections IV, V, and VI were done under the following conditions: 40-70 μl O_2 consumption/ml/hr (1.79-3.13 mM/hr), 37°C, 8 ml aqueous volume, and rate constant equal to 6.71. Solution tensions were controlled from 0.2 torr (0.28 μM) to 150 torr (210 μM). Carrier gas was usually 20% O_2, 5% CO_2, 75% N_2 and controlled gas was 70% O_2, 5% CO_2, 25% N_2. Under some circumstances 5% CO_2, 95% N_2 and 35% O_2, 5% CO_2 and 60% N_2 were used. The percent fluctuations of the solution oxygen tension at the different oxygen tensions is given in Figure III-20. The maximum deviations about the average were measured,

Figure III-19. Controller function at different respiration rates. Yeast suspensions with oxygen consumption rates of 10-100 µl O_2/ml/hr (0.45-4.5 mM/hr) were placed in the incubating vessel. Incubation medium was sodium phosphate buffer (50 mM, pH 7.0), containing glucose (10 mM). Total volume was 8 ml in each case. Temperature was 37°C. Incubations were maintained for 20 min after control was attained or a maximum of 30 min. Controlled gas was 30% O_2, 70% N_2 with 100% N_2 as carrier gas, or 100% O_2 with compressed air as carrier gas. The set point was 76 torr. The range of fluctuation of $P(O_2)$ about the average value is expressed by the bars.

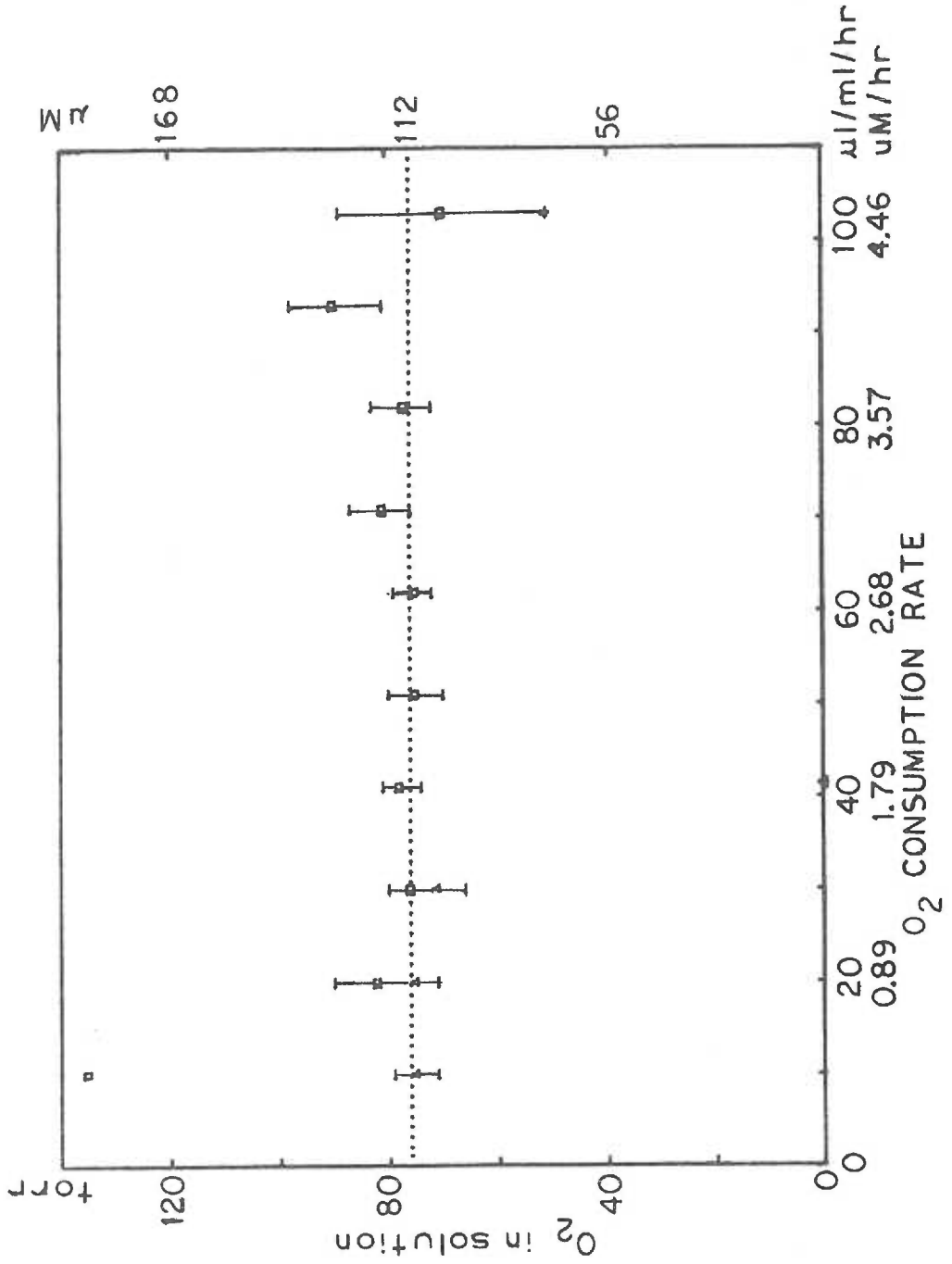
torr
120
80
40
0
O_2 in solution
uM
168
112
56
0
20
40
60
80
100 µl/ml/hr
0.89
1.79
2.68
3.57
4.46 uM/hr
O_2 CONSUMPTION RATE

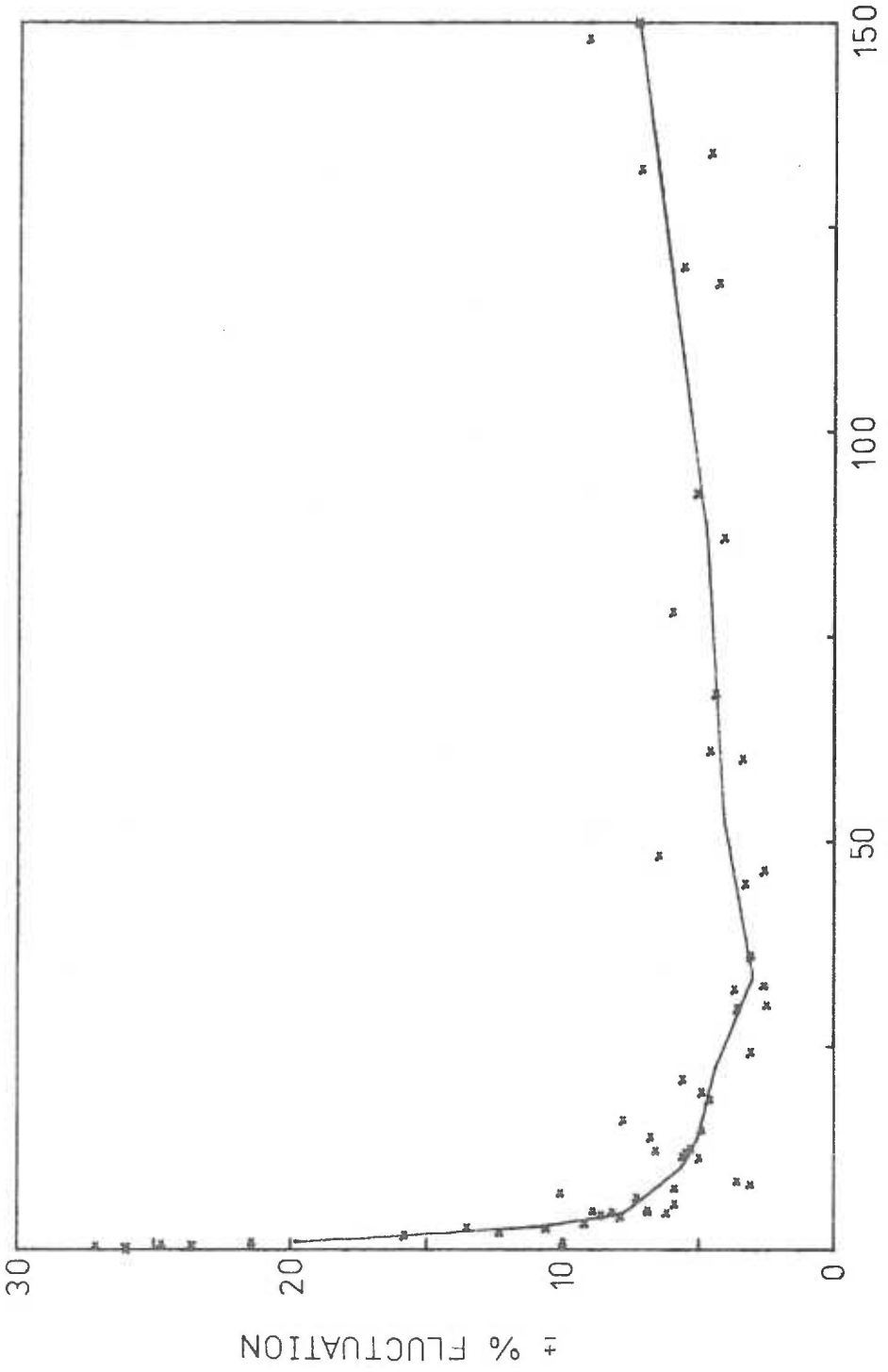
± % FLUCTUATION
30
20
10
0
50
100
150
P(O_2) (torr)

divided by the average, multiplied by 100% and then by 0.5 to express as $\pm$ percent fluctuation. From this figure, one can see that the average percent fluctuation is $\pm$ 20% at 1 torr (1.4 μM), $\pm$ 15% at 2 torr (2.8 μM), $\pm$ 11% at 3 torr (4.2 μM), and less than $\pm$ 7% at 4 torr (5.6-210 μM).

Rapid approach to a desired steady state solution $P(O_2)$ was obtained by dilution of cells into solutions equilibrated with low oxygen tensions at 37°C. This solution was then pipetted into the incubation vessel, and the oxygen analyzing system turned on. The vessel was then flushed with 95% O_2, 5% CO_2 or 95% N_2, 5% CO_2 until the desired oxygen tension was approached (1-3 min). Gas flow through the oxystat was then started with the valve preset to give the desired $P(O_2)$ in solution. After 2-3 min, the controller mode was switched from manual to automatic and steady state maintained.

III.E. Discussion

High oxygen consumption rates by isolated mammalian cells makes study of cellular metabolism as a function of oxygen tension technically difficult (Wilson et al., 1974). Development of an instrument that can maintain constant $P(O_2)$ in cellular suspensions is an important breakthrough in research of hypoxia and oxygen metabolism. The oxystat allows study of oxygen utilizing systems in intact cells as a function of oxygen tensions even though the system under

investigation consumes only a very small fraction of the total oxygen. In addition, it allows direct analysis of metabolite levels in cells at different steady state oxygen tensions. The intracellular function and control of oxidases may be examined under highly defined conditions. Oxygen tension is measured continually throughout the incubation and can be maintained at a predetermined value. The approach to this value is rapid, and once attained can be maintained indefinitely. The carbon dioxide concentration can be established at a constant value by inclusion of CO_2 at the same percentage in both carriers and controlled gases.

The instrument as described has been tested over the oxygen tension range of 0.2-150 torr (2.8-210 μM) with isolated rat hepatocytes. Incubations below 1 torr (1.4 μM) are of limited value because of relatively large $P(O_2)$ fluctuations. Inclusion of hemoglobin or myoglobin (2 mg/ml) increases the apparent solubility of oxygen and improves performance below 1 torr; however, these additions may interfere with the assay of cellular metabolism. The ability of the instrument to perform to 1 torr (1.4 μM) with isolated hepatocytes is probably due to reduced oxygen consumption rate at this low oxygen tension (Longmuir, 1957; see Section IV). The instrument may also be useful for hyperoxia studies (> 150 torr; > 210 μM) and is limited only by the oxygen transfer constant. The theoretical upper limit for $P(O_2)_f$ in a system of known R at atmospheric pressure can be

calculated for this instrument using Equation III-5 with K between 12 and 5 (4-10 ml volume).

The carrier and controlled gases were chosen for the experiments reported (Sections IV, V and VI) so that oxygen tension could be preset at any value between 1 and 150 torr (1.4 and 210 μM). Repetitive experiments at a single desired $P(O_2)_f$ can be performed with much less variability by choosing carrier and controlled gases with a much smaller difference in oxygen content.

The ability of the instrument to maintain constant $P(O_2)_f$ was demonstrated for an 8 ml volume with oxygen consumption rate between 10 and 80 μl/ml/hr (0.45 and 3.57 mM/hr). At lower oxygen consumption rates maintenance of constant $P(O_2)_f$ becomes progressively easier as $P(O_2)_f$ approaches $P(O_2)_g$. Above 80 μl O_2/ml/hr, control becomes increasingly difficult.

Although only cellular systems were examined, the instrument is likely to be useful for oxygen consuming enzymatic or chemical systems. It has greater versatility and control than manometric systems, closed polarographic systems or the respirograph. In addition, the principle may be applicable to studies of perfused organs or to oxygenation of blood by heart-lung machines.

IV. RESPIRATION AND ENERGETICS OF ISOLATED HEPATOCYTES

Changes in adenylate concentrations and lactate/pyruvate occur during hypoxia and have been implicated in altered cell function and subsequent pathology (Section I.B.). Many parameters may be used as indicators of cellular energetics. Some of those which are most commonly used are: ATP concentration, the ratio of ATP to ADP, the phosphorylation state potential ([ATP]/[ADP][Pi]), adenylate energy charge (([ATP]+1/2[ADP])/([ATP]+[ADP]+[AMP])), cytoplasmic $NADH/NAD^+$ and mitochondrial $NADH/NAD^+$. Because of varying experimental circumstances, no single parameter is universally measurable or useful. However, all of these parameters appear to be qualitatively related under most physiological situations. A list of these values under oxygenated conditions is given in Table IV-A. Oxygen consumption by isolated hepatocytes is given in Table IV-B.

Decreased oxygen availability to hepatocytes alters these parameters in predictable directions. Decreased rate of oxygen consumption occurs when oxygen tension is lowered below the critical oxygen tension (Chance et al., 1964; Jobsis, 1972). Total cellular redox state becomes more negative as reflected in a greater degree of reduction of reducible components (Ballard, 1971; Chance et al., 1962). ATP concentration decreases and AMP increases with decreased $P(O_2)$ (Atkinson, 1968; Ballard, 1970).

Table IV-A. Metabolite levels in isolated hepatocytes (mmole/kg).

ATP	2.57	Krebs et al., 1974
	2.12	Meijer and Williamson, 1974
	2.21	
	2.28 ± 0.46	This research
ADP	0.87	Krebs et al., 1974
	0.32	Wilson et al., 1974
	0.48	
	0.72	Meijer and Williamson, 1974
	0.77	
AMP	0.35	Krebs et al., 1974
Pi (1 mM Pi incubating medium)	2.16	Wilson et al., 1974
	2.93	
Lactate/pyruvate (intact liver)	7.52	Veech et al., 1970
β-Hydroxybutyrate/ acetoacetate	0.35	Wilson et al., 1974
	0.34	
	0.49	Meijer and Williamson, 1974
	0.35	

Table IV-B. Oxygen consumption by isolated hepatocytes. Conditions as listed; all were at 37°C.

	μmole O_2/min/gm (wet weight)	
Endogenous, fasted	1.94 ± 0.05	Berry, 1974
Endogenous, fed	2.5	Wilson, 1974
	0.7 - 2.2	Quistorff et al., 1973
Endogenous, fed	1.88 ± 0.31	This research

Determination of the oxygen dependence of mitochondrial respiration in the liver (Section I.B.5.b.) has been studied at three levels of organization: intact liver, isolated cells, and isolated mitochondria. Ballard (1970, 1971) measured redox and energetic changes in the liver in intact animals as a function of inspired oxygen. These data are discussed in Section I.B.5.b. Longmuir (1957) measured oxygen consumption by isolated hepatocytes as a function of oxygen tension and observed a respiratory "$Km(O_2)$" of about 0.38 torr (0.5 μM). This measurement provides an indication of the oxygen tension at which energetic changes due to oxygen concentration may occur. However, the cells may have been damaged due to the method of preparation. Measurements of adenylate and redox changes were not made so these energetic parameters are not available. Studies on oxygen consumption, pyridine nucleotide reduction, and cytochrome c reduction in isolated mitochondria show that $P(O_2)$ at half maximal changes for these functions occur at 0.02-0.2 torr (0.03-0.3 μM) (Sugano et al., 1974). Mitochondrial oxygen consumption has been shown to be dependent upon ATP and ADP concentrations (Christensen et al., 1971) and the redox state has been shown to be related to cytoplasmic energetics (Wilson et al., 1974a, b). The direct applicability of mitochondrial values to cellular metabolism is doubtful because of the altered metabolic environment of the subcellular fraction. The present research on isolated cells provides a continuity

between studies on subcellular and intact liver. It examines the adenylate pool, lactate/pyruvate, and oxygen consumption as a function of oxygen tension and provides reference values to which other hypoxic changes can be compared.

IV.A. Respiratory Rate as a Function of Oxygen Tension

The oxygen tension tracing as a function of time for an incubation of isolated hepatocytes is given in Figure IV-1. An estimation of the first derivative of this plot is given as the $\Delta P(O_2)$/second as a function of $P(O_2)$ in Figure IV-2. From this and similar tracings, the oxygen tension for half maximal respiration by isolated hepatocytes was determined to be 1.45 ± 0.21 torr (2.03 ± 0.29 μM) (N = 6). The $P(O_2)$ at which deviation from zero order with regard to oxygen consumption could be observed was 14 torr (19.6 μM).

The double reciprocal plot of the rate of oxygen consumption as a function of oxygen tension is given in Figure IV-3. The linear least squares line for these points gives an apparent $Km(O_2)$ equal to 1.36 ± 0.13 torr (1.90 ± 0.18 μM), and a maximal respiration equal to 20.8 μl O_2/mg protein/hr (29.1 μM/hr). The theoretical curve for this system assuming Michaelis kinetics is shown in Figure IV-2.

Figure IV-1. Polarographic tracing of oxygen consumption by isolated hepatocytes. Isolated hepatocytes (3×10^6 cells/ml) were placed in thermostatted polarographic cell equipped with Clark-type electrode connected through amplifier and analog-digital converter to PDP-11 computer. Oxygen tension recordings were registered at 10 sec^{-1} and averaged to give 1/sec data.

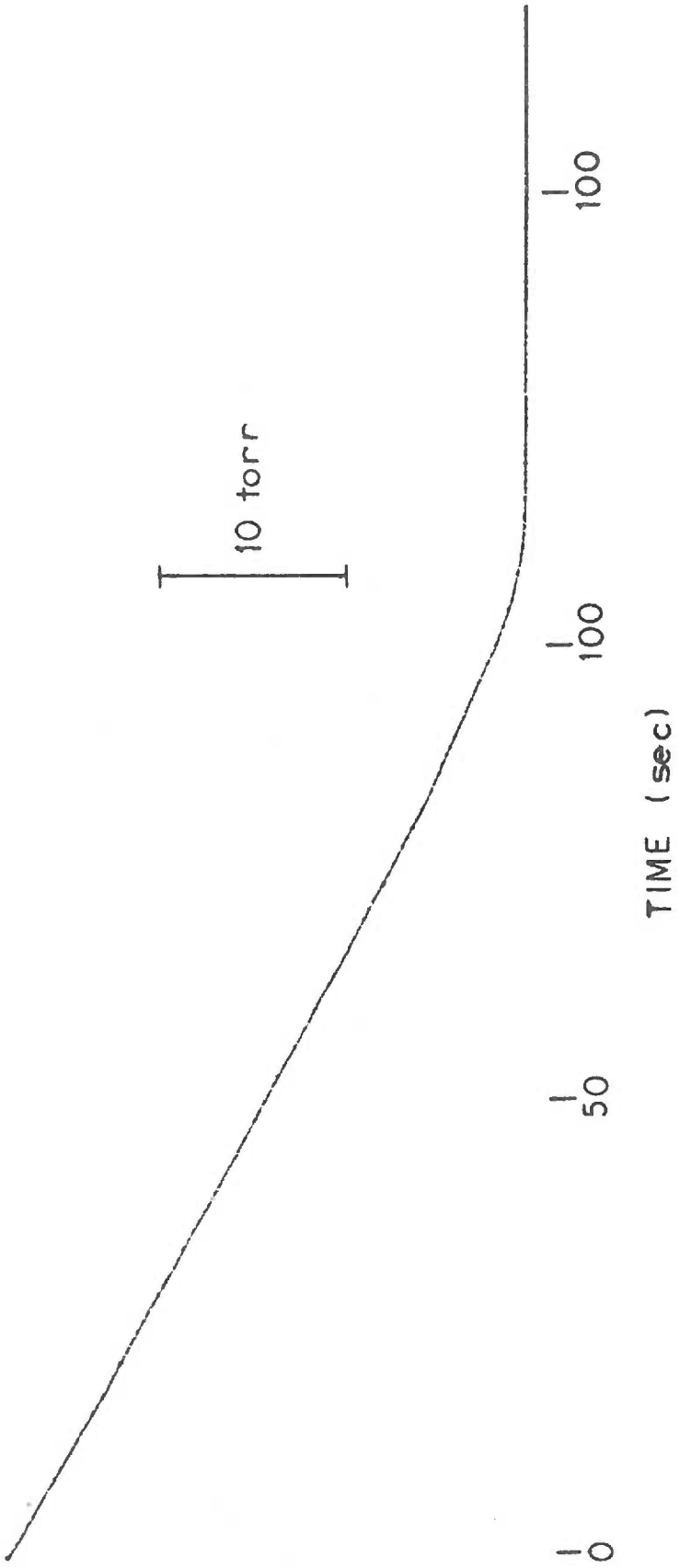
10 torr
0
50
100
100
TIME (sec)

Figure IV-2. Hepatocyte respiration rate as a function of oxygen tension. Isolated hepatocytes (3×10^6 cells/ml) were placed in thermostatted polarographic cells equipped with Clark-type electrode connected through amplifier and analog-digital converter to PDP-11 computer. Oxygen tension recordings were registered at 10 sec^{-1} and averaged to give 1 sec data. The change in $P(O_2)$/sec was then plotted as a function of $P(O_2)$ with an 11 point smoothing routine (see Appendix IV). The data thus represent the rate of oxygen consumption as a function of oxygen tension. the solid line represents oxygen consumption with the measured Q_{O_2} and $Km(O_2)$ = 1.3 torr (1.8 μM) assuming Michaelis kinetics are applicable.

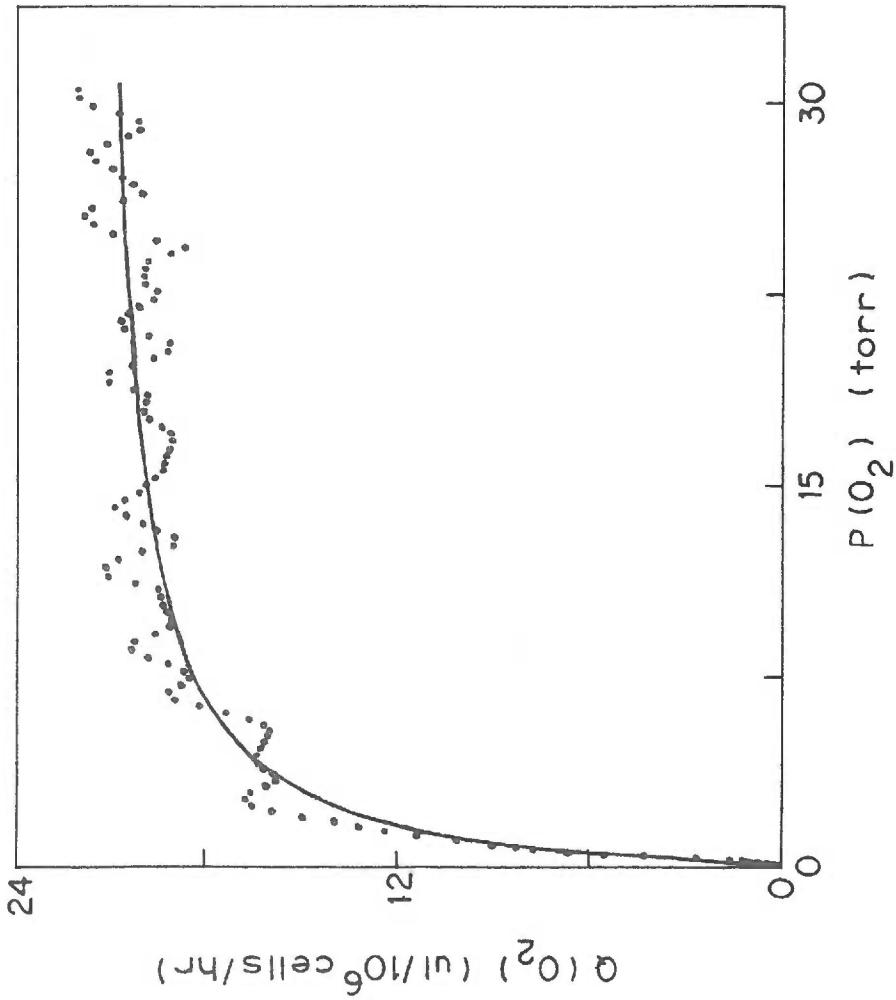
24
12
0
0
15
30
P (O_2) (torr)
Q (O_2) (ul/10^6 cells/hr)

Figure IV-3. Double reciprocal plot of oxygen consumption rate and oxygen tension. Data same as Figure IV-2 and plotted by computer (see Appendix IV).

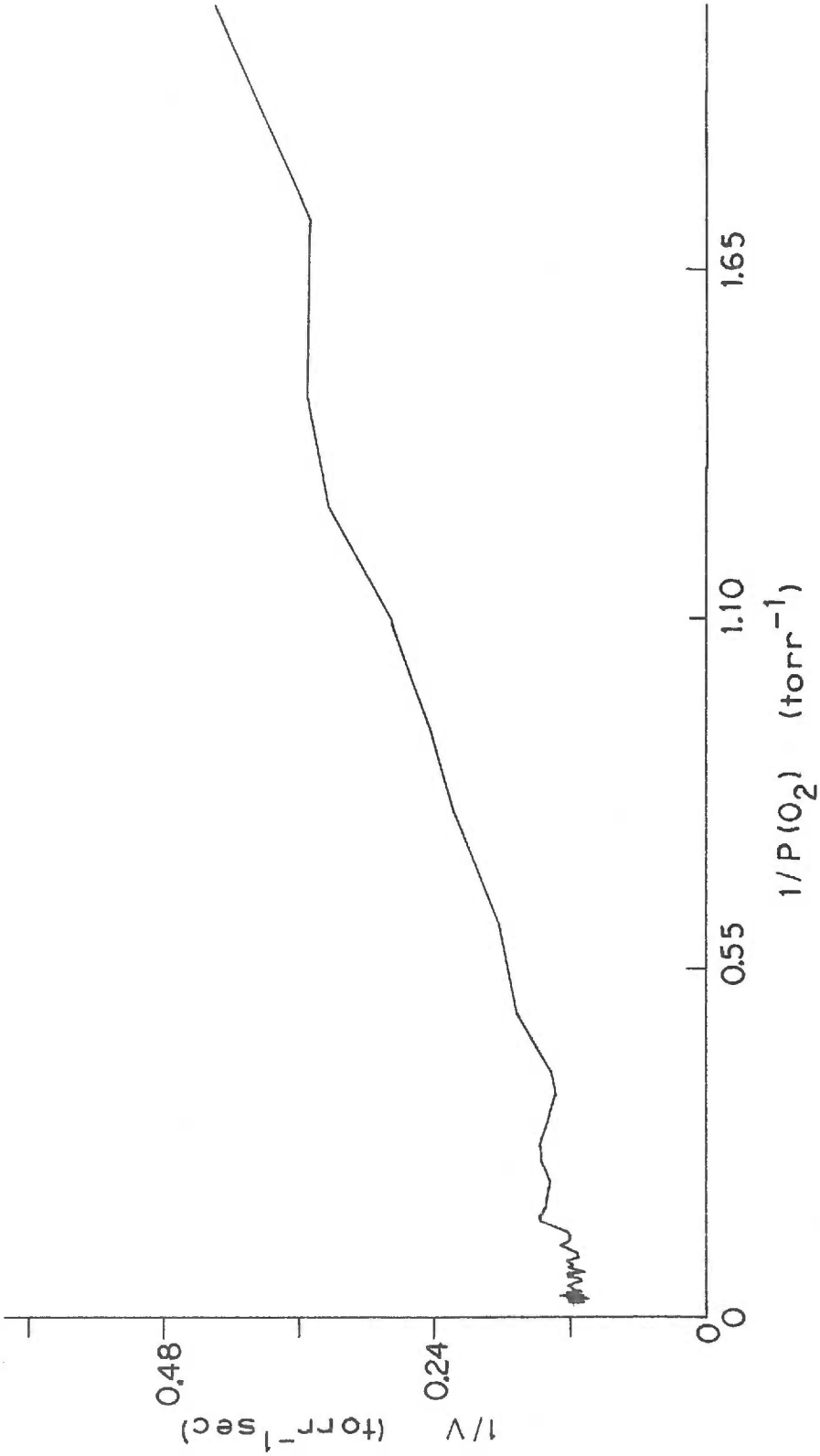
0.48
0.24
0
1/V (torr⁻¹sec)
0
0.55
1.10
1.65
1/P(O2) (torr⁻¹)

IV.B. Lactate and Pyruvate Concentrations as a Function of Oxygen Tension

IV.B.1. Lactate and Pyruvate Partitioning between Hepatocytes and Medium

Estimation of the fraction of total incubation lactate and pyruvate that was contained in the cells was performed by separation of the cells from the suspending volume and assaying the levels in the suspending medium or cell fraction relative to the total incubation (see Section II.D). The partitioning of lactate and pyruvate in four different cell preparations is shown in Table IV-C and IV-D. Cells were isolated by the perfusion method, incubated at 37°C for 30 min under 20% O_2, 5% CO_2, 75% N_2. Cell concentration was 3×10^6 cells/ml in 8 ml modified Hank's medium. Incubation mixtures were centrifuged at 50 g for 3 min and supernatant decanted. To 6 ml of supernatant was added 1 ml 2 N H_2SO_4. The pellet volume was estimated from tube plus pellet weight minus tube weight assuming the density for cells to be 1.07 gm/ml (Krebs et al., 1974). Volume of cells was estimated from cell count and 7.25 $\mu l/10^6$ cells (Krebs et al., 1974). Concentration in cells was calculated from total pellet concentration using calculated cell volume as a percent of total cell volume and the supernatant concentration as an estimate for packing volume concentration

$$C_{cells} + V_{cells} + C_{supernatant} \times V_{packing} = C_{pellet} \times V_{pellet},$$

Table IV-C. Lactate partitioning between cells and suspending medium. Isolated hepatocytes were incubated at 37°C for 30 min at room temperature under 20% O_2, 5% CO_2, 75% N_2. Cell concentration was 3×10^6 cells/ml in modified Hank's medium. Cells were centrifuged at 50 x g for 5 min, supernatant decanted and both portions quenched with 2 N H_2SO_4.

Preparation	Lactate (mM)		Cells/supernatant (P/S)	% of Total in pellet
	Cells	Supernatant		
CP4-11	2.68	0.920	2.91	74.4
CP4-14	1.92	0.737	2.61	72.2
CP4-15	2.11	0.984	2.14	68.3
CP4-16	2.54	0.967	2.63	72.4
Avg.	2.31 ± 0.36	0.902 ± 0.113	2.57 ± 0.32	71.8 ± 2.6

Table IV-D. Pyruvate partitioning between cells and suspending medium (see Table IV-C).

	Pyruvate (mM)		Cells/supernatant (P/S)	% of Total in pellet
	Cells	Supernatant		
CP4-11	0.241	0.130	1.85	65.0
CP4-14	0.206	0.109	1.89	65.4
CP4-15	0.177	0.096	1.84	64.8
CP4-16	0.228	0.126	1.81	64.4
Avg.	0.213 ± 0.028	0.115 ± 0.016	1.85 ± 0.03	64.9 ± 0.4

where C refers to concentration and V refers to volume of the various components. The cell volume ranged from 63-72% of the pellet volume. The percent of the total lactic acid which was found in the cells was 71.8 ± 2.6. For pyruvic acid the value was 64.9 ± 0.4%.

IV.B.2. Lactic Acid Concentration in Hepatocytes as a Function of Oxygen Tension

The lactic acid concentration in incubation mixtures containing 3×10^6 hepatocytes/ml in modified Hank's medium was measured after maintenance at 37°C at fixed oxygen tensions. The oxygen tensions ranged from zero to 150 torr (210 μM). After 10 min at constant solution $P(O_2)$ the system was quenched by injection of 2 N H_2SO_4. The protein was removed by centrifugation and the lactic acid measured fluorometrically. The partitioning value determined above for the same cell concentration was used to calculate the lactic acid concentration in the cells as a function of oxygen tension. The results from three cell preparations are shown in Figure IV-4. The initial increase in lactic acid concentration above 0.5 mM is observed as oxygen tension is lowered below about 20 torr (28 μM). Half maximal change occurs around 9 torr (12.6 μM).

Figure IV-4. Cellular lactate and pyruvate concentrations as a function of solution $P(O_2)$. Isolated hepatocytes (3×10^6 cells/ml) were incubated in modified Hank's medium at fixed oxygen tensions for 10 min at 37°C, then quenched by injection of 2 N H_2SO_4. Lactate was measured by an enzymatic assay utilizing lactate dehydrogenase and measuring the increase in fluorescence of NADH due to addition of lactate. Pyruvate was measured by an enzymatic assay utilizing lactate dehydrogenase and measuring the decrease in absorbance due to loss of NADH upon addition of pyruvate. Data are expressed as intracellular concentration after correction for differences in cellular and suspending medium concentrations. Data from three cell preparations, n = 15.

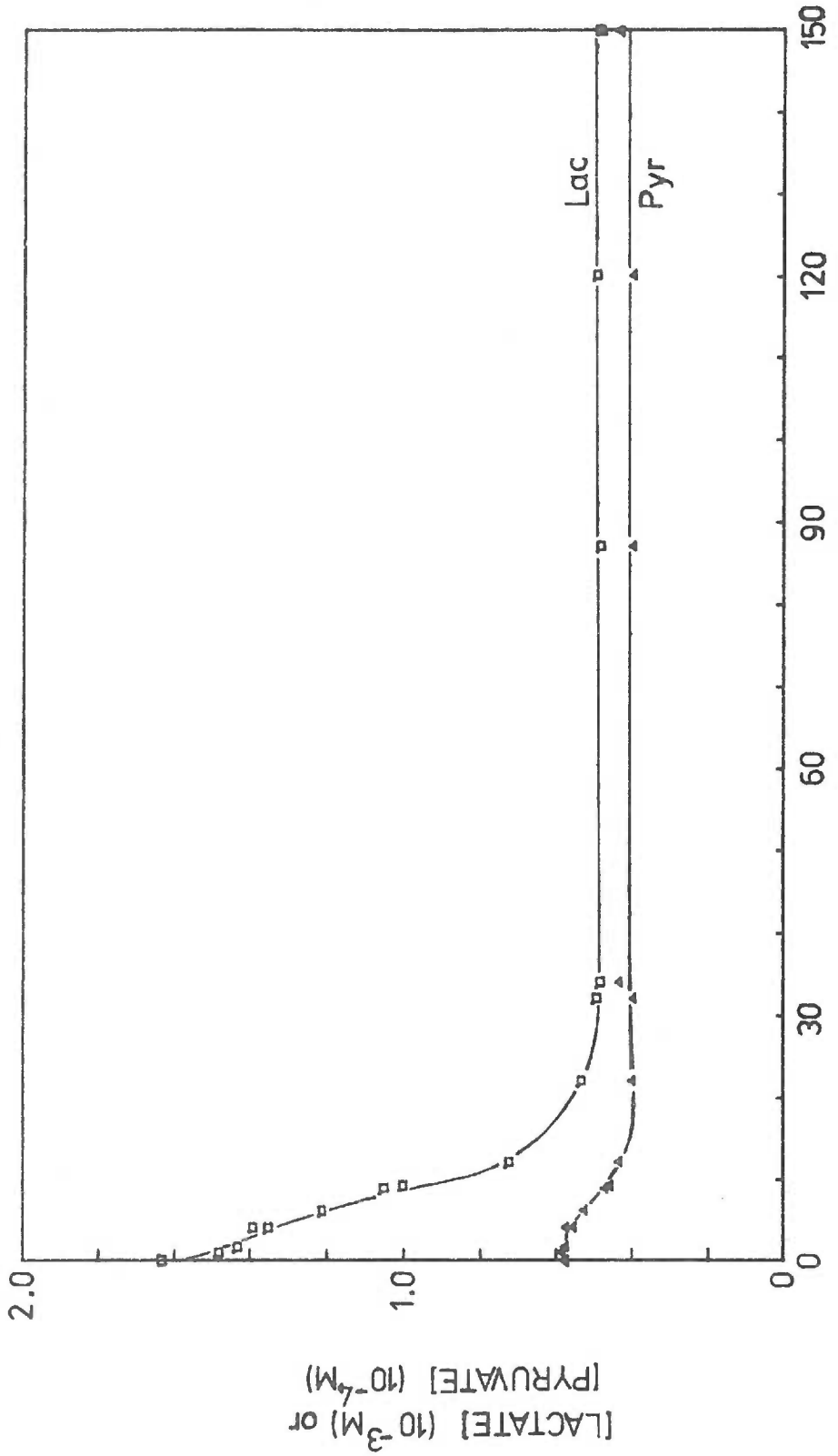
Lac
Pyr
0
30
60
90
120
150
P(O_2) (torr)
0
1.0
2.0
[LACTATE] (10^{-3}M) or
[PYRUVATE] (10^{-4}M)

IV.B.3. Pyruvic Acid Concentration in Hepatocytes as a Function of Oxygen Tension

Pyruvic acid concentration as a function of oxygen tension was measured spectrophotometrically on the deproteinated cell suspensions used for lactic acid determinations (Section IV.B.2.). The partitioning data for pyruvate given in Section IV.B.1. were used for calculation of cellular concentrations as given in Figure IV-4. Above 20 torr (28 μM), pyruvate concentration was about 0.4×10^{-4} M. An increase in pyruvate concentration was observed at 16 torr (22.4 μM) and a half maximal change at about 8 torr (11.2 μM).

IV.B.4. Cellular Lactate to Pyruvate and Cytoplasmic NAD^+ to NADH Ratios as a Function of Oxygen Tension

The ratio of cellular concentrations of lactate and pyruvate as a function of oxygen tension was calculated from the data in Section IV.B.2. and IV.B.3. The results are given in Figure IV-5. The average lactate:pyruvate for oxygen tensions above 25 torr (35 μM) was 11.9 ± 0.2. The oxygen tension at which a detectable increase in this ratio occurred was 20 torr (28 μM). The half maximal change in lactate:pyruvate ratio occurred at about 9 torr (12.6 μM).

The cytoplasmic NAD^+:NADH ratio was calculated from the lactate to pyruvate ratio using the measured equilibrium constant, 1.1×10^{-4} M, determined by Williamson et al. (1967) for the lactic

Figure IV-5. Lactate to pyruvate ratio in isolated hepatocytes as a function of solution oxygen tension. Data from Figure IV-4 expressed as ratio of intracellular lactate to intracellular pyruvate.

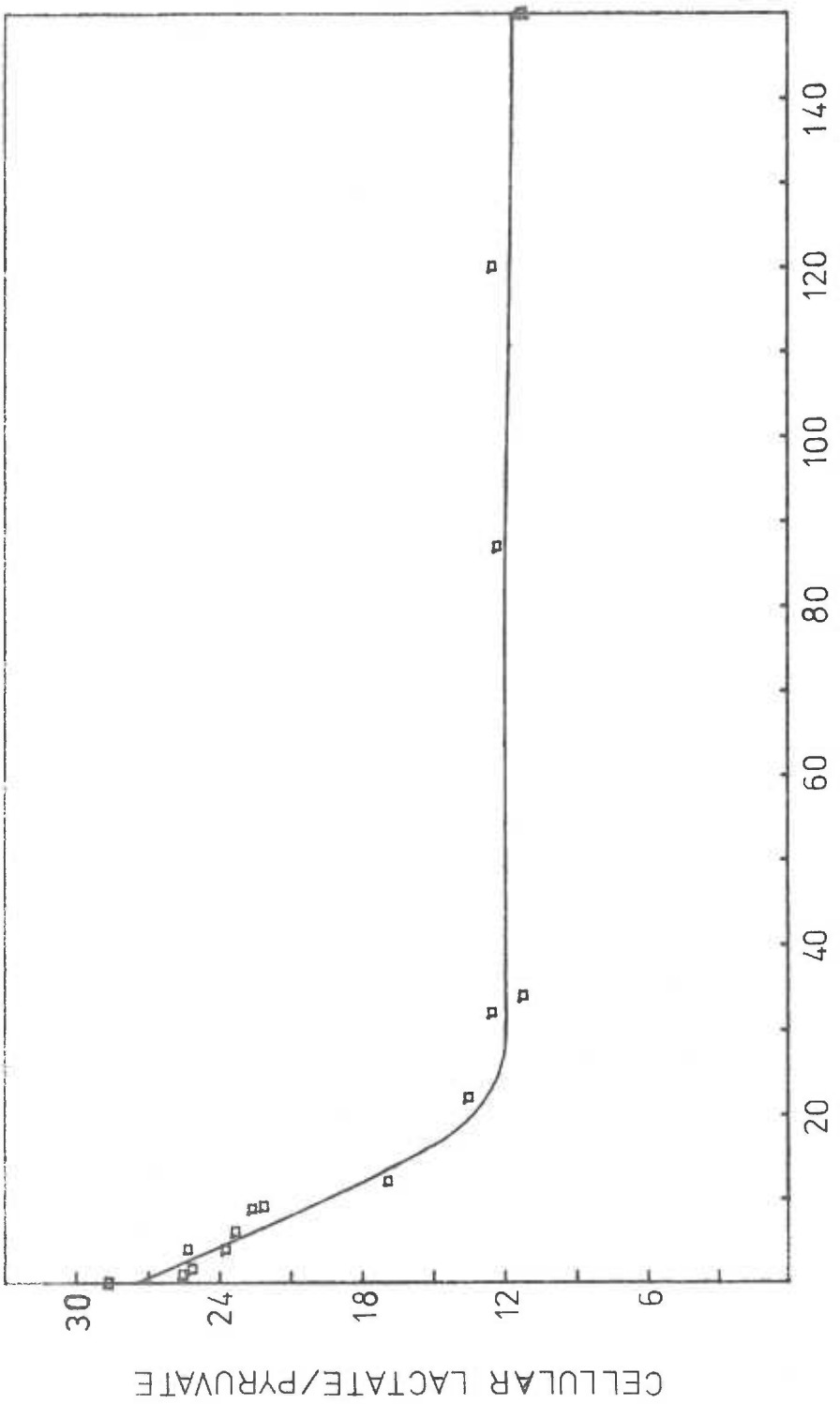
CELLULAR LACTATE/PYRUVATE
30
24
18
12
6
20
40
60
80
100
120
140
P(O2) (torr)

dehydrogenase catalyzed reaction and assuming that the reaction was at equilibrium at pH 7.0.

$$K = \frac{[\text{pyruvate}][\text{NADH}][H^+]}{[\text{lactate}][NAD^+]}$$

The results are shown in Figure IV-6. The average NAD^+: NADH measured for oxygen tension above 25 torr (35 μM) was 763 ± 44. The critical $P(O_2)$ and $P(O_2)$ for half maximal change are the same as those for the lactate:pyruvate ratio.

IV.C. Adenylate Concentrations as a Function of Oxygen Tension

IV.C.1. ATP Partitioning between Cells and Medium

Isolated hepatocytes were incubated at 37°C for 30 min in modified Hank's medium under 20% O_2, 5% CO_2, 75% N_2. The cells were centrifuged for 3 min at 50 x g and the supernatant removed. Each fraction was deproteinated with 2 N H_2SO_4 and assayed by the luciferase assay for ATP. The cellular ATP concentration was found to be 2.40 ± 0.34 mM for four cell preparations after corrections were applied for extracellular packing volume as discussed in Section IV.B.1. The average suspending medium concentration was 0.0089 ± 0.0031 mM. The percent of total incubation ATP estimated to occur intracellularly was 99.2 ± 0.3.

Figure IV-6. Cytoplasmic NAD^+/NADH as a function of solution $P(O_2)$. Calculated according to Williamson et al. (1967) from data in Figure IV-5. Line represents three point smoothing.

IV.C.2. ATP, ADP and AMP Concentrations as a Function of Oxygen Tension

Isolated hepatocytes were incubated at 37°C in modified Hank's medium at constant incubation oxygen tensions containing 5% CO_2. Oxygen tensions were maintained with the oxystat. Cell concentration was 3×10^6/ml in a total volume of 8 ml. Incubations were quenched after 10 min at constant oxygen tension with 1 ml 2 N H_2SO_4. Protein was removed by centrifugation and the adenylates assayed as described in Section II. Data from three cell preparations are given in Figure IV-7. ATP, ADP and AMP concentrations in the suspension at oxygen tension above 20 torr (28 μM) were 48.6 ± 1.0 μM, 8.2 ± 0.4 μM and 2.6 ± 0.6 μM. Using the estimation of Krebs et al. that the average hepatocyte volume is 7.25×10^3 μl, and the above determination that >99% of ATP is intracellular, [ATP] is 2.24 mM. Assuming that both ADP and AMP are similarly partitioned, the intracellular ADP concentration is about 0.36 mM and that for AMP is about 0.12 mM. ATP concentration decreases at 10 torr (1.4 μM) and below while ADP and AMP concentrations increase. The most dramatic changes occur in ATP and AMP concentrations; half maximal changes occur for both at about 3 torr (4.2 μM).

Figure IV-7. Concentration of ATP, ADP, and AMP as a function of solution $P(O_2)$. Isolated hepatocytes (3×10^6 cells/ml) were incubated in modified Hank's solution at fixed oxygen tensions for 10 min at $37^{\circ}C$, then quenched by injection of 2 N H_2SO_4. ATP, ADP, and AMP were measured by the luciferase assay and are expressed as concentration in total incubation. Data from three cell preparations, n = 15.

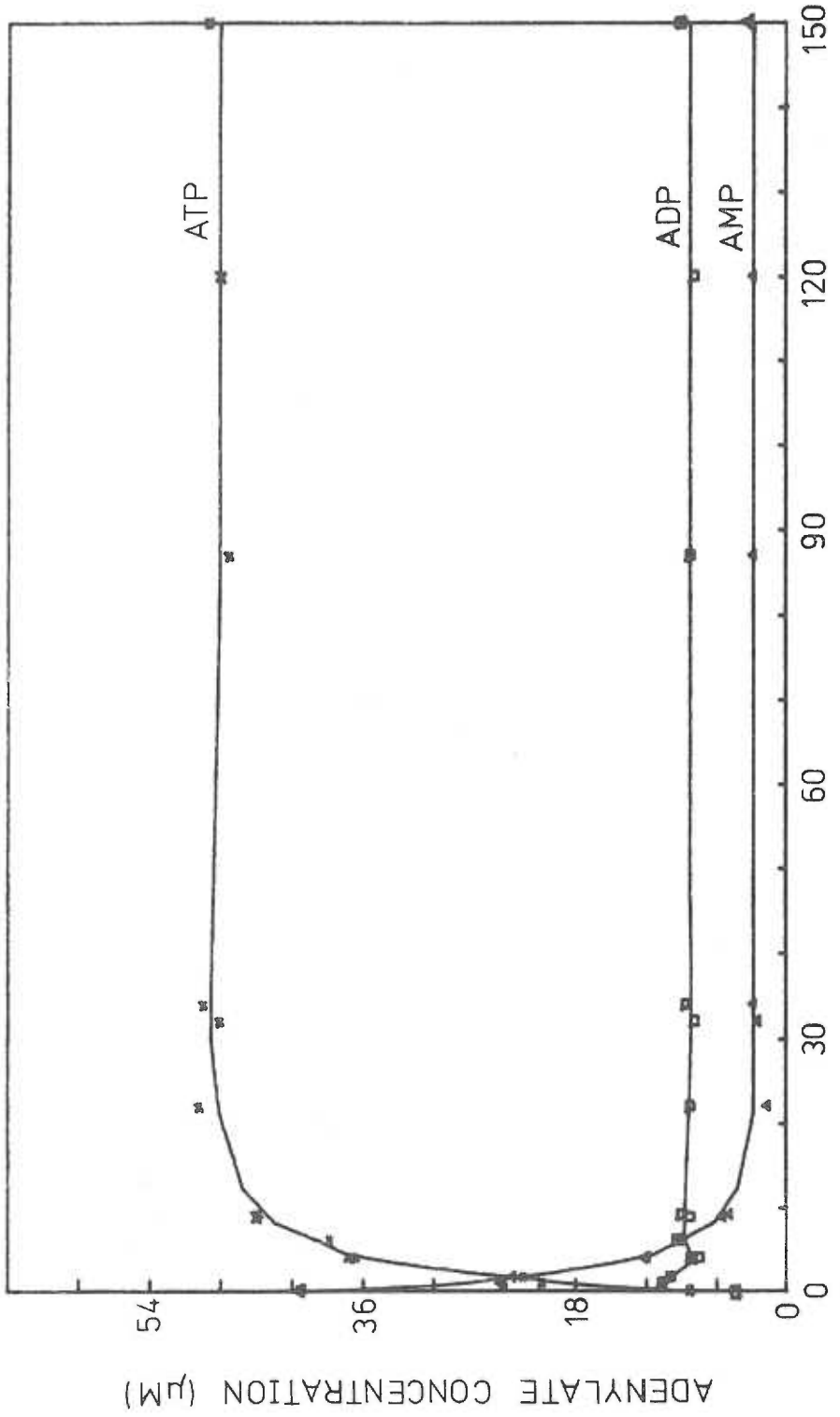
ATP
ADP
AMP
0
18
36
54
0
30
60
90
120
150
ADENYLATE CONCENTRATION (μM)
P(O2) (torr)

IV.C.3. ATP:ADP and Adenylate Energy Charge as a Function of Oxygen Tension

The ATP to ADP ratio as a function of oxygen tension was calculated from the data in the previous section and is shown in Figure IV-8. This ratio was found to be 5.9 ± 0.3 for oxygen tensions greater than 20 torr (28 μM). The first decrease in this ratio was observed at about 10 torr (14 μM) so that the critical $P(O_2)$ is between 10 and 20 torr (14 and 28 μM). The $P(O_2)$ at half maximal change in this ratio was 5 torr (7 μM).

The adenylate energy charge was calculated from the above data using the equation of Atkinson (1968):

$$E.C. = \frac{[ATP] + 1/2[ADP]}{[ATP] + [ADP] + [AMP]}$$

The energy charge as a function of oxygen tension is given in Figure IV-9. The critical $P(O_2)$ was approximately 20 torr (28 μM) and the half maximal change was observed to be about 2 torr (2.8 μM). The energy charge above 20 torr (28 μM) was found to be 0.89 ± 0.01.

IV.D. Discussion

Longmuir (1957) measured respiration by isolated liver cells at low oxygen concentrations and obtained an apparent $Km(O_2)$ equal to 0.5 μM at 40°C. Improved methodology for hepatocyte preparation (Berry and Friend, 1969; Section II) necessitated reexamination of this

Figure IV-8. ATP to ADP ratio as a function of oxygen tension. Isolated hepatocytes (3×10^6 cells/ml) were incubated in modified Hank's solution at fixed oxygen tensions for 10 min at 37°C, then quenched by injection of 2 N H_2SO_4. ATP and ADP were measured by the luciferase assay in the suspension. Computer drawn line represents three point smoothing.

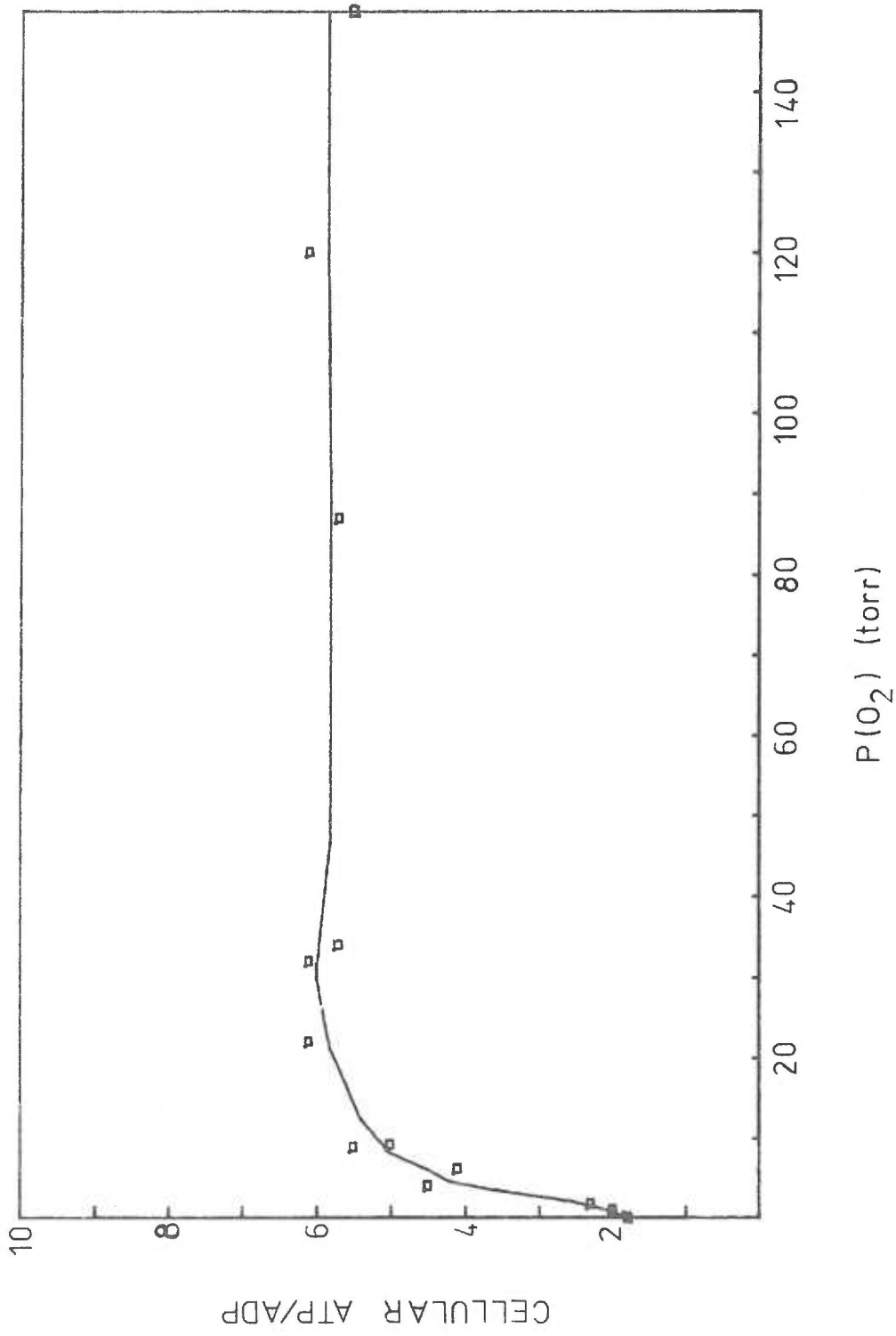
CELLULAR ATP/ADP
10
8
6
4
2
20
40
60
80
100
120
140
P(O2) (torr)

Figure IV-9. Adenylate energy charge as a function of oxygen tension. Isolated hepatocytes (3×10^6 cells/ml) were incubated in modified Hank's medium at fixed oxygen tensions for 10 min at 37°C, then quenched by injection of 2 N H_2SO_4. ATP, ADP and AMP were measured by the luciferase assay. Adenylate energy charge is expressed as (ATP + 1/2 ADP) / (ATP + ADP + AMP). Data from three cell preparations, n = 15. Computer drawn line represents three point smoothing.

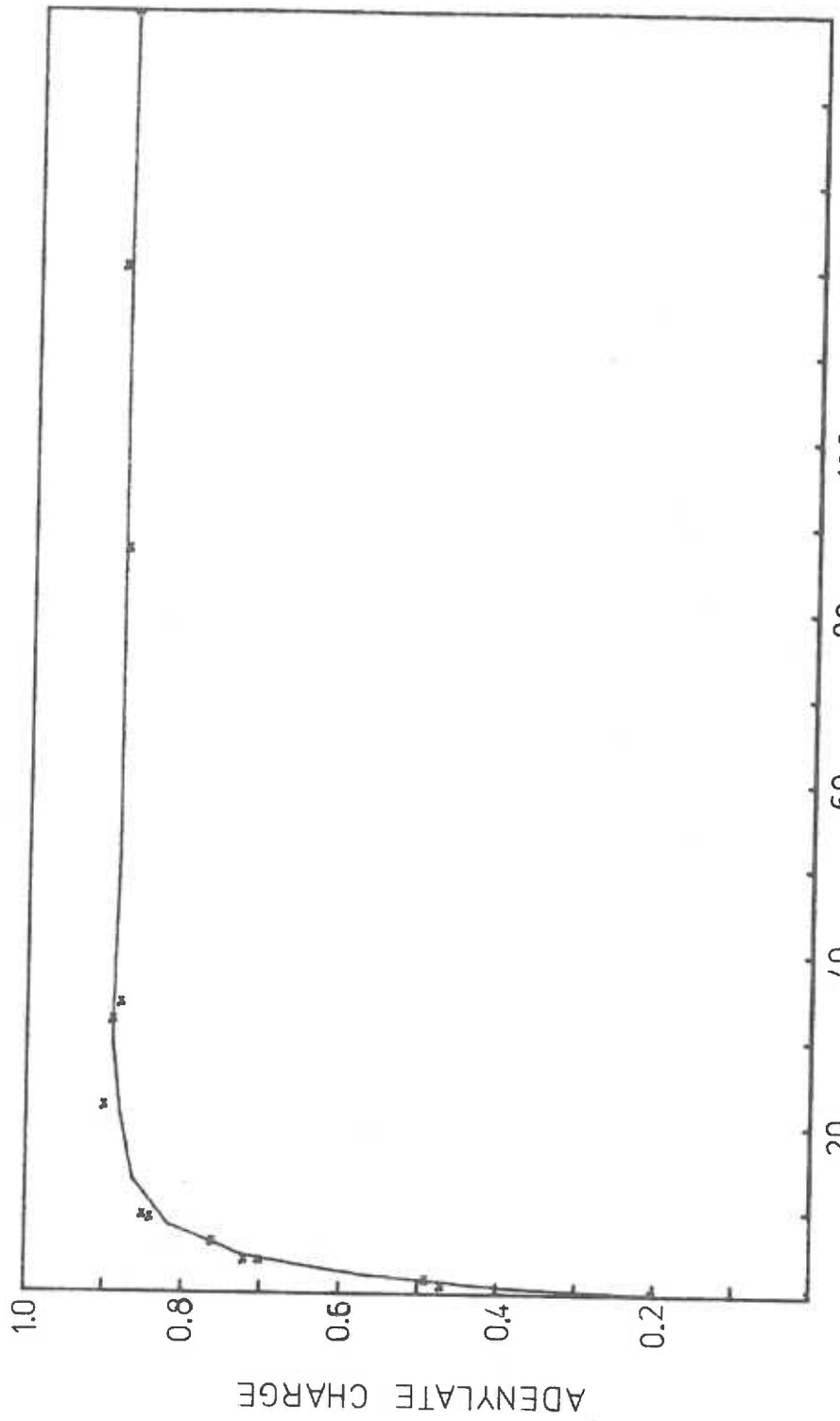
ADENYLATE CHARGE
1.0
0.8
0.6
0.4
0.2
20
40
60
80
100
120
140
P(O2) (torr)

value and yielded the higher value, 1.36-1.45 torr. Corresponding changes in adenylate pools and lactate/pyruvate indicate their close dependence upon cellular oxygen consumption. The results are in marked contrast to the oxygen dependence of respiration by isolated mitochondria and submitochondrial particles which have an apparent $Km(O_2)$ of 0.02 to 0.05 μM (Chance, 1957, 1965; Chance et al., 1965; Sugano et al., 1974). This difference is probably due to both intracellular oxygen tension gradient (Boag, 1970) and to a difference between respiratory control in isolated mitochondria and intact cells. Petersen et al. (1974) showed that the apparent $Km(O_2)$ for mitochondrial respiration is dependent upon the ratio ATP:ADP; the apparent $Km(O_2)$ in the presence of high ATP:ADP is increased over the uncoupled state 3 value. Since respiratory studies on isolated mitochondria are frequently performed with low ATP:ADP, reported values may not reflect the in vivo oxygen dependence of mitochondrial respiration (Section I.B.).

V. DRUG METABOLISM BY THE CYTOCHROME P-450 SYSTEM

Cytochrome P-450 is a carbon monoxide binding hemoprotein (Garfinkel, 1958; Klingenberg, 1958; Omura and Sato, 1964) which occurs in mammalian hepatic microsomes and is a component of a system involved in a variety of metabolic mixed function oxidations (for reviews, see Gillette, 1971; Gillette, Davis and Sasame, 1972; Gunzalus et al., 1974; Orrenius and Ernster, 1974). The multiple activities are involved in normal endogenous metabolism and in modifications of xenobiotics (Mason, North and Venneste, 1965). The reactions include "the oxidation of alkanes and aromatic compounds, the epoxidation of alkenes, polycyclic hydrocarbons, and halogenated benzenes, the dealkylation of the secondary and tertiary amines, the conversion of amines to N-oxide, hydroxylamine, and nitroso derivatives, the oxidative cleavage of ethers and organic thiophosphate esters, and the conversion of phosphothionates to their phosphate derivatives. In addition, these enzymes may catalyze the reduction of azo-compounds and nitro-compounds to primary aromatic amines and possibly the reductive cleavage of halogenated alkanes, such as carbon tetrachloride, to free radicals" (Gillette et al., 1972).

The hepatic cytochrome P-450 system contains several components which interact in a complex and only partially resolved fashion. This is illustrated schematically in Figure V-1 for the

Figure V-1. Cytochrome P-450 reaction scheme. Proposal 1. A proposal for the mixed function oxidase process catalyzed by the NADPH-cytochrome P-450 reductase/cytochrome P-450 system (Mason, 1973). See text for details.

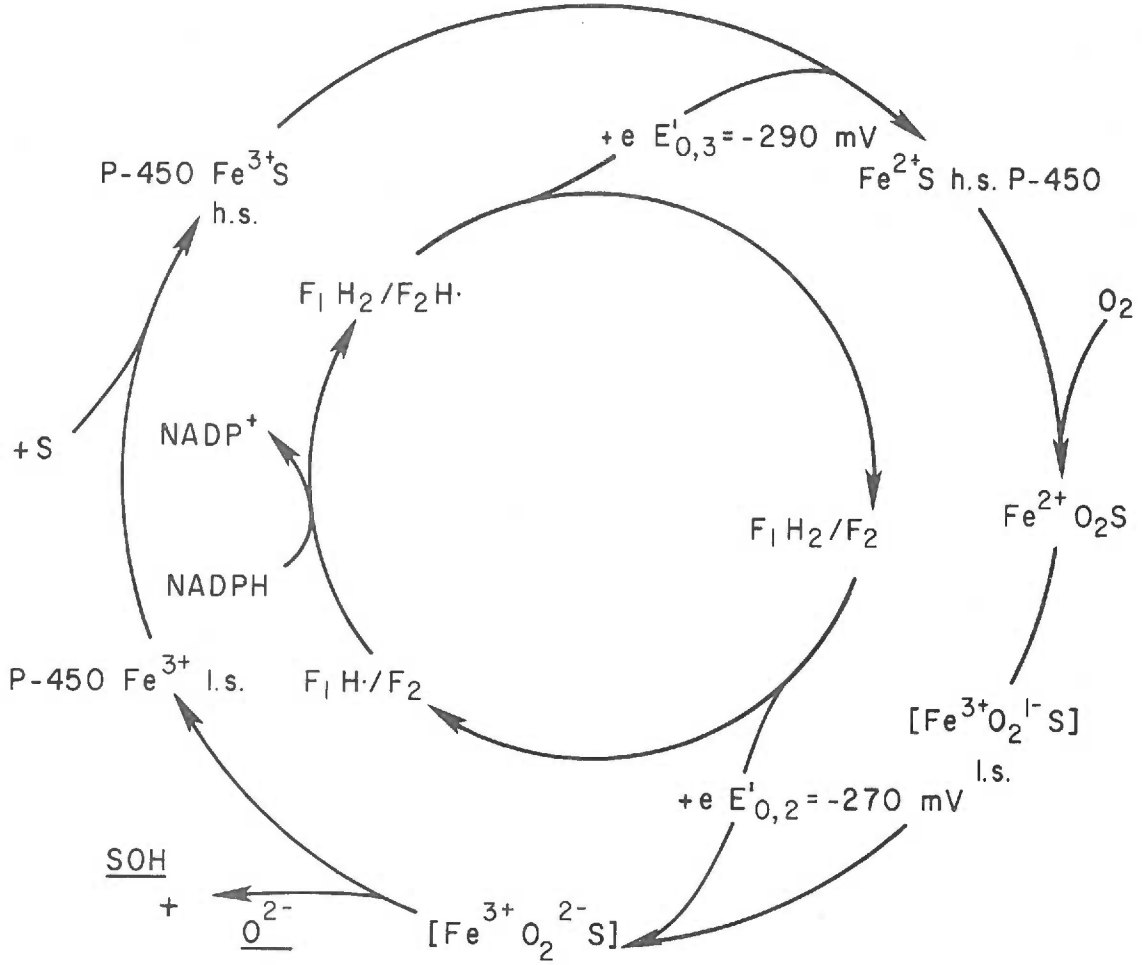
P-450 $Fe^{3+}S$ h.s.
+e $E'_{0,3}$ = -290 mV
$Fe^{2+}S$ h.s. P-450
O_2
$F_1H_2/F_2H\cdot$
+S
$NADP^+$
F_1H_2/F_2
$Fe^{2+}O_2S$
NADPH
P-450 Fe^{3+} l.s.
$F_1H\cdot/F_2$
$[Fe^{3+}O_2{}^{1-}S]$ l.s.
+e $E'_{0,2}$ = -270 mV
SOH
+
O^{2-}
$[Fe^{3+}O_2{}^{2-}S]$

NADPH-cytochrome P-450 system. Oxidized cytochrome P-450 binds substrate to undergo a low spin to high spin transition which can be observed spectrally (Schenkman, Remmer and Estabrook, 1967). This complex may then undergo a one-electron reduction, perhaps by an electron donation from a low potential flavin in NADPH-cytochrome P-450 reductase (Iyanagi, Makino and Mason, 1974). The reduced substrate complex combines with oxygen and undergoes a subsequent one-electron reduction with production of products and regeneration of low-spin ferric cytochrome P-450. Presence of a 418 nm absorbance following introduction of oxygen to the reduced-substrate bound Pseudomonas cytochrome P-450 has been interpreted to indicate the oxygenated species (Gunsalus, Tyson and Lipscomb, 1973). The second electron may be passed to the complex from the reductase in the half-reduced form with the production of the O_2 stable flavoprotein semiquinone (Iyanagi et al., 1974). The two-electron reduction of the flavoprotein by NADPH then completes the reaction cycle.

An alternative proposal (Figure V-2) has been made based upon the requirement of two electrons per molecule for reduction of cytochrome P-450 under anaerobic conditions (Guengerich, Ballon and Coon, 1975). Substrate binds to the oxidized form and undergoes a two-electron reduction (the second electron acceptor is represented by C in the figure). This complex binds oxygen with consequent hydroxylation of substrate and release of water, leaving the oxidized form of the enzyme.

Figure V-2. Cytochrome P-450 reaction scheme. Proposal 2. A proposed scheme for hydroxylation reactions catalyzed by liver microsomal cytochrome P-450 (Guenerich et al., 1975). RH represents substrate, and C represents unknown electron acceptor.

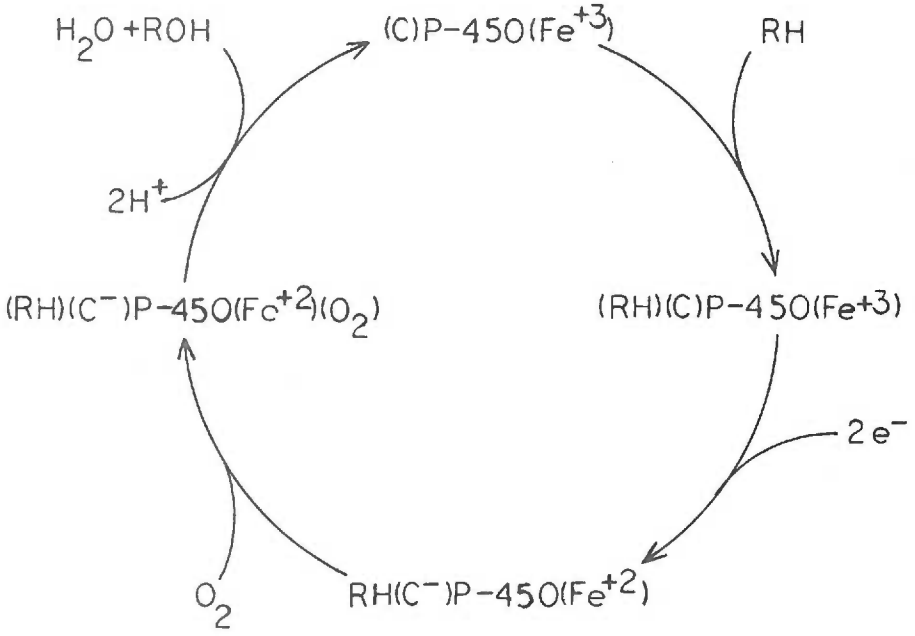
H_2O +ROH
(C)P-450(Fe^{+3})
RH
$2H^+$
(RH)(C^-)P-450(Fe^{+2})(O_2)
(RH)(C)P-450(Fe^{+3})
2 e^-
O_2
RH(C^-)P-450(Fe^{+2})

The numerous detoxification reactions catalyzed by the microsomal cytochrome P-450 system, which are so essential in an organism's encounter with its environment, may be impaired during hypoxia (Sanvordeker and Lambert, 1974). This is of particular importance in the clinical administration of drugs, since excretion of many of these compounds is dependent upon hepatic hydroxylation. Thus, the pharmacologic activity of a drug may be altered in an hypoxic patient. Alterations in metabolism or threshold response have been reported as a consequence of hypoxia for pentobarbital (Buemel et al., 1970) and sulfadiazine, isoniazid and p-aminopropiophenone (Mustala and Azarnoff, 1969).

The oxygen dependence of cytochrome P-450 oxidations has been studied for hepatic microsomes, perfused rat liver, and the Pseudomonas putida cytochrome P-450 system; apparent $Km(O_2)$ values (Table V-A) range from 1-5.4 μM (0.76-4.1 torr) for hepatic microsomes. The relationship of these values to intracellular function has not been established. Microsomes have a high rate of autoxidation which is oxygen dependent and interferes with the Km determination (Choi, 1971; Kerekjarto and Staudinger, 1966). In addition, metabolic controls existing in cells may be lost in microsomes. Finally, if a significant intracellular oxygen tension gradient exists, drug metabolism in cells and intact tissue could be oxygen dependent at oxygen tensions much above the 1-5 μM range determined for microsomes.

Table V-A. $Km(O_2)$ values for the cytochrome P-450 mixed function oxidation.

Tissue	Conditions	$Km(O_2)$ (μM)	$Km(O_2)$ (torr)	Reference
Microsomes, rat liver	TPNH only as substrate (autoxidation)	0.1	0.076	Estabrook (1964)
Perfused rat liver	CO difference spectra	0.4	0.30	Brauser, Sies & Bucher; also citing Schindler (1964) and Chance (1965)
Microsomes, dog liver	Coumarin, 6.3 μM NADPH 0.12 μM	1	0.76	Kratz and Staundinger (1966)
Microsomes, dog liver	Acetanilid; 5 hr aging	4.8	3.6	Kerekiarto and Staudinger (1966)
	24 hr aging	10.7	8.1	
	48 hr aging	21.9	16.6	
Pseudomonas putida, P-450 system	4-methylbenzoate	1.9	1.4	Bernhardt, Erdin, Staudinger & Ullrich (1973)
	3, 4-dimethoxybenzoate	3.8	2.9	
	4-ethoxybenzoate	10	7.6	
	N-methyl-4-aminobenzoate	51	39	
	4-methylbenzoate	63	48	
Microsomes, male rats	No addition (autoxidation)	2.23	1.7	M. J. Choi (1971)
	Aniline, 1 mM	5.3	4.0	
	Ethylmorphine, 2 mM	1.2	0.91	
	Ethylmorphine, PB induced	5.4	4.1	
	Ethylmorphine, 3 MC induced	4.1	3.1	
Microsomes, male rats	Steroid 11β -hydroxylase	9	6.4	Ando and Horie (1971)

The purpose of this research is to determine the functional dependence of drug metabolism on oxygen tension in intact isolated hepatocytes.

Drug metabolism by hepatocytes isolated by the enzymatic method (Section II) has recently been reported (Moldeus et al., 1964). They observed that the need for added cofactors is eliminated and that metabolism occurs at a rate comparable to microsomes plus an NADPH generating system. Further, uptake of alprenolol and hexobarbital by these cells was shown to be rapid (van Bahr et al., 1974) so that uptake is not limiting for metabolism. Metabolism of alprenolol and hexobarbital were chosen for examination because of the background work available on substrate uptake and metabolism in hepatocytes and measurements of the apparent Km of these substrates. The apparent Michaelis constant for alprenolol metabolism is about 10 μM (Moldeus et al., 1974) and for hexobarbital in microsomes is 0.145 mM (Gillette, 1971; Wolf et al., 1974). Phenyramidol was chosen as a substrate because of the availability of a simple and rapid assay system (Gerber et al., 1974). Experiments were performed on the oxygen dependence of hexobarbital, phenyramidol and alprenolol metabolism at saturating substrate concentrations in cells from non-induced rats. Additional experiments at subsaturating hexobarbital concentration and in phenobarbital-induced and 3-methylcholanthrene induced hepatocytes were performed to obtain information on the physiological importance of this oxygen dependence and on the multiplicity of cytochrome P-450. Available methods were used for quantitation of cytochrome P-450 in

hepatocytes, and new methods based upon addition of submitochondrial particles containing cytochrome $\underline{a}_3$, and microsomes containing cytochrome P-450 were developed (Section II.E.4.).

V.A. Quantitation of Cytochrome $\underline{a}_3$ and Cytochrome P-450 in Hepatocytes

V.A.1. Quantitation of Cytochrome $\underline{a}_3$ with Method of Additions

The cytochrome $\underline{a}_3$ content of isolated hepatocytes was estimated from plots of the $\Delta OD_{428.5-455}$ for the CO asc TMPD minus asc TMPD difference spectrum with additions of mitochondrial particles containing known amounts of cytochrome $\underline{a}_3$ (Section III.E.4.a.). Figure V-3a shows the difference spectrum of cells and cells plus increments of cytochrome $\underline{a}_3$. Final ascorbate concentration was 8.2 mM, and TMPD concentration was 0.15 mM. The plot of $\Delta OD_{428.5-445}$ as a function of additions is given in Figure V-3b. The x-intercept of this plot gives a direct measure of the cytochrome $\underline{a}_3$ content of the hepatocytes. The cytochrome $\underline{a}_3$ content of four preparations (Table V-B) was found to be 0.058 ± 0.001 nmoles/mg protein.

V.A.2. Quantitation of Cytochrome P-450 with Additions of Cytochrome $\underline{a}_3$

The carbon monoxide difference spectrum of dithionite reduced hepatocytes with added increments of cytochrome $\underline{a}_3$ is given in Figure V-4a. The $\Delta OD_{450-490}$ is plotted as a function of cytochrome $\underline{a}_3$ additions in Figure V-4b. Extrapolation of $\Delta OD_{450-490}$ to zero

Figure V-3. Carbon monoxide difference spectrum of ascorbate plus TMPD reduced isolated hepatocytes with additions of submitochondrial particles. Cells were solubilized by homogenization in 50 mM phosphate buffer (pH 7.5) containing 25% glycerol and 1% Lubrol WX. Final concentration of cells was adjusted to give 1.3-1.5 mg protein/ml containing additions of submitochondrial particles to give 0-0.5 nmole cytochrome $\underline{a}_3$/ml. Three ml fractions were transferred to sample and reference cuvettes and a baseline recorded. The sample cuvette was then bubbled with CO for 1 min followed by addition of 25 µl ascorbate (1 M, pH 7.0) and 30 µl TMPD (15 mM) to both sample and reference cuvettes. After 30 min the difference spectrum was recorded as shown in a. The $\Delta OD_{428.5-445}$ as a function of mitochondrial cytochrome $\underline{a}_3$ additions is presented in b.

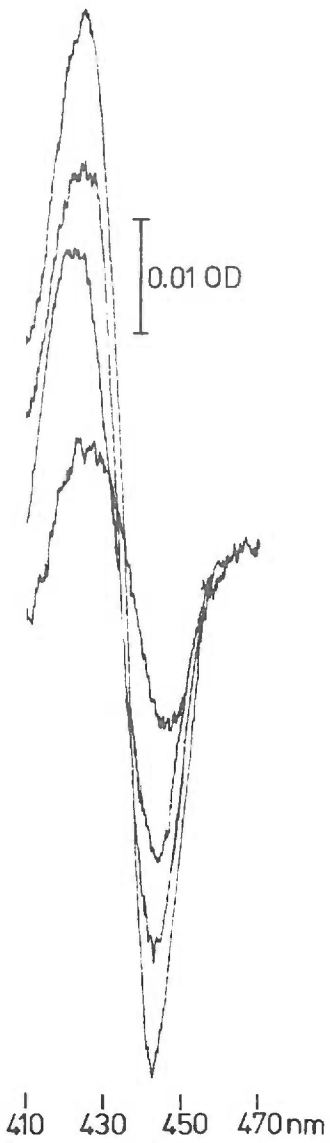
0.01 OD
410
430
450
470nm

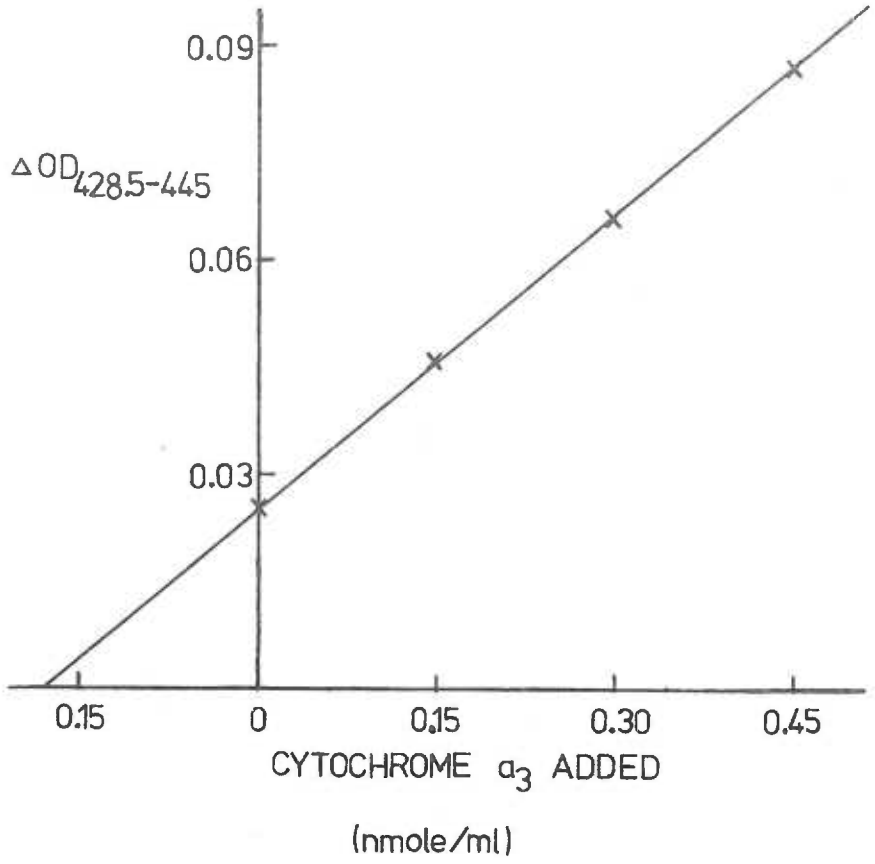
0.09
0.06
0.03
ΔOD428.5-445
0.15
0
0.15
0.30
0.45
CYTOCHROME a3 ADDED
(nmole/ml)

Table V-B. Cytochrome $\underline{a}_3$ and cytochrome P-450 content of isolated hepatocytes.

a. Cytochrome $\underline{a}_3$ and cytochrome P-450 determinations using methods of additions (Figures V-3 and V-4).

	CP5-11	CP5-12	CP5-14	CP5-15
Cytochrome $\underline{a}_3$	0.058 nmole cyt. $\underline{a}_3$ / mg pro	0.057	0.057	0.058
Cytochrome P-450 method of additions with microsomal particles	0.23 nmole P-450/ mg pro	0.22	0.22	0.21
Cytochrome P-450 method of additions with microsomal particles	0.24	0.215	0.22	0.21

b. Cytochrome P-450 content as determined by simplified mathematical subtraction of cytochrome oxidase (Section V.A.2) and method of Ghazarian et al. (1974), from Figure V-5b.

	CP5-13	CP5-16	CP5-17	CP5-19
$\Delta OD_{450-490}$CO DITH minus DITH CO asc TMPD minus asc TMPD	0.23	0.21	0.20	0.20
CO DITH minus CO asc TMPD	0.22	0.20	0.22	0.22

Figure V-4. Carbon monoxide difference spectrum of dithionite reduced isolated hepatocytes with additions of submitochondrial particles. Cells and submitochondrial particles were prepared as in Figure V-3. The sample cuvette was bubbled with CO for 1 min and a few crystals of dithionite were added to each cuvette. Spectra were recorded after 15 min (a) and $\Delta OD_{450-490}$ plotted as a function of mitochondrial additions (b). Extrapolation to zero cytochrome $\underline{a}_3$ concentration determined in Figure V-3 allowed calculation of cytochrome P-450 concentration (see text). Cell concentration was 2.75 mg pro/ml.

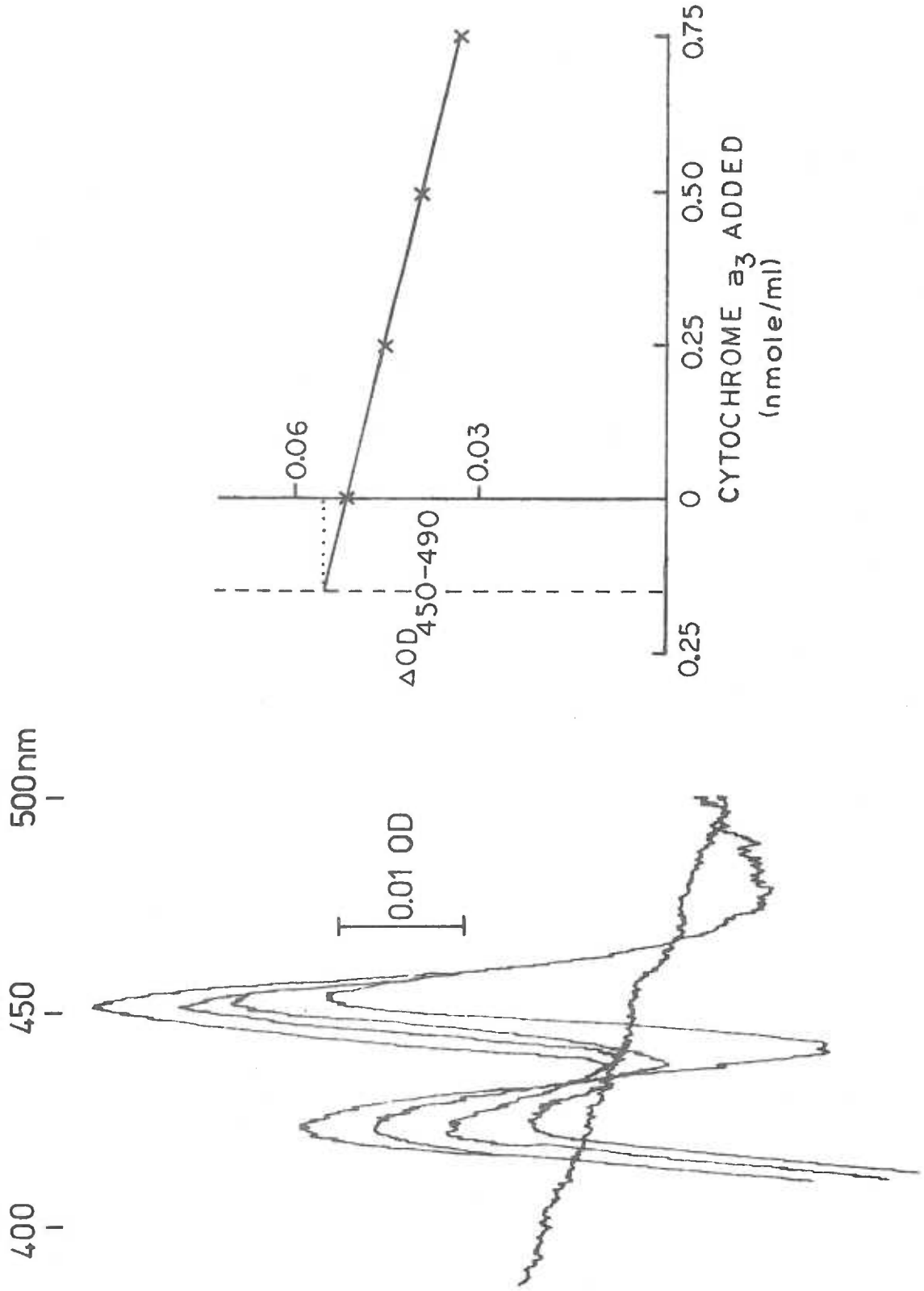
400
450
500nm
0.01 OD
ΔOD 450-490
0.06
0.03
0
0.25
0.50
0.75
0.25
CYTOCHROME a3 ADDED
(nmole/ml)

cytochrome $\underline{a}_3$ using the cytochrome $\underline{a}_3$ content determined in Section V.A.1 gives the $\Delta OD_{450-490}$ contributed from cytochrome P-450 assuming no other chromophores contribute to this absorbance difference. The extinction value 91 mM^{-1} cm^{-1} (Amura and Sato, 1964) was used with this corrected $\Delta OD_{450-490}$ to obtain cellular cytochrome P-450 content. The results from four preparations (Table V-B) gave 0.22 $\pm$ 0.01 nmoles cytochrome P-450/mg protein.

A simplified method for cytochrome P-450 estimation was performed by subtracting the $\Delta OD_{450-490}$ for the carbon monoxide difference spectrum of the ascorbate + TMPD reduced form from the carbon monoxide difference spectrum of the dithionite reduced form (see Section II.E.4.b.). The resulting ΔOD was used with the extinction value of Omura and Sato to calculate the P-450 content. The results from four non-induced cell preparations, given in Table V-B, had an average equal to 0.21 $\pm$ 0.02 nmoles cytochrome P-450/mg protein.

V.A.3. Quantitation of Cytochrome P-450 by Method of Additions with Microsomes

The method of Ghazarian et al. (1974) for selective visualization of cytochrome P-450 in the presence of cytochrome $\underline{a}_3$ was used with a method of additions of microsomes. A typical series of spectra is given in Figure V-5a. The x-intercept of a plot of

Figure V-5. Cytochrome P-450 determination in hepatocytes by the method of Ghazarian et al. (1974). Cells were solubilized by homogenization in 50 mM phosphate buffer (pH 7.5) containing 25% glycerol and 1% Lubrol WX. Final concentrations of cells (a and b) were adjusted to give 0.5 mg protein/ml containing added microsomes to give 0, 0.65, 1.3 or 1.95 nmole added cytochrome P-450. Three milliliter fractions were transferred to sample and reference cuvettes and the baseline recorded. CO was bubbled for 1 min through each cuvette. Additions of 25 µl ascorbate (1 M, pH 7.0) and 30 µl TMPD (15 mM) were made to the reference and sample cuvettes, followed by a few crystals of dithionite to the sample cuvette. After 30 min, spectra were recorded (a). The plot of $\Delta OD_{450-490}$ as a function of microsomal additions (b) may then be used to calculate cytochrome P-450 concentration. Dithionite minus ascorbate + TMPD difference spectrum (c) was recorded from 650 to 400 nm with 2.3 mg protein/ml.

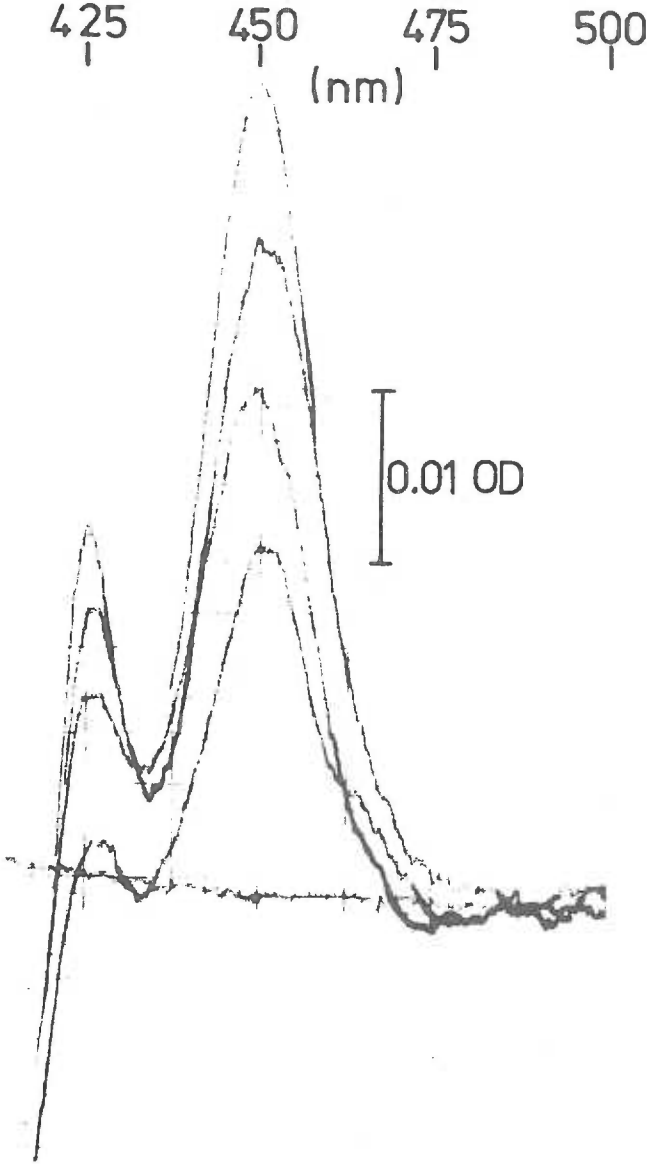
425
450
475
500
(nm)
0.01 OD

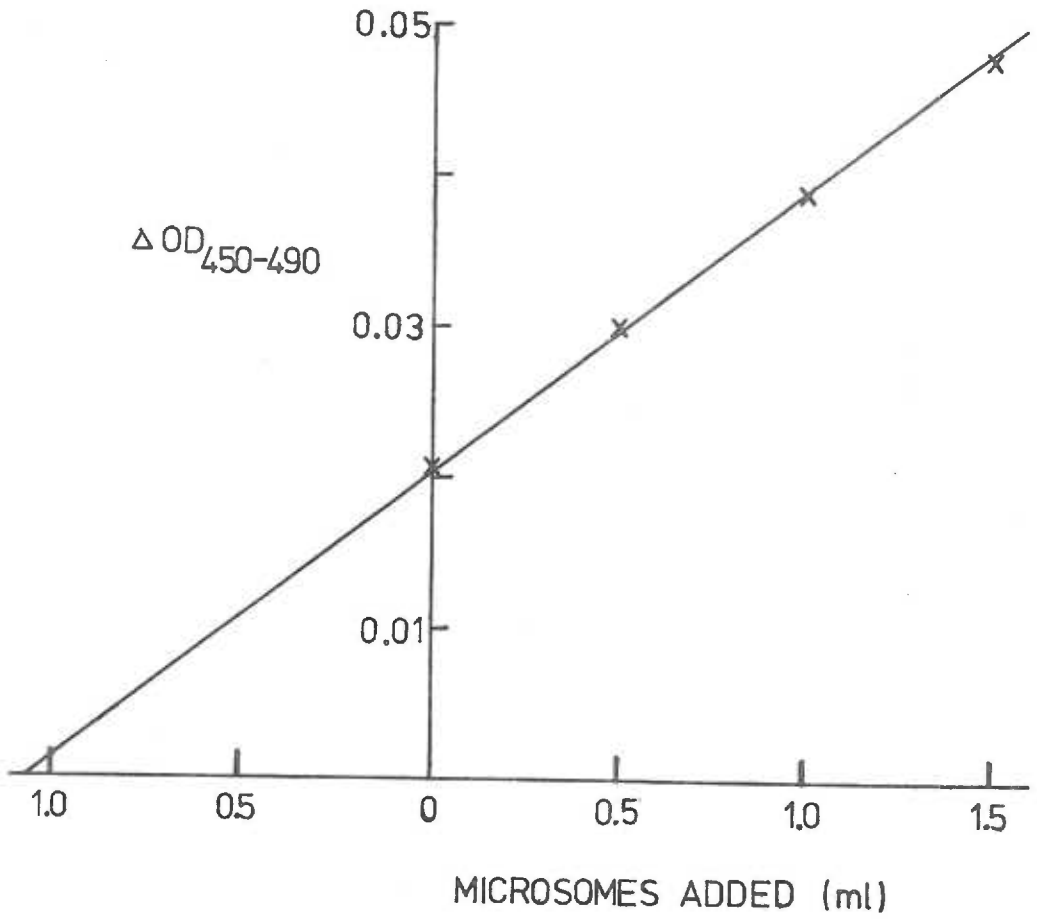
0.05
0.03
0.01
ΔOD450-490
1.0
0.5
0
0.5
1.0
1.5
MICROSOMES ADDED (ml)

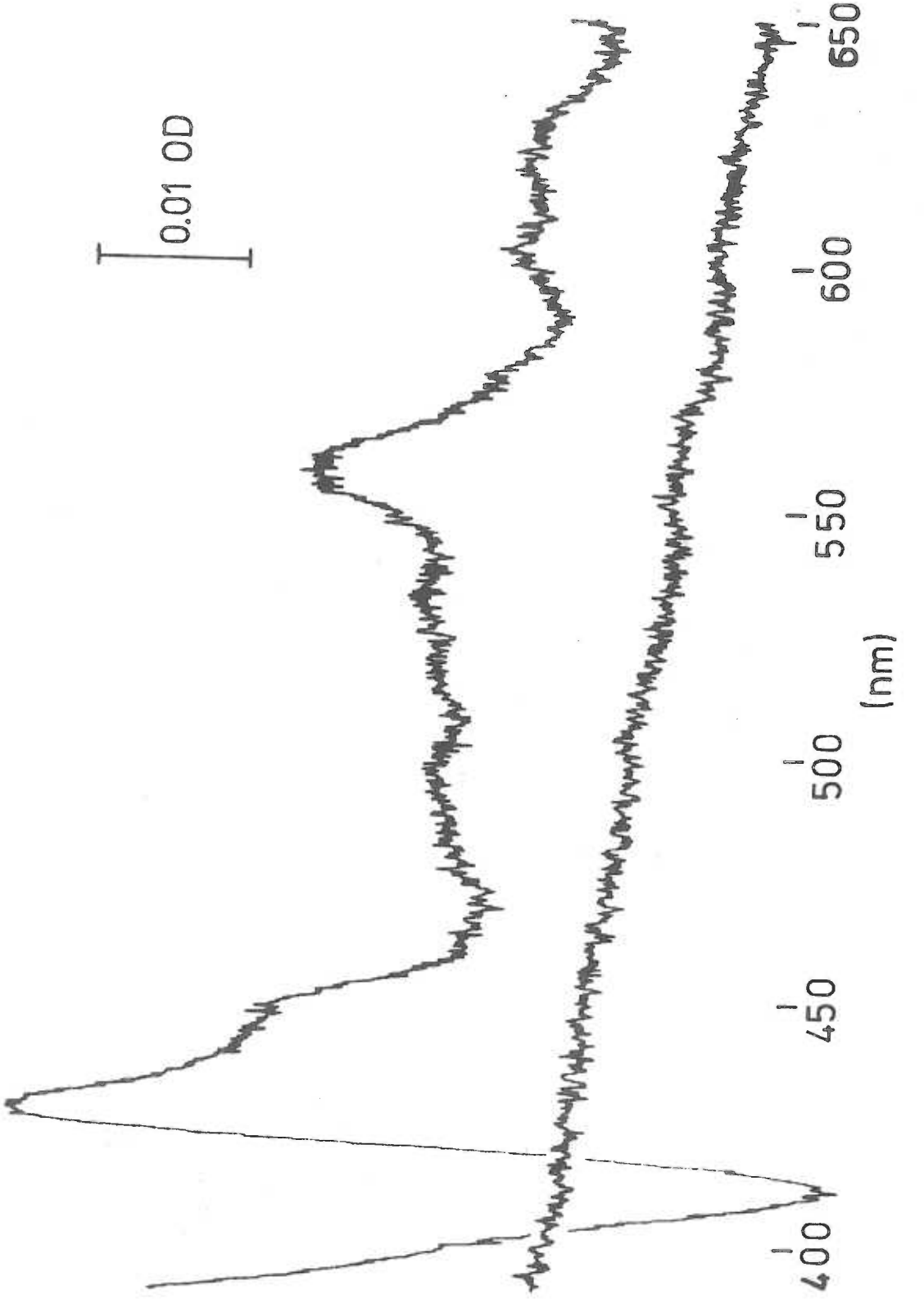
0.01 OD
400
450
500
550
600
650
(nm)

$\Delta OD_{450-490}$ as a function of known microsomal cytochrome P-450 additions (Figure V-5b) gives the cellular cytochrome P-450 content. The results of four non-induced hepatocyte preparations, given in Table V-B, was 0.22 ± 0.01 nmoles cytochrome P-450/mg protein. The effective extinction coefficient for cytochrome P-450 calculated from the $\Delta OD_{450-490}$ and the extrapolated cytochrome P-450 content was 76 mM^{-1} cm^{-1} for isolated non-induced hepatocytes.

To test the affect of mitochondrial components on the $\Delta OD_{450-490}$ for this assay, the method of additions with submitochondrial particles was used. The results showed that components present in mitochondria which are reduced by dithionite but not by ascorbate + TMPD also affect the $\Delta OD_{450-490}$. This is confirmed by the absorbance change at 450 in the dithionite minus ascorbate + TMPD difference spectrum (Figure V-5c).

V.B. Metabolism of Phenyramidol HCl

V.B.1. Determination of Optimal Conditions for Incubations

Metabolism of phenyramidol as a function of time by isolated hepatocytes is shown in Figure V-6 for non-induced and phenobarbital induced rats. Cells were incubated at 3×10^6 cells/ml (modified Hank's medium, 19 ml total volume, 37°C under 95% O_2, 5% CO_2) in a plastic, 125-ml Erlenmeyer flask in a gyrotory shaker. After

Figure V-6. Phenyramidol metabolism by isolated hepatocytes. Non-induced cells were incubated at 3 x 10^6 cells/ml (modified Hank's medium, 37°C under 95% O_2, 5% CO_2) in a plastic 125 ml Erlenmeyer flask (0 and X) or in special incubation vessel (△ and □). Phenobarbital induced cells were incubated at 3 x 10^6 cells/ml (modified Hank's medium, 37°C under 95% O_2, 5% CO_2) in a plastic 125 ml Erlenmeyer flask. Suspension volume was 19 ml in Erlenmeyer flask and 8 ml in special vessel. After 5 min equilibration, substrate was added to give a concentration of 0.1 mM. Samples were removed at indicated times and assayed for substrate loss as described in text.

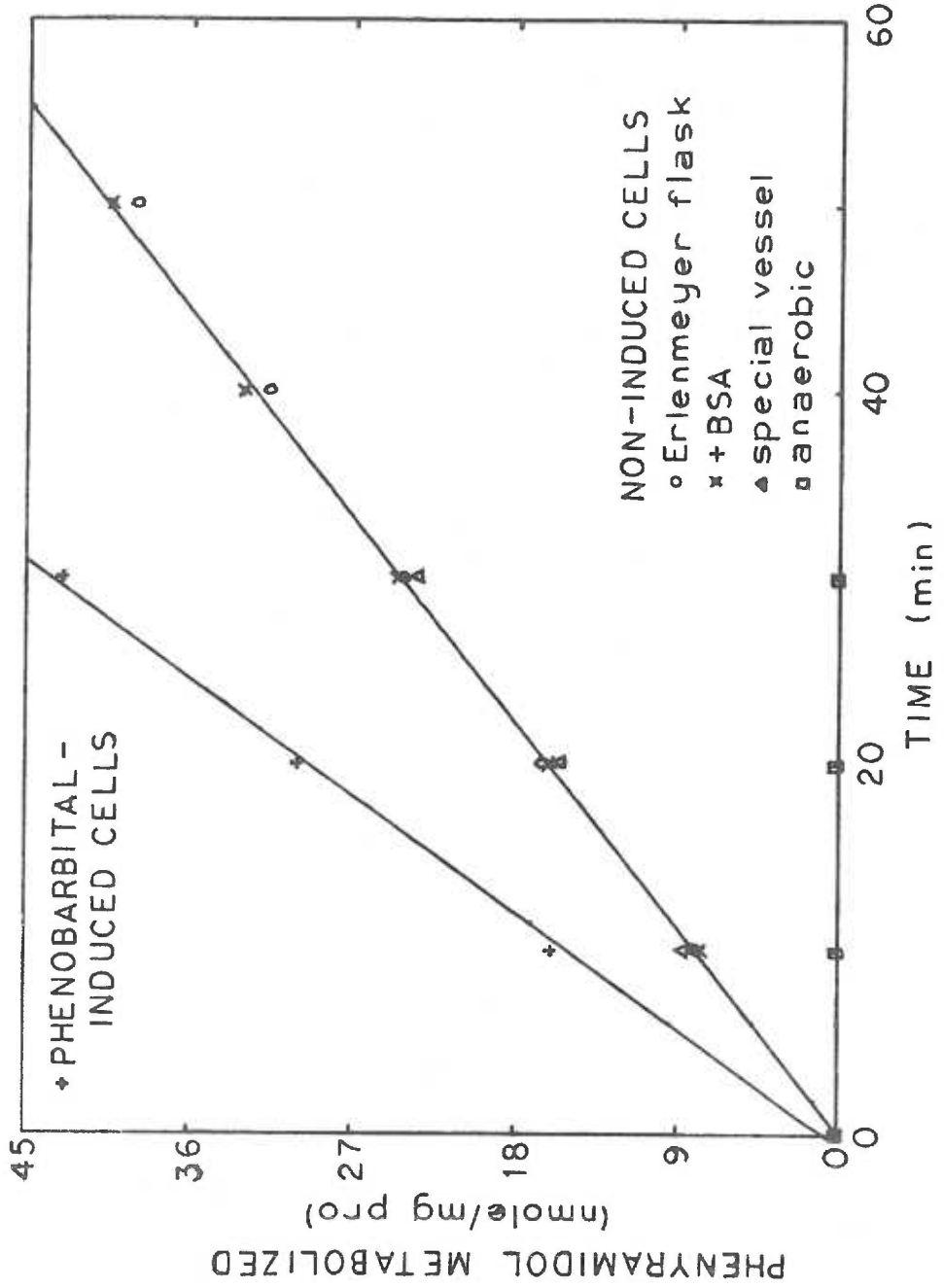
PHENYRAMIDOL METABOLIZED
(nmole/mg pro)
45
36
27
18
9
0
0
20
40
60
TIME (min)
+ PHENOBARBITAL-
INDUCED CELLS
NON-INDUCED CELLS
o Erlenmeyer flask
x + BSA
▲ special vessel
□ anaerobic

5 min equilibration, 1 ml phenyramidol solution (2 mM in modified Hank's medium, equilibrated to 37°C under 95% O_2, 5% CO_2) was added. Aliquots were removed at designated times and pipetted into 9 ml 100 mM phosphate buffer, pH 6.8 plus 10 ml butyl chloride for assay. Metabolism was linear for 30-50 min in all preparations examined. Metabolism per mg protein is independent of cell concentration in this concentration range (Figure V-7).

Since in the assay of phenyramidol metabolism, loss of substrate is measured, a minimal initial substrate concentration is required for optimal measurement. Consequently, the metabolism as a function of substrate concentration was measured as shown in Figure V-8. Aliquots of isolated hepatocyte suspensions (7.6 ml, 2×10^6 cells/ml modified Hank's medium) were incubated in 25 ml Erlenmeyer flasks in a gyrotory shaker (37°C; 95% O_2, 5% CO_2) for 5 min. Modified Hank's medium (0.4 ml) containing phenyramidol HCl to give final concentrations of 2-100 mM was added. After 5 min incubations, 1 ml from each flask was pipetted into 10 ml butyl chloride plus 9 ml 100 mM phosphate buffer (pH 6.8) for extraction and assay. The apparent cellular Km for this metabolism in below 10 μM; a reasonable approximation from these data is about 3-5 μM. The measured spectral binding constant for phenyramidol by microsomes is 5 μM (Figure V-9). An initial concentration of phenyramidol which would provide substrate saturation throughout the incubation, but allow

Figure V-7. Phenyramidol metabolism as a function of cell concentration. Incubation conditions and assay as described in Figure V-8 with varied cell concentration and initial phenyramidol concentration equal to 0.1 mM.

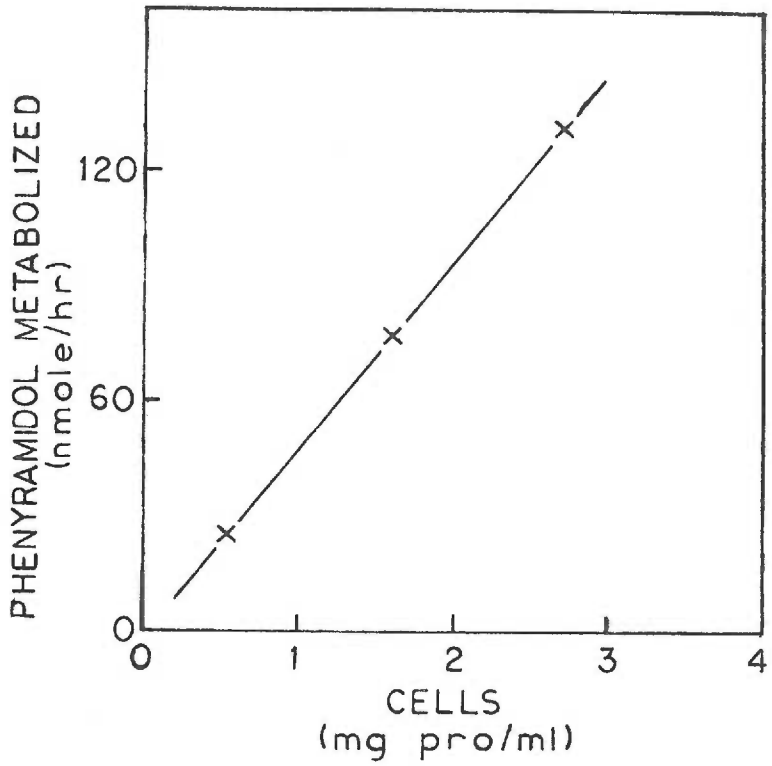
PHENYRAMIDOL METABOLIZED
(nmole/hr)
120
60
0
0
1
2
3
4
CELLS
(mg pro/ml)

Figure V-8. Phenyramidol metabolism by isolated hepatocytes as a function of initial phenyramidol concentration. Aliquots (7.6 ml) of isolated hepatocyte suspensions (2×10^6 cells/ml modified Hank's medium) were incubated in 25 ml Erlenmeyer flasks in a gyrotory shaker (37°C; 95% O_2, 5% CO_2) for 5 min. Modified Hank's medium (0.4 ml) containing phenyramidol HCl to give final concentrations of 2-100 mM was added. Initially, and after 5 min, 1 ml samples were removed and assayed to determine rate of substrate concentration decrease as described in the text.

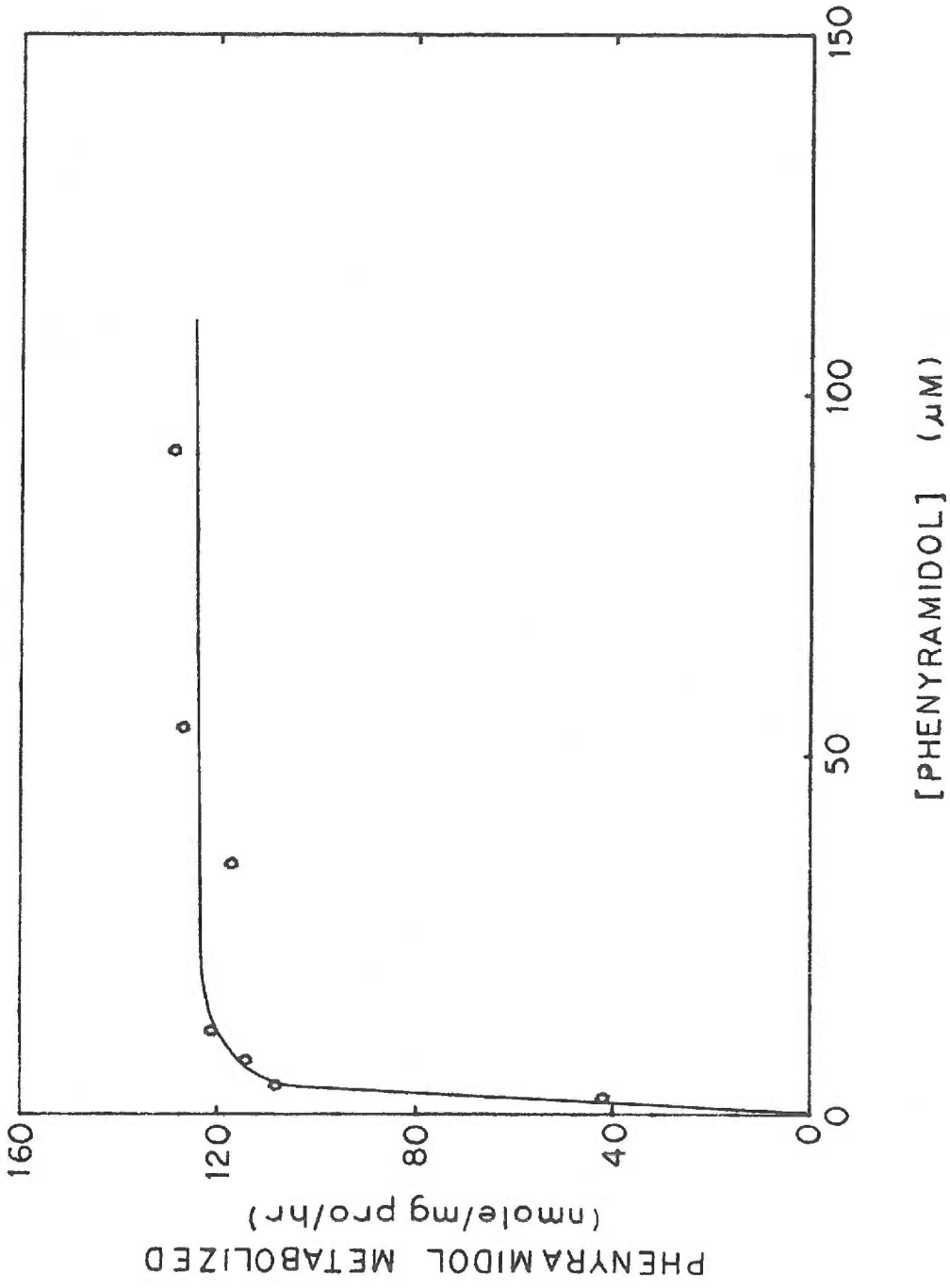
PHENYRAMIDOL METABOLIZED
(nmole/mg pro/hr)
160
120
80
40
0
0
50
100
150
[PHENYRAMIDOL] (μM)

Figure V-9. Phenyramidol induced difference spectrum in microsomes. Microsomes were prepared and solubilized as described in text. One to 10 µl aliquots of phenyramidol solution (4.7 mM) were added to 1 ml microsomes in the sample cuvette and an equivalent volume of distilled water added to the microsomes in the reference cuvette. The baseline was subtracted (2) and the double reciprocal plot (b) of $\Delta OD_{385-419}$ nm against phenyramidol concentration used to calculate the apparent spectral binding constant.

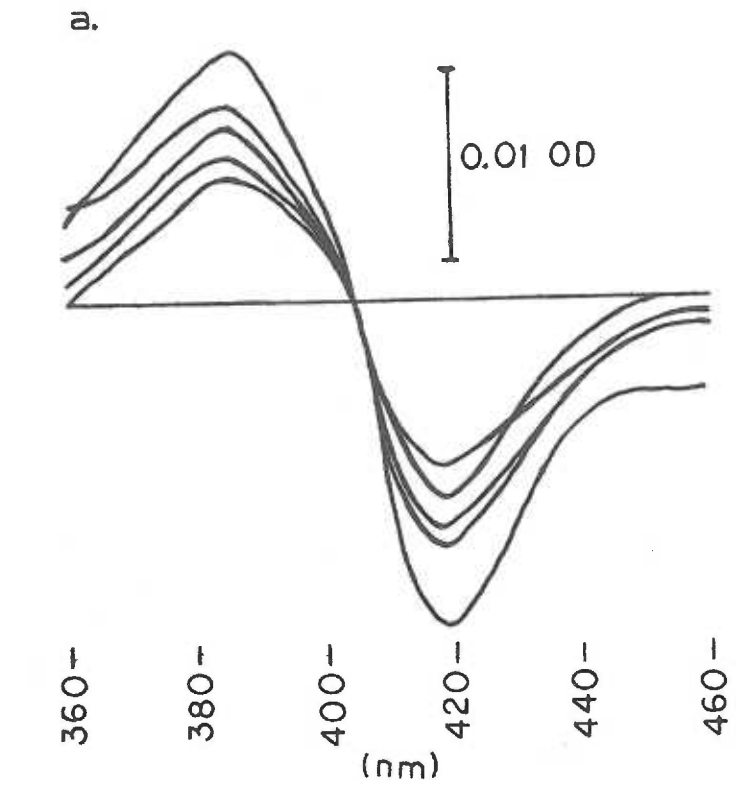
a.
0.01 OD
360
380
400
420
440
460
(nm)

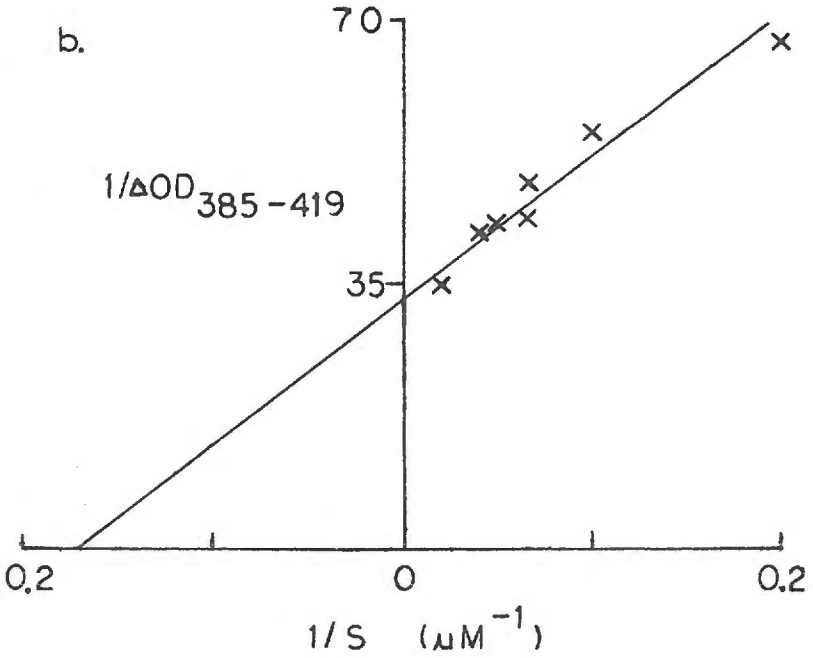
b.
70
1/ΔOD385-419
35
0.2
0
0.2
1/S (μM-1)

optimal quantitation of metabolite loss was chosen to be 0.1 mM.

The binding of phenyramidol by cytochrome P-450 in isolated hepatocytes is very rapid; maximal absorbance change occurred within the time required for mixing and observation with the Cary 14 (about 15 sec). The difference spectrum (microsomes + drug) - (microsomes) was typical of a type I compound: absorbance maximum at 385 nm, minimum at 419 nm.

Since preliminary characterization of drug metabolism for phenyramidol, hexobarbital, and alprenolol was performed in Erlenmeyer flasks with gyrotory shaking but the metabolism relative to oxygen tension was to be performed in a special incubation vessel, an experiment to compare the two systems was performed. The results (Figure V-6) were identical. Addition of bovine serum albumin (15 mg/ml) had little effect during a 30 min incubation. At 40 and 50 min, however, metabolism without BSA decreased slightly relative to the incubation containing BSA.

To determine if any phenyramidol metabolism was oxygen independent, cells were incubated in the special incubation vessel under 95% N_2, 5% CO_2 until anaerobicity, as measured by the oxygen electrode. Phenyramidol (0.4 ml, 2.1 mM) in modified Hank's medium equilibrated to 95% N_2, 5% CO_2 was then added to 8 ml in the vessel. One milliliter aliquots were removed with a gas-tight

Hamilton syringe after 0, 10, 20 and 30 min and assayed by the extraction and spectrophotometric method. There was no oxygen independent metabolism (Figure V-6).

To determine the stability of drug metabolism as a function of length of hepatocyte storage at $0^{\circ}C$, hepatocytes were assayed for phenyramidol metabolism after 0, 1, 2, 3, 4, and 5 hours at $0^{\circ}C$. Metabolism decreased little for 3 hr; the loss averaged less than 2% per hr for 5 hr storage (Figure V-10).

V.B.2. Metabolism as a Function of Oxygen Tension

Eight milliliter total volume samples non-induced hepatocyte suspension (2×10^6 cells/ml in modified Hank's medium) were pipetted into the special incubation vessel. Oxygen tension was brought to desired value and 0.4 ml phenyramidol solution (2.1 mM phenyramidol in modified Hank's medium, equilibrated with 95% N_2, 5% CO_2) was added. After 10 min at desired $P(O_2)$, 1 ml samples were removed and assayed for rate of substrate loss. Each cell preparation was observed at 4-6 different oxygen tensions, along with zero time and anaerobic incubations. Metabolic rates as a function of oxygen tension for 20 incubations are shown in Figure V-11. The critical $P(O_2)$ was approximately 11 torr (15.4 μM). The $P(O_2)$ at half-maximal metabolic rate was 2.6 torr (3.6 μM). The apparent

Figure V-10. Metabolism of phenyramidol by hepatocytes as a function of length of storage of hepatocytes at 0°C. Hepatocytes were prepared as previously described and stored at about 10^7 cells/ml modified Hank's solution at 0°C. Phenyramidol metabolism was assayed as in Figure V-6 and expressed as nmole metabolized/mg protein/hr as a function of storage time.

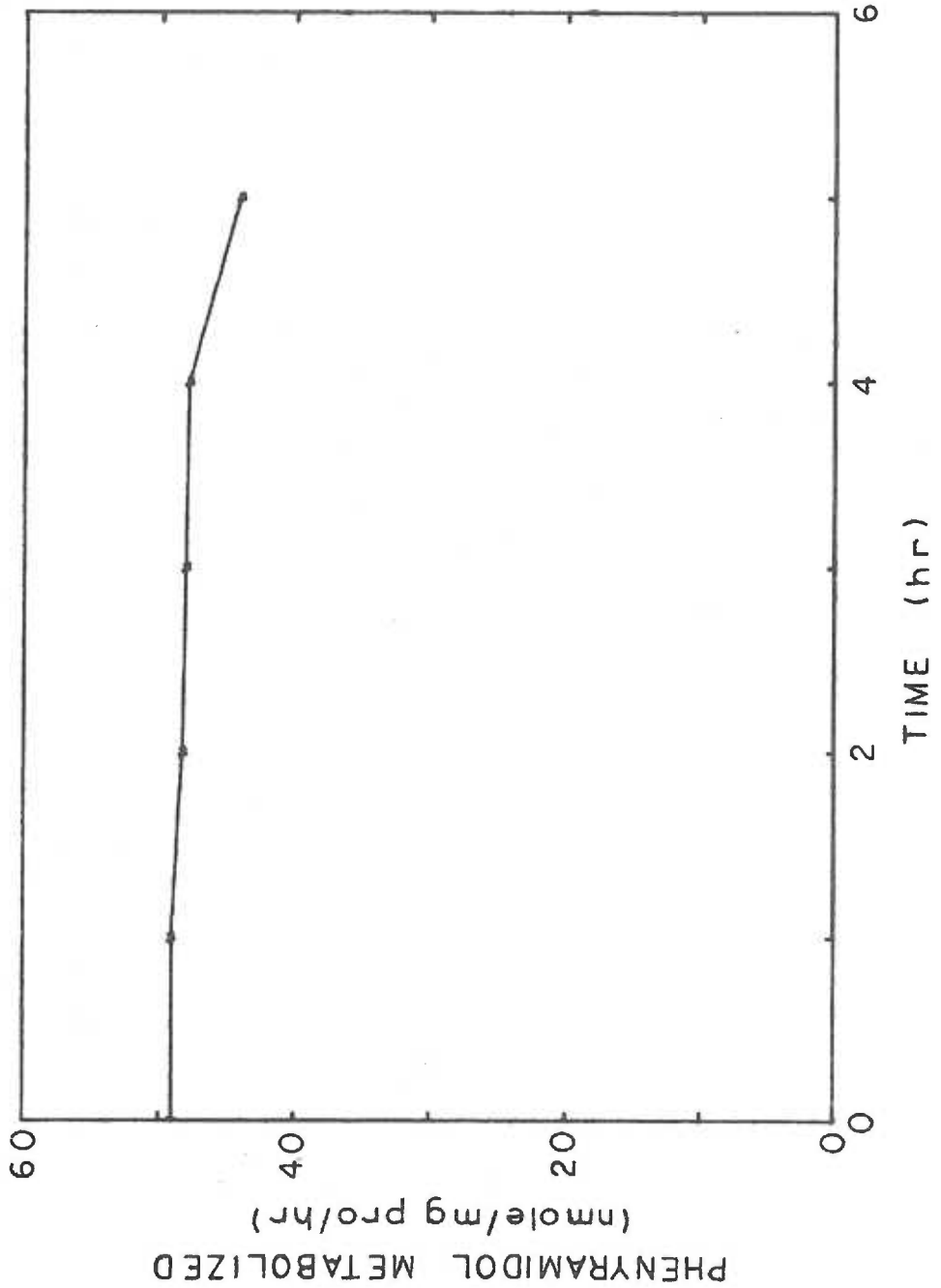
PHENYRAMIDOL METABOLIZED
(nmole/mg pro/hr)
60
40
20
0
0
2
4
6
TIME (hr)

Figure V-11. Phenyramidol metabolism by isolated hepatocytes as a function of oxygen tension. Hepatocytes (2×10^6 cells/ml, 8 ml volume) were brought to a desired $P(O_2)$. Phenyramidol was added to give 100 μM. After 10 min, 1 ml was pipetted into 9 ml phosphate buffer (100 mM, pH 6.8) plus 10 ml butyl chloride and unmetabolized substrate extracted. Metabolic rate was calculated from substrate loss. Data from four cell preparations, n = 20.

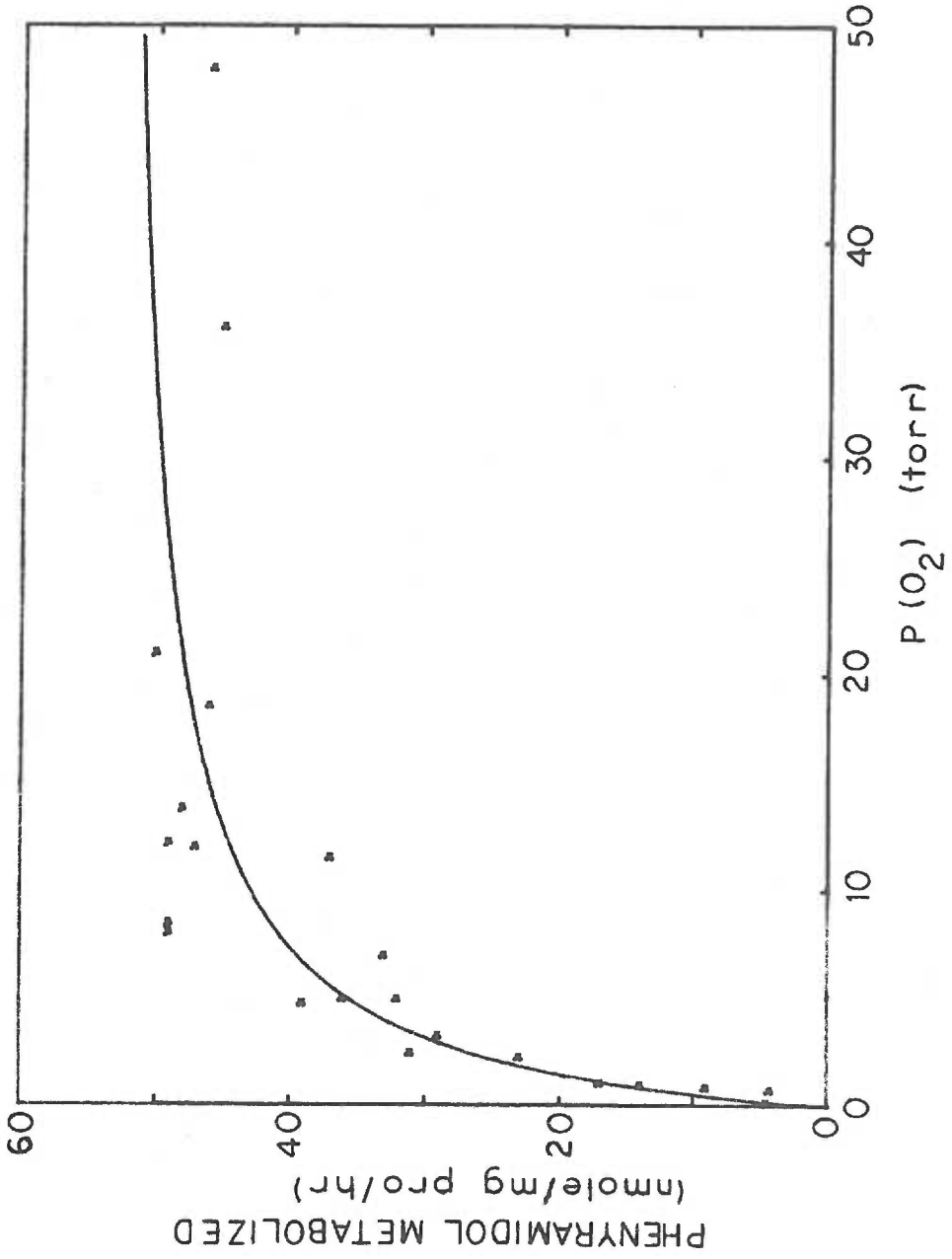
PHENYRAMIDOL METABOLIZED
(nmole/mg pro/hr)
0
20
40
60
0
10
20
30
40
50
P (O_2) (torr)

maximal metabolic rate was 46.0 ± 4.0 nmoles/mg protein/hr. The turnover number was calculated to be 0.058 sec^{-1}.

The double reciprocal plot, phenyramidol metabolic rate as a function of oxygen tension (Figure V-12), points fitted by the linear least squares method, had an intercept corresponding to an apparent cellular $Km(O_2)$ = 2.6 torr (3.6 μM) with a standard error of estimate of 0.4 torr (0.56 μM). Apparent cellular Vmax was 56 nmoles/mg protein. The Michaelis plot using these values for Km and V max is given in Figure V-11.

V.C. Metabolism of Hexobarbital by Isolated Hepatocytes

V.C.1. Metabolism as a Function of Time

The metabolism of hexobarbital by isolated hepatocytes from non-induced rats at 0.5 mM hexobarbital is given in Figure V-13. Cells were incubated at 2.3 x 10^6 cells/ml modified Hank's medium in a gyrotory shaker at 37°C. Hexobarbital was added to give a final concentration of 0.5 mM and samples taken at 0', 10', 20', and 30'. Results are expressed as nmole product/mg protein and nmole substrate loss/mg protein after corrections with the measured partition coefficients of Gerber et al. (1971).

Figure V-12. Double reciprocal plot of rate of phenyramidol metabolism as a function of solution $P(O_2)$ (data of Figure V-11).

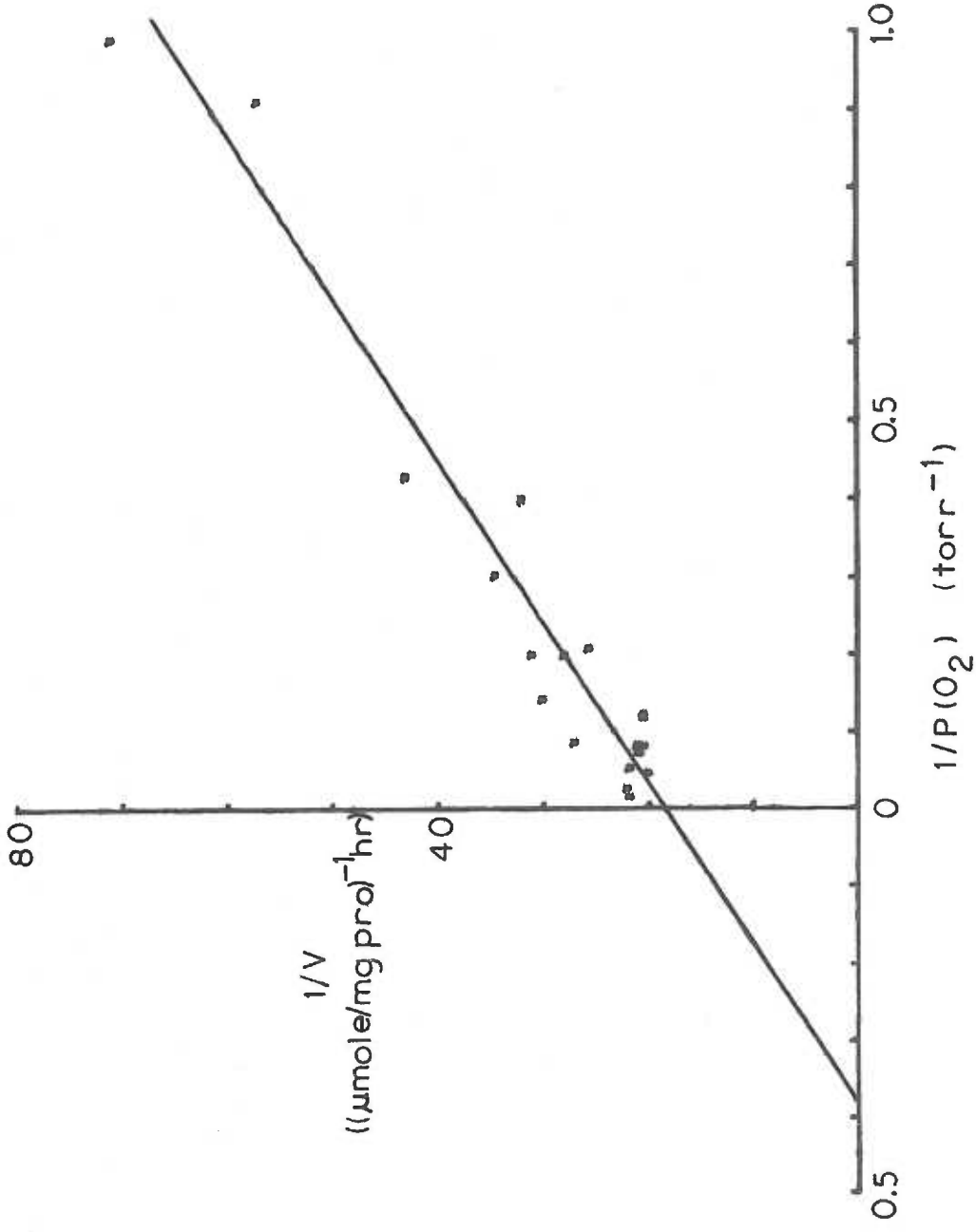
80
40
0
0.5
0.5
1.0
1/V
((μmole/mg pro)$^{-1}$hr)
1/P(O$_2$) (torr^{-1})

Figure V-13. Hexobarbital metabolism as a function of time. Isolated hepatocytes (24 ml, 3.6×10^6 cells/ml) were incubated in a 125 ml Erlenmeyer flask at $37^{\circ}C$ in a gyrotory shaker under 95% O_2, 5% CO_2. Hexobarbital was added (final concentration of 0.5 mM) and 2 ml samples taken at 0, 5, 10, 15, 20, 30 and 40 min for assay as described in text. Line is linear least squares fit for first five points.

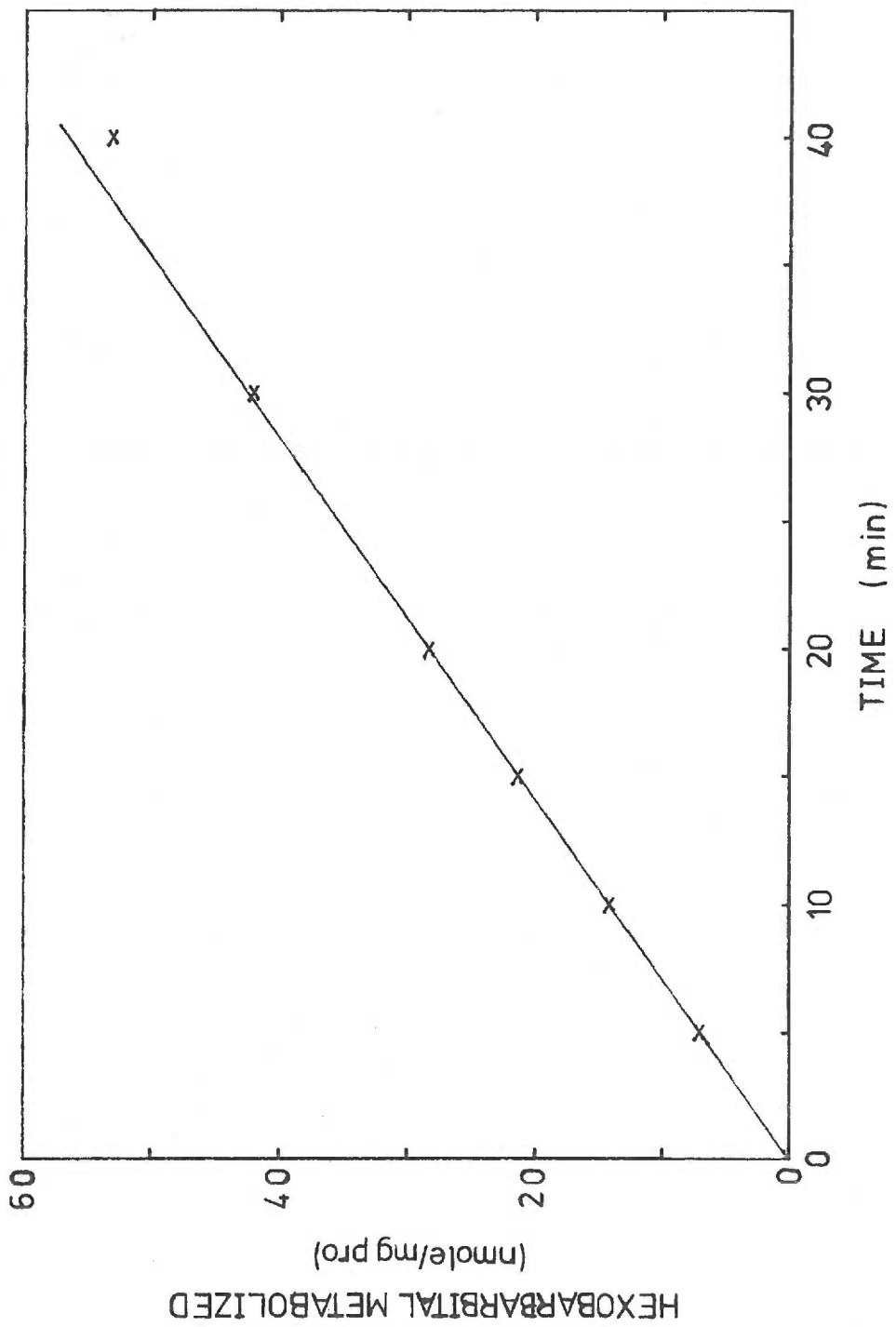
HEXOBARBARBITAL METABOLIZED
(nmole/mg pro)
0
20
40
60
0
10
20
30
40
TIME (min)

V.C.2. Metabolism by Non-induced Hepatocytes as a Function of Oxygen Tension with 0.5 mM Hexobarbital

Isolated hepatocytes were suspended to a final concentration of 2.3×10^6/ml in modified Hank's medium. Eight milliliter samples were transferred to the special incubation vessel and equilibrated to 37°C and the desired solution $P(O_2)$ with gases containing 5% CO_2. Hexobarbital solution (0.2 ml) was added. The suspension $P(O_2)$ was maintained with the oxystat for 10 min at desired values. A 4 ml aliquot was then removed and mixed with 6 ml 100 mM phosphate buffer (pH 6.8) plus 10 ml butylchloride and extracted. Results, expressed as nmole product formed/mg protein/hr relative to zero time controls for 20 incubations from six cell preparations, are given in Figure V-14. The $P(O_2)$ at half maximal metabolic rate was about 3.5 torr (4.9 μM) and the critical $P(O_2)$ was 14 torr (19.6 μM). The maximal velocity was 84.4 ± 4.3 nmole /mg protein/hr. The double reciprocal plot of rate against oxygen tension is given in Figure V-15. The apparent cellular $Km(O_2)$ as determined by the x-intercept of the linear least squares fit curve is 4.6 torr (6.4 μM) and the standard error of estimate is ± 1.2 torr (1.7 μM). The apparent cellular Vmax is 99.9 nmole /mg protein/hr. The turnover number was calculated to be 0.10 sec^{-1}.

Figure V-14. Hexobarbital metabolism by non-induced hepatocytes as a function of $P(O_2)$. Cells (2.3×10^6 cells/ml, 8 ml total volume) were brought to desired $P(O_2)$. Hexobarbital was then added to give 0.5 mM. After 10 min, 4 ml was removed and rapidly pipetted into 6 ml 100 mM phosphate buffer (pH 6.8) plus 10 ml butyl chloride. For details of extraction see text. Data represent hydroxylated products remaining in aqueous phase after extraction. Data from six cell preparations, n = 20.

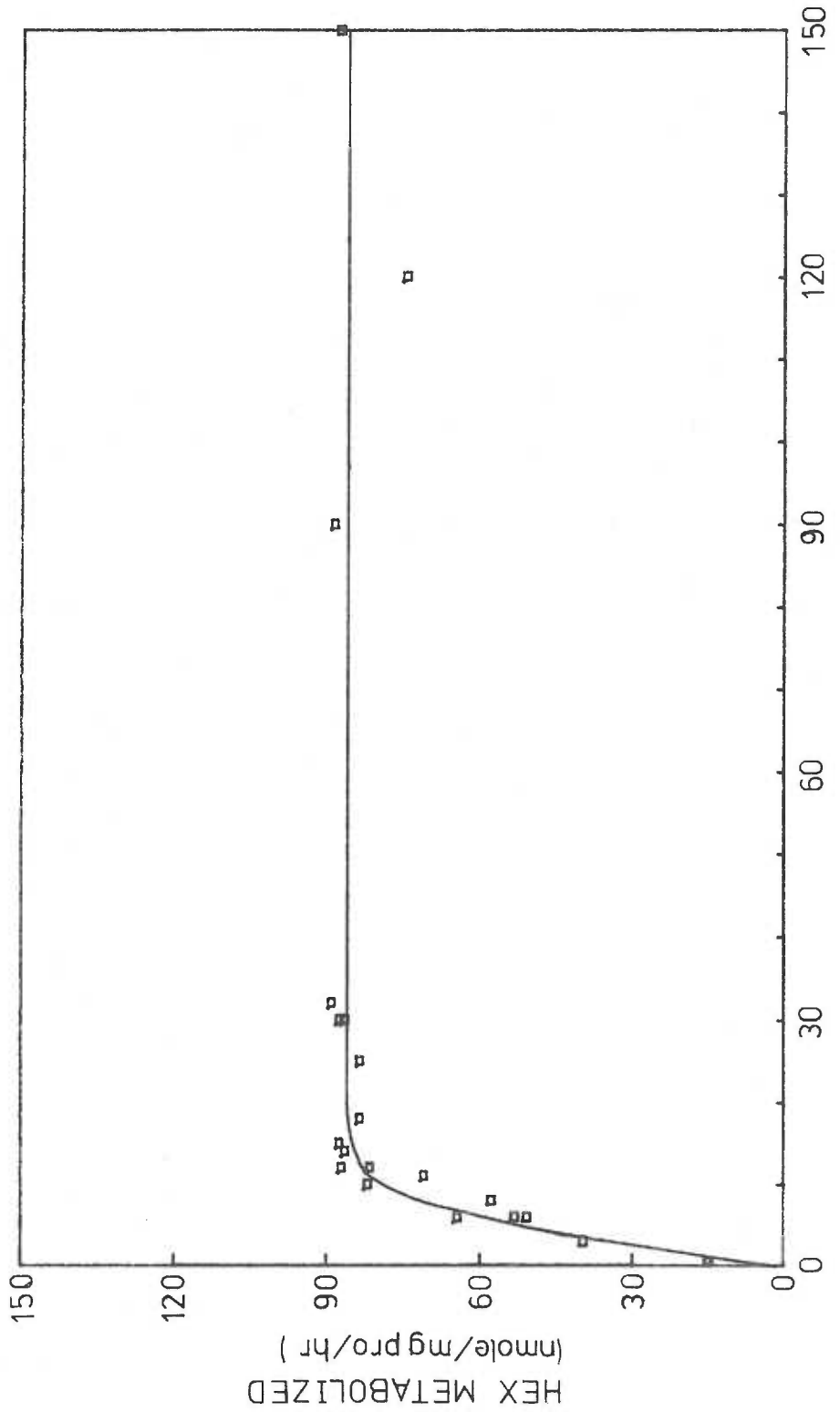
HEX METABOLIZED
(nmole/mg pro/hr)
150
120
90
60
30
0
0
30
60
90
120
150
P(O2) (torr)

Figure V-15. Double reciprocal plot of hexobarbital metabolism by non-induced hepatocytes and solution $P(O_2)$. Data same as in Figure V-14.

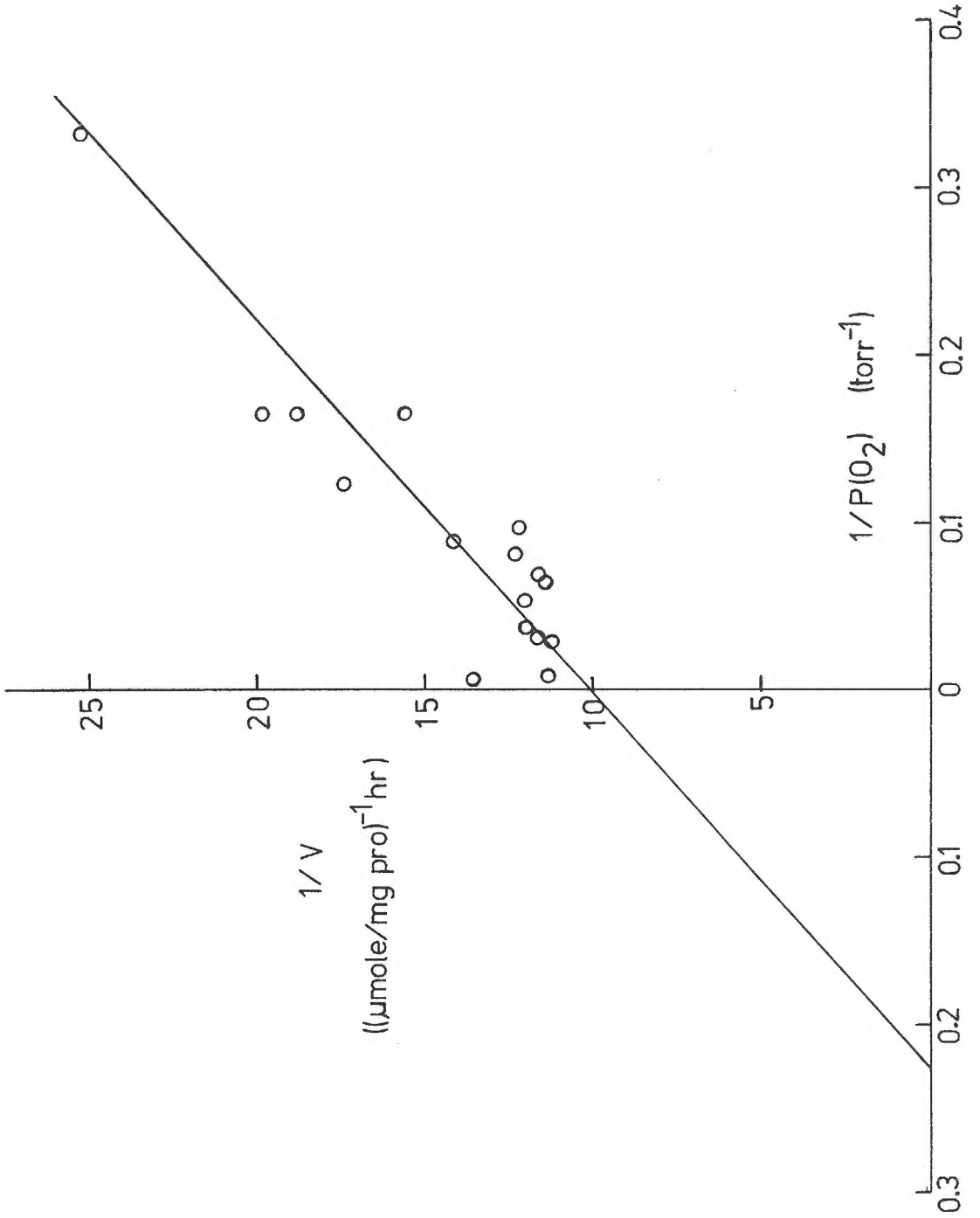
25
20
15
10
5
0
0.1
0.2
0.3
0.1
0.2
0.3
0.4
1/ V
((μmole/mg pro)$^{-1}$hr)
1/ P(O$_2$) (torr^{-1})

V.C.3. Metabolism by Non-induced Hepatocytes as a Function of Oxygen Tension with 0.1 mM Hexobarbital

Cells (2×10^6 cells/ml) were preincubated as above, and after desired $P(O_2)$ was achieved, hexobarbital was added to give a final concentration of 0.1 mM. The metabolism as a function of oxygen tension is given in Figure V-16. The estimated $P(O_2)$ for half maximal metabolism was 1.7 torr (2.4 μM); the critical $P(O_2)$ was about 5 torr (7 μM). Hexobarbital was metabolized at saturating oxygen tensions at a rate of 51.6 ± 2.0 nmole /mg/protein/hr.

V.C.4. Metabolism as a Function of Oxygen Tension by Phenobarbital Induced Hepatocytes

Rats were injected with phenobarbital as described in Section II.C and hepatocytes prepared. Cells (8 ml total volume, 2.3×10^6 cells/ml) were brought to desired $P(O_2)$. Hexobarbital (0.2 ml) was then added to a final concentration of 0.5 mM. After 10 min at constant oxygen tension, 4 ml was removed, extracted, and assayed for product formed. The results from four preparations are given in Figure V-17. The critical $P(O_2)$ was about 10 torr (14 μM) and the $P(O_2)$ at half maximal velocity was about 0.5 torr (0.7 μM). The maximal velocity was 147 ± 7 mole /mg protein/hr.

Figure V-16. Hexobarbital metabolism by isolated hepatocytes as a function of $P(O_2)$ at 0.1 mM hexobarbital. Cells were suspended in 8 ml total volume modified Hank's medium at approximately 2.0×10^6/ml and equilibrated to the desired oxygen tension. Hexobarbital was then added to 0.1 mM. After 10 min, 4 ml was removed and pipetted into 10 ml BuCl + 6 ml 100 mM phosphate buffer (pH 6.8) for extraction.

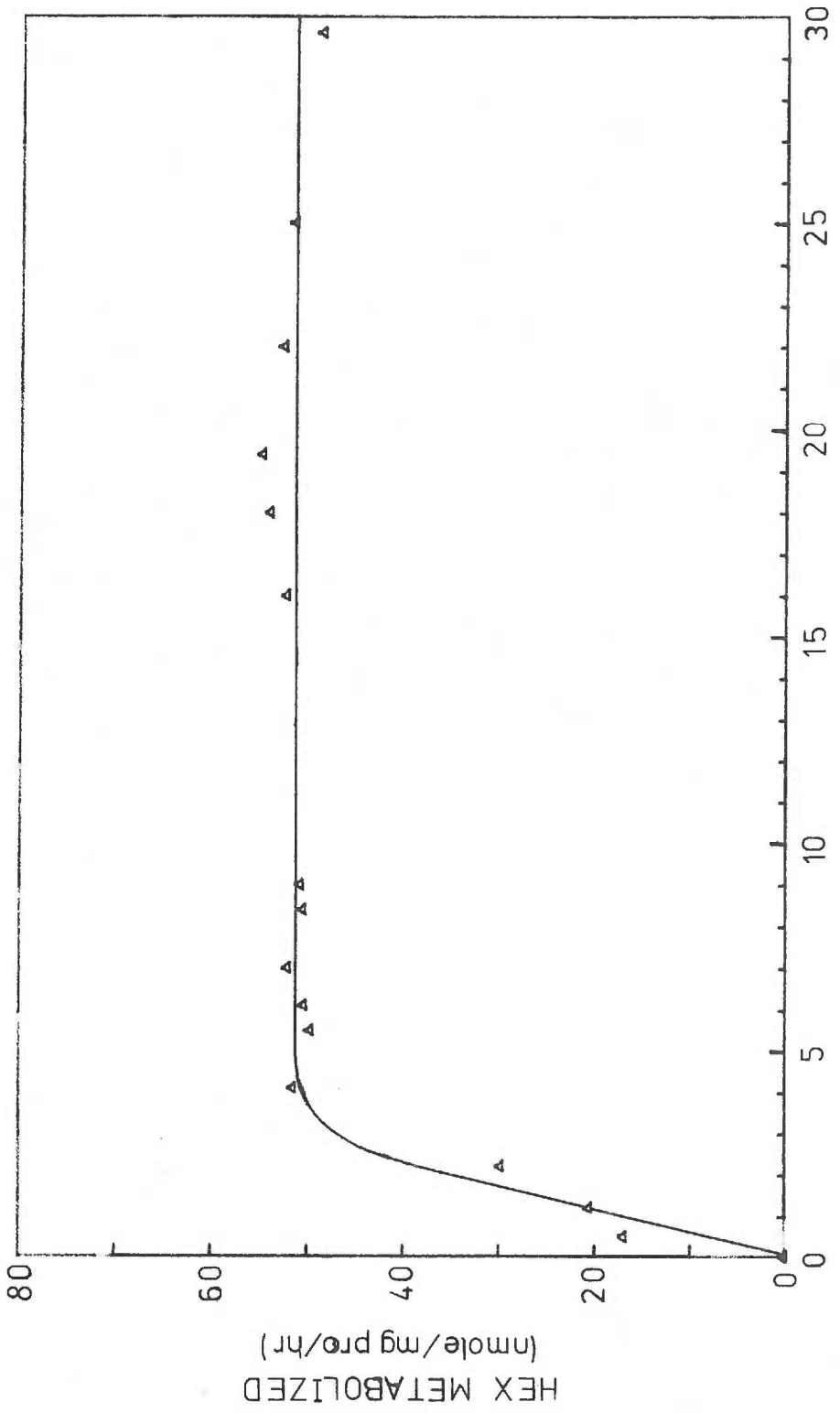
HEX METABOLIZED
(nmole/mg pre/hr)
80
60
40
20
0
0
5
10
15
20
25
30
P(O2) (torr)

Figure V-17. Hexobarbital metabolism by phenobarbital induced rat hepatocytes as a function of $P(O_2)$. Cells (2.3×10^6 cells/ml, 8 ml total volume) were brought to desired $P(O_2)$. Hexobarbital was then added to give 0.5 mM. After 10 min, 4 ml was removed and rapidly pipetted into 6 ml 100 mM phosphate buffer (pH 6.8) plus 10 ml butyl chloride. For details of extraction see text. Data represent hydroxylated products remaining in aqueous phase after extraction. Data from four cell preparations, n = 15.

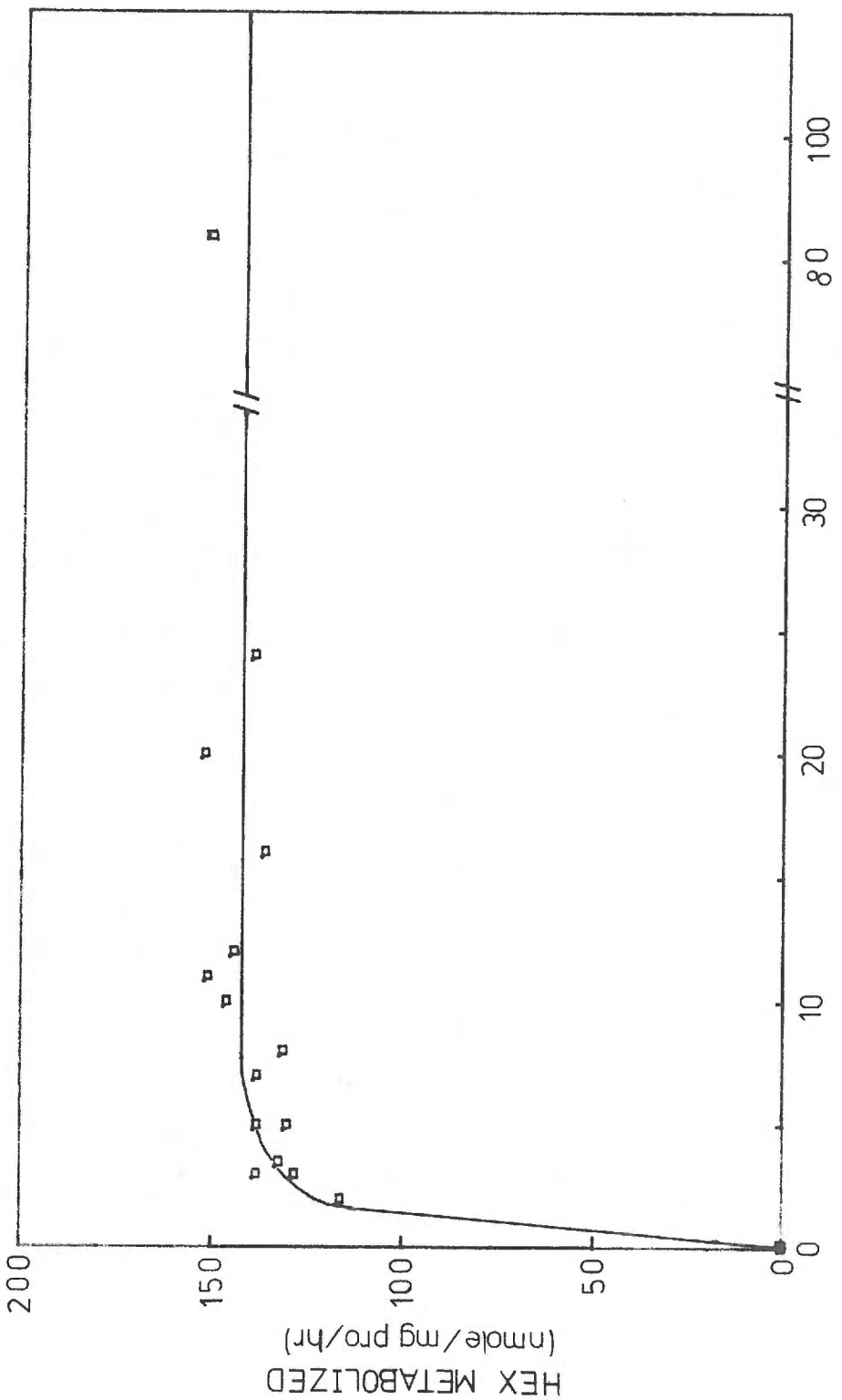
HEX METABOLIZED
(nmole/mg pro/hr)
200
150
100
50
0
0
10
20
30
80
100
P(O2) (torr)

V.C.5. Metabolism as a Function of Oxygen Tension by 3-Methylcholanthrene Induced Hepatocytes

Rats were injected with 3-methylcholanthrene as described in section II.C.1.a. and cells prepared by the perfusion method. Cells (2.3×10^6 cells/ml) were incubated as above at desired constant oxygen tensions with 0.5 mM hexobarbital. After 10 min 4 ml was removed, extracted, and assayed for product formed. The results from four preparations are given in Figure V-18. The critical $P(O_2)$ was 12 torr (17 μM), and the $P(O_2)$ at half maximal metabolic rate was 2.6 torr (3.6 μM). The maximal velocity was 101 ± 5.6 nmole/mg protein/hr.

V.D. Metabolism of Alprenolol by Isolated Hepatocytes

V.D.1. Metabolism as a Function of Time

Isolated hepatocytes from non-induced rats were prepared by the perfusion method as previously described. Twenty milliliter volumes of cells (2.3×10^6 cells/ml) were incubated in a 125 ml Erlenmeyer flask in a gyrotory shaker at 37°C under 95% O_2, 5% CO_2. After 5 min, alprenolol was added to final concentration, 44 μM. Samples were removed for assay of substrate loss at 0, 5, 10, 15, 20, 25 and 30 min. The results are shown in Figure V-19.

Figure V-18. Hexobarbital metabolism by 3-methylcholanthrene induced isolated hepatocytes as a function of $P(O_2)$. Cells (2.3×10^6 cells/ml, 8 ml total volume) were brought to desired $P(O_2)$. Hexobarbital was then added to give 0.5 mM. After 10 min, 4 ml was removed and rapidly pipetted into 6 ml 100 mM phosphate buffer (pH 6.8) plus 10 ml butyl chloride. For details of extraction see text. Data represent hydroxylated products remaining in aqueous phase after extraction. Data from four cell preparations, n = 12.

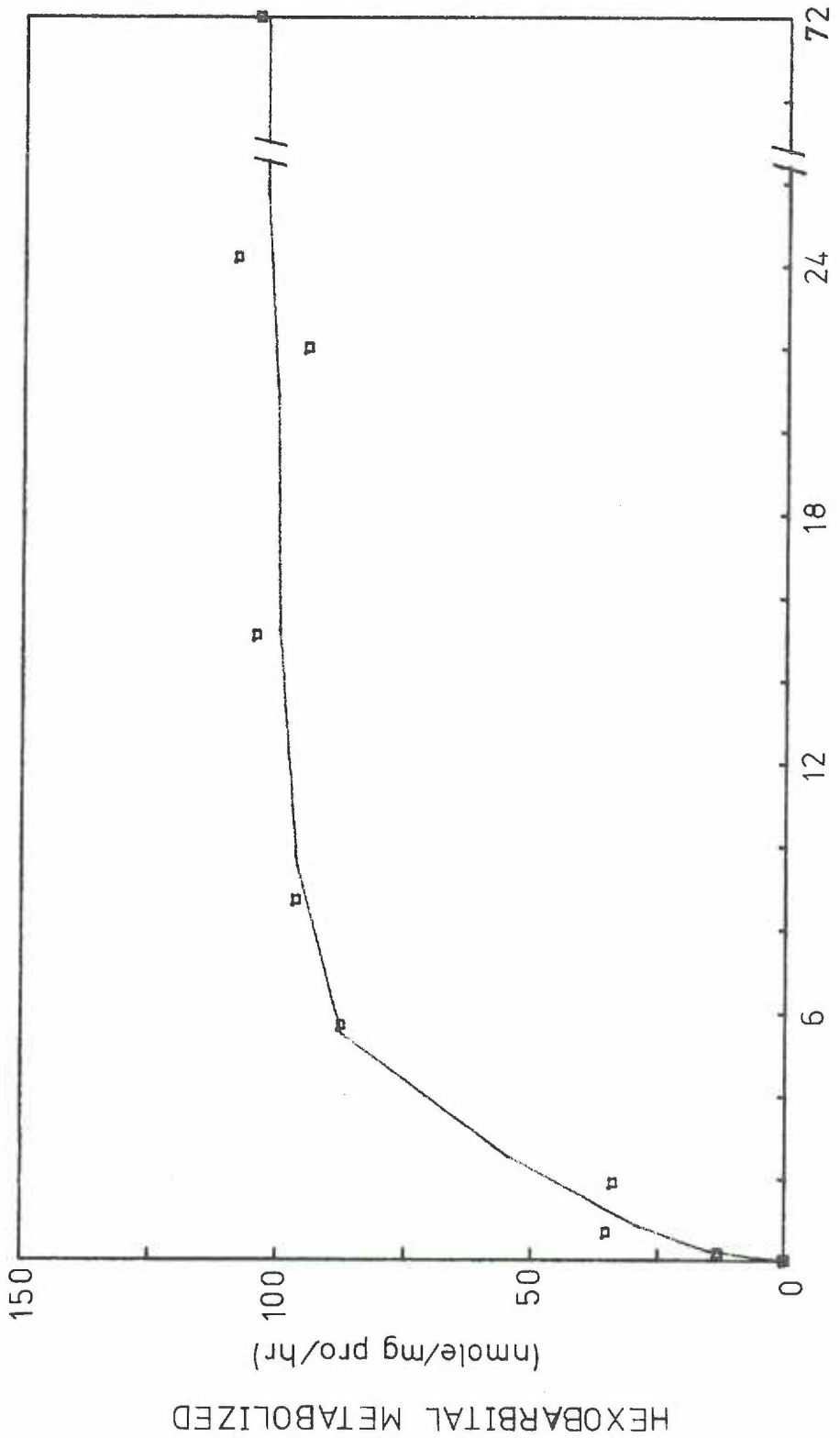
HEXOBARBITAL METABOLIZED
(nmole/mg pro/hr)
150
100
50
0
6
12
18
24
72
P(O2) (torr)

Figure V-19. Alprenolol metabolism by isolated hepatocytes. Isolated hepatocytes (20 ml total volume; 2.3×10^6 cells/ml) from non-induced rats were incubated in a 125 ml plastic Erlenmeyer flask in a gyrotory shaker at 37°C in modified Hank's medium under 95% O_2, 5% CO_2. After 5 min, alprenolol was added to give a final concentration of 44 μM. Samples were removed for assay of substrate loss at zero time and subsequently at 5 min intervals. Results were expressed as nmoles/mg protein.

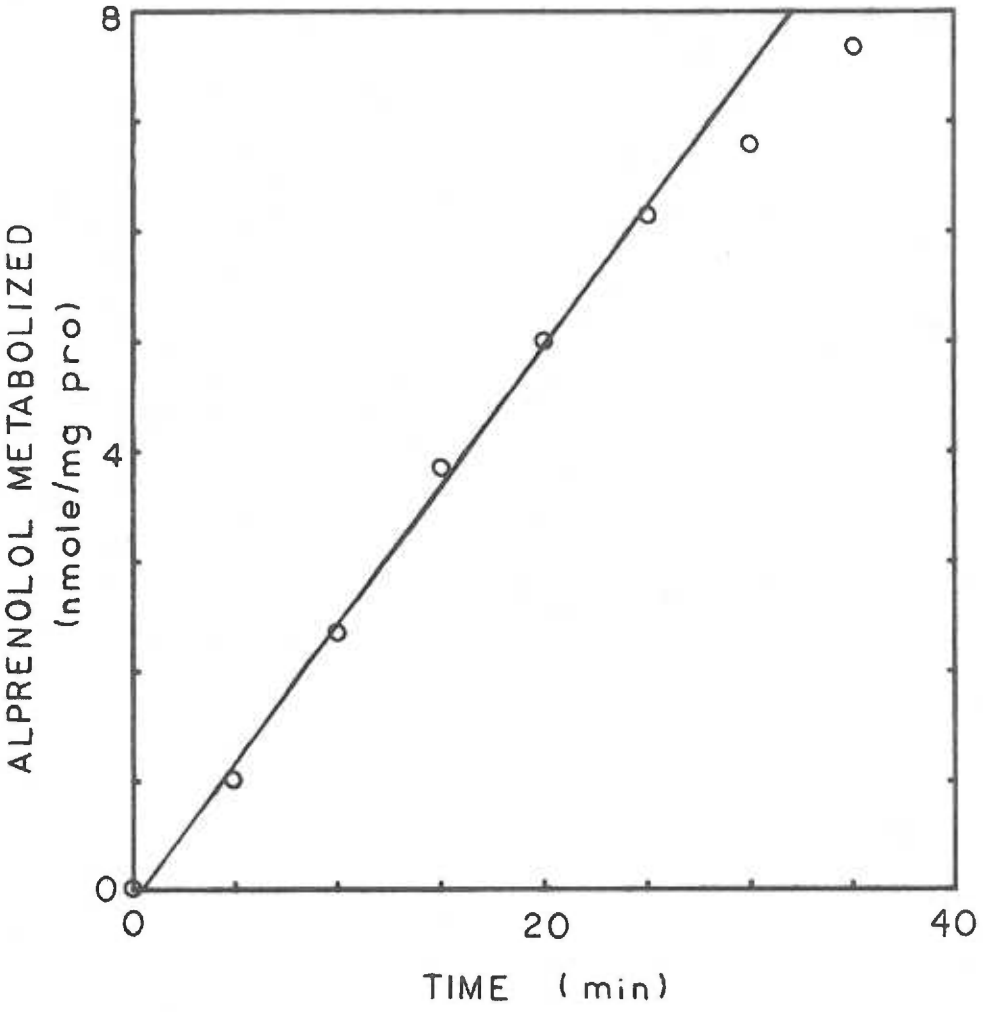
ALPRENOLOL METABOLIZED
(nmole/mg pro)
8
4
0
0
20
40
TIME (min)

Metabolism is expressed in nmole /mg protein and was linear for about 25 min.

V.D.2. Metabolism as a Function of Oxygen Tension

Isolated hepatocytes (2.3×10^6 cells/ml) were pipetted into the special incubation vessel and brought to the desired $P(O_2)$ as previously described. Alprenolol was added to 44 μM, and the oxygen tension was maintained constant for 10 min. An aliquot of 4 ml was transferred to an extraction tube containing 1 ml 10 N NaOH and the unreacted substrate removed by extraction with 10 ml n-hexane. The metabolic rate for alprenolol as measured by substrate loss is plotted as a function of oxygen tension in Figure V-20. The data represent 15 incubations from five cell preparations. The critical $P(O_2)$ was 24 torr (33.6 μM) and the $P(O_2)$ at half maximal metabolic rate was 7 torr (9.8 μM). Maximal metabolism was 14.2 ± 1.0 nmole /mg protein/hr. The calculated turnover number was 0.018 sec^{-1}.

V.E. Discussion

Metabolism rates of alprenolol, hexobarbital and phenyramidol by isolated intact cells without added cofactors are comparable to rates for isolated microsomes plus cofactors (Gerber et al., 1972, 1974; Moldeus et al., 1974). The oxygen dependencies of the

Figure V-20. Alprenolol metabolism by isolated hepatocytes as a function of $P(O_2)$. Cells (2.3×10^6 cells/ml, 8 ml total volume) were brought to desired $P(O_2)$. Alprenolol was then added to give 44 μM. After 10 min, 4 ml was removed and rapidly pipetted into tube containing 1 ml 10 N NaOH; 10 ml n-hexane was then added to extract unreacted substrate as described in text. Metabolic rate was determined from the rate of substrate disappearance. Data from five cell preparations, n = 15.

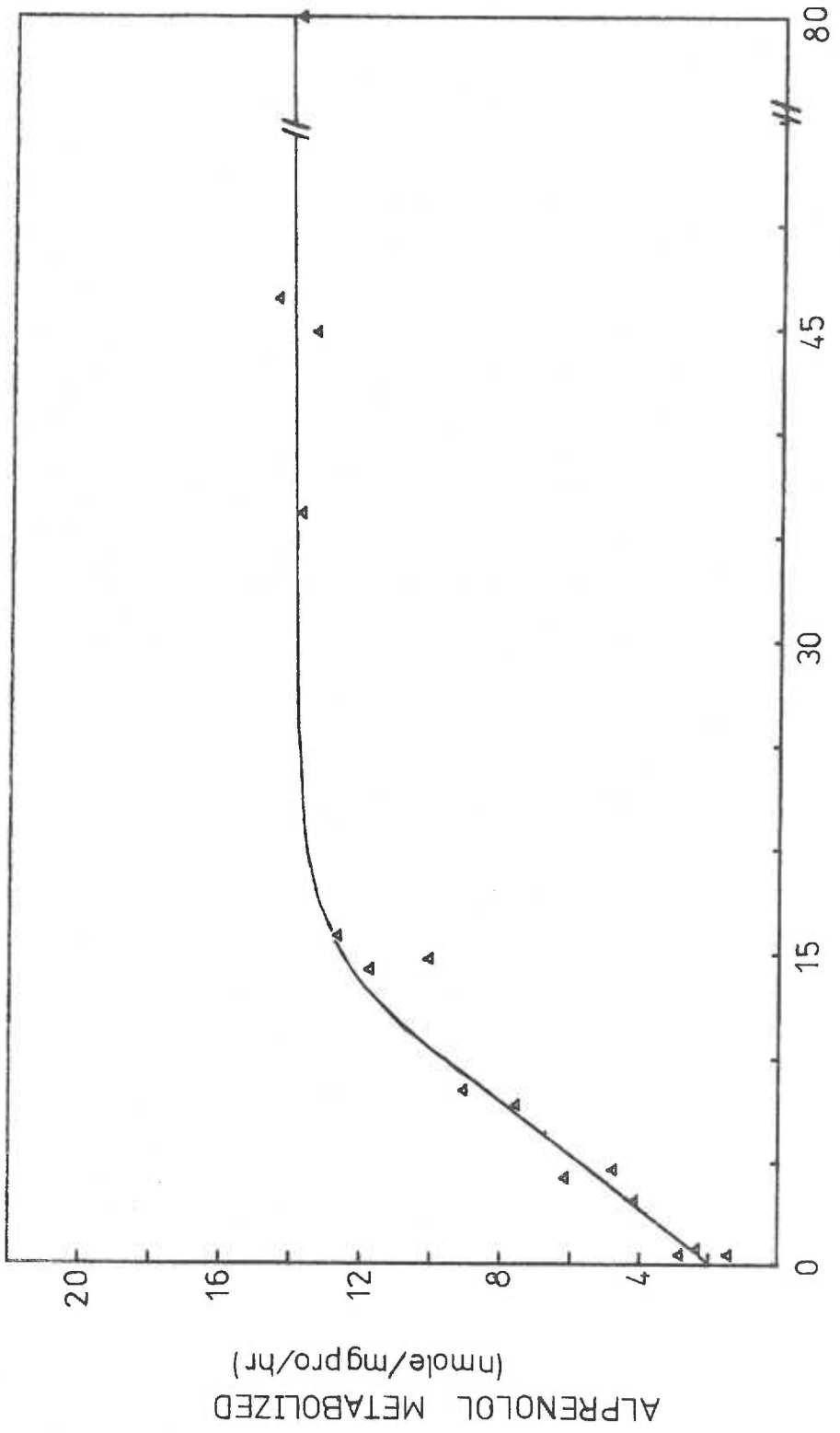
ALPRENOLOL METABOLIZED
(nmole/mg pro/hr)
20
16
12
8
4
0
15
30
45
80
P(O2) (torr)

metabolism of these substrates (Table VII-C) are similar to values reported for isolated microsomes (Table V-A). This suggests that there is no difference in control of the two systems and only a minimal oxygen tension gradient between the suspending medium and the endoplasmic reticulum. It is not clear whether the apparent cellular $Km(O_2)$ represents a true affinity of the cytochrome(s) for oxygen, a kinetic limitation in the multistep reaction sequence, a diffusion limited process, or a decreased availability of reducing equivalents due to failure of energy dependent transhydrogenation.

The occurrence of $Km(O_2)$ values in the same range as cytochrome oxidase (Section IV) and in the lower "normal" cellular oxygen tension (Section I) indicates that hepatic mixed function oxidation may be oxygen dependent under normal in vivo conditions. This may be important in control of oxygen utilizing pathways and lead to decreased function during hypoxia. The clinical manifestations of such an oxygen dependence in hypoxic patients is obvious (Section I).

Whether multiple specificity and spectral characteristics of cytochromes P-450 are due to different forms of one protein or due to different proteins with similar properties has been a matter of query for several years. Hangen, van der Hoeven and Coon (1975) recently separated and characterized multiple forms of cytochrome P-450. They showed that these forms have different electrophoretic mobilities in polyacrylamide gels in the presence of sodium dodecyl sulfate and

that they have different oxidative activities with different substrates. This provides strong evidence that cytochrome P-450 in hepatic microsomes is a group of enzymes rather than a single enzyme and thus limits the interpretation of experiments based upon physical techniques, such as optical and ESR spectroscopy, and of activity studies on the mixture of forms. The lower apparent cellular $Km(O_2)$ for 0.1 mM compared to 0.5 mM hexobarbital concentration suggests that either two cytochrome systems with different O_2 affinities are operative or that the system functions more efficiently at low substrate concentrations. The decrease in apparent cellular $Km(O_2)$ due to phenobarbital induction suggests induction of a protein with greater oxygen affinity or induction of a component rate controlling in the process. The increase in apparent cellular $Km(O_2)$ due to 3-MC induction indicates induction of a low affinity component or a less efficient reductase system. Change in cytochrome P-450 and reductase components due to induction are known (Gillette et al., 1972; Haugen et al., 1975) so that either or both explanations may prove to be correct.

The typical method of cytochrome P-450 quantitation using the carbon monoxide difference spectrum of the dithionite reduced compound and the extinction coefficient of Omura and Sato (1964) is not valid if other carbon monoxide binding pigments which absorb in the 450 to 490 nm region are present. Reduced cytochrome $\underline{a}_3$

present in mitochondria binds carbon monoxide to produce a strong negative absorption with a peak at 445 nm (Vanneste, 1966; Vanneste and Vanneste, 1965). Since cytochrome oxidase is frequently present in systems in which cytochrome P-450 quantitation is desired, a simple method without interference is needed. This is of particular importance in studies of cytochrome P-450 in isolated cells or mitochondria. In the reduced CO minus reduced difference spectrum of cytochrome $\underline{a}_3$, the negative absorbance at 460 nm is only 4% of that at 445 nm while the cytochrome P-450 absorbance is 52% of that at 450 nm (Kowal, Simpson and Estabrook, 1970). Consequently, the absorbance change at 460 nm minus 490 nm was used to quantitate cytochrome P-450 content in cultured adrenal cells. Mason, Estabrook and Purvis (1973), using the same technique, expressed the adjusted extinction of the dithionite reduced carbon monoxide difference spectrum of cytochrome P-450 as 52 mM^{-1} cm^{-1}. They added increasing amounts of cytochrome $\underline{a}_3$ to microsomes and showed a peak shift from 450 to 460 nm as well as a dramatic reduction in peak height. The $\Delta OD_{460-490}$ also showed a decrease as cytochrome $\underline{a} + \underline{a}_3$ was increased. Thus, this technique for cytochrome P-450 quantitation is not useful without previous knowledge of cytochrome $\underline{a}_3$ concentration, and with this knowledge, requires modification of the effective extinction coefficient to correct for the contribution from cytochrome $\underline{a}_3$.

A different approach to observing cytochrome P-450 in the presence of cytochrome $\underline{a}_3$ was used by Ghazarian et al. (1974) for isolated renal mitochondria. They utilized the difference in redox potentials of the carbon monoxide complexes of cytochrome $\underline{a}_3$ and cytochrome P-450 to provide a difference spectrum of cytochrome P-450 without interference from cytochrome $\underline{a}_3$. Malate (or dithionite) in the presence of carbon monoxide produces the reduced CO species of both cytochromes in the sample cuvette while ascorbate and TMPD (in the presence of antimycin A) produces only CO · cytochrome $\underline{a}_3$ in the reference cuvette. The difference spectrum shows a large 450 nm absorbance which is apparently primarily due to cytochrome P-450. However, this spectrum is not necessarily valid for P-450 quantitation with Omura and Sato's extinction value since other chromophores with redox potentials between or near malate and ascorbate are present in mitochondria and may be contributing to this difference. In the present work, the applicability of these methods to cytochrome P-450 quantitation in isolated hepatocytes was examined. The method of additions allowed accurate quantitation of cytochrome P-450 by extrapolating to zero cytochrome $\underline{a}_3$ concentration.

In measurement of total cytochrome P-450 in microsomes (Omura and Sato, 1964) the carbon monoxide difference spectrum of the dithionite reduced form has an extinction coefficient of 91 mM^{-1}

VI. TYROSINE DEGRADATION

Tyrosine is degraded in mammals primarily by a single multi-enzyme pathway as shown in Figure VI-1. The high activities of these enzymes in the liver relative to other tissues suggests that the hepatic function determines the ability of the entire organism to carry out this metabolism (Fellman et al., 1972; Lin and Knox, 1958). The first enzyme, tyrosine aminotransferase (TAT; EC 2.6.1.5), catalyzes the transfer of the amine group on tyrosine to 2-oxoglutarate with formation of p-hydroxyphenylpyruvate and glutamate. The reaction is reversible and has a ping-pong mechanism (Litwack and Cleland, 1968; Rosenberg and Litwack, 1970). The p-hydroxyphenylpyruvate (pHPP) is oxidized to homogentisate (HG) by p-hydroxyphenylpyruvate oxidase (pHPPO; EC 1.14.2.2). The oxygen-dependent reaction involves an interesting side chain transfer, a decarboxylation, and an hydroxylation (oxygen incorporation from molecular oxygen; Lindblad, Lindstedt and Lindstedt, 1970; Yasunobu et al., 1958). The mechanism is thought to be analogous to the 2-oxo acid-dependent oxidases (Lindblad et al., 1970). Homogentisate is oxidized to maleylacetoacetate by an oxygen-dependent ring-cleavage catalyzed by homogentisate oxidase (HGO; EC 1.13.1.5). The reaction requires ferrous ion and results in incorporation of a molecule of oxygen into the product (Crandall et al., 1960).

Figure VI-1. Phenylalanine and tyrosine degradation and possible side reactions. Dark arrows indicate normal pathway. Enzymes are indicated by numbers: 1, phenylalanine hydroxylase; 2, tyrosine amino transferase; 2a, L-amino acid oxidase; 3, p-hydroxyphenylpyruvic acid oxidase; 4, homogentisic acid oxidase; 5, phenylalanine amino transferase.

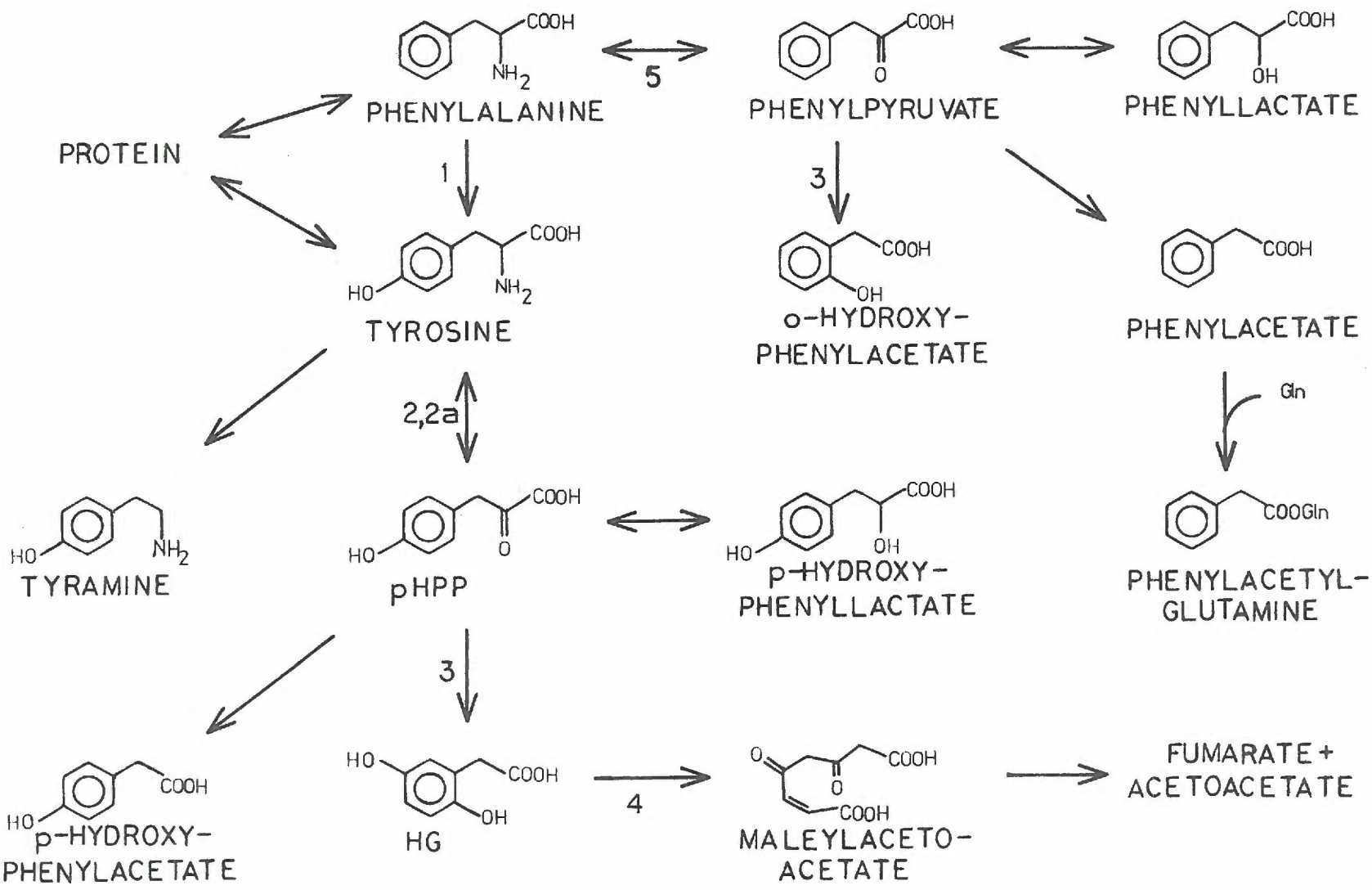
PHENYLALANINE
PHENYLPYRUVATE
PHENYLLACTATE
PROTEIN
TYROSINE
o-HYDROXY-
PHENYLACETATE
PHENYLACETATE
TYRAMINE
pHPP
p-HYDROXY-
PHENYLLACTATE
PHENYLACETYL-
GLUTAMINE
p-HYDROXY-
PHENYLACETATE
HG
MALEYLACETO-
ACETATE
FUMARATE +
ACETOACETATE
1
2,2a
3
4
5
Gln

Intracellular control of tyrosine metabolism is not fully understood (Figure VI-2). TAT has the lowest specific activities of the three enzymes. This suggests that TAT is the rate limiting enzyme in the pathway. However, the TAT reaction is reversible, and it is possible that the pHPPO reaction could be rate limiting if its rate is submaximal. The metabolite, pHPP, could itself modulate TAT activity by product inhibition or by a shift in the TAT reaction equilibrium (David, Dairman and Udenfriend, 1974). Modulation of tyrosine degradation may also occur through inhibition of TAT by HG (Civin, Wilson and Brown, 1970). Thus, if decreased HGO activity resulted in an increased level of HG, the rate of tyrosine conversion to pHPP could be decreased by TAT inhibition. Both pHPPO and HGO are oxygen dependent enzymes, and therefore, their in vivo function may be modulated by cellular $P(O_2)$. The apparent $Km(O_2)$ of pHPPO is about 10^{-4} M (76 torr) (Fellman et al., 1972), and the apparent $Km(O_2)$ of HGO is about 10^{-3} M (760 torr) (Flamm and Crandall, 1963). Since normal liver oxygen tensions appear to range from about 1-40 torr (Lubbers, 1973), oxygen tension must have an important affect on the activity of these oxidases in vivo. Decreased function is likely to result in accumulation of either pHPP or HG, which could have an inhibitory affect on tyrosine degradation. In addition, 2-oxoglutarate or glutamate concentrations, or their ratio, may control the process through the TAT reaction.

Figure VI-2. Metabolic control of tyrosine degradation.

1. Substrate level control may be exerted by both 2-oxoglutarate and tyrosine since both have subsaturating concentrations *in vivo* for the TAT reaction.

2. Glutamate and pHPP concentrations may affect the overall reaction rate by the reverse reaction.

3. If the TAT reaction is at or near equilibrium, then all four reactants are important to rate control. Under this condition the degradative rate is determined by [pHPP], [O_2] and pHPPO activity.

4. O_2 may exert control by:
   a. altered mitochondrial function. Redox state becomes more reduced, thereby altering glutamic dehydrogenase equilibrium. Increased glutamate/2-oxoglutarate could cause increased reverse TAT reaction.

   b. Decreased pHPPO reaction. The resultant decrease could diminish overall rate if TAT reaction is at equilibrium and pHPPO reaction is rate determining. Alternatively, pHPP could decrease overall rate by product inhibition of TAT or by increasing reverse TAT reaction.

   c. Decreased HGO reaction. The resultant HG inhibits TAT and thus could decrease overall degradation rate if TAT is rate determining.

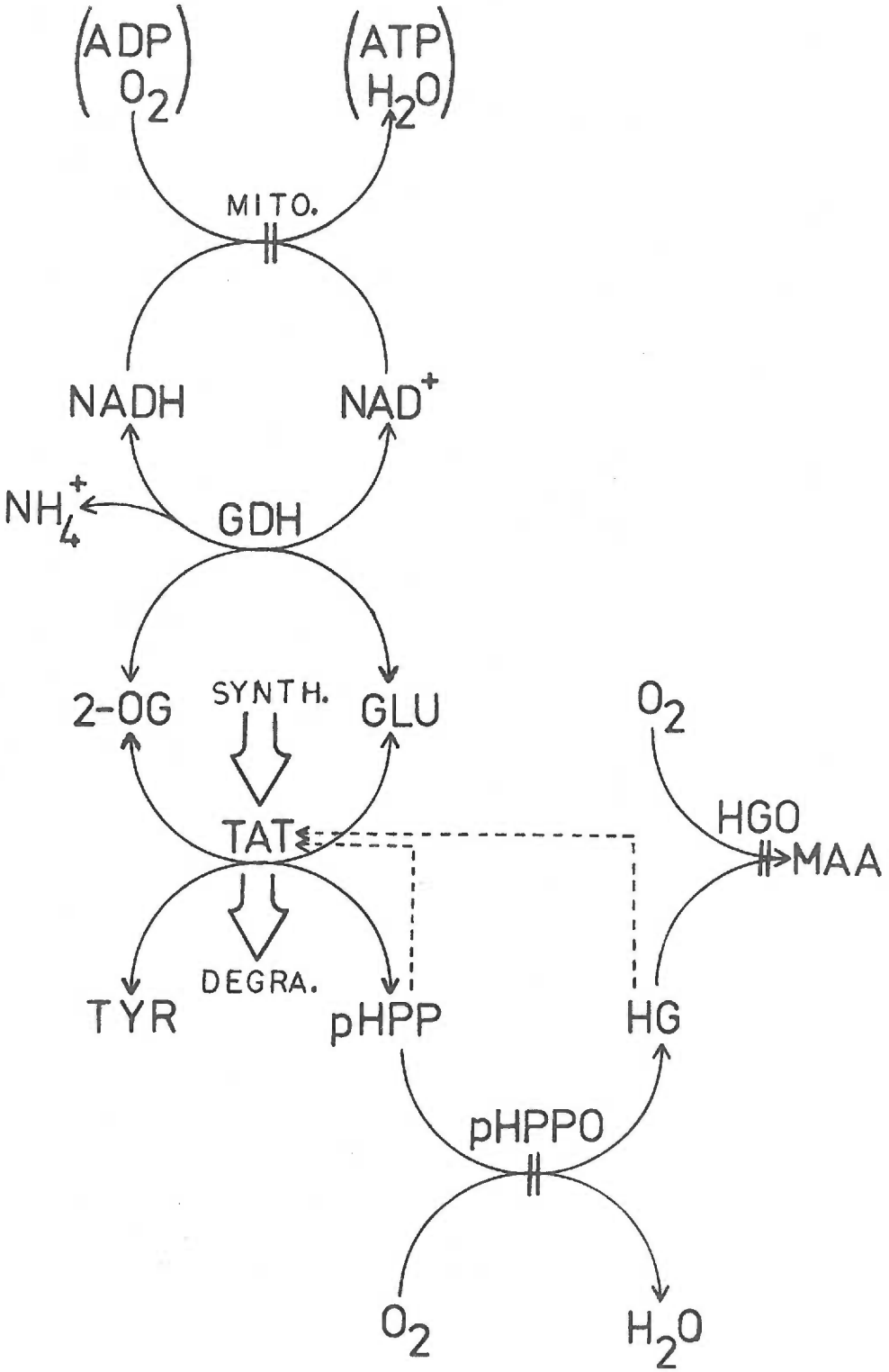
ADP
O2
ATP
H2O
MITO.
NADH
NAD+
NH4+
GDH
2-OG
SYNTH.
GLU
O2
HGO
MAA
TAT
DEGRA.
TYR
pHPP
HG
pHPPO
O2
H2O

The use of isolated cells to study the affect of oxygen tension on tyrosine degradation seemed advantageous since use of cells eliminates tissue diffusion problems yet retains metabolic integrity. In this research the suitability of hepatocytes for the study of tyrosine degradation and the affect of oxygen tension on this metabolism is examined.

VI. A. Specific Activities of Tyrosine Degradative Enzymes in Hepatocytes

Hepatocytes were prepared from fed, non-induced rats, homogenized and assayed for tyrosine aminotransferase, p-hydroxyphenylpyruvate oxidase, and homogentisate oxidase activities under conditions chosen to approximate maximum activities (Section II.B.). The results are expressed in Table VI-A as μmole product formed/hr/mg total cellular protein. Also shown are the activities as measured in liver homogenate.

VI.B. Tyrosine, pHPP, and HG Partitioning between Cells and Incubation Medium

Estimation of the fraction of tyrosine, pHPP, and HG in the total incubation mixture that was contained in the cells was performed by separation of the cells from the suspending medium by centrifugation at 50 x g for 3 min, and assaying the metabolites in both the pellet (cells) and supernatant (suspending medium). Corrections were then

Table VI-A. Specific activities of enzymes involved in tyrosine degradation in isolated cells and intact liver. Values are expressed in μmoles product formed/mg protein/hr. All assays were run at 37°C under conditions assumed to give maximal activity. Values expressed are the averages ± 1 S.D. for multiple determinations on at least three rat livers. Numbers in parentheses are the total number of determinations.

Enzyme	Cells	Liver
TAT	0.501 ± 0.130 (6)	0.406 ± 0.043 (4)
pHPPO	0.232 ± 0.021 (6)	0.256 ± 0.011 (3)
HGO	1.96 ± 0.30 (6)	2.09 ± 0.26 (3)

made for packing volume as described in Section IV. B. 1. The cell concentration was 3.0×10^6 cells/ml in modified Hank's medium containing 0.22 mM tyrosine. Incubations were maintained at 37°C under 20% O_2, 5% CO_2, 75% N_2 for 30 min prior to centrifugation. The results are given in Table VI-B.

VI. C. Tyrosine Uptake by Isolated Hepatocytes

To determine the rate of tyrosine uptake by isolated rat liver cells, ^3H tyrosine (3.3 mCi/mmole) was added to isolated cells and aliquots removed at 1-4 min intervals for collection of cells on 0.45 μ millipore filters. The incubations were performed in the special incubation vessel (Section III) at 37°C with gentle stirring. Medium 199 was used as the incubating medium. The initial tyrosine concentration was 0.3 mM. Millipore filters with collected cells were incubated overnight in 0.5 ml NCS tissue solubilizer and counted in toluene-PPO-POPOP. Counts on filters were plotted as a function of time. The intercept of a linear least squares analysis of the initial time points was subtracted from each value to correct for counts retained in the volume of the filter. These data were divided by cell concentration and plotted as a function of time (Figure VI-3). The initial rate of label uptake corresponded to 19.2 nmole tyrosine/hr/10^6 cells or 12.8 nmole /hr/mg protein. After about 10 min, this rapid phase of label uptake subsided and no further uptake was apparent for the remainder of the experiment.

Table VI-B. Partitioning of metabolites between pellet and suspending medium. Cells were incubated 30 min under 20% O_2, 5% CO_2 at 37°C, centrifuged 2 min at 600 rpm (50 x g), supernatant decanted and both fractions deproteinated with H_2SO_4 and centrifugation. Metabolites determined and expressed in terms of concentration in the volume of each fraction. Incubation medium was modified Hank's medium.

	Average pellet	Average supernatant	% of Total as pellet
HG	15.5 ± 4.2 μM	[illegible] ± 0.84 μM	88.2 ± 2.0
pHPP	0.101 ± 0.069 mM	0.013 ± 0.007 mM	91.6 ± 1.9
Tyrosine	0.41 ± 0.08 mM	0.22 ± 0.01 mM	62.2 ± 1.6
Glutamate	1.30 ± 0.18 mM	0.54 ± 0.20 mM	69.2 ± 6.9

Figure VI-3. Tyrosine uptake by isolated hepatocytes. ^{3}H tyrosine was added to isolated hepatocytes suspension and uptake of radiolabel by the cells assayed as a function of time. See text for details.

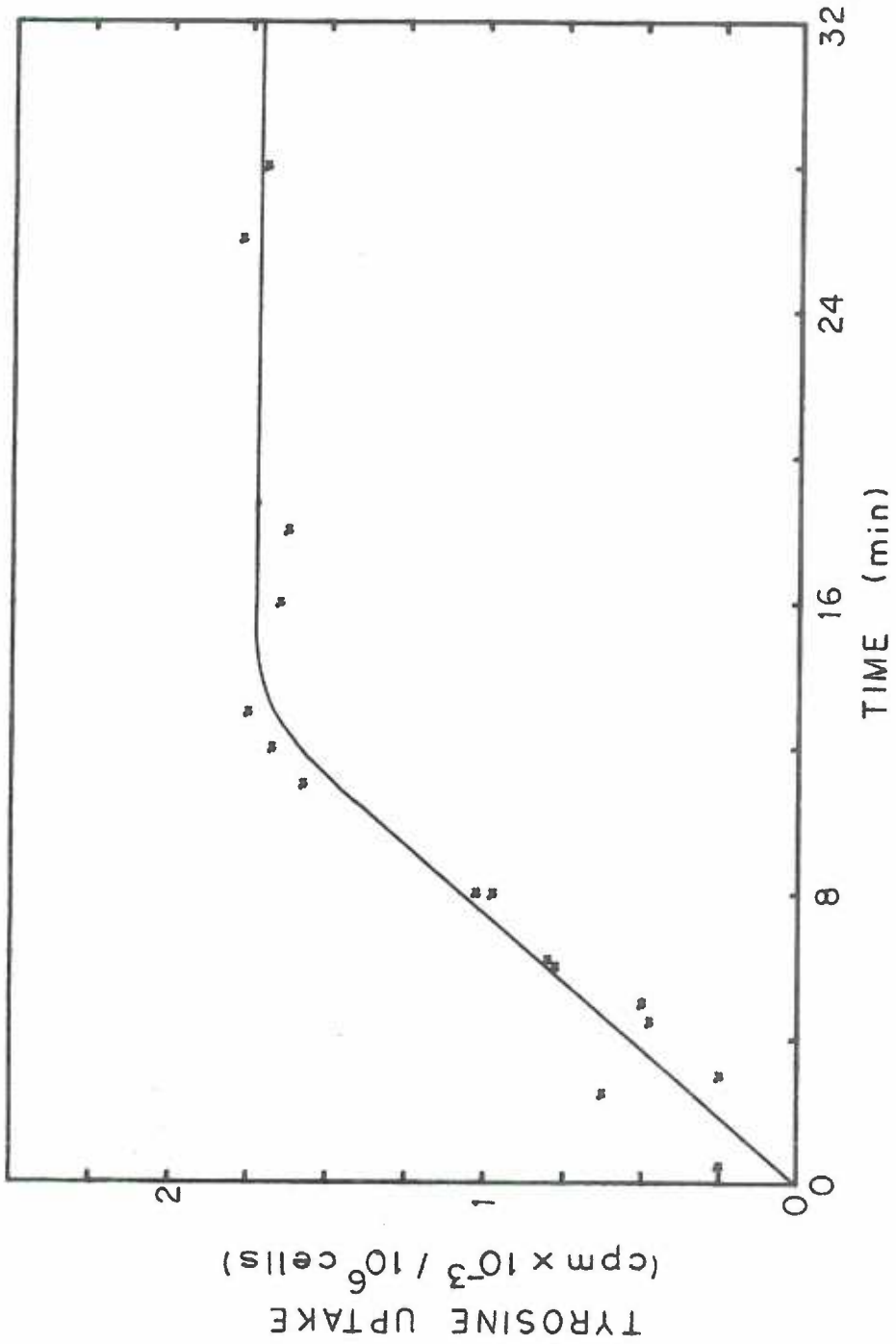
TYROSINE UPTAKE
(cpm x 10⁻³ / 10⁶ cells)
0
1
2
0
8
16
24
32
TIME (min)

To check these results, 1 ml aliquots were taken at 3, 10 and 22 min from incubation as above, centrifuged for 3 min and supernatants decanted. Metabolism was stopped by addition of H_2SO_4. Fractions were centrifuged to remove the protein, and assayed for tyrosine content and radioactivity. The results are given in Table VI-C. These results indicate that by 13 min equilibration of label is nearly complete. It further shows that the tyrosine concentration in the cells is not the same as the concentration in the medium.

Incorporation of ^3H tyrosine into protein was assayed in incubations as above at 10 and 20 min. One milliliter samples were acidified with 0.15 ml 2 N H_2SO_4 and centrifuged. The protein was collected on millipore filters (0.45 μ) and the filters placed in scintillation vials. NCS tissue solubilizer (0.5 ml) was added and the vials sealed and shaken for 20 hr. Ten milliliter toluene-PPO-POPOP was added and samples were counted after 24 hr. There was no significant incorporation of radiolabel into the acid precipitable fraction under these conditions. This indicates that incorporation of tyrosine into protein during this short incubation is insignificant relative to tyrosine uptake and degradation rates (see below).

VI. D. pHPP Concentration as a Function of Oxygen Tension

Isolated hepatocytes (3×10^6 cells/ml) in modified Hank's

Table VI-C. Tyrosine uptake by isolated hepatocytes. Isolated hepatocytes (3×10^6 cells/ml) were incubated at 37°C in modified Hank's medium containing 0.30 mM tyrosine. ^{3}H-Tyrosine was added and distribution of label and tyrosine between cells and suspending medium was measured at indicated times after centrifugation.

Time (min)	Fraction	Volume (ml)	Tyrosine (mM)	Label (dpm/ml)	Specific activity (μCi/μmole)
0	supernatant	0.659	0.30	-	1.00[1]
	pellet	0.402	0.35	-	-
13	supernatant	0.736	0.31	7.45×10^5	1.08
	pellet	0.234	0.36	7.45×10^5	0.93
25	supernatant	0.847	0.28	5.58×10^5	0.98
	pellet	0.133	0.42	10.8×10^5	1.06

[1] Calculated from amount of label added.

medium containing 0.22 mM tyrosine were pipetted into the incubation vessel and equilibrated to 37°C and the desired $P(O_2)$. Ten minutes was allowed for equilibration followed by control of oxygen tension for 10 min with the oxystat. One milliliter 2 N H_2SO_4 was then injected to quench the system. Protein was removed by centrifugation, and pHPP was extracted with 2 volumes ethyl acetate. The ethyl acetate was then re-extracted with 3 ml 200 mM phosphate buffer (pH 8.0). NaOH (0.1 ml 10 N) was then added/ml buffer to convert the pHPP to the corresponding benzaldehyde. The benzaldehyde was measured spectrophotometrically at 331 nm. The results are shown in Figure VI-4 as pHPP concentration in suspension as a function of oxygen tension. Using the partitioning information determined above, the intracellular concentration as a function of oxygen tension can be calculated as on the right hand axis. The half maximal change in pHPP concentration as a function of oxygen tension occurred at approximately 7 torr (9.8 μM). A detectable increase was observable at 50 torr (70 μM).

VI.E. HG Concentration as a Function of Oxygen Tension

Isolated hepatocytes were incubated and extracted as described in Section VI.D. Homogentisate content in the phosphate buffer extract was measured by the colorimetric assay of Fellman et al.

Figure VI-4. p-Hydroxyphenylpyruvate concentration in hepatocyte suspension as a function of oxygen tension. Hepatocytes (3×10^6 cells/ml, 6 ml total volume) were incubated in modified Hank's medium containing 0.22 mM tyrosine at 37°C for 10 min at the desired $P(O_2)$. The system was quenched with 1 ml 2 N H_2SO_4, centrifuged to remove the protein, and 5 ml extracted with 2 volumes of ethylacetate to remove pHPP. The ethyl acetate was then reextracted with 3 ml phosphate buffer (200 mM, pH 8.0). The pHPP was converted to the corresponding benzaldehyde by addition of NaOH, which was measured spectrophotometrically at 331 nm. Data are expressed as pHPP concentration (μM) as a function of partial pressure of oxygen. Solid line represents three point smoothing. Dotted line is limit of detectability. Data from three preparations, n = 15.

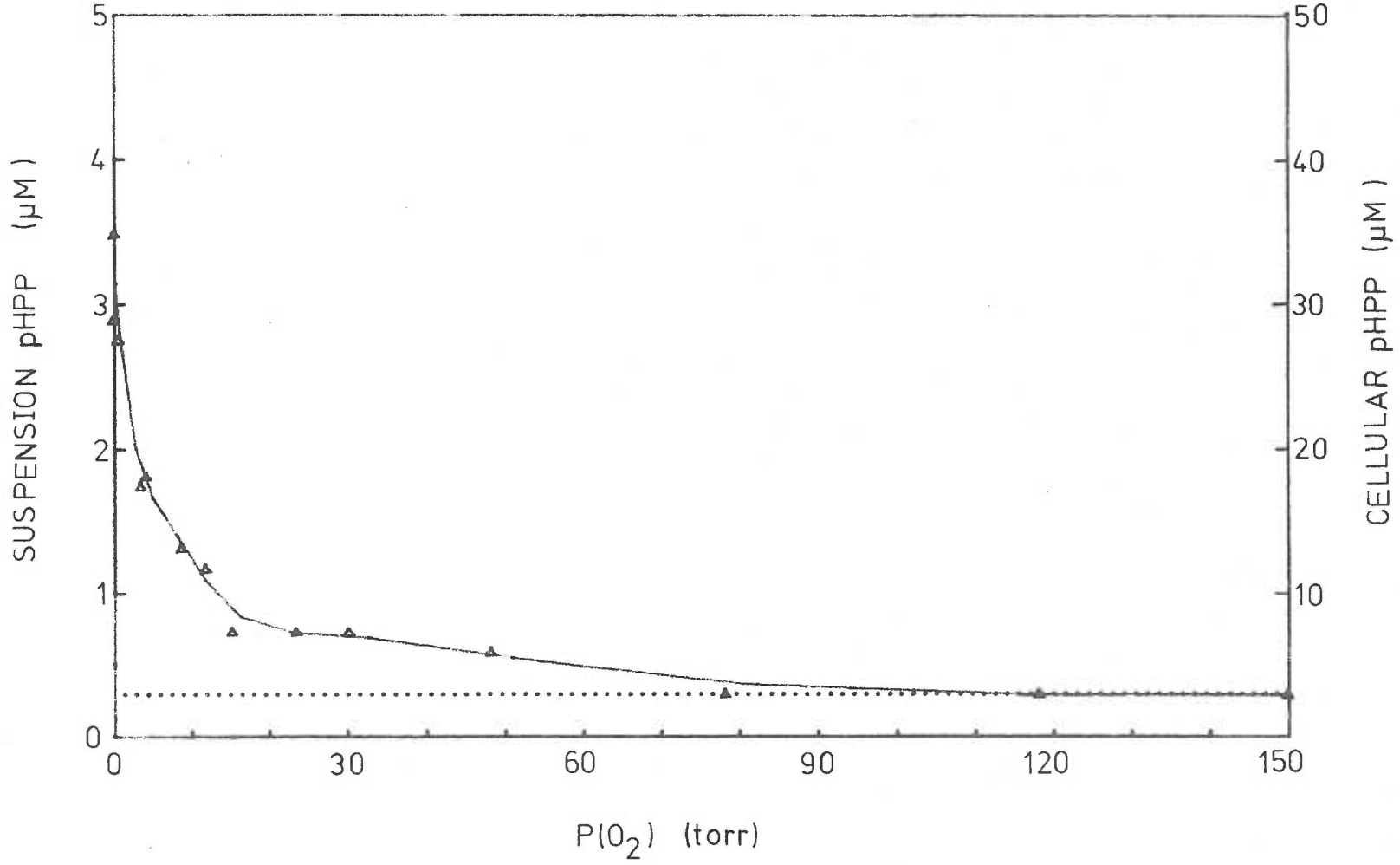
SUSPENSION pHPP (μM)
CELLULAR pHPP (μM)
P(O2) (torr)
0
1
2
3
4
5
10
20
30
40
50
0
30
60
90
120
150

(1972). The HG content in the incubation as a function of oxygen tension is given in Figure VI-5. Using the partitioning data in Section VI.B, the intracellular content can be estimated as shown on the right hand axis. The half maximal change in HG concentration as a function of oxygen tension was 15 torr (21 μM); however, a detectable increase in concentration was observed at 50 torr (70 μM).

VI.F. Rate of Tyrosine Loss as a Function of Oxygen Tension

Isolated hepatocytes were incubated as described in Section VI.D. The acidified incubation mixture was assayed for tyrosine content by the fluorometric method of Waalkes and Udenfriend (1957). Tyrosine loss was calculated relative to a zero time control for the 10 min incubation and is shown in Figure VI-6 as nmole loss/mg protein/hr as a function of oxygen tension. As seen in this graph, tyrosine degradation increased as oxygen tension decreased from 150 torr (210 μM) to 12 torr (16.8 μM), then decreased as oxygen tension approached zero. The maximal measured rate of loss was 72 nmole /mg protein/hr; this value is much less than the maximal values measured for the individual enzymes.

An iterative process with the PDP 11 was used to calculate $Km(O_2)$, K_m(pHPP) and Vmax for the enzyme to provide a best fit of the rate of pHPPO reaction with measured pHPPA and oxygen

Figure VI-5. Homogentisic acid concentration in solution as a function of oxygen tension. Hepatocytes (3×10^6 cells/ml, 6 ml total volume) were incubated in modified Hank's medium containing 0.22 mM tyrosine at $37^{\circ}C$ for 10 min at the desired $P(O_2)$. The system was then quenched with 1 ml 2 N H_2SO_4. The acidified mixture was centrifuged to remove protein and 5 ml removed for extraction of homogentisate with 2 volumes ethyl acetate. Nine milliliters of the ethyl acetate phase was then reextracted with 3 ml phosphate buffer (200 mM, pH 8.0). Homogentisate concentration was estimated by the colorimetric assay of Fellman et al. (1972) relative to homogentisate standards. Data are expressed as homogentisate concentration (μM) as a function of partial pressure of oxygen. Computer drawn line represents three point smoothing. Data from three cell preparations, n = 15.

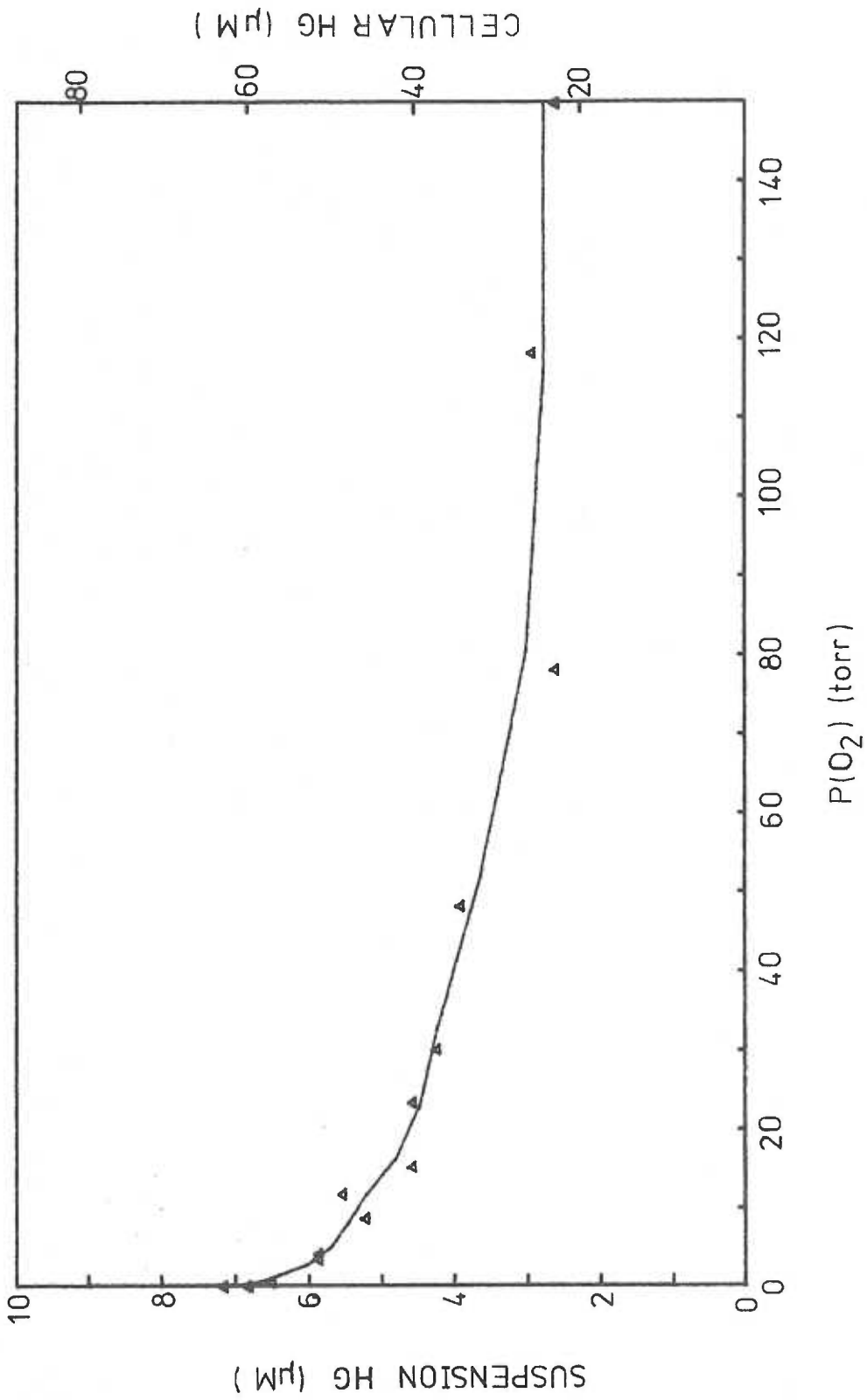
SUSPENSION HG (μM)
CELLULAR HG (μM)
P(O2) (torr)
0
2
4
6
8
10
20
40
60
80
100
120
140

Figure VI-6. Tyrosine degradation by isolated hepatocytes as a function of oxygen tension. Cells were incubated at 3×10^6 cells/ml in modified Hank's solution containing 0.22 mM tyrosine. Oxygen tension was brought to desired level and maintained for 10 min before quenching with H_2SO_4. Data represent tyrosine loss during 10 min relative to zero time tyrosine concentration. Computer drawn line connects points for oxygen tension below 12 torr and represents three point smoothing above 12 torr.

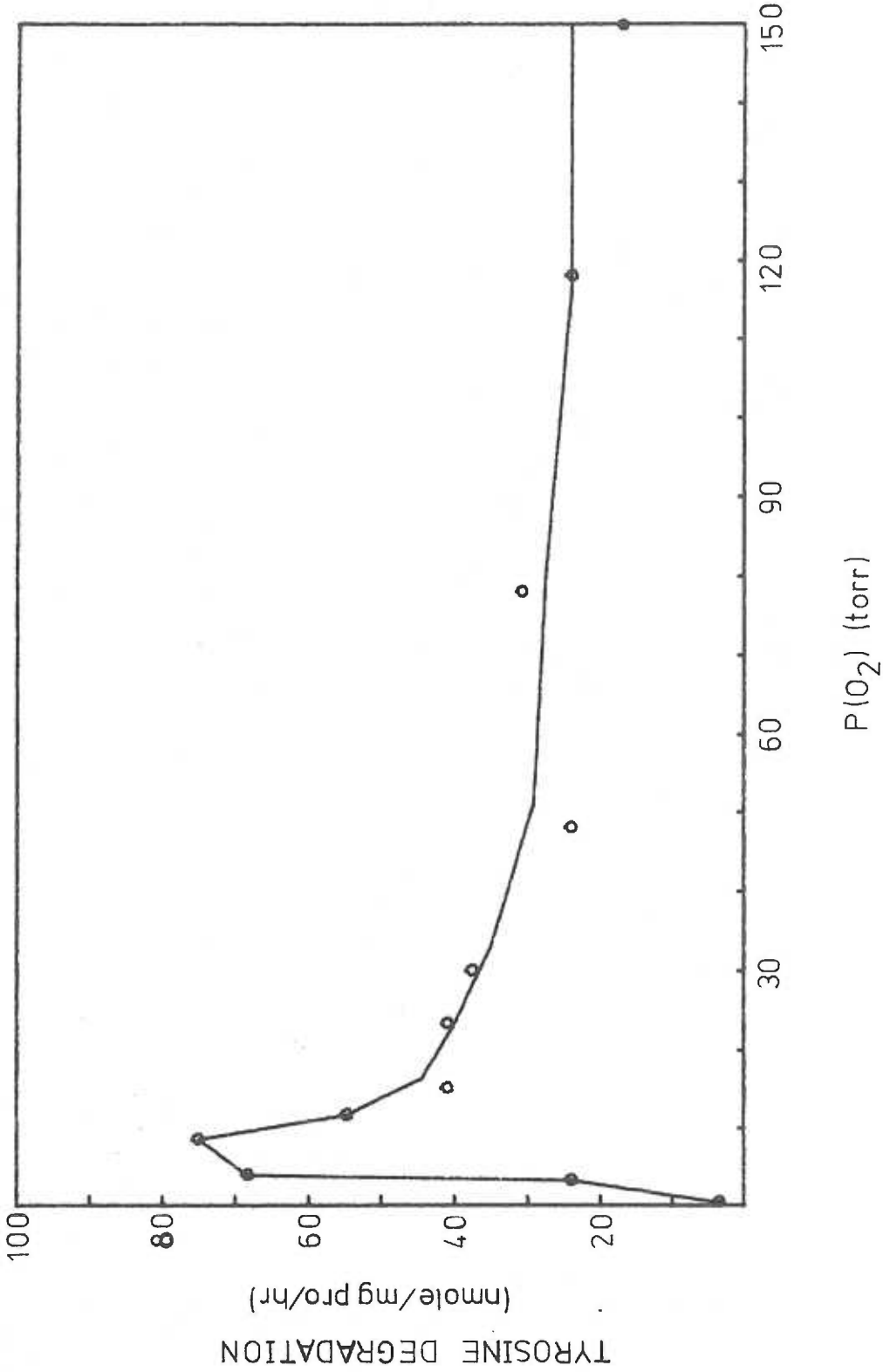
TYROSINE DEGRADATION
(nmole/mg pro/hr)
100
80
60
40
20
30
60
90
120
150
P(O2) (torr)

concentrations to the measured rates of tyrosine degradation. This program is given in Appendix IV and assumes independent additions of the two substrates. The best fit was found to have a $Km(O_2)$ of 38 torr, Km(pHPP) of 198 μM and Vmax of 612 nmole /mg protein/ hr, and is shown in Figure VI-7, curve a. A better visual fit was obtained with the measured Vmax of 232 nmole /mg protein/hr as shown in curve b. This fit was obtained using a Km(pHPP) of 70 μM and a $Km(O_2)$ of 7.6 torr.

VI. G. Discussion

Isolated intact hepatocytes allow study of tyrosine degradation with intracellular control parameters maintained. The cells have normal enzyme contents and are only moderately permeable to tyrosine, pHPP, HG and glutamate. Thus, the pathway from tyrosine to maleylacetoacetic acid is intact and may be used for specific metabolic studies, e.g., hypoxia. Intracellular pools of metabolites can be measured, and overall rate of tyrosine loss estimated.

Tyrosine loss at oxygen tensions 70 torr (98 μM) or greater is about 0.030 μmole /mg protein/hr. Maximal activities of TAT, pHPPO, and HGO are all greater than 0.20 μmole /mg protein/hr. This low rate of degradation compared to maximal activities suggests that this pathway is functioning submaximally under normal conditions. This may occur as a consequence of low tyrosine concentration

Figure VI-7. Computer estimated tyrosine degradation rate. Circles represent actual measured degradation rate as in Figure VI-6. Curve a is predicted rate using measured pHPP concentrations, and values for $Km(O_2)$, Km(pHPP) and Vmax obtained by an iterative process to provide a best fit between predicted rates and actual rates. Curve b is drawn using measured Vmax value and a visual best fit by varying Km(pHPP) and $Km(O_2)$ from their reported literature values. See text for details.

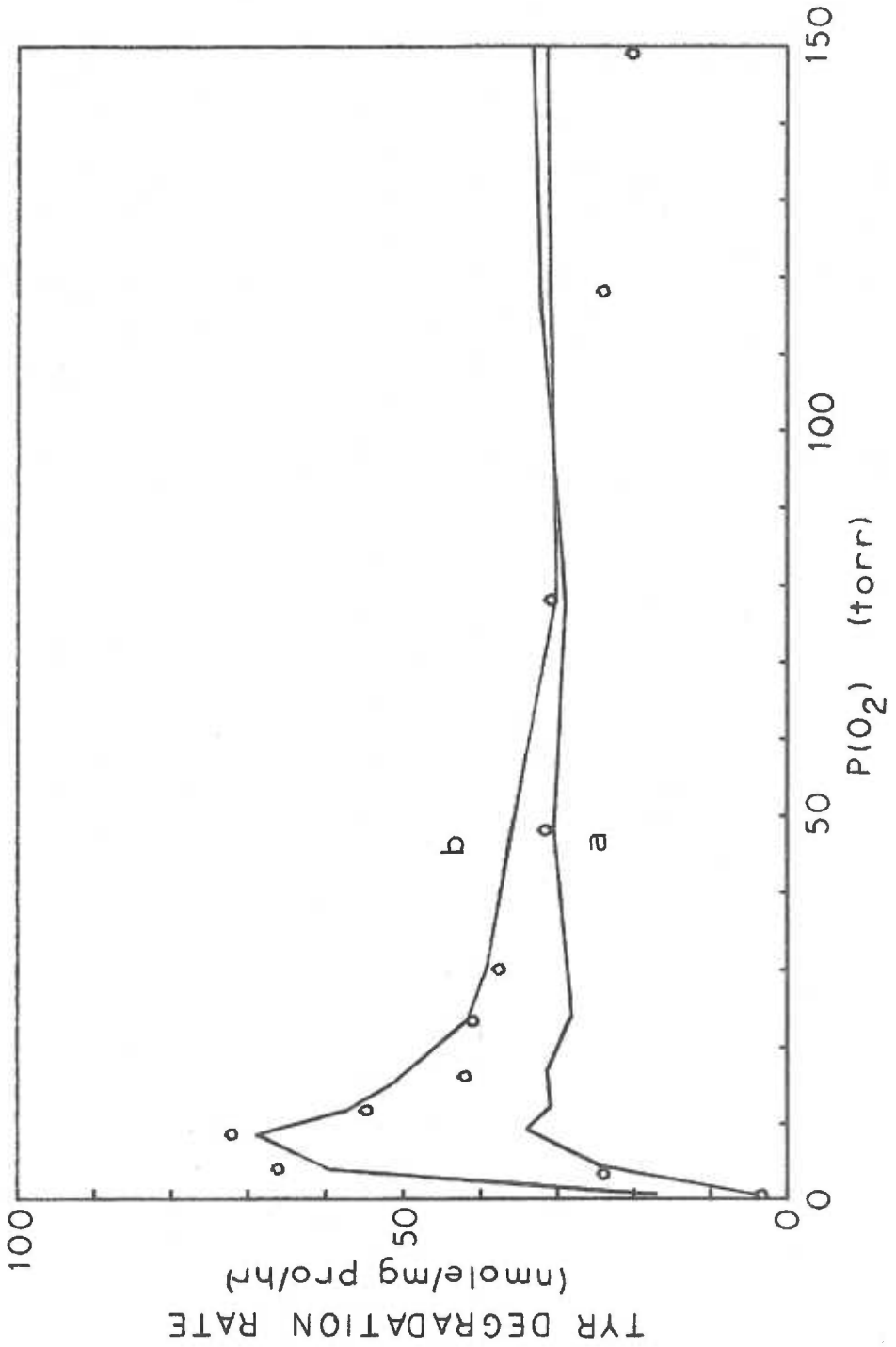
TYR DEGRADATION RATE
(nmole/mg pro/hr)
100
50
0
0
50
100
150
P(O2) (torr)
b
a

(0.44 mM), compared to the Km for tyrosine (1.5 mM; Jakoby and La Du, 1964). Alternatively, if the TAT reaction is at equilibrium, the low rate could be a consequence of low pHPP concentration (< 10 μM) relative to the Km of pHPPO for pHPP (50 μM, Fellman et al., 1972).

This research demonstrates the dependence of tyrosine degradation on oxygen tension in the normal hepatic oxygen tension range (1-40 torr; 1.4-56 μM). Metabolite concentrations and overall rate of tyrosine loss are both affected. The precise method of control is not clear and may involve one or more of the factors presented in Figure VI-2. Computer simulation (Figure VI-7) suggests that O_2 dependent function of pHPPO may be important. The increased concentration of pHPP and HG at oxygen tensions at which lactate or pyruvate remained unchanged (Section IV) indicates that redox independent metabolic control exists.

The greater sensitivity to oxygen limitation of tyrosine degradation compared to mitochondrial function supports the hypothesis that primary metabolic oxygen deficiencies may be important in the pathology of hypoxia (section I.B.). Although no direct studies on this possibility are available for the tyrosine pathway, interference of metabolic processes may occur, e.g., p-hydroxyphenylpyruvate (2 mM) is a potent inhibitor of sterol synthesis in rat liver (Ranganathan and Ramasarma, 1973), and phenylpyruvate (a close

structural analog of pHPP) is a potent inhibitor of gluconeogenesis (Arinze and Patel, 1973). This provides a plausible mechanism for metabolic changes during hypoxia and indicates a need for further studies on metabolic oxidases during hypoxia.

VII. SUMMARY AND CONCLUSIONS

The introduction of this dissertation provides an operational definition, a brief history, and a review of the biochemistry of hypoxia. The central role of oxygen utilizing enzymes in metabolism is discussed. A new theory of hypoxic pathology is proposed that includes metabolic in addition to bioenergetic changes. The major points of the theory are:

1) The primary biochemical events in hypoxia are enzymic oxygen deficiencies.

2) All physiological and pathological changes must be related to these primary changes. They can be related by three biochemical parameters (Figure I-1), concentration changes of substrate or products of oxidases, ATP (or other high energy intermediate) deficiency, or more negative redox potential.

3) Oxidases are selectively affected depending upon their oxygen affinity, conveniently expressed in terms of apparent $Km(O_2)$.

4) Not all metabolic changes due to hypoxia are deleterious (e.g., decreased pH is protective against anoxic damage; Bing et al., 1973; Pentilla and Trump, 1974).

A model system for the study of hypoxia on a cellular level is developed in this research to examine the feasilibity of this theory. Isolated intact rat hepatocytes were used so that all cells are

exposed to the same oxygen tension during incubation. The cells were extensively characterized (summarized in Table VII-A) and maintain properties similar to normal intact tissue.

An oxystat was designed which provides a desired oxygen tension (1-150 torr; 1.4-210 μM) in a suspension of respiring hepatocytes. Characteristics of the system are summarized in Table VII-B.

Metabolite levels and enzyme catalyzed reaction rates were used as indicators of metabolic function at fixed oxygen tensions. $P(O_2)$ at half maximal metabolic change and at first detectable metabolic change (critical $P(O_2)$) are summarized in Table VII-C. Cellular respiration, adenylate energy charge and cytoplasmic redox potential had roughly the same dependence upon oxygen. Drug metabolism and tyrosine degradation were more sensitive to oxygen limitation than these bioenergetic changes. This supports the hypothesis that metabolic changes other than those related to cytochrome oxidase function may be important in hypoxia.

The major conclusions of this research are:

1) The study of metabolism of isolated hepatocytes as a function of oxygen tension with the aid of newly developed oxystat provides a useful model for examining the biochemistry of hypoxia.

2) Decreased respiration and altered adenylate concentrations and redox state are apparent at only moderately hypoxic oxygen tensions in spite of the extremely low values of respiratory $Km(O_2)$

Table VII-A. Summary of characteristics of isolated hepatocytes. Cells were prepared by the method of Berry and Friend (1969). All cell incubations performed in modified Hank's medium.

Cell yield	$2.03 \pm 1.93 \times 10^8$ cells
% Excluding 0.2% trypan blue	90.6 ± 2.9 %
Protein content	1.59 ± 0.13 mg/10^6 cells
$Q_{O_2}^{cell}$ (37°C, polarographic assay)	20.1 ± 3.4 µl O_2/10^6 cells/hr (0.90 ± 0.15 µmoles/10^6 cells/hr)
$Q_{O_2}^{pro}$ (37°C, polarographic assay)	13.8 ± 1.2 µl O_2/mg pro/hr (0.62 ± 0.05 µmoles/mg pro/hr)
Stimulation of respiration by 0.5 mM ADP	None
Stimulation of respiration by 10 mM pyruvate	None
ATP content (assuming 7.25 mg wet wt/10^6 cells)	2.28 ± 0.46 mmoles/kg wet wt
ADP content	0.36 mmoles/kg wet wt
AMP content	0.12 mmoles/kg wet wt
Adenylate energy charge (as isolated, $P(O_2) \approx 150$ torr)	0.91
Lactic dehydrogenase activity retained after 1 hr	92.6 ± 3.1 %
Contamination by other cell types as judged by electron microscopy	< 1%
Percent of cells retaining regions of cell contact	7.9%
Glucose synthesis from pyruvate (cells from starved rats)	1.74 nmoles/10^6 cells/min
Pyruvate content (as isolated)	0.213 ± 0.028 mM
Lactate content (as isolated)	2.31 ± 0.36 mM

(Continued on next page)

Table VII-A. (Continued)

Cytoplasmic NAD^+/NADH (calculated from lactate/ pyruvate according to Williamson et al., 1967)	763 ± 44
Cytochrome $\underline{a}_3$ content (spectrophotometric)	0.058 ± 0.001 nmole /mg pro
Cytochrome P-450 content (spectrophotometric)	0.22 ± 0.01 nmole /mg pro
Phenyramidol metabolism (0.1 mM)	
Non-induced	46.0 ± 4.0 nmole /mg pro/hr
Phenobarbital induced	91 nmoles/mg pro/hr
Alprenolol metabolism (44 μM), Non-induced	14.2 ± 1.0 nmole /mg pro/hr
Hexobarbital metabolism (0.5 mM)	
Non-induced	84.4 ± 4.3 nmole/mg pro/hr
0.1 mM, non-induced	51.6 ± 2.0 nmole/mg pro/hr
0.5 mM, phenobarbital induced	147 ± 7 nmole/mg pro/hr
0.5 mM, 3-MC induced	101 ± 5.6 nmole/mg pro/hr
Tyrosine aminotransferase activity	0.501 ± 0.130 μmole product/mg pro/hr
pHPPO activity	0.232 ± 0.021 μmole product/mg pro/hr
HGO activity	1.96 ± 0.30 μmole product/mg pro/hr
Tyrosine content (0.22 mM tyrosine in incubation mixture)	0.41 ± 0.08 mM
Initial rate of tyrosine uptake	12.8 nmole/mg pro/hr
Rate of tyrosine degradation ($P(O_2) > 50$ torr)	30 nmole/mg pro/hr
pHPP content ($P(O_2) > 50$ torr)	2 μM
HG content ($P(O_2) > 50$ torr)	27 μM

Table VII-B. Summary of oxystat characteristics.

Aqueous volume	3-20 ml
Mixing time	2 sec
Oxygen transfer constant (K) 8 ml volume	6.71 ± 0.07 hr^{-1}
$t_{1/2}$ for gas-liquid O_2 equilibration	2.9 min
Rate of water evaporation (gas flow - 65 ml min^{-1})	1.28 % hr^{-1}
Loss of hepatocyte viability (modified Hank's medium + 15 mg BSA/ml)	2.9 % /30 min
Washout time for gas (80 ml min^{-1})	30 sec
Aqueous P(O_2) range	1-150 torr (1.4-210 μM)
Respiratory rate range	10-80 μl O_2/ml/hr (0.12-1.00 μM/sec)
Time required to reach steady state	2-3 min
Fluctuation at steady state (4-150 torr)	< ± 7%
(3 torr)	± 11%
(2 torr)	± 15%
(1 torr)	± 20%

Table VII-C. Summary of critical $P(O_2)$ and half maximal $P(O_2)$ values. Values with asterisk represent least squares intercept of double reciprocal plot of data ± standard error of estimate. Other data ± 1 S.D. All experiments at 37°C in modified Hank's medium.

Parameter	Condition	Half maximal $P(O_2)$ (torr)	Critical $P(O_2)$ (torr)
Respiration rate		1.45 ± 0.21 1.36 ± 0.13*	14
ATP		3	20
ADP		-	-
AMP		3	20
ATP/ADP		5	20
ATP + 1/2ADP/ATP + ADP + AMP)		1.3	20
Lactate		9	20
Pyruvate		8	16
Lactate/pyruvate		9	20
$NADH/NAD^+$		9	20
Hexobarbital metabolism			
	0.5 mM hex, non-induced	4.5 ± 1.2*	14
	0.1 mM hex, non-induced	1.7	5
Alprenolol metabolism			
	44 mM alp, non-induced	7.0 ± 1.1*	24
Phenyramidol metabolism			
	0.1 mM phen, non-induced	2.6 ± 0.4*	11
Hexobarbital metabolism			
	0.5 mM hex, phenobarbital induced	0.5	10
	0.5 mM hex, 3-MC induced	2.6	12
pHPP			
	0.22 mM tyrosine	7	50
HG			
	0.22 mM tyrosine	15	50

reported for isolated mitochondria. This is interpreted to suggest that mitochondrial function in intact cells is under strong metabolic regulation which is not present in isolated mitochondria.

3) The oxygen dependence of drug hydroxylation in hepatocytes is similar to that observed in microsomes suggesting a minimal oxygen tension gradient from extracellular space to endoplasmic reticulum and lack of non-endoplasmic reticulum metabolic controls. A direct oxygen dependence is also apparent under moderately hypoxic conditions indicating that drug metabolism may be altered in clinical cases of hypoxia.

4) Isolated cells may be used to study tyrosine degradation if suitable controls regarding substrate uptake and metabolite partitioning are observed. Tyrosine degradation is operating submaximally in hepatocytes relative to maximal activities of individual enzymes in this pathway. The rate of degradation and metabolite levels as a function of oxygen tension suggest substrate level control. Additional modes of control are discussed; oxygen concentration may affect this pathway directly as a substrate at submaximal concentration or indirectly through metabolite changes related to redox changes.

5) Metabolic dependence upon oxygen occurs over a wide range of oxygen tension (e.g., 0-50 torr for pHPP), including that considered "normoxia" (1-40 torr). Therefore, alterations in metabolism due to oxygen tensions may have a regulatory function.

6) Different oxidase systems in intact cells (e.g., cytochrome P-450 and tyrosine degradative pathway) have different dependencies upon oxygen. This confirms data on isolated enzymes and suggests that each metabolic system must be considered separately with regard to function during hypoxia. Many metabolic oxidases are more sensitive to oxygen deprivation than cytochrome oxidase and therefore should be considered separately in hypoxic pathology.

REFERENCES

Abbott, M. T. & Udenfriend, S. α-Ketoglutarate-coupled dioxygenases. In O. Hayaishi (ed.), Molecular mechanisms of oxygen activation. New York: Academic Press, 1974. pp. 167-214.

Ackerman, E. & Brill, A.S. Magnetic and spectrophotometric studies of the kinetics of the catalysis of xanthine oxidation by xanthine oxidase from cow's milk. Biochim. Biophys. Acta, 1962, 56, 397-412.

Adachi, K., Iwayama, Y., Tanioka, H., & Takeda, Y. Purification and properties of homogentisate oxygenase from Pseudomonas fluorescens. Biochim. Biophys. Acta, 1966, 118, 88-97.

Altman, P. L. Handbook of circulation, edited by D. S. Dittmer and R.M. Grebe. Wright-Patterson Air Force Base, Ohio: Wright Air Development Center, 1959. pp. 115-134.

Altman, P. L., & Dittmer, D.S. Blood and other body fluids. Washington, D.C.: Federation of Societies for Experimental Biology, 1961. pp. 191-199.

Altman, P. L., & Dittmer, D.S. (Eds.). Respiration and circulation. Biological handbooks series. Bethesda, Maryland: Federation of American Societies for Experimental Biology, 1971. pp. 424-437.

Anderson, N. G. The mass isolation of whole cells from rat liver. Science, 1953, 117, 627-628.

Ando, N., & Horie, S. Studies on P-450. VIII. Effects of steroids on the reaction with oxygen and the rate of reduction of partially purified P-450 from adrenocortical mitochondria. J. Bio hem. (Tokyo), 1971, 70, 557-570.

Araki, T. Ueber die Bildung von Milchsaure und Glycose im Organismus bei sauerstoffmangel. Hoppe-Seylers z. physiol. Chem., 1890, 15, 335.

Aschenbrenner, V., Zak, R., Cutilletta, A.F., & Rabinowitz, M. Effect of hypoxia on degradation of mitochondrial components in rat cardiac muscle. Am. J. Physiol., 1971, 221, 1418-1425.

Aschoff, J., & Pohl, H. Rhythmic variation in energy metabolism. Fed. Proc., 1970, 29, 1541-1552.

Atkinson, D.E. Enzymes as control elements in metabolic regulation. In P.D. Boyer (ed.), The enzymes (3rd ed), Vol. 1. New York: Academic Press, 1970. pp. 461-489.

Atkinson, M.R., & Morton, R.K. Free energy and the biosynthesis of phosphates. In M. Florkin and H.S. Mason (eds.), Comparative biochemistry, Vol. II. New York: Academic Press, 1960. pp. 1-95.

Bagchi, S.P., & Zarycki, E.P. In vivo hydroxylation of phenylalanine to tyrosine in brain. Fed. Proc., 1970, 29, 680. (Abstract).

Bain, W.H., & Harper, A.M. (Eds.). Blood flow through organs and tissues. Baltimore: The Williams and Wilkins Company, 1967. 515 p.

Ballard, F.J. Kinetic studies with cytosol and mitochondrial phosphoenolpyruvate carboxy kinases. Biochem. J., 1970, 120, 809-814.

Ballard, F.J. Regulation of gluconeogenesis during exposure of young rats to hypoxic conditions. Biochem. J., 1971, 121, 169-178.

Ballard, F.J. The development of gluconeogenesis in rat liver. Controlling factors in the newborn. Biochem. J., 1971, 124, 265-274.

Barcroft, J. Anoxemia. Lancet, 1920, 2, 485-489.

Barman, T.E. Enzyme handbook (2 volumes). New York: Springer, 1969. 928 p.

Baur, H., & E. Pfaff. Permeability of cholephilic substances with isolated liver cells. Naunyn-Schmiedeberg's Archives of Pharmacology, 1972, 274: R 16. (Abstract).

Baumel, I., DeFeo, J.J., & Lal, H. Effect of acute hypoxia on brain sensitivity and metabolism of barbiturates in mice. Psychopharmacologia, 1970, 17, 193-197.

Baumel, I., Schatz, R., DeFeo, J.J., & Lal, H. Protection against m-fluorotyrosine convulsions and lethality in mice exposed to hypobaric hypoxia. J. Pharm. Pharmacol., 1969, 21, 475-476.

Bendixen, H.H., & Laver, M.B. Hypoxia in anesthesia: a review. Clinical Pharmacology and Therapeutics, 1964, 6, 510-539.

Bergstrom, S. Prostaglandins: members of a new hormonal system. Science, 1967, 157, 382-391.

Bergstrom, S., Carlson, L.A., & Weeks, J.R. The prostaglandins: a family of biologically active lipids. Pharmacol. Rev., 1968, 20, 1-48.

Bernhardt, F.H., Erdin, N., Staudinger, H., & Ullrich, V. Interactions of substrates with a purified 4-methoxybenzoate monooxygenase system (o-dimethylating) from Pseudomonas putida. Eur. J. Biochem., 1973, 35, 126-134.

Berry, M.N. Energy dependent reduction of pyruvate to lactate by intact isolated parenchymal cells from rat liver. Biochem. Biophys. Res. Commun., 1971, 44, 1449-1456.

Berry, M.N. Energy metabolism of endogenous metabolism and gluconeogenesis in liver cells from normal and hyperthyroid rats. In Lundquist, F. and Tygstrup, N. (eds.), Regulation of hepatic metabolism. New York: Academic Press, 1974. pp. 568-578.

Berry, M.N., & Friend, D.S. High yield preparation of isolated rat liver parenchymal cells. J. Cell Biol., 1969, 43, 506-520.

Berry, M.N., & Kun, E. Rate-limiting steps of gluconeogenesis in liver cells as determined with the aid of fluoro-dicarboxylic acids. Eur. J. Biochem., 1972, 27, 395-400.

Berry, M.N., & Werner, H.V. Additional comments on the preparation of isolated liver cells. In Lundquist, F. and Tygstrup, N. (eds.), Regulation of hepatic metabolism. New York: Academic Press, 1974. pp. 751-753.

Bert, P. La Pression barometrique recherches de physiologie, Paris: Masson, 1878. Translated into English by M.A. Hitchcock and F.A. Hitchcock. Columbus, Ohio: College Book Co., 1943.

Bicher, H.I. Autoregulation of oxygen supply to brain tissue. In Bruley, D.F. and Bicher, H.I. (Eds.), Oxygen transport to tissue, Part A. New York: Plenum Press, 1973. pp. 215-222.

Bicher, H.I., & Bruley, D.F. (eds.). Oxygen transport to tissue, Part B. New York: Plenum Press, 1973. pp. 637-1161.

Bing, O.H.L., Brooks, W.W., & Messer, J.V. Heart muscle viability following hypoxia: Protective effect of acidosis. Science, 1973, 180, 1297-1298.

Biorck, G. Hematic compounds in mammalian heart and skeletal muscle. Am. Heart J., 1956, 52, 624-639.

Birnie, J.H., & Grayson, J. Observations on temperature distribution and liver blood flow in the rat. J. Physiol., 1952, 116, 189-201.

Bjorkheim, I., & Gustafsson, J. Mitochondrial ω-hydroxylation of cholesterol side chain. J. Biol. Chem., 1974, 249, 2528-2535.

Bloch, E.H. The terminus of hepatic arterioles and the functional unit of the liver as determined by microscopy of the living organ. Ann. N.Y. Acad. Sci., 1970, 170, 78-86.

Boag, J.W. Oxygen diffusion and oxygen depletion problems in radiobiology. Current Topics in Radiation Research, 1969, 5, 141-196.

Bock, R.M., Ling, N.-S., Morell, S.A., & Lipton, S.H. Ultraviolet absorption spectra of adenosine-5'-triphosphate and related 5'-ribonucleotides. Arch. Biochem. Biophys., 1956, 62, 253-264.

Bongiovanni, A.M., Eberlein, W.R., Goldman, A.S., & New, M. Disorders of adrenal steroid biogenesis. Recent Prog. Hormone Res., 1967, 23, 375-449.

Boxer, G.E., & Devlin, T. Pathways of intracellular hydrogen transport. Science, 1961, 134, 1495-1501.

Boyle, R. New pneumatical experiments about respiration. Phil. Trans. Roy. Soc. (London), 1970, 5, 2011-2032.

Brachfeld, N., Ohtaka, Y., Klein, I., & Kawade, M. Substrate preference and metabolic activity of the aerobic and the hypoxic turtle heart. Circulation Res., 1972, 31, 453-467.

Bradley, S.E., Ingelfinger, F.J., Bradley, G.P., & Curry, J.J. The estimation of hepatic blood flow in man. J. Clin. Invest., 1945, 24, 890-897.

Branster, M.V., & Morton, R.K. Isolation of intact liver cells. Nature, 1957, 180, 1283-1284.

Brauer, R.W., Leong, G.F., Holloway, R.J., & Krebs, J.S. Parameters controlling oxygen uptake of the intact rat liver--respiration rate and the definition of hepatic hypoxia. In J.P. Schade and W.H. McMenemey, Selective vulnerability of the brain in hypoxemia. Philadelphia: F.A. Davis Co., 1963. pp. 273-294.

Brighton, C.T., & Krebs, A.G. Oxygen tension of nonunion of fractured femurs in the rabbit. Surg. Gynecol. Obstet., 1972, 135, 379-385.

Brown, H., & Hardwick, D.F. (eds.). Intermediary metabolism of the liver. Springfield, Ill.: Charles C. Thomas, Publisher, 1973. 187 p.

Brown, R.M., Kehr, W., & Carlsson, A. Functional and biochemical aspects of catecholamine metabolism in brain under hypoxia. Brain Research, 1975, 85, 491-509.

Bublitz, C. A direct assay for liver phenylalanine hydroxylase. Biochim. Biophys. Acta, 1969, 191, 249-256.

Bruley, D.F. Mathematical considerations for oxygen transport to tissue. In Bicher, H.I. and Bruley, D.F. (Eds.), Oxygen transport to tissue, Part B. New York: Plenum Press, 1973. pp. 749-759.

Bruley, D.F., & Bicher, H.E. (eds.). Oxygen transport to tissue, Part A. New York: Plenum Press, 1973. pp. 1-633.

Burns, B., & Gurtner, G.H. A specific carrier for oxygen and carbon monoxide in the lung and placenta. Drug Met. and Disposition, 1973, 1, 374-379.

Burns, J.J. Interactions of environmental agents and drugs. Environmental Research, 1969, 2, 352-359.

Bywaters, E.G.L., & Glynn, L.E. Connective tissue disorders. In R.H.S. Thompson and I.D.P. Wootton (Eds.), Biochemical disorders in human disease, 3rd edition. New York: Academic Press, 1970. pp. 723-750.

Calder, R.M. Effect of nicotinic acid on anoxia in rats. Proc. Soc. Exp. Biol. Med., 1948, 68, 642-646.

Case, R.B., Nasser, M.G., & Crampton, R.S. Biochemical aspects of early myocardial ischemia. Am. J. Cardiol., 1969, 24, 766-775.

Catchpole, H.R., & Gersh, I. Pathogenic factors and pathological consequences of decompression sickness. Physiol. Rev., 1947, 27, 360-397.

Cater, D.B., & Silver, I.A. Quantitative measurements of oxygen tension in normal tissues and in the tumors of patients before and after radiotherapy. Acta Radiol., 1960, 53, 233-256.

Cater, D.B., & Silver, I.A. Microelectrodes and electrodes used in biology. In D.J. Ives and G.J. Janz, Reference electrodes. New York: Academic Press, 1961. pp. 464-523.

Chance, B. Cellular oxygen requirements. Fed. Proc., 1957, 16, 671-680.

Chance, B. Reaction of oxygen with the respiratory chain in cells and tissues. J. Gen. Physiol., 1965, 49, 163-188.

Chance, B., & Hagihara, B. Direct spectroscopic measurements of interaction of components of the respiratory chain with ATP, ADP, phosphate and uncoupling agents. In A.N.M. Sissakian (Ed.), Proc. Vth Intl. Cong. Biochem, Vol. 5. New York: Pergamon Press, 1963. pp. 3-33.

Chance, B., Cohen, P., Jobsis, F., & Schoener, B. Intracellular oxidation-reduction states in vivo. Science, 1962, 137, 499-508.

Chance, B., Schoener, B., & Schindler, F. The intracellular oxidation reduction state. In F. Dickens and E. Neil (Eds.), Oxygen in the animal organism. New York: The Macmillan Co., 1964. pp. 367-388.

Choi, M.J. Kinetics of the utilization of molecular oxygen by the microsomal drug-metabolizing system of the liver. Master of Science thesis, Univ. of Minnesota, 1971.

Chvapil, M., Hurych, J., & Ehrlichova, E. The influence of various oxygen tensions upon proline hydroxylation and the metabolism of collagenous and non-collagenous proteins in skin slices. Z. Physiol. Chem., 1968, 349, 211-217.

Clark, L.C., Jr. Monitor and control of blood and tissue oxygen tensions. Trans. Am. Soc. Artificial Organs, 1956, 2, 41-45.

Civin, M., Wilson, C., & Brown, C.B. Tyrosine transaminase: Inactivation by tyrosine metabolic end products. Biochim et Biophys. Acta, 1970, 206, 78-86.

Clark, J.K., & Barker, H.G. Studies of renal oxygen consumption in man. I. The effect of tubular loading (PAH), water diuresis and osmotic (mannitol) diuresis. J. Clin. Invest., 1951, 30, 745-750.

Cohen, M.M. Biochemistry of cerebral anoxia, hypoxia and ischemia. Monogr. in Neural Sciences, 1973, 1, 1-49.

Cohen, P.J. The effects of decreased oxygen tension on cerebral cirulation, metabolism, and function. In J.D. Hatcher and D.B. Jennings (Eds.), Proc. Int. Symp. Cardiovasc. Respir. Effects Hypoxia. New York: Karger, Basel, 1966, 81-102.

Cohen, P.J. The metabolic function of oxygen and biochemical lesions of hypoxia. Anesthesiology, 1972, 37, 148-177.

Collins, J.M., McDevitt, D.G., Shanks, R.G., & Swanton, J.G. The cardio-toxicity of isoprenaline during hypoxia. Brit. J. Pharmacol., 1969, 36, 35-45.

Conney, A.H. Pharmacological implications of microsomal enzyme induction. Pharmacol. Rev., 1967, 19, 317-366.

Conney, A.H., & Burns, J.J. Metabolic interactions among environmental chemicals and drugs. Science, 1972, 178, 576-586.

Conney, A.H., Levine, W., Jacobson, M., and Kuntzman, R. Effects of drugs and environmental chemicals on steroid metabolism. Clin. Pharmacol. Ther., 1973, 14, 727-741.

Copenhaver, W.M., Bunge, R.P., & Bunge, M.B. Bailey's textbook of histology. 16th edition. Baltimore: The Williams and Wilkins Co., 1971. 485 p.

Crandall, D.I., Krueger, R.C., Anan, F., Yasunobu, K., & Mason, H.S. Oxygen transfer by the homogentisate oxidase of rat liver. J. Biol. Chem., 1960, 235, 3011-3015.

Crosley, A.P., Jr., Brown, J.F., Huston, J.H., Emanuel, D.A., Tuchman, H., Castillo, C., & Rowe, G.G. The adaptation of the nitrous oxide method to the determination of renal blood flow and in vivo renal weight in man. J. Clin. Invest., 1956, 35, 1340-1344.

Cutroneo, K.R., Guzman, N.A., & Sharawy, M.M. Evidence for a subcellular vesicular site of collagen prolyl hydroxylation. J. Biol. Chem., 1974, 249, 5989-5994.

Danielsson, H. Mechanisms of bile acid biosynthesis. In P.D. Nair and D. Kritchevsky (Eds.), The bile acids, Vol. 2. New York: The Plenum Press.

Danielsson, H., & Sjovall, J. Bile acid metabolism. Ann. Rev. Biochem., 1975, 44, 233-253.

Davies, P.W., & Brink, F., Jr. Microelectrodes for measuring local oxygen tension in animal tissues. Rev. Sci. Instrum., 1942, 13, 524-533.

Davis, J.N., Carlsson, A., MacMillan, V., & Siesjo, B.K. Brain tryptophan hydroxylation: Dependence on arterial oxygen tension. Science, 1973, 182, 72-74.

Davison, A.N. Lipid metabolism of nervous tissue. In A.N. Davison and J. Dobbing, Applied neurochemistry. Philadelphia: F.A. Davis Co., 1968. pp. 178-221.

Davy, H. Elements of agricultural chemistry, 4th edition. London: Longman, Reed, Orme, Brown and Green, 1827.

Deetjen, P. Normal and critical oxygen supply of the kidney. In D.W. Lubbers, U.C. Luft, G. Thews, & E. Witzleb (Eds.), Oxygen transport in blood and tissue. Stuttgart: Georg Thieme Verlag, 1968. pp. 212-226.

Degn, H., & Wohlrab, H. Measurement of steady state values of respiration rate and oxidation levels of respiratory pigments at low oxygen tensions. A new technique. Biochim. Biophys. Acta, 1971, 245, 347-355.

De Luca, H.F., & Cohen, P.P. Methods for preparation and study of tissues and enzymes. In W.W. Umbreit, R.H. Burris, & J.F. Stauffer (Eds.), Manometric methods, 4th edition. Minneapolis: Burgess Publishing Co., 1964. pp. 114-123.

Diamondstone, J.I. Assay of tyrosine transaminase by conversion of p-hydroxyphenyl-pyruvate to p-hydroxybenzaldehyde. Analytical Biochem., 1966, 16, 395-401.

Di Carlo, F.J., Haynes, L.J., Coutinho, C.B., & Phillips, G.E. Pentobarbital sleeping time and RES stimulation. J. Reticuloendothel. Soc., 1965, 2, 367-378.

Dickens, F. Anaerobic glycolysis, respiration and the Pasteur effect. In J.B. Sumner and K. Myrback (Eds.), The enzymes, Vol. II, Part I. New York: Academic Press, 1951. pp. 624-683.

Dickens, F., & Neil, E. (eds.). Oxygen in the animal organism. New York: The Macmillan Co., 1964. 694 p.

Diczfalusy, E., & Diczfalusy, A. (eds.). Karolinska symposia on research methods in reproductive endocrinology. 4th Symposium: Perfusion techniques. Stockholm: Karolinska Institutet, 1971. 375 p.

Dittmer, D.S., & Grebe, R.M. (eds.). Handbook of respiration. Philadelphia: W.B. Saunders Co., 1958. pp. 272-273.

Dixon, M. Manometric methods. Cambridge: Cambridge University Press, 1934. 122 p.

Downing, S.E. Autonomic influences on cardiac function in systemic hypoxia. In J.D. Hatcher and D.B. Jennings (Eds.), Proc. Int. Symp. Cardiovasc. Respir. Effects Hypoxia. New York: Karger. Basel, 1966. pp. 208-231.

Duncan, J. Document No. 4957. Laboratory of Chemical Neurobiology, Allan Memorial Institute of Psychiatry, McGill University, Montreal, Canada, 1972.

Effron, M.L. Familial hyperprolinemia. New England J. Med., 1965, 272, 1243-1254.

Eggleton, P., & Eggleton, G.P. The inorganic phosphate and a labile form of organic phosphate in the gastrocnemius of the frog. Biochem. J., 1927, 21, 190-195.

Ernsting, J. Respiration and anoxia. In J.A. Gillies (Ed.), A textbook of aviation physiology. Oxford: Pergamon Press, 1965. pp. 214-263.

Estabrook, R. In T.E. King, H.S. Mason, and M. Morrison (Eds.), Oxidases and related redox systems. New York: John Wiley and Sons, 1964. p. 833.

Estabrook, R.W., Peterson, J., Baron, J., & Hildebrandt, A. The spectrophotometric measurement of turbid suspensions of cytochromes associated with drug metabolism. Meth. Pharmac., 1972, 2, 303-350.

Everett, N.B., Simmons, B., & Lasher, E.P. Distribution of blood (Fe^{59}) and plasma (I^{131}) volumes of rats determined by liquid nitrogen freezing. Circul. Research, 1956, 4, 419-424.

Farber, E. Biochemical pathology. Ann. Rev. Pharmac., 1971, 11, 71-96.

Farber, E. ATP and cell integrity. Fed. Proc., 1973, 32, 1534-1539.

Feinstein, M.B. Effects of experimental congestive heart failure, oubain and asphyxia on the high-energy phosphate and creatine content of the guinea pig heart. Circul. Research, 1962, 10, 333-346.

Felig, P. Amino acid metabolism in man. Ann. Rev. Biochem., 1975, 44, 933-955.

Fellman, J.H., Fujita, T.S., & Roth, E.S. Assay, properties and tissue distribution of p-hydroxyphenylpyruvate hydroxylase. Biochim. Biophys. Acta, 1972, 284, 90-100

Fisher, D.B., & Kaufman, S. The inhibition of phenylalanine and tyrosine hydroxylases by high oxygen levels. J. Neurochem., 1972, 19, 1359-1365.

Fishman, A.P. Respiratory gases in the regulation of pulmonary circulation. Physiol. Review, 1961, 41, 214-280.

Flamm, W.G., & Crandall, D.F. Purification of mammalian homogentisate oxidase and evidence for the existence of ferrous mercaptans in the active center. J. Biol. Chem., 1963, 238, 389-396.

Foltz, E.L., Page, R.G., Sheldon, W.F., Wong, S.K., Tuddenham, W.J., & Weiss, A.J. Factors in variation and regulation of coronary flow in intact anesthetized dogs. Am. J. Physiol., 1950, 162, 521-537.

Fridovich, I. Competitive inhibition of xanthine oxidase by urea and guanidium ion. J. Biol. Chem., 1964, 239, 3519-3521.

Fridovich, I., & Handler, P. Xanthine oxidase. V. Differential inhibition of the reduction of various electron acceptors. J. Biol. Chem., 1962, 237, 916-921.

Fulco, A.J. Metabolic alteration of fatty acids. Ann. Rev. Biochem., 1974, 43, 215-241.

Garfinkel, D. Studies on pig liver microsomes. I. Enzymatic and pigment compositions of different microsomal fractions. Arch. Biochem. Biophys., 1958, 77, 493-509.

Gatt, S., & Barenholz, Y. Enzymes of complex lipid metabolism. Ann. Rev. Biochem., 1973, 42, 61-90.

Gaylor, J.L., Miyake, Y., & Yamano, T. Stoichiometry of 4-methyl sterol oxidase of rat liver microsomes. J. Biol. Chem., 1975, 250, 7159-7167.

Gentz, J., Jagenburg, R., & Zetterstrom, R. Tyrosinemia. J. Pediatrics, 1965, 66, 670-696.

Gerber, N., Lynn, R., Holcomb, R., Welles, W.L., & Bush, M.L. The metabolism of hexobarbital in mice and methodology for isolation and quantitation of its metabolites in vivo and in vitro. J. Pharmac. Exp. Therap., 1971, 177, 234-245.

Gerber, N., Seibert, R.A., Desiderio, D.M., & Thompson, R.M. Studies on the metabolism and pharmacology of α[(2-pyridylamino)methyl]benzyl alcohol hydrochloride (phenyramidol hydrochloride) in rodents. Drug Met. and Disp, 1974, 2, 140-147.

Gerstl, B., Tavaststjerna, M.G., Hayman, R.B., Smith, J.K., & Eng, L.F. Lipid studies of white matter and thalamus of human brain. J. Neurochem., 1963, 10, 889-902.

Ghazarian, J.G., Jefcote, C.R., Knutson, J.C., Orme-Johnson, W.H., & De Luca, H.F. Mitochondrial cytochrome P-450. A component of chick kidney 25-hydroxycholecalciferol-1α-hydroxylase. J. Biol. Chem., 1974, 249, 3026-3033.

Ghazarian, J.G., Schnoes, H.K., & De Luca, H.F. Mechanism of 25-hydroxychole calciferol 1α-hydroxylation. Incorporation of oxygen-18 into the 1α position of 25-hydroxycholecalciferol. Biochemistry, 1973, 12, 2555-2558.

Gibson, J.G., Seligman, A.M., Peacock, W.C., Aub, J.C., Fine, J., & Evans, R.D. The distribution of red cells and plasma in large and minute vessels of the normal dog, determined by radioactive isotopes of iron and iodine. J. Clin. Invest., 1946, 25, 848-857.

Gillette, J.R. Factors affecting drug metabolism. Ann. N.Y. Acad. Sci., 1971, 179, 43-66.

Gillette, J.R., & Mitchell, J.R. (eds.). Concepts in biochemical pharmacology, Part 3. Berlin and New York: Springer, 1975.

Gillette, J.R., Davies, D.S., & Sasame, H.A. Cytochrome P-450 and its role in drug metabolism. Ann. Rev. Pharmacol., 1972, 12, 57-84.

Goad, L.J. Sterol biosynthesis. In T.W. Goodwin (Ed.), Natural substances formed biologically from mevalonic acid. New York: Academic Press, 1970. pp. 45-77.

Goldman, R.H., & Harrison, D.C. Effects of hypoxia and hypercarbia on myocardial catecholamines. J. Pharmacol. Exp. Ther., 1970, 174, 307-314.

Goodman, D.S., Huang, H.S., Kanai, M., & Shiratori, T. The enzymatic conversion of all-trans β-carotene into retinal. J. Biol. Chem., 1967, 242, 3543-3554.

Goodridge, A.G. Regulation of fatty acid synthesis in isolated hepatocytes prepared from the livers of neonatal chicks. J. Biol. Chem., 1973, 248, 1924-1931.

Goresky, C.A. The lobular design of the liver: its effect on uptake processes. In F. Lundquist and N. Tygstrup (Eds.), Regulation of hepatic metabolism. New York: Academic Press, 1974. pp. 808-819.

Grant, M.E. , & Prockop, D.J. The biosynthesis of collagen (first of three parts). New Eng. J. Med., 1972a, 286, 194-199.

Grant, M.E., & Prockop, D.J. The biosynthesis of collagen (second of three parts). New Eng. J. Med., 1972b, 286, 242-249.

Grant, M.E., & Prockop, D.J. The biosynthesis of collagen (third of three parts). New Eng. J. Med., 1972c, 286, 291-300.

Green, H.D., Lewis, R.N., Nickerson, D., & Heller, A.L. Blood flow, periferol resistance and vascular tonus, with observations on the relationship between blood flow and cutaneous temperature. Am. J. Physiol., 1944, 141, 518-536.

Green, I.D. The circulation in anoxia. In J.A. Gillies (Ed.), A textbook of aviation physiology. Oxford: Pergamon Press, 1965. pp. 264-269.

Greven, K. Der O_2-Diffusionskoeffizient von Leber, Nierensinde and Hirnrinde unter verschiedenen Bedingungen. Pflugers Arch Ges. Physiol., 1960, 271, 14-22.

Grim, E. The flow of blood in the mesenteric vessels. In W.F. Hamilton (Ed.), Handbook of physiology, Section 2. Circulation, 3 volumes. Washington, D.C.: American Physiological Society, 1965. pp. 1439-1456.

Grote, J., & Thews, G. Die Bedingungen fur die Sauerstoffversorgung des Herzmuskel gewebes. Pflugers Arch. Ges. Physiol., 1962, 276, 142-165.

Grunewald, W. The influence of the three dimensional capillary pattern on the intercapillary oxygen diffusion--A new composed model for comparison of calculated and measured oxygen distribution. In H.I. Bicher and D.F. Bruley (Eds.), Oxygen transport to tissue, Part B. New York: Plenum Press, 1973. pp. 5-17.

Grunnet, N. Mechanism for transfer of reducing equivalents (as NADH) from the cytosol to mitochondria and the need for such transfer in ethanol metabolism. In F. Lundquist and N. Tygstrup (Eds.), Regulation of hepatic metabolism. New York: Academic Press, 1974. pp. 520-527.

Guegerich, F.P., Ballou, D.P., & Coon, M.J. Purified liver microsomal cytochrome P-450 electron-accepting properties and oxidation reduction potential. J. Biol. Chem., 1975, 250, 7405-7414.

Gunsalus, I.C., Pederson, T.C., & Sligar, S.G. Oxygenase-catalyzed biological hydroxylations. Ann. Rev. Biochem., 1975, 44, 377-407.

Gunsalus, I.C., Tyson, C.A., & Lipscomb, J.D. Cytochrome P-450 reduction and oxygenation systems. In T.E. King, H.S. Mason, & M. Morrison (Eds.), Oxidases and related redox systems. Baltimore: University Park Press, 1973. pp. 583-603.

Gurdjian, E.S., Stone, W.E., & Webster, J.E. Cerebral metabolism in hypoxia. Arch. Neurol. Psychiat., Chicago, 1944, 51, 472-477.

Gurdjian, E.S., Webster, J.E., & Stone, W.E. Cerebral constituents in relation to blood gases. Am. J. Physiol., 1949, 156, 149-157.

Gurtner, G.H., & Burns, B. The role of cytochrome P-450 of placenta in facilitated oxygen diffusion. Drug Met. and Disp., 1973, 1, 368-373.

Gustafsson, J. Biosynthesis of cholic acid in rat liver 24-hydroxylation of 3α, 7α, 12α-trihydroxy-5β-cholestanoic acid. J. Biol. Chem., 1975, 250, 8243-8247.

Haldane, J.S. In Barcroft, J. Anoxemia. Lancet, 1920, 2, 485-489.

Haldane, J.S., & Priestley, J.G. Respiration. (New edition). New Haven: Yale University Press, 1935. 478 p.

Halley, M.M., Reemtsman, K., & Creech, O., Jr. Cerebral blood flow, metabolism, and brain volume in extracorporeal circulation. J. Thoracic Surg., 1958, 36, 506-518.

Hamberg, M. Metabolism of prostaglandins in rat liver mitochondria. Eur. J. Biochem., 1968, 6, 135-146.

Hamberg, M., Israelsson, U., & Samuelsson, B. Metabolism of prostaglandin E_2 in guinea pig liver. Ann. N.Y. Acad. Sci., 1971, 180, 164-180.

Hamberg, M., Samuelsson, B., Bjorkhem, I., & Danielsson, H. Oxygenases in fatty acid and steroid metabolism. In O. Hayaishi (Ed.), Molecular mechanisms of oxygen activation. New York: Academic Press, 1974. pp. 29-85.

Hamilton, W.F. (Section Editor). Handbook of physiology, Section 2, Circulation. 3 Volumes. Washington, D.C.: American Physiological Society, 1965. 2765 p.

Handler, P., Rajagopalan, K.U., & Aleman, U. Structure and function of iron-flavo proteins. Fed. Proc., 1964, 23, 30-38.

Harden, A., & Young, W.J. The alcoholic ferment of yeast-juice. Proc. Roy. Soc. (London), 1906, B 77.

Harris, P., & Gloster, J. The effects of acute hypoxia on lipid synthesis in the rat heart. Cardiology, 1971/72, 56, 43-47.

Harrison, D.C., Robinson, M.D., & Kleiger, R.E. Role of hypoxia in digitalis toxicity. Am. J. Med. Sci., 1969, 256, 352-359.

Hartman, B.K. J. of Histochem. and Cytochem., 1973, 21, 312-332.

Haugen, D.A., van der Hoeven, T.A., & Coon, M.J. Purified liver microsomal cytochrome P-450 separation and characterization of multiple forms. J. Biol. Chem., 1975, 250, 3567-3570.

Haung, Y.L., & Ebner, K.E. Induction of tyrosine aminotransferase in isolated liver cells. Biochim. Biophys. Acta, 1969, 191, 161-163.

Hayaishi, O. Oxygenases (oxygen transferring enzymes). In T.P. Singer (Ed.), Biological oxidation. New York: John Wiley and Sons, 1968. pp. 581-601.

Hayaishi, O. Enzymic hydroxylation. Ann. Rev. Biochem., 1969, 38, 21-44.

Hayaishi, O. General properties and biological functions of oxygenases. In O. Hayaishi (Ed.), Molecular mechanisms of oxygen activation. New York: Academic Press, 1974. pp. 1-28.

Hayaishi, O. Molecular mechanisms of oxygen activation. New York: Academic Press, 1974.

Hayaishi, O., Katagiri, M., & Rothberg, S. Mechanism of the pyrocatechase reaction. J. Am. Chem. Soc., 1955, 77, 5450-5451.

Hayaishi, O., & Nozaki, M. Nature and mechanisms of oxygenases. Science, 1969, 164, 389-396.

Hayano, M. Oxygenases in lipid and steroid metabolism. In O. Hayaishi (Ed.), Oxygenases. New York: Academic Press, 1962. pp. 181-240.

Hems, R., Ross, B.D., Berry, M.N., & Krebs, H.A. Gluconeogenesis in the perfused rat liver. Biochem. J., 1966, 101, 284-292.

Henry, H.L., & Norman, A.W. Studies on calciferol metabolism. IX. Renal 25-hydroxy-vitamin D_3-1-hydroxylase. Involvement of cytochrome P-450 and other properties. J. Biol. Chem., 1974, 249, 7529-7535.

Henry, P.D., Sobel, B.E., & Braunwald, E. Maintenance of viability of the hypoxic perfused guinea pig heart by glucose and insulin. Am. J. Physiol., 1974, 226, 309-313.

Herndon, J.H., Jr., Steinberg, D., & Uhlendorf, B.W. Refsum's disease: defective oxidation of phytanic acid in tissue cultures derived from homozygotes and heterozygotes. New Eng. J. Med., 1969, 281, 1034-1038.

Heyrovsky, J. Rec. trav. chim. du Payes-Bas, 1925. 44, 1. Cited in Longmuir, I.S. The oxygen electrode, pp. 219-237. In F. Dickens and E. Neil (Eds.), Oxygen in the animal organism. New York: The Macmillan Co., 1964. 694 p.

Hill, D.K. Oxygen tension and the respiration of resting frog's muscle. J. Physiol., 1948, 107, 479-495.

Hills, B.A. Respiration of tissue as a medium of heterogeneous permability. Bull. Math. Biophys., 1970, 32, 219-235.

Hinman, J.W. Prostaglandins. Ann. Rev. Biochem., 1972, 41, 161-178.

Horowitz, D., Lovenberg, W., Engelman, K., & Sjoerdsma, A. Monoamine oxidase inhibitors, tyramine, and cheese. J. Am. Med. Assoc., 1964, 188, 1108-1110.

Howard, R.B., Christensen, H.K., Gibbs, F.A., & Pesch, L.A. The enzymatic preparation of isolated intact parenchymal cells from rat liver. J. Cell Biol., 1967, 35, 675-684.

Howard, R.B., & Pesch, L.A. Respiratory activity of intact, isolated parenchymal cells from rat liver. J. Biol. Chem., 1968, 243, 3105-3109.

Huckabee, W.E. Relationships of pyruvate and lactate during anaerobic metabolism. I. Effects of infusion of pyruvate or glucose and of hyperventilation. J. Clin. Invest., 1958, 37, 244-254.

Hunt, T.K., & Pai, M.P. The effect of varying ambient oxygen tensions on wound metabolism and collagen synthesis. Surg. Gynecol. Obstet., 1972, 135, 561-567.

Hutten, H., Thews, G., & Vaupel, P. Some special problems concerning the oxygen supply to tissue as studied by an analogue computer. In H.I. Bicher and D.F. Bruley (Eds.), Oxygen transport to tissue, Part B. New York: Plenum Press, 1973. pp. 25-31.

Hutton, J.J., Jr., Tappel, A.L., & Udenfriend, S. Cofactor and substrate requirements of collagen proline hydroxylase. Arch. Biochem. Biophys., 1967, 118, 231-240.

Iaccarino, M., Boeri, E., & Scardi, V. Preparation of purified 3-hydroxyanthranilic acid oxidase from rat and ox liver. Biochem. J., 1961, 78, 65-69.

Ichikawa, Y., & Yamano, T. Preparation and physiochemical properties of functional hemoprotein P_{450} from mammalian tissue microsomes. Biochim. Biophys. Acta, 1970, 200, 220-240.

Ichiyama, A., & Nakamisa, S. Tryptophan 5-monooxygenase (mammalian brainstem)--an assay method. Method. in Enzymol., 1970, 17, 449-459.

Ikeda, M., Fahien, L.A., & Udenfriend, S. A kinetic study of bovine adrenal tyrosine hydroxylase. J. Biol. Chem., 1966, 241, 4452-4456.

Inaba, T., Umeda, T., Mahon, W.A., Ho, J., & Jeejeebhoy, K.N. Isolated rat hepatocytes as a model to study drug metabolism: Dose-dependent metabolism of diphenylhydantoin. Life Sciences, 1975, 16, 1227-1232.

Ingebretsen, W.R., Jr., & Wagle, S.R. A rapid method for the isolation of large quantities of rat liver parenchymal cells with high anabolic rates. Biochem. Biophys. Res. Communications, 1972, 47, 403-410.

Irreverre, F., Mudd, S.H., Heizer, W.D., & Laster, L. Sulfite oxidase deficiency: studies of a patient with mental retardation, dislocated ocular lenses, and abnormal urinary excretion of S-sulfo-L-cysteine, sulfite and thio sulfate. Biochem. Med., 1967, 1, 187-217.

Isherwood, F.A., Mapson, L.W., & Chen, Y.T. Synthesis of L-ascorbic acid in rat liver homogenates. Conversion of L-gulono- and L-galactono-γ-lactone and the respective acids into L-ascorbic acid. Biochem. J., 1960, 76, 157-171.

Israelsson, U., Hamberg, M., & Samuelsson, B. Biosynthesis of 19-hydroxyprostaglandin A_1. Eur. J. Biochem., 1969, 11, 390-394.

Iyanagi, T., Makino, N., & Mason, H.S. Redox properties of the reduced nicotinamide adenine dinucleotide phosphate-cytochrome P-450 and reduced nicotinamide adenine dinucleotide-cytochrome b_5 reductases. Biochemistry, 1974, 13, 1701-1710.

Jacob, S.T., & Bhargava, P.M. A new method for the preparation of liver cell suspensions. Exp. Cell Res., 1962, 27, 453-467.

Jarvik, M.E. Drugs used in the treatment of psychiatric disorders. In L.S. Goodman and A. Gilman (Eds.), The pharmacological basis of therapeutics, 3rd edition. New York: The Macmillan Co., 1965. pp. 159-214.

Jennings, R.B. Early phase of myocardial ischemic injury and infraction. Am. J. Cardiol., 1969, 24, 753-765.

Jobsis, F.F. Basic processes in cellular respiration. In W.O. Fenn and H. Rahn (Eds.), Handbook of Physiology, Vol. 1. Respiration, Chapter 2. Baltimore: Waverly Press, 1964. pp. 63-124.

Jobsis, F.F. Oxidative metabolism at low PO_2. Fed. Proc., 1972, 31, 1404-1413.

Jobsis, F.F. Intracellular metabolism of oxygen. Am. Rev. of Resp. Disease, 1974, 110, 58-63.

Johnson, M.E.M., Das, N.M, Butcher, F.R., & Fain, J.N. The regulation of gluconeogenesis in isolated rat liver cells by glucagon, insulin, dibutyryl cyclic adenosine monophosphate and fatty acids. J. Biol. Chem., 1972, 247, 3229-3235.

Kalckar, E.M. (ed.). Biological phosphorylations: development of concepts. Englewood Cliffs, N.J.: Prentice-Hall, Inc., 1969. pp. 10-19, 170-177, 318-325, 376, 382-385, 416-419.

Kaltenbach, J.P. The preparation of whole cell suspensions obtained from solid mammalian tissues. Exp. Cell Res., 1954, 7, 568-571.

Kastle, J.H. The oxidases and other oxygen-catalysts concerned in biological oxidations. Bull. U.S. Hyg. Lab. no. 59. Washington, D.C.: Government Printing Office, 1910. 164 p.

Katz, A.M. Congestive heart failure. Role of altered myocardial cellular control. New Eng. J. Med., 1975, 293, 1184-1191.

Katz, R. Growth phase and rotenone sensitivity in Torulopsis utilis: Difference between exponential and stationary phase. FEBS Letters, 1971, 12, 153-156.

Kaufman, S., & Fisher, D.B. Pterin-requiring aromatic amino acid hydroxylases. In O. Hayaishi (Ed.), Molecular mechanisms of oxygen activation. New York: Academic Press, 1974. pp. 285-369.

Klebanoff, S.J. Role of the superoxide anion in the myeloperoxidase-mediated antimicrobial system. J. Biol. Chem., 1974, 249, 3724-3728.

Keilin, D. Cytochrome and respiratory enzymes. Proc. Roy. Soc. (London), B, 1929, 106, 206-252.

Keilin, D. The history of cell respiration and cytochrome. Cambridge: Cambridge Univ. Press, 1966. 359 p.

Kennedy, E.P., & Lehninger, A.L. Oxidation of fatty acids and tricarboxylic acid cycle intermediates by isolated rat liver mitochondria. J. Biol. Chem., 1949, 179,

Kent, K.M., Goodfriend, T.L., McCallum, Z.T., Dempsey, P.J., & Cooper, T. Ionotropic agents in hypoxic cat myocardium: depression and potentiation. Circulation Research, 1972, 30, 196-204.

Kessler, M., Bruley, D.F., Clark, L.C., Jr., Lubbers, D.W., Silver, I.A., & Strauss, J. Oxygen supply. Theoretical and practical aspects of oxygen supply and microcirculation of tissue. Baltimore: University Park Press, 1973. 312 p.

Kessler, M., Gornandt, L., & Lang, H. Correlation between oxygen tension and hemoglobin dissociation curve. In M. Kessler, D.F. Bruley, L.C. Clark, Jr., D.W. Lubbers, I.A. Silver, and J. Strauss, Oxygen supply. Baltimore: University Park Press, 1973. pp. 156-159.

Kessler, M., Lang, H., Sinagowitz, E., Rink, R., & Hoper, J. Homeostasis of oxygen supply in liver and kidney. In D.F. Bruley and H.I. Bicher (Eds.), Oxygen transport to tissue, Part A. New York: Plenum Press, 1973. pp. 351-360.

Kessler, M., Lang, H., & Starlinger, H. J. Physiol. (Paris), 1972, 65 (supp.), 249A.

Kety, S.S. Regional circulation of the brain under physiological conditions--possible relationship to selective vulnerability. In J.P. Schade and W.H. McMenemey (Eds.), Selective vulnerability of the brain in hypoxemia. Philadelphia: F.A. Davis Co., 1963. pp. 21-26.

Kety, S.S., & Schmidt, C.F. The effects of altered arterial tensions of carbon dioxide and oxygen on cerebral blood flow and cerebral oxygen consumption of normal young men. J. Clin. Invest., 1948, 27, 484-492.

Kety, S.S., & Schmidt, C.F. The nitrous oxide method for the quantitative determination of cerebral blood flow in man: Theory, procedure and normal values. J. Clin. Invest., 1948, 27, 476-483.

King, T.E. The Keilin-Hartree heart muscle preparation. Meth. Enz., 1967, 10, 202-208.

Kirk, J.E., & Laursen, T.J.S. Diffusion coefficients of various solutes for human aortic tissue with special reference to variation in tissue permeability with age. J. Geront., 1955, 10, 288-302.

Kitagawa, H. Chem. Pharm. Bull. (Tokyo), 1968, 16, 1589.

Klein, J.R., & Olsen, N.S. Effect of convulsive activity upon the concentration of brain glucose, glycogen, lactate and phosphates. J. Biol. Chem., 1947, 167, 747-756.

Klingenberg, M. Pigments of rat liver microsomes. Arch. Biochem. Biophys., 1958, 75, 376-386.

Kopin, I.J., & Gordon, E.K. Origin of norepinephrine in the heart. Nature, 1963, 199, 1289.

Kornberg, A. Lactic dehydrogenase of muscle. Meth. Enz., 1955, 1, 441-454.

Kowal, J., Simpson, E.R., & Estabrook, R.W. Adrenal cells in tissue culture. J. Biol. Chem., 1970, 245, 2438-2443.

Krasnow, N., Neill, W.A., Messer, J.V., & Gorlin, R. Myocardial lactate and pyruvate metabolism. J. Clin. Invest., 1962, 41, 2075-2085.

Kratz, F., & Staudinger, H. Kinetische Untersuchungen zur Hydroxyliesung von Cumarin mit Lebermikrosomen von Kaninchen. Zeitschr. Physiol. Chemie, 1965, 343, 27-34.

Krebs, H.A. The intermediate metabolism of carbohydrates. Lancet, 1937, 2, 736-738.

Krebs, H.A., Cornell, N.W., Lund, P., & Hems, R. Isolated liver cells as experimental material. In F. Lundquist and N. Tygstrup (Eds.), Regulation of hepatic metabolism. New York: Academic Press, 1974. pp. 726-750.

Krishner, N. Epinephrine, norepinephrine, and related compounds. Methods in Hormone Research, 1968, 1, 383-410.

Krogh, A. The rate of diffusion of gases through animal tissues with some remarks on the coefficient of invasion. J. Physiol., 1919, 52, 391-415.

Krogh, A. The anatomy and physiology of capillaries. New Haven, Conn.: Yale Univ. Press, 1922.

Kronenberg, R., Hamilton, F.N., Gabel, R., Hickey, R., Read, D.J.C., & Severinghaus, J. Comparison of three methods for quantitating respiratory response to hypoxia in man. Respiratory Physiology, 1972, 16, 109-125.

Kunze, K. Normal and critical oxygen supply to the muscle. In D.W. Lubbers, U.C. Luft, G. Thews, and E. Witzleb (Eds.), Oxygen transport in blood and tissue. Stuttgart: George Thieme Verlag, 1968. pp. 198-208.

Kupfer, D., & Rosenfeld, J. A sensitive radioactive assay for hexobarbital hydroxylase in hepatic microsomes. Drug Met. and Disp., 1973, 1, 760-765.

Kuramoto, K., Murata, K., Lie, H.Y., Yazaki, Y., & Ikeda, M. Effect of sympathetic nerve on the coronary circulation and myocardial oxygen consumption. Japanese Circulation J., 1970, 34, 1098-1099.

Kurien, V.A., & Oliver, M.F. Metabolic cause for arrhythmias during acute myocardial hypoxia. Lancet, 1970, 1, 813-815.

Lardy, H.A., & Ferguson, S.M. Oxidative phosphorylation in mitochondria. Ann. Rev. Biochem., 1969, 38, 991-1034.

Larner, J. Intermediary metabolism and its regulation. Englewood Cliffs, N.J.: Prentice-Hall, Inc., 1971. 308 p.

Lasfargues, E.Y. Cultivation behavior in vitro of the normal mammary epithelium of the adult mouse. Anat. Rec., 1957, 127, 117-129.

Lehninger, A.L. Bioenergetics, 2nd edition. Menlo Park, Calif.: W.A. Benjamin, Inc., 1971. 245 p.

Lehninger, A.L. Biochemistry, 2nd edition. New York: Worth Publishers, Inc., 1975. 1104 p.

Lemberg, M.R. Cytochrome oxidase. Physiol. Rev., 1969, 49, 48-121.

Lenfant, C., & Torrance, J. Role of oxygen dissociation curve in hypoxia. Ann. Int. Med., 1969, 70, 1108. (Abstract).

Leroux, A., Junien, C., Kaplan, J-C., & Bamberger, J. Generalized deficiency of cytochrome b_5 reductase in congenital methaemoglobinaemia with mental retardation. Nature, 1975, 258, 619-620.

Levine, S. Anoxic ischemic encephalopathy in rats. Am. J. Pathol., 1960, 36, 1-17.

Lin, E.C.C., & Knox, W.E. Specificity of the adaptive response of tyrosine-α-ketoglutarate transaminase in the rat. J. Biol. Chem., 1958, 233, 1186-1189.

Lindblad, B., Lindstedt, G., & Lindstedt, S. The mechanism of enzymic formation of homogentisate from p-hydroxyphenylpyruvate. J. Am. Chem. Soc., 1970, 92, 7446-7449.

Lindstedt, G., Lindstedt, S., Midtvedt, T., & Tofft, M. The hydroxylation of γ-butyrobetaine to carnitine. Biochem. J., 1967, 103, 19P.

Lipmann, F. Metabolic generation and utilization of phosphate bond energy. Adv. in Enzymology, 1941, 1, 99-162.

Lipmann, F. Pasteur effect. In A Symposium on Respiratory Enzymes. Madison: Univ. of Wisconsin Press, 1941-42. pp. 48-73.

Litwack, G., & Cleland, W.W. Studies on the tyrosine aminotransferase mechanism. Biochemistry, 1968, 7, 2072-2079.

Lockard, I. Existing anatomical parameters and the need for further determinations for various tissue structures. In H.I. Bicker and D.F. Bruley (Eds.), Oxygen transport to tissue, Part B. New York: Plenum Press, 1973. pp. 803-811.

Longmuir, I.S. Respiration rate of bacteria as a function of oxygen concentration. Biochem. J., 1954, 57, 81-87.

Longmuir, I.S. Respiration rate of rat liver cells at low oxygen concentrations. Biochem. J., 1957, 65, 378-382.

Longmuir, I.S. The oxygen electrode. In F. Dickens and E. Neil (Eds.), Oxygen in the animal organism. New York: The MacMillan Co., 1964. pp. 219-237.

Longmuir, I.S., & McCabe, M. Cyanide and azide insensitive tissue respiration. New York: VIth Internatl. Cong. Biochem, 1964.

Longmuir, I.S., & Bourke, A. The measurement of the diffusion of oxygen through respiring tissues. Biochem. J., 1960, 76, 225-229.

Longmuir, I.S., & McCabe, M. Tissue adaption to oxygen lack. J. Theoret. Biol., 1965, 8, 124-129.

Longmuir, I.S., & Rees, W.A. Preparation of cell suspensions from rat livers. Nature, 1956, 177, 997.

Longmuir, I.S., Martin, D.C., Gold, H.J., & Sun, S. Non-classical respiratory activity of tissue slices. Microvascular Research, 1971, 3, 125-141.

Loomis, M.E. An enzymatic fluorometric method for the determination of lactic acid in serum. J. Lab. & Clin. Med., 1961, 57, 966-969.

Losse, B., Schuchhardt, S., Niederle, N., & Benzing, H. The histogram of local oxygen pressure (PO_2) in the dog myocardium and the PO_2 behavior during transitory changes of oxygen administration. In D.F. Bruley and H.I. Bicher (Eds.), Oxygen transport to tissue, Part A. New York: Plenum Press, 1973. pp. 535-540.

Lowenstein, J.M. The tricarboxylic acid cycle. In D.M. Greenberg (Ed.), Metabolic pathways, 3rd edition, Vol. 1. New York: Academic Press, 1967. pp. 146-270.

Lowry, O.H., Rosebrough, N.J., Farr, A.L., & Randall, R.J. Protein measurement with the folin phenol reagent. J. Biol. Chem., 1951, 193, 265-275.

Lubbers, D.W. The oxygen pressure field of the brain and its significance for the normal and critical oxygen supply of the brain. In D.W. Lubbers, U.C. Luft, G. Thews, and E. Witzleb (Eds.), Oxygen transport in blood and tissue. Stuttgart: Georg Thieme Verlag, 1968. pp. 124-139.

Lubbers, D.W. The meaning of the tissue oxygen distribution curve and its measurement by means of Pt-electrodes. In F. Kreuzer and H. Herzog (Eds.), Oxygen pressure recording in gases, fluids and tissues. New York: Karger, Basel, 1969. pp. 112-123.

Lubbers, D.W. Opening remarks. In M. Kessler, D.F. Bruley, L.C. Clark, Jr., D.W. Lubbers, I.A. Silver, & J. Strauss (Eds). Oxygen supply. Baltimore: University Park Press, 1973. pp. 1-2.

Lubbers, D.W. Local tissue PO_2: its measurement and meaning. In M. Kessler, D.F. Bruley, L.C. Clark, Jr., D.W. Lubbers, I.A. Silver, & J. Strauss (Eds.), Oxygen supply. Baltimore: University Park Press, 1973. pp. 151-155.

Lubbers, D.W., Luft. U.C., Thews, G., & Witzleb, E. (Eds.). Oxygen transport in blood and tissue. Stuttgart: Georg Thieme Verlag, 1968.

Lundgren, C.E.G., & Zederfeldt, B.H. Influence of low oxygen pressure on wound healing. Acta Chir. Scand., 1969, 135, 555-558.

Lundquist, F., & Tygstrup, N. (eds.). Regulation of hepatic metabolism. New York: Academic Press, 1974. 828 p.

McMurray, W.C., & Magee, W.L. Phospholipid metabolism. Ann. Rev. Biochem., 1972, 41, 129-160.

MacMillan, V., & Siesjo, B.K. Critical oxygen tensions in the brain. Acta Physiol. Scand., 1971, 82, 412-414.

Mahler, H.R., & Cordes, E.H. Biological chemistry, 2nd edition. New York: Harper and Row, 1971. 1009 p.

Majno, G. Death of liver tissue. In Ch. Rouiller (Ed.), The liver. Vol. II. New York: Academic Press, 1964. pp. 267-313.

Marshall, B.E., & Wyche, M.Q., Jr. Hypoxemia during and after anesthesia. Anesthesiology, 1972, 37, 178-209.

Mason, H.S. Mechanisms of oxygen metabolism. Adv. in Enzymology, 1957, 19, 79-223.

Mason, H.S. Mechanisms of oxygen metabolism. Science, 1957, 125, 1185-1188.

Mason, H.S. Comment in general discussion following session C in symposium entitled Oxygen in the animal organism. F. Dickens and E. Neil (Eds.), Oxygen in the animal organism. New York: The Macmillan Co., 1964. p. 357.

Mason, H.S. Oxidases. Ann. Rev. Biochem., 1965, 34, 595-634.

Mason, H.S., Fowlks, W.B., & Peterson, E.W. Oxygen transfer and electron transport by the phenolase complex. J. Am. Chem. Soc., 1955, 77, 2914-2915.

Mason, H.S., North, J.C., & Vanneste, M. Microsomal mixed function oxidations: the metabolism of xenobiotics. Fed. Proc., 1965, 24, 1172-1180.

Mason, J.I., Estabrook, R.W., & Purvis, J.L. Testicular cytochrome P-450 and iron-sulfur protein as related to steroid metabolism. Ann. N.Y. Acad Sci., 1973, 212, 406-419.

Massey, V., Ganther, H., Brunley, P.E., & Curti, B. D-amino acid oxidase. In T.E. King, H.S. Mason, and M. Morrison (Eds.), Oxidases and related redox systems. New York: John Wiley and Sons, 1964. pp. 335-352.

Mayow, J. Tractatibus quinque Medico-Physic, 1974. In Alembic Club Reprints, No. 17. Edinburgh: The Alembic Club, 1907. pp. 73-75.

McGinty, D.A. The regulation of respiration. XXV. Variations in the lactic acid metabolism of the intact brain. Am. J. Physiol., 1929, 88, 312-325.

McKerns, K.W. (ed). Functions of the adrenal cortex. 2 Volumes. New York: Appleton-Century-Crofts, 1968. 1176 p.

Mellman, M.A., & Hanson, R.W. (eds). Energy metabolism and the regulation of metabolic processes in mitochondria. New York: Academic Press, 1972. 296 p.

Meijer, A.J., & Williamson, J.R. Transfer of reducing equivalents across the mitochondrial membrane. Biochim. Biophys. Acta, 1974, 333, 1-11.

Metzger, H. PO_2 histograms of three dimensional systems with homogenous and inhomogenous microcirculation--a digital computer study. In H.I. Bicher and D.F. Bruley (Eds.), Oxygen transport to tissue, Part B. New York: Plenum Press, 1973. pp. 18-24.

Mills, E., & Slotkin, T.A. Catecholamine content of the carotid body in cats ventilated with 8-40% oxygen. Life Sciences, 1975, 16, 1555-1562.

Milne, M.D. Some abnormalities of amino acid metabolism. In R.H.S. Thompson and I.D.P. Wootton (Eds.), Biochemical disorders in human disease, 3rd edition. New York: Academic Press, 1970. pp. 553-607.

Miyake, Y., Mochizaki, S., Yamaro, T., & Aki, K. Symp. Enz. Chem. (Japan), 1960, 14, 73; Cited in Hayaishi, O. Enzymic hydroxylation. Ann. Rev. Biochem., 1962, 31, 25-46.

Moldeus, P., Grundin, R., Vadi, H., & Orrenius, S. A study of drug metabolism linked to cytochrome P-450 in isolated rat liver cells. Eur. J. Biochem, 1974, 46, 351-360.

Molinoff, P.B., & Axelrod, J. Biochemistry of catecholamines. Ann. Rev. Biochem., 1971, 40, 465-500.

Montgomery, M.R., & Rubin, R.J. Oxygenation during inhibition of drug metabolism by carbon monoxide or hypoxic hypoxia. J. Appl. Physiol., 1973, 35, 505-509.

Monthly Vital Statistics Report, 1974. Annual summary for the United States. Volume 22, No. 13, p. 20.

Moore, K.E., & Dominic, J.A. Tyrosine hydroxylase inhibitors. Fed. Proc., 1971, 30, 859-870.

Moret, P.R. Myocardial metabolic changes in chronic hypoxia. Cardiology, 1971/72, 56, 161-172.

Mortimore, G.E., Woodside, K.H., & Henry, J.E. Compartmentation of free valine and its relation to protein turnover in perfused rat liver. J. Biol. Chem., 1972, 247, 2776-2784.

Mudd, S.H., Irreverre, F., & Laster, L. Sulfite oxidase deficiency in man: Demonstration of the enzymatic defect. Science, 1967, 156, 1599-1602.

Mustala, O.O., & Azarnoff, D.L. Effect of oxygen tension on drug levels and pharmacological action in the intact animal. Proc. Soc. Exp. Biol. Med., 1969, 132, 37-41.

Myers, J.D. The hepatic blood flow and splanchnic oxygen consumption of man; their estimation from urea production or bromosulphalein excretion during catheterization of the hepatic veins. J. Clin. Invest., 1947, 26, 1130-1137.

Nicholas, H.J., & Aexel, R.T. Biosynthesis of cholesterol in cell-free extracts of adult rat brain. Fed. Proc., 1967, 26, 342.

Nichols, P., & Chance, B. Cytochrome c oxidase. In O. Hayaishi (Ed.), Molecular mechanisms of oxygen activation. New York: Academic Press, 1974. pp. 479-534.

Niinikoski, J., & Hunt, T.K. Oxygen tensions in healing bone. Surg. Gynecol. Obstet., 1972, 134, 746-750.

Nordenskiold, Erik. The history of biology. A survey. New York: Tudor Publishing Co. Originally issued as Biologins Historia, 1920-24, Stockholm, Bjorck and Borjesson.

Novick, W.J. Effect of oxygen tension on monoamine oxidase activity. Biochem. Pharmacol., 1966, 15, 1009-1012.

Nozaki, M. Non-heme iron dioxygenase. In O. Hayaishi (Ed.), Molecular mechanisms of oxygen activation. New York: Academic Press, 1974. pp. 135-165.

Ogasawara, N., Gander, J.E., & Henderson, L.M. Purification and properties of 3-hydroxyanthranilate oxygenase from beef kidney. J. Biol. Chem., 1966, 241, 613-619.

Olsen, N.S., & Klein, J.R. Effect of cyanide on the concentration of lactate and phosphates in brain. J. Biol. Chem., 1947, 167, 739-746.

Olson, J.S., Ballou, D.P., Palmer, G., & Massey, V. The reaction of xanthine oxidase with molecular oxygen. J. Biol. Chem., 249, 4350-4362.

Omura, T., & Sato, R. The carbon monoxide-binding pigment of liver microsomes. I. Evidence for its hemoprotein nature. J. Biol. Chem., 1964, 239, 2370-2378.

Opie, L.H. Substrate utilization and glycolysis in the heart. Cardiology, 1971/72, 56, 2-21.

Opie, L.H., & Mansford, K.R.L. Value of lactate and pyruvate measurements in the assessment of the redox state of free nicotinamide-adenine dinucleotide in the cytoplasm of perfused rat heart. Eur. J. Clin. Invest., 1971, 1, 295-306.

Opitz, E., & Schneider, M. The oxygen supply of brain and the mechanism of deficiency effects. Ergebn. Physiol., 1950, 46, 126-260.

Orme-Johnson, N.R., Orme-Johnson, W.H., Hansen, R.E., Beinert, H., & Hatefi, Y. In T.E. King, H.S. Mason, and M. Morrison (Eds.), Oxidases and related redox systems. Baltimore: University Park Press, 1973. pp. 769-797.

Orrenius, S., & Ernster, L. Microsomal cytochrome P-450-linked monoxygenase systems in mammalian tissues. In O. Hayaishi (Ed.), Molecular mechanisms of oxygen activation. New York: Academic Press, 1974. pp. 215-244.

Orrenius, S., Wilson, B.J., von Bahr, C., & Schenkman, J.B. On the significance of drug induced spectral changes in liver microsomes. In G.S. Boyd and R.M.S. Smellie (Eds.), Biological hydroxylation mechanisms. Biological Society Symposium No. 34. London: Academic Press, 1972. pp. 55-77.

Osaki, S., Walter, C., & Frieden, E. The ascorbate oxidase activity of chelex treated ceruloplasmin. Biochem. Biophys. Res. Commun., 1963, 12, 1-7.

Osaki, S., Johnson, D.A., and Freiden, E. The possible significance of the ferrous oxidase activity of ceruloplasmin in normal human serum. J. Biol. Chem., 1966, 241, 2746-2751.

Oshino, N., & Chance, B. The properties of sulfite oxidation in perfused rat liver; interaction of sulfite oxidase with the mitochondrial respiratory chain. Arch. Biochem. Biophys, 1975, 170, 514-528.

Parrilla, R., Ohkawa, K., Lindros, K.O., Zimmerman, U.-J.P., Kobayaishi, K., & Williamson, J.R. Functional compartmentation of acetaldehyde oxidation in rat liver. J. Biol. Chem., 1974, 249, 4926-4933.

Paul, K.G. Peroxidases. In P.D. Boyer, H. Lardy, and K. Myrback (Eds.), The enzyme, 2nd edition, Vol. 8. New York: Academic Press, 1963. pp. 227-274.

Pelkonen, R., & Kivirikko, K.I. Hydroxyprolinemia, an apparently harmless familial metabolic disorder. New Eng. J. Med., 1970, 283, 451-456.

Pembrey, M.S. Chemistry of respiration. In E.A. Schafer, Textbook of physiology, Vol. I. Edinburgh and London: Young J. Pentland, 1898. pp. 692-784.

Penttila, A., & Trump, B.F. Extracellular acidosis protects Erlich ascites tumor cells and rat renal cortex against anoxic injury. Science, 1974, 185, 277-278.

Perkins, J.F., Jr. Historical development of respiratory physiology. In W.O. Fenn and H. Rahn (Section Editors), Handbook of physiology, Section 3. Respiration, Vol. 1. Washington, D.C.: American Physiological Society, 1964. pp. 1-62.

Peters, J.P., & van Slyke, D.D. Quantitative clinical chemistry, Vol. I. Baltimore: Williams and Wilkins Co., 1932. pp. 578-593.

Pickles, V.R. Prostaglandins. Nature, 1969, 224, 221-225.

Pinchot, G.B. Mechanisms of oxidative phosphorylation--observations and speculation. Perspect. Biol. Med., 1965, 8, 180-195.

Poillon, W.N. Tyrosine hydroxylase of sheep brain: Some catalytic and chemical properties of the detergent-solubilized, partially purified enzyme. J. Neurochem. 1970, 21, 729-741.

Pool, P.E., Covell, J.W., Chidsey, C.A., & Braunwald, E. Myocardial high energy phosphate stores in acutely induced hypoxic heart failure. Circulation Res., 1966, 19, 221-229.

Price, J.M., Yess, N., Brown, R.R., & Johnson, S.A.M. Tryptophan metabolism, A hitherto unreported abnormality occurring in a family. Arch. Dermatol., 1967, 95, 462-472.

Prough, R.A., & Burke, M.D. The role of NADPH-cytochrome c reductase in microsomal hydroxylation reactions. Arch. Biochem. Biophys., 1975, 170, 160-168.

Pullman, M.E., & Schatz, G. Mitochondrial oxidations and energy coupling. Ann. Rev. Biochem., 1967, 36, 539-610.

Quistorff, B., Bondesen, S., & Grunnet, N. Preparation and biochemical characterization of parenchymal cells from rat liver. Biochim. Biophys. Acta, 1973, 320, 503-516.

Rabinowitz, J.L., & Hercker, E.S. Incomplete oxidation of palmitate and leakage of intermediary products during anoxia. Arch. Biochem. Biophys., 1974, 161, 621-627.

Ramwell, P.W., & Shaw, J.E. Biological significance of the prostaglandins. Recent Prog. Hormone Res., 1970, 26, 139-187.

Randerath, K., & Randerath, E. Thin-layer separation methods for nucleic acid derivatives. Meth. Enz., 1967, 12, 323-347.

Reivich, M. Dimensions and maximum diffusion distance of capillaries: vertebrate tissues. In P. L. Altman and D. S. Dittmer (Eds.), Biological handbooks. Bethesda, Md.: Federation of American Societies for Experimental Biology, 1971. pp. 453-454.

Ridge, J. W. The distribution of cytochrome-oxidase activity in rabbit brain. Biochem. J., 1967, 102, 612-617.

Robbins, K. C. In vitro enzymatic omega oxidation of medium-chain fatty acids in mammalian tissues. Arch. Biochem. Biophys., 1968, 123, 531-538.

Robbins, S. L., & Angell, M. Basic pathology. Philadelphia: W. B. Saunders Co., 1971. p. 13.

Rosenberg, J. S., & Litwack, G. Liver cytosol tyrosine aminotransferase. Product inhibition and interaction with substrates. J. Biol. Chem., 1970, 245, 5677-5684.

Runnstrom, J., & Michaelis, L. Correlation of oxidation and phosphorylation in hemolysed blood in presence of methylene blue and pyocyanine. J. Gen. Physiol., 1935, 18, 717-727.

Russell, J. A., & Crook, L. Comparison of metabolic responses of rats to hypoxic stress produced by two methods. Am. J. Physiol., 1968, 214, 1113-1116.

Rydstrom, J., Teixeisa da Cruz, A., & Ernster, L. Factors governing the kinetics and steady state of the mitochondrial nicotinamide nucleotide transhydrogenase system. Eur. J. Biochem., 1970, 17, 56-62.

Salford, L. G., Plum, F., & Seisjo, B. K. Graded hypoxia-oligemia in rat brain. I. Biochemical alterations and their implications. Arch. Neurol., 1973, 29, 227-233.

Salomon, E. Theorie des Reststomes den mar bei polarisiesten Electroden beobachtet. Z. Physik. Chem., 1897, 24, 55-80.

Samuelsson, B. Biosynthesis of prostaglandins. Prog. Biochem. Pharmac., 1969, 5, 109-128.

Samuelsson, B., Granstrom, E., Green, K., Hamberg, M., & Hammarstrom, S. Prostaglandins. Ann. Rev. Biochem., 1975, 44, 669-695.

Sano, S. 2-4-Bis-(β-hydroxypropionic acid) deuteroporphyrinogen IX, a possible intermediate between coproporphyrinogen III and protoporphyrin IX. J. Biol. Chem., 1966, 241, 5276-5283.

Sano, S., & Granick, S. Mitochondrial coproporphyrinogen oxidase and protoporphyrin formation. J. Biol. Chem., 1961, 236, 1173-1180.

Sanvordeker, D.R., & Lambert, H.J. Environmental modification of mammalian drug metabolism and biological response. Drug Metabolism Reviews, 1974, 3, 201-229.

Sapirstein, L.A., & Goldman, H. Adrenal blood flow in the albino rat. Am. J. Physiol., 1959, 196, 159-162.

Savitzky, A., & Golay, M.J.E. Smoothing and differentiation of data by simplified least squares procedures. Anal. Chem., 1964, 36, 1627-1639.

Schenkman, J.B., Remmer, H., & Estabrook, R.W. Spectral studies of drug interaction with hepatic microsomal cytochrome. Mol. Pharmacol., 1967, 3, 113-123.

Scheuer, J. Myocardial metabolism in cardiac hypoxia. Am. J. Cardiol., 1967, 19, 385-392.

Scheuer, J., & Stezoski, S.W. Effect of alkalosis upon the mechanical and metabolic response of the rat heart to hypoxia. J. Molec. Cell. Cardiol., 1972, 4, 599-610.

Schindler, F.J. Doctoral dissertation, Univ. of Pennsylvania, 1964.

Schmahl, F.W., Betz, E., Dettinger, E., & Hohorst, H.J. Oxygen tension, energy-rich phosphate and electrical activity of the brain cortex of the cat during controlled hypoxia. In D.W. Lubbers, U.C. Luft, G. Thews, and E. Witzleb (Eds.), Oxygen transport in blood and tissue. Stuttgart: Georg Thieme Verlag, 1968. pp. 140-145.

Schmeling, V.S., Mayer, G., Diehl, H., Ullrich, V., & Standinger, H. Untersuchungen zur Kinetik der L-Kynurenin-3-hydroxylase und des Cytochroms b_5 in Rattenlebermitochondrien. Z. Physiol. Chemie, 1969, 350, 349-356.

Schneider, W.C., & Potter, V.R. The assay of animal tissue for respiratory enzymes. J. Biol. Chem., 1943, 149, 217-227.

Schreiber, G., & Schreiber, M. Protein synthesis in single cell suspensions from rat liver. J. Biol. Chem., 1972, 247, 6340-6346.

Scholz, R., Hansen, W., & Thurman, R.G. Interaction of mixed function oxidation with biosynthetic processes. I. Inhibition of gluconeogenesis by aminopyrine in perfused rat liver. Eur. J. Biochem., 1973, 38, 64-72.

Schuchhardt, S. Comparative physiology of the oxygen supply. In M. Kessler, D.F. Bruley, L.C. Clark, Jr., D.W. Lubbers, I.A. Silver, & J. Strauss. Oxygen supply. Baltimore: University Park Press, 1973. pp. 223-229.

Scholander, P.F. Oxygen transport through hemoglobin solutions. Science, 1960, 131, 585-590.

Selkurt, E. Renal function. In E. Selkurt (Ed.), Physiology, 3rd edition. Boston: Little, Brown and Company, 1971. pp. 487-527.

Shukita, M., & Hall, P.F. Cytochrome P-450 from bovine adrenocortical mitochondria: an enzyme for the side chain cleavage of cholesterol. I. Purification and properties. J. Biol. Chem., 1973, 248, 5598-5604.

Sies, H., & Kandel, M. Positive increase of redox potential of the extramitochondrial NADP(H) system by mixed function oxidations in hemoglobin-free perfused rat liver. FEBS Letters, 1970, 9, 205-208.

Siesjo, B.K., & Messeter, K. Factors determining intracellular pH. In B.K. Seisjo and S.C. Sorensen (Eds.), Ion homeostasis of the brain. Copenhagen: Munksgaard, 1971. pp. 244-262.

Siesjo, B.K., & Nilsson, L. The influence of arterial hypoxemia upon labile phosphates and upon extracellular and intracellular lactate and pyruvate concentrations in the rat brain. Scand. J. Clin. Lab. Invest., 1971, 27, 83-96.

Silver, I.A. The measurement of oxygen tension in healing tissue. Prog. Resp. Res., 1969, 3, 124-135.

Simpson, E.R., & Estabrook, R.W. Mitochondrial malic enzyme: The source of reduced nicotinamide adenine dinucleotide phosphate for steroid hydroxylation in bovine adrenal cortex mitochondria. Arch. Biochem. Biophys., 1969, 129, 384-395.

Sinagowitz, E., Rahmer, H., Rink, R., Gornandt, L., & Kessler, M. Local oxygen supply in intra-abdominal organs and in skeletal muscle during hemorrhagic shock. In D.F. Bruley and H.I. Bicher (Eds.), Oxygen transport to tissue, Part A. New York: Plenum Press, 1973. pp. 505-511.

Sirek, A., & Sirek, O.V. Serotonin: A review. The Canadian Medical Assoc. J., 1970, 102, 846-849.

Smialek, M., & Hamberger, A. The effects of moderate hypoxia and ischemia on cytochrome oxidase activity and protein synthesis in brain mitochondria. Brain Res., 1970, 17, 369-371.

Smith, L. Cytochromes a, a_1, a_2, and a_3. Method. Enz., 1955, 2, 732-740.

Sobel, B.E. Salient biochemical features in ischemic myocardium. Circulation Res., 1974, 34 & 35 (suppl. III), 173-181.

Solomon, S., Bird, C.E., Ling, W., Iwamiza, M., & Young, P.L.M. Formation and metabolism of steroids in the fetus and placenta. Recent Prog. Hormone Res., 1967, 23, 297-347.

Sourkes, T.L., & Heneage, P. Some studies on the oxidative metabolism of the adrenal gland. Endocrinology, 1952, 50, 73-82.

Stainsley, W.N. Some critical oxygen tensions and their physiological significance. In J.D. Hatcher and D.B. Jennings (Eds.), Proc. Int. Symp. Cardiovasc. Respir. Effects Hypoxia. New York: Karger, Basel, 1966. pp. 29-40.

Stainsby, W.N., & Otis, A.B. Blood flow, blood oxygen tension, oxygen uptake and oxygen transport in skeletal muscle. Am. J. Physiol., 1964, 206, 858-866.

Stanley, P.E., & Williams, S.G. Use of the liquid scintillation spectrometer for determining adenosine triphosphate by the luciferase enzyme. Anal. Chem., 1969, 29, 381-392.

Statistical Bulletin, 1974. Incidence of disability lasting eight days or more. Vol. 55, p. 11.

Staudinger, H., & Zubzycki, Z. Zur kinetik der mikrosomalen NADPH-Oxydation. Z. Physiol. Chemie, 1963, 332, 109-120.

Stenger, R.J., & Spiro, D. Structure of the cardiac muscle cell. Am. J. Med., 1961, 30, 653-665.

Stoffel, W. Sphingolipids. Ann. Rev. Biochem., 1971, 40, 57-82.

Stone, W.E., Marshall, C., & Nims, L.F. Chemical changes in the brain produced by injury and anoxia. Am. J. Physiol., 1941, 132, 770-775.

Swash, M., Moffett, A.M., & Scott, D.F. Tyramine activates the EEG in epileptic patients. Nature, 1975, 258, 749-750.

Tada, K., Ito, H., Wada, Y., & Arakawa, T. Congenital tryptophanuria with dwarfism. Tokoku J. Exp. Med., 1963, 80, 118-134.

Tai, R.C., & Chang, H.-K. Oxygen transport in heterogeneous tissue. J. Theor. Biol., 1974, 43, 265-276.

Takahashi, G.H., Fatt, I., & Goldstick, B. Oxygen consumption rate of tissue measured by a micropolarographic method. J. Gen. Physiol., 1967, 50, 317-335.

Tanaka, T., & Knox, W.E. The nature and mechanism of the tryptophan pyrrolase (peroxidase-oxidase) reaction of Pseudomonas and rat liver. J. Biol. Chem., 1959, 234, 1162-1170.

Taurog, A. Thyroid peroxidase and thyroxine biosynthesis. Recent Prog. Hormone Res., 1970, 26, 189-247.

Wittenberg, J.B. Oxygen transport: A new function proposed for myoglobin. Biol. Bull., 1959, 117, 402.

Wittenberg, J.B. Myoglobin-facilitated oxygen diffusion: role of myoglobin in oxygen entry into muscle. Physiol. Rev., 1970, 50, 559-636.

Wolf, C.R., Elcombe, C.R., Illing, H.P.A., Bridges, J.W., Nimmo-Smith, R.H., King, L.J., & Netter, K.J. Measurement of substrate-induced oxygen uptake during microsomal drug oxidation using a gold microelectrode. Xenobiotica, 1975, 5, 173-181.

Wolff, J. Disorders of iodine metabolism. In R.H.S. Thompson and I.D.P. Wootton (Eds.), Biochemical disorders in human disease, 3rd edition. New York: Academic Press, 1970. pp. 379-449.

Wood, J.D. A possible role for γ-aminobutyric and in the homeostatic control of brain metabolism under conditions of hypoxia. Exp. Brain Res., 1967, 4, 81-84.

Wood, J.D., & Watson, W.J. The effect of hyperoxia and hypoxia on free and bound γ-aminobutyric acid in mammalian brain. Canadian J. Biochem., 1969, 47, 994-997.

Wurtman, R.J., & Zervas, N.T. J. Neurosurg., 1974, 40, 34-36.

Wykle, R.L., & Lockmiller, J.M.S. The biosynthesis of plasmologens by rat brain: Involvement of the microsomal electron transport system. Biochim. Biophys. Acta, 1975, 380, 291-298.

Yagi, K., Nagatsu, T., & Ozawa, T. Inhibitory action of chlorpromazine on the oxidation of D-amino-acid in the diencephalon part of the brain. Nature, 1956, 177, 891-892.

Yamaguchi, K., Sakakibara, S., Asamizu, J., & Ueda, I. Induction and activation of cysteine oxidase of rat liver. II. The measurement of cysteine metabolism in vivo activity of cysteine oxidase. Biochim. Biophys. Acta, 1973, 297, 48-59.

Yamamato, S., & Block, K. Enzymatic studies on the oxidative cyclizations of squalene. In T.W. Goodwin (Ed.), Natural substances formed biologically from mevalonic acid. Biochemical Society Symposium No. 29. New York: Academic Press, 1970. pp. 35-43.

Yousef, I.M., & Kuksis, A. Release of chylomicrons by isolated cells of rat intestinal mucosa. Lipids, 1972, 7, 380-386.

Zervas, N.T., Nori, H., Negora, M., Wurtman, R.J., Larin, F., & Lavyne, M.H. Reduction in brain dopamine following experimental cerebral ischemia. Nature, 1974, 247, 283-284.

Kerekiarto, B.V., γ Staudinger, H. Die Sauerstoffabhangigkeit der Hydroxylierung von Acetanilid zu 4-Acetamino-phenol durch kaninchenlebermikromen. Zeitschr. Physiol. Chemie, 1966, 347, 7-17.

APPENDICES

APPENDIX I

A CHRONOLOGY OF DISCOVERIES RELEVANT TO THE PHYSIOLOGY AND BIOCHEMISTRY OF HYPOXIA

1603 Fabricus described valves in arteries.

1615 Harvey formulated idea of circulation.

1658 Swammerdam described red blood cells (not published until 1738); Malpighi independently described red blood cells in 1665.

1661 Malpighi described alveoli of lungs; Malpighi described closed capillary circulation.

1660-1670 Boyle used air-pump to evacuate a vessel containing sparrow or candle; concluded that some anonymous component of air was necessary for life; obtained "air" from blood using vacuum pump.

1667 Robert Hooke used bellows to keep air passing through the lungs of a dog to show that the physical motion of breathing was not necessary for life, but rather only continual fresh air was necessary.

1668 Hooke noted that blood exposed to air became brighter red.

1669 Lower demonstrated blood in pulmonary vein is of arterial color before it reaches the heart.

1668-1674 Mayow concludes that a single substance is required for both combustion and life.

1755 Joseph Black established "fixed air" (CO_2) was given off by animals and by burning charcoal.

1771 Priestley showed that a sprig of mint restores foul air.

1772 Rutherford found that after "fixed air" was removed from vitiated air, a large portion remains which cannot support life (discovery of nitrogen).

1770-1774 Scheele and Priestley independently produced oxygen. Scheele called it "fire air" and interpreted it in terms of the phlogiston theory. Priestley showed it is consumed by animals and produced by plants. Also showed it turns blood bright red.

1780-1789 Lavoisier demonstrated that during respiration and combustion the same amount of heat is produced for the same amount of "eminently respirable air" (oxygen) consumed. He and Seguin found that the same amount of oxygen is consumed whether an animal breathed more or less oxygen than is present in the atmosphere. They found that oxygen consumption is influenced by exercise, digestion and external temperature.

1783 Montgolfier brothers developed hot air balloon.

1791 Spallanzani showed oxygen consumed by tissue sections, CO_2 produced. Not published until 1808 under the name of Senebier. Confirmed by Liebig (1850) and Pfluger (1872) but not generally accepted until 1890's.

1804 Robertson reached 26,000 ft in balloon and was greatly affected by altitude sickness.

1804 Wollaston demonstrated guaiacum turns blue in presence of oxygen and light (also shown by Brande in 1806).

1810, 1820 Planche showed that horse radish roots turned guaiacum blue.

1812 Vogel showed that H_2 and O_2 can combine at low temperatures in the presence of charcoal.

1812 Legallois discovered respiratory center; Hering discovered self regulation of breathing.

1818 Thenard discovered hydrogen peroxide.

1824 Liebig showed that carbohydrates, fats and protein are combusted by the body.

1837 Berzelius formulated theory of catalysis and suggested its role in living tissues.

1837 Magnus developed blood-gas apparatus.

1840 Schonbein discovered ozone.

1849 Hutchinson obtained pressure-volume curves for human lung.

1850 Liebig studied muscle respiration and concluded respiration occurs in muscle tissue; that blood acts only as a carrier of oxygen, CO_2.

1857 Hoppe-Seyler showed quantity of oxygen in blood did not follow Henry's law of solution.

1858 Claude Bernard showed CO displaces oxygen from blood.

1862 Glaisher and Coxwell made 29,000 ft trip in balloon. Glaisher described symptoms of altitude sickness.

1862 Hoppe-Seyler determined oxy-hemoglobin absorption spectrum.

1863 Holmgren found oxygen content of venous blood is less than arterial blood.

1864 Stokes determined deoxy-hemoglobin absorption spectrum.

1868 Pfluger showed both CO_2 excess and oxygen deficiency stimulated breathing.

1872 Paul Bert obtained a first oxy-hemoglobin dissociation curve.

1875 Tissandier made balloon flight in which two scientists died from oxygen deprivation.

1876 Hoppe-Seyler showed cyanide inhibits tissue oxygen consumption.

1877 Walter showed that poisoning by acid stimulates respiration.

1877 Oertmann found that frogs with their blood replaced by normal saline consumed as much oxygen and released as much CO_2 as normal frogs.

1878 Paul Bert showed that physiological affects of high altitudes were due to oxygen deprivation; points out that acclimatization to decreased oxygen partial pressure occurs; verified that the oxygen carrying capacity of the blood is increased in hypoxia.

1882 Zuntz formulated concept of residual volume in the lung.

1885 Miescher-Rusch produced evidence that resting ventilation is primarily regulated by CO_2.

1886 MacMunn described histohaematin and myohaematin.

1890 Araki found lactic acid production during hypoxia.

1890-1891 Vialt showed that the number of red corpuscles/unit volume of blood is increased at high altitudes.

1891 Rubner showed that the law of conservation of energy applies to the living body.

1893 Haldane showed quantitative role of CO_2 in regulation of respiration.

1894 Bertrand described laccase.

1896 Bertrand described tyrosinase.

1897 Spitzer studied indophenol oxidase reaction; Solomon discovered that oxygen reduction affected current of platinum wire.

1898 Linossier demonstrated blueing of guaiacum by extracts of plants and animals in presence of H_2O_2; termed activity peroxidase.

1901 Loew established catalase decomposes peroxide.

1904 Bohr, Hasselbach and Krogh discovered that addition of CO_2 to blood decreases affinity for oxygen.

1906 Zuntz and coworkers showed that respiratory volume increased during acclimatization to hypoxia.

1906 Harden and Young discovered stimulatory affect of inorganic phosphate and NAD on alcoholic fermentation.

1907 Fletcher and Hopkins found accumulation of lactic acid in muscle following electrical stimulation of contraction.

1908-1909 Henderson applied mass action law to CO_2-bicarbonate system.

1908-1925 Warburg used improved manometric methods to study tissue respiration; searched for oxygen activating ferment.

1909 Sorenson developed electrometric methods for measuring blood acidity.

1910 Kroghs showed that diffusion alone was sufficient to account for oxygen uptake by the lungs.

1911-1914 Battelli and Stern studied succinate and p-phenylenediamine oxidation.

1912-1922 Wieland advanced theory of hydrogen activation by dehydrogenases.

1913 Pikes Peak expedition: found that hemoglobin increase parallels red blood cell increase during acclimatization.

1917 Hasselbalch introduced log version of mass action law and clarified the relationship between pH, CO_2 tension, total CO_2 and bicarbonate in the blood.

1918-1920 Krogh studied diffusion of oxygen through tissue.

1920 Barcroft classified types of oxygen deficiencies.

1919-1920 Haggard and Henderson found that increased breathing during hypoxia resulted in alkalosis with a consequent decrease in urinary excretion of ammonia and acid.

1922 Krogh described in detail the anatomy and physiology of capillaries.

1923 Lumsden showed caudal pons responsible for sustained inspiratory drive.

1923 Warburg concluded that glycolysis supplied energy requirements in mammalian cells analogous to fermentation in bacteria.

1923 Keilin rediscovered histohaematins (cytochromes) and demonstrated changes in their oxidation state during respiratory activity.

1924 Hill and coworkers showed lactic acid accumulation during exercise is related to oxygen debt (also shown by Bang, 1935).

1925 Heyrovsky developed polarographic electrode system.

1926-1928 Heymans and Heymans showed reflex stimulation of breathing during hypoxia.

1926 Warburg recognized "Pasteur effect" as link between respiration and glycolysis.

1926 DeCastro described microscopic anatomy of the carotid body and suggested that it is involved in respiratory control.

1927 Eggleton and Eggleton observed that acid labile phosphoric ester is decreased in muscle fatigue.

1929 Keilin proposed that cytochromes function as a link between the dehydrogenases and oxygen consumption.

1929 Fiske and Subbarow isolated ATP from muscle.

1930 Engelhardt discovered that phosphorylation is coupled to respiration.

1934-1938 Szent-Gyorgyi showed the catalytic effect of dicarboxylic acids on respiration.

1937 Kalckar showed that phosphorylation is related to oxygen consumption.

1937 Krebs proposed the tricarboxylic acid cycle.

1939, 1940 Belitster and Tsybokova and, independently, Ochoa, determined P:O ratios.

1939-1941	Lipmann suggested that ATP plays a central role in the transfer of energy.
1941	Marshall and Nims showed that phosphocreatine decreases in brain during short periods of anoxia.
1942	Davies and Brink made first accurate tissue oxygen tension measurement.
1948	Kennedy and Lehninger showed that the tricarboxylic acid cycle occurs in the mitochondria.
1949	Gardjian, Webster and Stone showed ATP decrease during severe hypoxia.
1951	Lehninger demonstrated that oxidative phosphorylation is coupled to electron transport in the respiratory chain.
1952-1957	Chance used platinum electrode and sensitive spectrophotometric methods to study oxygen utilization and cytochrome kinetics; provided a biochemical basis for tissue oxygen requirements.
1955	Mason and Hayaishi independently showed enzymatic incorporation of molecular oxygen into metabolites.
1959-1960	Wittenberg and Scholander independently discovered the facilitation of oxygen diffusion in solution by myoglobin and hemoglobin.
1961	Cater and Silver developed micro-oxygen-electrode for tissue studies.

APPENDIX II

Cell Preparation Data Sheet

Rat weight: 278 gm

Liver weight: 10.5 gm

Cell preparation: CP 3-29

Date: 10/26/73

Time: 10 AM

Weight of tube plus cells: 34.1 gm

Weight of tube: − 14.6 gm

volume of cell suspension: 19.5 gm

total cell yield 1:72 dilution	viable cell yield
431	395
301	280
406	366
1138	1041

$1138 \div 3 \times 2 \times 10^4 = 7.59 \times 10^6$ cells/ml

volume of cell suspension		cells/ml		total cell yield
19.5 ml	X	7.59×10^6	=	1.48×10^8

$$\text{viability} = \frac{\text{viable cells}}{\text{total cells}} = \frac{1041}{1138} = 91.5\% \text{ viable}$$

$$\frac{\text{protein}}{10^6 \text{ cells}} = \frac{10.6 \text{ protein/ml}}{7.59 \text{ cells/ml}} = 1.40 \text{ mg}/10^6 \text{ cells}$$

Respiration rate

span = 5.1

cell conc = 1.52×10^6

media = mod. Hanks

temperature = 37°C

speed of recorder = 50 sec/in

slope = 1.3/3 in

$$Q_{O_2}^{cell} = \frac{4.8 \mu l O_2}{5.1} \times \frac{1.3}{3 \text{ inch}} \times \frac{\text{inch}}{50 \text{ sec}} \times \frac{60 \text{ sec}}{\text{min}} \times \frac{60 \text{ min}}{\text{hr}} \times \frac{1}{1.52 \times 10^6} = \frac{19.3 \mu l O_2}{10^6 \text{ cells}/\text{hr}}$$

$Q_{O_2}^{pro} = Q_{O_2}^{cell}$ /protein/10^6cells = 13.8 $\mu l O_2$/mg pro/hr

APPENDIX III

OPERATION INSTRUCTIONS FOR THE OXYSTAT

A. General

Operator should be familiar with principles of control as described in Instrumentation Handbook published by the Hays Corporation. Determination of optimum controller settings is described in the instruction manual for the Hays Model 854 Universal Solid State Controller which would be consulted if settings other than those described below are needed.

B. Determination of Liquid Volume, Carrier and Controlled Gases

1. Measure or estimate the rate of oxygen consumption for the desired incubation mixture.

2. Consult Figure 1 to determine the permissible range of oxygen transfer constants for desired oxygen consumption rates.

3. Use Figure 2 to determine a suitable incubation volume to provide an acceptable oxygen transfer constant.

4. Use Figure 3 to calculate maximum and minimum percent oxygen inputs required so that carrier and controlled gas mixtures can be chosen. Draw a line from the origin to the value of K on the top or right margin. Draw a second line parallel to this line intersecting the ordinate at the percent oxygen corresponding to the

maximum desired percent oxygen in solution. Now, draw a vertical line corresponding to the desired oxygen consumption rate. The points at which this vertical line intersects the diagonal lines when read on the ordinate correspond to the maximum and minimum inputs percent oxygen to allow control over the desired range.

5. Using Figure 4, one can now choose the oxygen content of carrier and controlled gases and suitable flow rates for oxystat function in the desired range.

C. Operation of the Oxystat

1. Turn on water bath for bubbling towers and adjust to 37°C.

2. Start flow of carrier and controlled gases through the bubbling towers at about 80-100 ml/min. At least 2 hr should be allowed for equilibration.

3. Turn on oxygen analyzer and temperature control for water jacketed incubation vessel.

4. Place distilled, deionized water in incubation vessel and turn on magnetic stirrer to moderate speed. Allow 1-2 hr for equilibration and stabilization, or longer if electrode is freshly recharged. Oxygen electrode must be charged every four to five experiments or roughly every 2-3 weeks of continual experimentation. Calibration with known oxygen standards and determination of a "zero" oxygen tension is essential for every day of experimentation.

The "zero" is determined by addition of a few crystals of sodium dithionite. The oxygen standards may be either air or certified oxygen mixtures, air (21% O_2) and 2% O_2 (certified standard) are suitable.

5) Adjust zero on oxygen analyzer to give zero on controller process meter.

6. Calibrate oxygen analyzer so that air at 37°C on the 25% scale reads 100 on the process meter. Zero to 100 on the process meter now represents 0-159 torr on the 25% scale, and 0-636 on the 100% scale.

7. Turn on recorder and adjust to span the desired O_2 range, and calibrate with standards and dithionite.

8. Adjust gas flows as determined from Figure 4.

9. Check controller settings (proportional band at 500%, rate is off, and reset is at 0.1 rpm).

10. Set valve manually to position to give desired input percent oxygen (Figure 4).

11. Adjust set point to desired value.

12. Pipet solution into incubation vessel. Attempts should be made to have solution as near as possible to final desired incubation oxygen tension to minimize the time required to attain a constant solution tension. This may be achieved by dilution of the oxygen consuming component into solutions preequilibrated with various

oxygen tensions. Alternatively, the solution may be flushed with hydrated N_2 or O_2 to rapidly approach the desired value.

13. As the solution oxygen tension approaches the desired value on the process meter, the mode is switched from manual to auto.

14. If the valve moves more than 1/2 turn, the set point should be readjusted to prevent any further movement.

15. Oxygen tension in solution should stabilize within 5-10 min to the desired value.

D. Trouble Shooting

1. Oxystat functions best with valve between 60 and 90% open. Control below 60 may have some drift and above 90 may have oscillations.

2. Drift of steady state value normally indicates too little change in input oxygen as a result of deviation from set point. This may be caused by several factors:

a. valve is operating below 50% open

b. carrier flow is too high relative to controlled air flow

c. set point oxygen tension is outside the permissible control range for given conditions (see section B).

d. proportion band setting too high.

e. reset value too slow

3. Oscillations may result from a variety of factors. These oscillations may be continuous or damped, but for short term experiments neither can be tolerated.

a. proportional band setting too low

b. reset valve too fast

c. rate too high

d. valve operating above 90% open

e. carrier flow too low relative to controlled air flow

f. difference in percent oxygen content of carrier and controlled gases is too great

4. Switching mode from manual to automatic too soon can result in over-response of controller. This will initially result in a reversal of the direction of oxygen tension excursion followed by an overshoot. This problem can be corrected by returning to manual for about a minute before returning to automatic or by readjustment of set point.

Appendix Figure 1. Percent oxygen input required to maintain solution $P(O_2)$ equal to 38 torr (53 μM) as a function of oxygen transfer constant at fixed respiration rates. This series of curves was computer drawn according to the equation $R = K(P(O_2)_g - P(O_2)_f)$. R was fixed at 20, 40, 60, or 80 μl O_2/ml/hr (0.89, 1.79, 2.68, or 3.57 mM/hr). $P(O_2)_f$ was set at 5% O_2 (38 torr, 53 μM). $P(O_2)_g$ was calculated as a function of K between 0 and 15 hr^{-1}. To determine K for experiments, choose curve drawn with R closest to desired respiration rate. Determine point on curve where slope is -1 and draw vertical line through this point intersecting the abscissa. This abscissa value is the minimum value of K to maintain solution oxygen tension between 1 and 150 torr (1.4-140 μM).

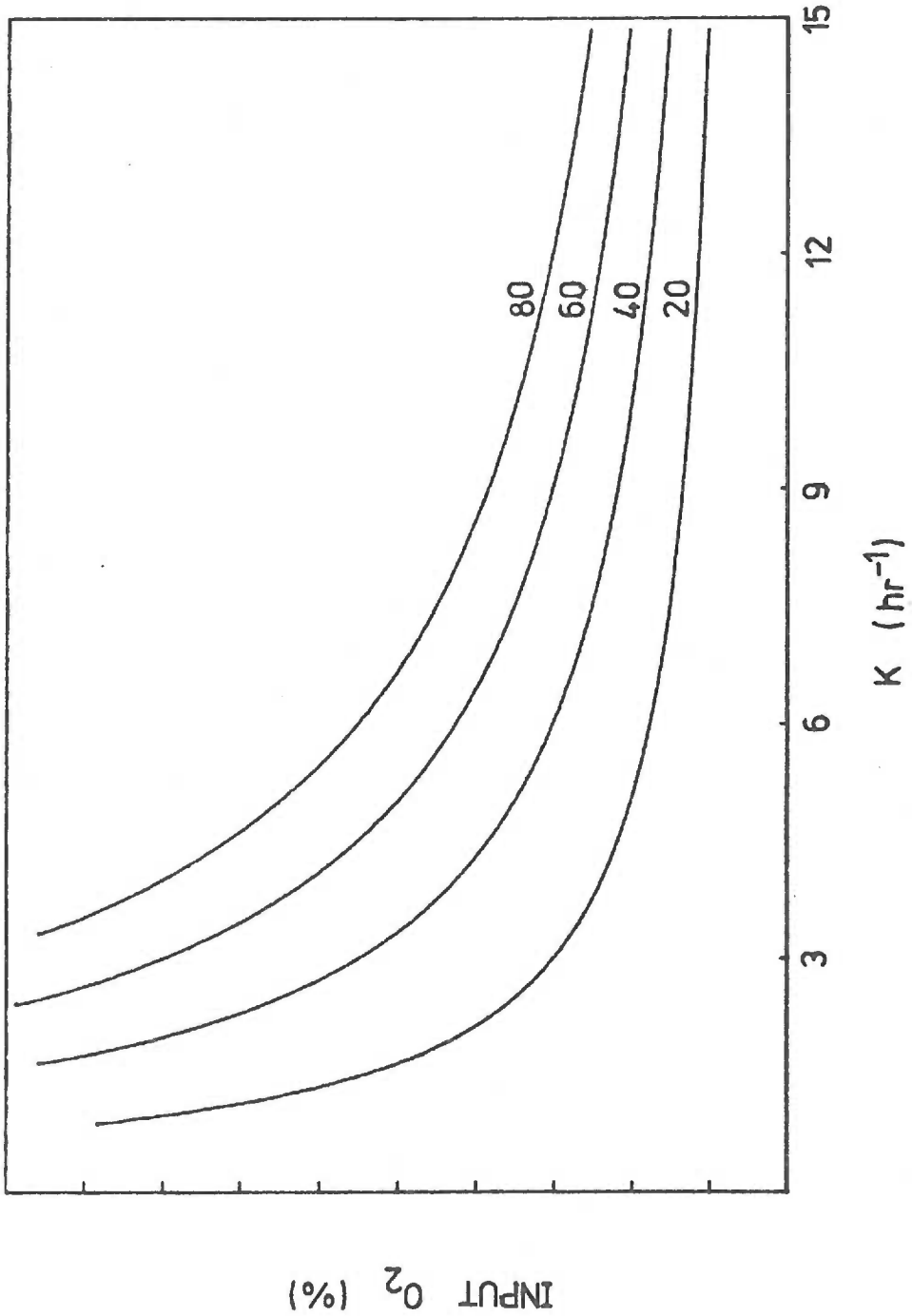
80
60
40
20
3
6
9
12
15
K (hr⁻¹)
INPUT O2 (%)

Appendix Figure 2. Oxygen transfer constant at different solution volumes.

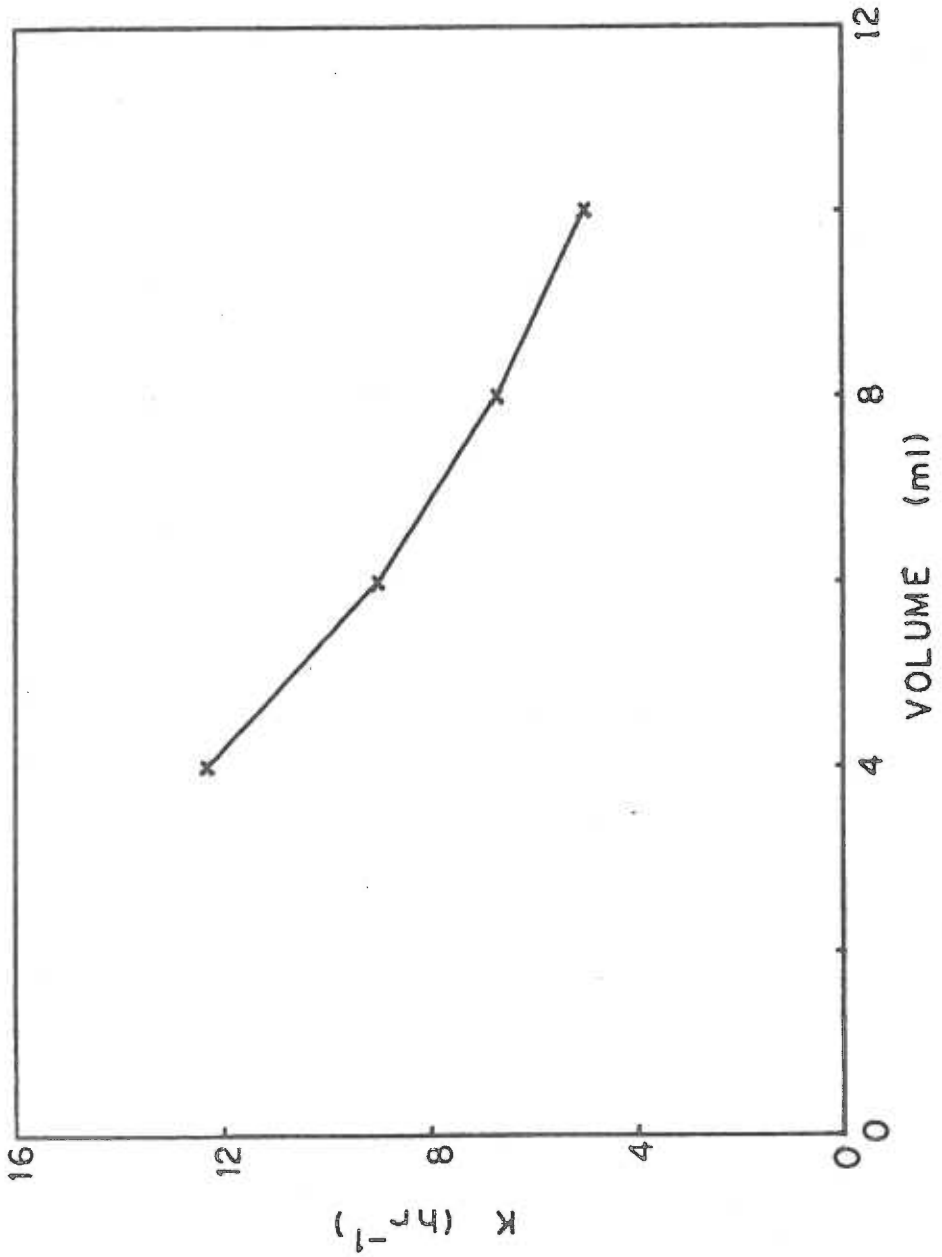
K (hr⁻¹)
16
12
8
4
0
0
4
8
12
VOLUME (ml)

Appendix Figure 3. Percent oxygen input required to maintain a solution $P(O_2)$ as a function of respiration rate. Draw a line from the origin to the desired value of K on upper or right margin. Draw a second line parallel to this line intersecting the ordinate at the maximum desired percent oxygen solution. Draw a vertical line corresponding to the desired oxygen consumption rate. The points at which the vertical line intersects the diagonal lines corresponds to the maximum and minimum input oxygen when read on the ordinate.

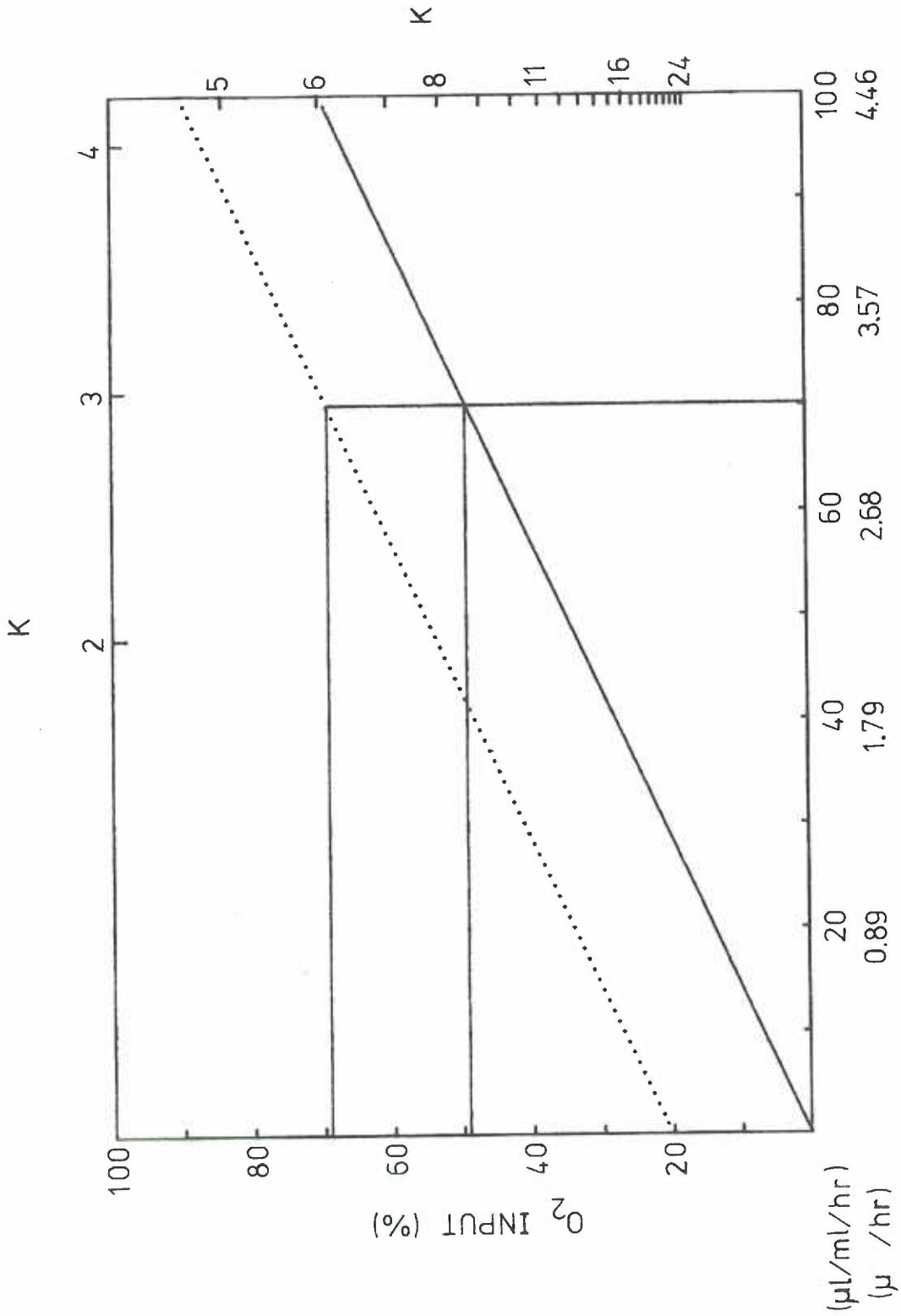

OXYGEN CONSUMPTION RATE

Appendix Figure 4. Percent oxygen in mixed gas as a function of valve position for various controlled and carrier gases. Points were calculated from the defined percent oxygen in the controlled and carrier gases, the flow rate for the carrier gas, and the flow rate of the controlled gas as a function of valve position according to the equation:

$$\%\ O_2 \text{ mixed} = \frac{(\%\ O_2 \text{ carrier}) \times (\text{flow rate carrier}) + (\%\ O_2 \text{ controlled}) \times (\text{flow rate controlled})}{(\text{flow rate carrier}) + (\text{flow rate controlled})}$$

A = 30% O_2 carrier gas (20 ml/min, 95% O_2 controlled gas (94 ml/min)

B = 20% O_2 carrier gas (20 ml/min, 70% O_2 controlled gas (94 ml/min)

C = 20% O_2 carrier gas (30 ml/min), 70% O_2 controlled gas (60 ml/min)

D = 0% O_2 carrier gas (30 ml/min), 70% O_2 controlled gas (60 ml/min)

E = 0% O_2 carrier gas (20 ml/min), 35% O_2 controlled gas (94 ml/min)

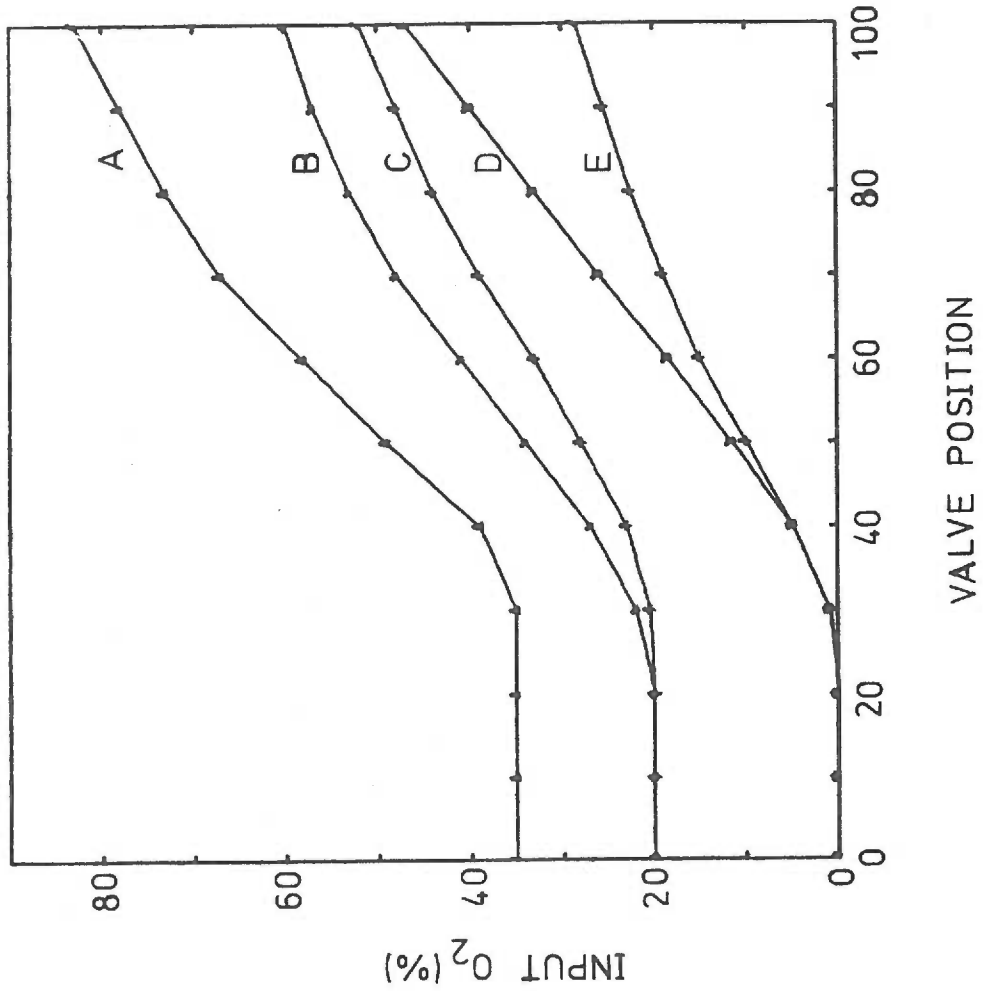
A
B
C
D
E
0
20
40
60
80
100
0
20
40
60
80
VALVE POSITION
INPUT O_2 (%)

APPENDIX IV

COMPUTER PROGRAMS

```
C:FOCAL-11,LFOCA-A

  1.01 T "STANDARD DEVIATION PROGRAM"!
  1.10 A "N", N,!
  1.11 S Y=0;S G=0
  1.20 F I=1,N; T %2, I;A "X", X(I),!
  1.30 F I=1,N;D 2
  1.40 T "AVG= "; T %4.03 Y/N,!
  1.50 F I=1,N;S Z(I)=(X(I)-Y/N)↑2
  1.60 F I=1,N; D 3
  1.70 S H=G/(N-1);T "VAR= ", H,!
  1.80 T "STD. DEV.= ", FSQT(H),!
  1.90 Q

  2.10 S Y=Y+X(I)

  3.10 S G=G+Z(I)
*



C:FOCAL-11,LFOCA-A

  1.01 T "LINEAR LEAST SQUARES PROGRAM",!
  1.10 T "PLTL",!;A "# OF STDS", N,;
  1.60 A "X-AXIS: LOWER LIMIT", X1,!
  1.70 A "UPPER LIMIT", X2,!
  1.80 A "Y AXIS: LOWER LIMIT", Y1,!
  1.90 A "UPPER LIMIT", Y2,!

  2.10 S XA=X2-X1;S YA=Y2-Y1
  2.20 F I=1,N;T %2 I;A "X",X(I),;A "Y",Y(I),!
  2.30 F I=1,N;S X(I)=X(I)-X1;S Y(I)=Y(I)-Y1
  2.40 F I=1,N;D 21
  2.50 A Z
  2.60 S D1=0;S D2=0;S D3=0;S L4=0;S D8=0
  2.70 F I=1,N;D 3
  2.80 S D5=D2↑2
  2.90 S D6=(D1-D2*D3/N)/(D4-D5/N);T "SLOPE=";T %6.05 D6,!
  2.91 S D7=D3/N-(D6*D2)/N;T "INTERCEPT=";T %6.05 D7,!
  2.92 F J=1,10;T %4 1E4* J/10,1E4*(D6*J*XA/10+D7)/YA,!
  2.98 A Z
  2.99 G 4.10

  3.01 S D1=X(I)*Y(I)+D1;S D2=X(I)+D2;S D3=Y(I)+D3;S D4=X(I)↑2+L4;
  3.10 S D8=Y(I)↑2+D8

  4.10 S D9=(D4-D1↑2/D8)/(N-2);
  4.15 T "X INTERCEPT=";T %6.05 -D7/D6,!
  4.20 T "STD ERROR OF ESTIMATE=";T %6.05 FSQT(D9)/FSQT(D4),!
  4.99 Q

 21.10 S PX=1E4*X(I)/XA;S PY=1E4*Y(I)/YA
 21.20 T %4,PX-30,PY+30,!,PX+30,PY-30,!,"-1000 -1000",!
 21.30 T PX-30,PY-30,!,PX+30,PY+30,!,"-1000 -1000",!
*
```

```
C:FOCAL-11,LFOCA-A

  1.01 C ONLINE O2 CONSUMPTION, DATA PRINTOUT
  1.10 X FX(-1,177550,2!9)
  1.20 F I=1,1E3;D 2.10;T %6.04 A(I),!
  1.29 X FX(-1,177550,1)
  1.30 A Y;G 4

  2.10 S P=0;F J=1,10;D 3.10

  3.10 S P=P+FADC(J);S A(I)=P/10

  4.10 C O2 CONSUMPTION PLOT
  4.20 A "PLOT TIME,SEC",N,!;A "INITIAL TIME,SEC",M,!
  4.30 A "O2 SPAN, 10MMS",O,!;A "MV",S,!;A "ZERO,MV",Q,!
  4.40 F I=M,M+N;D 5;T %4 1E4*(I-M)/N,1E4*(A(I)-Q)/S+1E4/7,!
  4.50 A Y;G 6.10

  5.01 C 11 POINT SMOOTH
  5.10 S D=-36*A(I-5)+9*A(I-4)+44*A(I-3)+69*A(I-2)+84*A(I-1)+89*A(I)
  5.11 S D1=-36*A(I+5)+9*A(I+4)+44*A(I+3)+69*A(I+2)+84*A(I+1)+D
  5.20 S A(I)=D1/429

  6.10 C RATE VS O2 PLOT
  6.20 F I=M,M+N;S B(I)=(2*(A(I-1)-A(I+1))+A(I-2)-A(I+2))/4
  6.30 S C(M)=0;F I=M+1,M+10;S C(I)=B(I)+C(I-1)
  6.40 S C=C(M+10)/10
  6.50 F I=M,M+N;T %4 1E4*(A(I)-Q)/S,1E4*B(I)/(2*C),!
  6.60 A Y

  7.10 C DOUBLE RECIPROCAL PLOT
  7.20 F I=M,M+N;T %4 1E4*(A(M)-Q)/((A(I)-Q)*100),1E4*(1/B(I))/(10/C),!


  8.10 X FX(-1,177550,2!9)
  8.20 F I=0,1E3;D 9.10;T %6.04 A(I)

  9.10 S P=0;F J=1,10;D 10

 10.10 S P=P+FADC(0);S A(I)=P/10
*


C:FOCAL-11,LFOCA-A
  1.01 C ITERATION PROGRAM FOR OBTAINING KM(O2)
  1.10 F I=1,12;A "V",V(I),"H",H(I),"O",O(I),!
  1.20 A "VMAX",V,"KH",KH,!
  1.30 S H=1E4;S A=-1
  1.40 F I=1,12;S C(I)=O(I)*((V/V(I))/(1+KH/H(I))-1)
  1.50 S Y=0;S G=0
  1.60 F I=1,12;S Y=Y+C(I)
  1.70 F I=1,12;S Z(I)=(C(I)-Y/12)!2
  1.80 F I=1,12;S G=G+Z(I)
  1.90 T %8.04 "V",V,"KH",KH,"KO",Y/12,"S.D.",FSQT(G/11),!

  3.01 I (A) 3.10,3.20,3.30
  3.10 I (FSQT(G/11)/(Y/12)-H) 4.10,4.20,4.20
  3.20 I (FSQT(G/11)/(Y/12)-H) 4.20,4.30,4.30
  3.30 I (B) 3.40,3.50,3.50
  3.40 I (FSQT(G/11)/(Y/12)-H) 4.30,4.40,4.40
  3.50 I (FSQT(G/11)/(Y/12)-H) 4.40,4.10,4.10

  4.10 S H=FSQT(G/11)/(Y/12);S A=-1;S V=V+.1*V;G 1.40
  4.20 S H=FSQT(G/11)/(Y/12);S A=0;S V=V-.1*V;G 1.40
  4.30 S H=FSQT(G/11)/(Y/12);S A=1;S B=-1;S KH=KH+.1*KH;G 1.40
  4.40 S H=FSQT(G/11)/(Y/12);S B=0;S KH=KH-.1*KH;G 1.40
*
```

```
C:FOCAL-11,LFOCA-A
 31.01 C MICHAELIS MENTON PLOT
 31.10 T "PLTL",!;A "X AXIS LIMIT=",X1,!;A "Y AXIS LIMIT=",Y1,!
 31.20 A "KM=",K,!;A "VM=",V,!
 31.30 F J=0,100;D 32

 32.20 T %4 1E2*J,1E2*V*X1*J/((K+(X1*J/100))*Y1),!
*
```

```
C:FOCAL-11,LFOCA-A
  4.00 C PLOT V VS P(O2) FOR 2-SUBSTRATE RANDOM KINETICS
  4.01 F I=1,12;A "P",P(I),"O",O(I),!
  4.04 A "KP",KP,"KO",KO,"V",V,!
  4.08 F I=1,12;S X(I)=V/((1+KP/P(I))*(1+KO/O(I)))
  4.09 T "PLTL",!;F I=1,12;T %4 1E4*O(I)/150,1E4*X(I)/100,!
  4.10 T "PLTT",!
  4.11 G 4.04
*
```

```
 1.01 C O2 UPTAKE RATE VS TIME FOR N OXIDASES

  1.10 T "PLTL", !; A "HOW MANY ENZYMES?", N,!
  1.20 F I=1, N; T %2, I; A "KM", K(I); A "VM", V(I)
  1.30 A "TIME SCALE", SX; A "FULL SCALE O2", SY,!
  1.40 S O=SY; S T=0; S DT =SX/200
  1.50 S V=0 ; F I=1,N; D 2
  1.55 S O=O-V*DT
  1.60 T %4 1E4*T/SX, 1E4*O/SY,!;S T=T+DT
  1.70 I (O) 1.8, 1.8, 1.5
  1.80 G

  2.20 S V1=V(I)/(1+K(I)/O); S V=V+V1

*
```

```
C:FOCAL-11,LFOCA-A

  1.01 C CALCULATION OF O2 CONSUMPTION RATE FOR A SYSTEM CONTAINING
  1.02 C N OXIDASES
  1.03 C ASSUMPTIONS; ASSUME 1 ALL SUB ARE SATURATING
  1.10 T "PLTL",!; A "HOW MANY ENZYMES?", N,!
  1.20 F I=1, N; T %2, I;A "KM", K(I); A "VM", V(I)
  1.30 A "FULL SCALE , O2", SX; A "RATE", SY,!
  1.40 F O=SX/100, SX/100, SX; D 2
  1.99 G

  2.10 S V=0; F I=1,N; S V1=V(I)/(1+K(I)/O); S V=V+V1
  2.20 T %4, 1E4*O/SX, 1E4*V/SY,!
*
```